Flavin-containing monooxygenases: Regulation, endogenous roles and dietary supplements

A thesis submitted to the University of London in partial fulfilment of the requirements for the degree of Doctor of Philosophy

by Lyndsey Houseman

Department of Biochemistry and Molecular Biology
University College London

February 2008

I, Lyndsey Houseman, confirm that the work presented in this thesis is my own. Where information has been derived from other sources, I confirm that this has been indicated in the thesis.

UMI Number: U591223

All rights reserved

INFORMATION TO ALL USERS
The quality of this reproduction is dependent upon the quality of the copy submitted.

In the unlikely event that the author did not send a complete manuscript
and there are missing pages, these will be noted. Also, if material had to be removed,
a note will indicate the deletion.

UMI U591223
Published by ProQuest LLC 2013. Copyright in the Dissertation held by the Author.
Microform Edition © ProQuest LLC.
All rights reserved. This work is protected against
unauthorized copying under Title 17, United States Code.

ProQuest LLC
789 East Eisenhower Parkway
P.O. Box 1346
Ann Arbor, MI 48106-1346

Abstract

To investigate the regulation of flavin-containing monooxygenase 5 (FMO5) by xenobiotics in mouse liver, a method for isolating primary mouse hepatocytes was designed. *Fmo5* expression was up-regulated by hormones (estradiol, progesterone), dietary supplements (lipoic acid) and other xenobiotics (rifampicin, ethanol) in primary mouse hepatocytes and HepG2 cells. Gene reporter assays showed that *Fmo5* expression in HepG2 cells is mediated by pregnane-x-receptor (PXR) ligands.

To uncover more about the endogenous role of FMOs, two knockout mouse models, *Fmo1, 2, 4* (-/-) and *Fmo5* (-/-), were studied. *Fmo1, 2, 4* (-/-) males weighed less and had less gonadal fat than their wild-type counterparts. The bodyweight of the *Fmo1, 2, 4* (-/-) females was greater than that of the wild-type females. Histology shows that the adipocytes in the *Fmo1, 2, 4* (-/-) male mice are 50% smaller than wild-type male adipocytes, and the liver histology shows the *Fmo1, 2, 4* (-/-) males had less fat in the liver compared to wild-type males. *Fmo1, 2, 4* (-/-) mice had higher plasma total-, HDL- and LDL-cholesterol than the wild-type mice. On a high-fat diet, the male *Fmo1, 2, 4* (-/-) mice gain weight and gonadal fat weight.

The *Fmo5* (-/-) mice have a similar bodyweight and fat weight to the wild-type animals, but *Fmo5* (-/-) mice have lower plasma HDL cholesterol and lower plasma iron than WT mice.

The results therefore show that a deficiency in FMOs interferes with endogenous fat metabolism.

Lipoic acid is an endogenous substrate of FMO1, so to see if the inability to metabolise lipoic acid is the reason for the lower bodyweight and fat weight in *Fmo1, 2, 4* (-/-) males, the mice were fed a 0.1% lipoic acid diet. All knock-out and wild-type mice lose a similar amount of weight. This implies that the metabolism of lipoic acid is not the fundamental endogenous role of FMOs.

Contents

List of Figures

Abbreviations

AhR	Aryl hydrocarbon receptor
BSA	Bovine serum albumin
C/EBP	CCAAT/enhancer-binding protein
CAR	Constitutive-activated receptor
CHD1L	chromodomain helicase DNA binding protein 1-like
CYP	Cytochrome P450
DPT	10-(N,N-dimethylaminopentyl)-2-(trifluoromethyl)phenothiazine
ER	Estrogen receptor
FAD	Flavin adenine dinucleotide
FAS	Fatty acid synthase
FBS	Fetal bovine serum
FCS	Fetal calf serum
FMO	Flavin-containing monooxygenase
GAPDH	Glyceraldehyde-3-phosphate dehydrogenase
GCR	Glucocorticoid receptor
GH	Growth hormone
GRE	Glucocorticoid responsive element
GST	glutathione *S*-transferase
GTA	Glycyrrhetinic acid
HBSS	Hank's buffered salt solution
HDL	High density lipoprotein
HIF-1	Hypoxia induced factor-1
HNF	Hepatocyte nuclear factor
HO	Haem-oxygenase
HSD	Hydroxysteroid dehydrogenase
IRS	Insulin response sequence
IVC	Inferior vena cava
KO	Knock-out
LARII	Luciferase Assay Reagent II
LB	Luria-Bertani
LDL	Low density lipoprotein
MW	Molecular weight
NADPH	Nicotinamide adenine dinucleotide phosphate
PB	Phenobarbital
PBREM	Phenobarbital response element
PBS	Phosphate buffered saline
PCR	Polymerase chain reaction
PEP	Phosphoenolpyruvate
PGC-1α	Peroxisome proliferators-activated receptor-γ co-activator 1α

PPAR	Peroxisome proliforator activated receptor
PRKAB2	AMP-activated protein kinase subunit beta-2
PXR	Pregnane-x-receptor
RLU	Relative light units
ROS	Reactive oxygen species
RT	Room temperature
RT-PCR	Reverse transcriptase-polymerase chain reaction
RXR	Retinoid-x-receptor
SDS	Sodium dodecyl sulphate
SEM	Standard error of the mean
SP1	Specificity protein-1
SRC-1	Steroid receptor coactivator-1
SSC	Standard saline citrate
STAT	Signal transducer and activator of transcription
TBE	Tris-borate-EDTA
TCDD	Tetrachloro-di-benzo-p-dioxin
TE	Tris-EDTA
TMA	Trimethylaminuria
UDPGT	UDP-glucuronyl transferase
USF	Upstream stimulatory factor
WT	Wild-type

A word about human and mouse gene and protein nomenclature

A human gene is written in italics and capital letters e.g. *FMO*, whereas the human protein is written in capitals e.g. FMO. In mice the protein is also written in capitals e.g. FMO, but the gene is written in italics with the first letter uppercase and the following letters lowercase e.g *Fmo*.

Acknowledgments

I'd obviously like to thank Professor Elizabeth Shephard for all her support and guidance. I greatly appreciated her understanding over the first year or so. Who'd of thought culturing primary mouse hepatocytes would be so tough?...

Many thanks to Dr Azara Janmohammed, who has been a great friend and a constant source of technical support and inspiration. Thank you Miss Asvi Francois and Mr Matthew Hancock who made the lab a fun and challenging place to be, I hope the next lab incumbents have strong constitutions, and like tea.

Thank you also to Mr Bilal Omar, whom I always enjoyed working with. It was great to have a fresh pair of eyes and someone to bounce ideas around with.

Thank you Dr Mina Edwards, who knows better than most how difficult it was to isolate the hepatocytes, and who was good enough to keep me going when it looked like we'd never crack it. Many thanks to Professor Ian Phillips, Dr Anoop Kumar and Mr Phillip Gates who were all kind enough to give me technical support and information at a moments notice.

I'd also like to thank Miss Alison Bradley and Mr Andrew Niewiarowski who have become two of my closest friends and who have been good enough to listen to me through the good times and bad.

My parents and my brother have been so supportive, since I first decided that Bunsen burners and frothing coloured liquids in flasks was the career I wanted for myself. Of course modern science turned out not to be like that at all. Although I do suspect there's only so much you can do with some dry ice and some coloured liquid. Thank you, I hope this thesis does you justice.

Finally, of course I'd like to thank Jim, for his support which has been immense, for listening to me harp on about mouse liver and for reminding me that a PhD was never supposed to be easy.

This research was very kindly funded by the Drummond Trust.

Chapter 1

Introduction

1 Introduction

1.1 Liver structure and function

The liver is the largest gland in the body and perhaps the most versatile organ. It is involved in many major physiological functions which can be divided into lipid metabolism, carbohydrate metabolism, protein metabolism, producer of bile, detoxification and excretion. Detoxification of course involves xenobiotic metabolism which is discussed in more detail below.

The human liver is comprised of several cell types where hepatocytes represent 90% of the tissue volume and 70% of the total cell population. The liver has a dual blood supply and is served mostly by the portal vein, which drains from the intestines, and by the hepatic artery. The portal vein, hepatic artery, bile duct and lymphatics enter the liver at a single point, the porta hepatis. Once inside the liver these vessels run in a connective tissue matrix and the assemblage is called the portal tract. This branches out to form the "portal tree". Each branch of the tree contains all four types of vessel. The hepatic vein also branches out amongst the liver and intermingles with the vessels from the portal tree (Rhoades, 2003).

Terminal portal venules and hepatic arteries deliver their blood to sinusoids formed by fenestrated endothelial cells. The functional part of the gland, the parenchyma, consists of hepatocytes, here the blood flows through the sinusoids, making contact with these cells. Unbound xenobiotics in the sinusoidal blood get taken up into the hepatocytes either by active transportation or by diffusion. This mode of transport very much depends upon how large the compound is, its charge and its lipophilicity. Having made contact with the hepatocytes the blood drains into the central vein and then to the hepatic artery. Blood leaves the liver via the hepatic veins, which join the ascending vena cava (Rhoades, 2003). The vasculature of the liver is shown in Figure 1.1.1.

1.1.1 Vasculature of the liver

The vasculature of the human liver and integration of bile ducts from the pancreas and gall bladder (excerpt from Merck.com).

1.2 The acinus-the functional unit of the liver

The acinus represents the functional unit of the liver and zones within the acinus centre around the blood supply. The acinus is the egg-shape delimiter around the terminal branches of the hepatic artery and portal vein (Figure 1.2.1). The area around the terminal portal vein and arteriole is the periportal zone. The area around the central vein is termed the perivenous or centrilobular zone. It is here that monooxygenase activity predominantly occurs (Bengtsson et al., 1987; Vaananen, 1986). There are phenotypic differences between hepatocytes as you move through the acinus. Genes are differentially expressed in the periportal and perivenous zones of the liver. This zonation appears to be dynamic, affected by the levels of oxygen, nutrients, hormonal signals (Jungermann and Katz, 1982) and xenobiotics (Buhler et al., 1992; Rich et al., 1989). The perivenous cells have the highest level of phase I and phase II enzymes, and genes from these cells also seem more sensitive to induction from xenobiotics (Baron et al., 1981; Buhler et al., 1992; Gooding et al., 1978). Hepatocytes that were isolated using digitonin-zonation showed that cytochrome P450 enzymes were more susceptible to induction from the perivenous compared with the periportal area (Bars et al., 1992). The zonation for the phase II enzymes, such as glutathione *S*-transferases and the UDP-glucuronyl transferases, appears to be less stark than that for phase I enzymes. This can often make the perivenous area more susceptible to damage because the phase II enzymes may not fully compensate for the high turn-over of toxic intermediates produced by the phase I enzymes (Bengtsson et al., 1987; Kera et al., 1987).

1.2.1 *Liver lobule and acinus*

Two representations of the liver lobule and the acinus (both excerpt from Merck.com).

1.3 Xenobiotic Metabolism

Xenobiotic metabolism is carried out by enzymes all over the body, but the main concentration of these enzymes is in the liver. Chemical reactions they preside over include oxidation, reduction, hydrolysis, conjugation and condensation. The result of these reactions can determine if a drug has a pharmacological or toxicological effect.

Xenobiotic metabolism can be split into two phases. Phase I enzymes functionalise the drug by uncovering or adding a reactive 'handle' for phase II enzymes to act upon. Phase II reactions essentially detoxify the drug, resulting in a hydrophilic product that can be excreted in the urine or bile.

There are several groups involved in phase I metabolism, the main two groups being the cytochromes P450 (P450) (the most prolific of the two) and the flavin-containing monooxygenases (FMO), both of which are discussed below. Other enzymes are involved such as peroxidases, amine oxidases, dehydrogenases, xanthine oxidases, but to a lesser degree.

1.4 Cytochromes P450

The major group of enzymes involved in xenobiotic metabolism are the cytochromes P450 (P450). These are a superfamily of haem-containing mixed-function oxidases, found bound to the endoplasmic reticulum in many cells. The mixed-function oxidase reaction conforms to this stoichiometry:

$$NADPH + H^+ + O_2 + RH \rightarrow NADP^+ + H_2O + ROH$$

Where RH represents an oxidisable drug and ROH is the hydroxylated metabolite. The overall reaction is catalysed by the P450 enzyme, which requires the presence of molecular oxygen, NADPH and NADPH-cytochrome P450 reductase.

The largest concentration of P450s is in the liver, although they are found throughout the body, most notably in the small intestine, kidney, skin (Murray et al., 1988) and lung (Hall et al., 1989). They are involved in the phase I metabolism of a massive variety of xenobiotics, although at most only 15 P450 enzymes are thought to be involved in exogenous metabolism. Besides xenobiotic metabolism P450s play a large

endogenous role. They are involved in cholesterol biosynthesis, vitamin D metabolism, bile acid metabolism and biosynthesis and catabolism of steroids ((Nelson, 1999).

There are four main P450 families involved in xenobiotic metabolism (CYP1-4), each with several sub-familes (e.g. CYP2A, CYP2B) and isoforms (e.g. CYP2B6). CYP2C9, CYP2D6 and CYP3A4 account for 60-70% of all phase I metabolism of drugs.

CYP3A4 is the most highly expressed P450 isoform in the human liver, approximately 30% of the total P450 content in the liver is represented by CYP3A4. Even more importantly it metabolises around half of the clinically important drugs in use today. This also means it is very important in the etiology of drug-drug interactions.

The human CYP3A4 family consists of 3 members; CYP3A4, CYP3A5 and CYP3A7 (Nelson et al., 1996). CYP3A7 is predominantly expressed in foetal liver (Komori et al., 1990) and metabolises retinoic acid (Chen et al., 2000). CYP3A4 is inducible by barbiturates, glucocorticoids and rifampicin in humans. It has the broadest substrate specificity of any P450 and is able to act upon compounds from acetaminophen (MW 151) to cyclosporine (MW 1201) (Combalbert et al., 1989). It is also able to metabolise pesticides (e.g. parathion) (Butler and Murray, 1997) and non-ionic detergents (Hosea and Guengerich, 1998).

CYP3A4's expression is under the control of several transcription factors, the most important of which are members of the orphan nuclear receptor family enabling CYP3A4's expression to be changed in response to environmental stimuli (see Section 1.17).

1.5 Flavin-containing monooxygenases (FMOs)

This small family of monooxygenases is the other prominent group of enzymes involved in phase I metabolism. FMOs were discovered in the 1960s in hepatic microsomes, not long after P450s were characterised, and were described as NADPH- and oxygen-requiring enzymes, able to metabolise dimethylaniline to its *N*-oxide (Ziegler and Pettit, 1966).

FMOs are flavoproteins containing a single FAD (Poulsen and Ziegler, 1979) and are important for the metabolism of a massive variety of dietary compounds, synthetic

environmental toxicants, natural plant alkaloids and therapeutics (Cashman, 2003). They are able to act upon such a range of xenobiotics because the energy required to drive the reaction is already available to the enzyme because the FAD moiety is already bound to oxygen as a peroxyflavin (Massey, 1994) (Figure 1.6.1). This intermediate is stable from minutes to hours *in vitro* at 4°C and so presumably this is the predominant form of FMO in the cell, waiting to bind a substrate (Jones and Ballou, 1986). Thus the tight fit of a substrate usually needed to lower the activation energy of a catalysed reaction is superfluous.

There are 5 functional human isoforms, FMO1-5, which preferentially act upon substrates containing nucleophiles such as nitrogen, sulphur, selenium and phosphorous. FMOs are expressed ubiquitously, found associated with the endoplasmic reticulum, but there are distinct differences between tissue, sex, developmental stage and species.

1.6 Expression of FMOs

FMO1 is the main liver isoform in mammals such as pig, rabbit, rat and mouse (Cherrington et al., 1998; Gasser et al., 1990; Lattard et al., 2002; Lawton et al., 1990), the exception being humans. In human liver the dominant isoform switches from FMO1 in the foetus to FMO3 in the days following birth (Dolphin et al., 1996; Koukouritaki et al., 2002). The expression of FMO3 is also switched on at this time in mice (Cherrington et al., 1998). Although the expression of FMO1 is switched off in humans after birth, it remains highly expressed in other organs, hence FMO1 in adult humans is extra-hepatic. FMO1 is expressed in human foetal and adult kidney (Dolphin et al., 1996; Krause et al., 2003; Zhang and Cashman, 2006), as well as human lung (Dolphin et al., 1996; Krueger et al., 2002a), brain (Zhang and Cashman, 2006), and intestine (Yeung et al., 2000). In mice FMO1 mRNA is found in the lung, kidney and brain (Janmohamed et al., 2004).

FMO2 is highly expressed in the lung of rabbits (Williams et al., 1984) and rhesus macaque (Yueh et al., 1997). FMO2 mRNA expression is the highest amongst the isoforms in human lung (Zhang and Cashman, 2006), however it is not expressed in the lung as a functional enzyme in most humans because of nonsense or frame-shift mutations in Caucasians and Asians (Dolphin et al., 1998; Furnes et al., 2003; Krueger et

al., 2002b). FMO2 mRNA is also found in human kidney and intestine (Zhang and Cashman, 2006), as well as mouse brain and kidney (Janmohamed et al., 2004).

FMO3 is thought to be the most important isoform in the human liver and is highly polymorphic. Mutations result in a dysfunctional enzyme which can reduce the enzyme's ability to *N*-oxygenate trimethylamine (TMA) (Dolphin et al., 1997). Un-metabolised, TMA is highly odorous and people who have a defective FMO3 are said to suffer from 'fish-odour syndrome' or trimethylaminuria. FMO3 is highly expressed in human liver and at low levels in human kidney and lung (Zhang and Cashman, 2006). FMO3 is also highly expressed in female mouse liver (Falls et al., 1995), and mRNA is seen at low levels in mouse kidney, lung and brain (Janmohamed et al., 2004).

FMO4 protein has not been observed, but low mRNA levels in mouse kidney, brain, liver and lung have been found (Janmohamed et al., 2004). In humans FMO4 mRNA is expressed at its highest levels in liver and kidney and to a lesser extent in foetal liver (Zhang and Cashman, 2006).

FMO5 is expressed in the liver of humans (Overby et al., 1995), rabbits (Atta-Asafo-Adjei et al., 1993), guinea pigs (Overby et al., 1995) and mice (Cherrington et al., 1998). The mRNA level in the liver is higher than any other FMO in humans (Zhang and Cashman, 2006) and mice (Janmohamed et al., 2004). But due to the lack of a suitable probe substrate, the contribution of FMO5 to xenobiotic metabolism is unclear. FMO5 levels are also high in mouse kidney, lung and brain (Janmohamed et al., 2004). In human foetal liver FMO5 mRNA levels are highest amongst the FMO isoforms. FMO5 mRNA is also seen at lower levels in human kidney, small intestine, lung and brain (Zhang and Cashman, 2006).

1.6.1 FMO catalytic cycle

The binding of NADPH and oxygen (a-d) to form the hydroperoxyflavin, this step happens relatively fast. FAD-OOH oxygenates the substrate (e). NADP and water are released and are the rate-limiting steps (f and g). Step h shows the possible mode of release of reactive oxygen species (ROS). Taken from (Schlaich, 2007).

1.7 FMO developmental expression

The developmental expression in humans describes FMO1 as the dominant foetal liver isoform (Dolphin et al., 1991). FMO1 is highly expressed in the human embryonic liver, and is down-regulated shortly after birth (Hines and McCarver, 2002). FMO3 is expressed at very low levels in human embryonic liver, but is up-regulated and detected in most individuals between 1-2 years of age, although its expression is highly variable (Koukouritaki et al., 2002). In mice FMO1 is found in the placenta between 12 and 18 days of pregnancy (Ishida et al., 2007). Also in mice both *Fmo1* and *Fmo5* are expressed at high levels in the newborn liver, with expression reaching a peak at 5 weeks, then declining with age (Janmohamed et al., 2004). FMO1 protein and mRNA is found at day 25 of gestation in the rabbit, but approximates to 10% of the adult amount. This rises rapidly after birth, where at 3 weeks it is 70-80% of the adult concentration (Larsen-Su et al., 2002). FMO2 which is highly expressed in the lung, increases during mid-late gestation in rabbits, a pattern that mirrors the increased levels of circulating progesterone. At parturition (where there are also higher levels of progesterone) FMO2 is increased in the kidney. The sub-cutaneous application of progesterone or dexamethasone also increases the FMO2 protein level in the lung as well as in the kidney (Lee et al., 1995). The same researchers found that FMO1 was induced over the period of mid-late gestation in rabbit liver. FMO1 mRNA levels were increased four-fold in response to progesterone or glucocorticoids. This study confirmed the findings of other experimenters (Devereux and Fouts, 1975).

In humans the switch over from FMO1 in the foetal liver to FMO3 in adult liver clearly has parallels in the switch over from CYP3A7 to CYP3A4, the major human liver P450 isoform.

1.8 Sex differences and hormonal effects on FMO expression

There are distinct sex-related differences in FMO expression in rodents, which are not seen in humans. What complicates the issue is that the hormonal control of FMO also displays species differences.

In the mouse FMO1 is the predominant form in male liver, in the female liver it is FMO3. This is because of the repressive effects of testosterone on FMO3 in the mouse. Treatment of castrated male mice with flutamide, an anti-androgen, increased FMO3 in the liver to female levels (Kloss et al., 1982). In the males, castration increased FMO3 as well as FMO1, whilst the re-introduction of testosterone only repressed FMO3 (Falls et al., 1997). FMO1 increased upon the treatment of intact males with 17β-estradiol, a slight increase in FMO3 was also observed (Falls et al., 1997). In ovariectomised females, the treatment with testosterone reduced hepatic FMO (FMO3) to male levels. Ovariectomy alone in females slightly reduced hepatic FMO activity, pointing to an inductive effect by female sex hormones. However, the subsequent addition of 17β-estradiol or progesterone resulted in no discernable effect on FMO levels (Falls et al., 1997). Gonadectomy in male and female mice had no effect on the expression of FMO5, implying a sex-independent expression profile (Falls et al., 1997).

In adult mouse liver FMO5 mRNA is the most highly expressed, in both males and females. FMO3 is second, but only in the female, followed by FMO1, which is expressed 5 times less than FMO5 (Janmohamed et al., 2004). In the kidney FMO1 mRNA is twice the level in males as in females and FMO5 is expressed six times more abundantly in the male than female kidney (Janmohamed et al., 2004). FMO3 levels in mouse kidney are barely detectable in both males and females. The relative amount of FMO3 protein in mouse kidney is low, and similar in males and females (Ripp et al., 1999).

In male rat liver FMO3 increases with age, so that FMO3 is the predominant form in the adult (compared to adult male mouse which is FMO1). FMO1 remains at a constant level with age. In young female rat liver it is FMO1 which is most highly expressed, but is un-detectable after 10 weeks of age, so that FMO3 becomes predominant in the adult, as its expression remains relatively unchanged (Lattard et al., 2002). The total activity of FMOs was seen to increase in male rat livers from 1 to 3 months of age, while FMO1-dependent activity remained the same over this time (Das and Ziegler, 1970). Studies using gonadectomy and hormone replacement point to positive regulation of FMO3 in male rat liver by testosterone, whilst in female rat liver there is a negative effect upon FMO1 by 17β-estradiol (Dannan et al., 1986). In primary

male rat hepatocytes the activity of FMO1 is repressed 56% after the treatment of the cells with 17β-estradiol for two weeks. Male sex hormones have no effect upon activity (Coecke et al., 1998). In the male rat kidney the expression profile is similar to that in the liver, where FMO1 remains at the same expression level with age whereas FMO3 expression increases after 6 weeks of age. A similar pattern is seen in female rat kidney to that in male kidney, which differs to that in female rat liver. FMO1 was repressed in female liver, but remains consistent in female kidney (Lattard et al., 2002).

In late gestation rabbit lung FMO (FMO2) is induced, but rabbit liver FMO (FMO1) is not (Devereux and Fouts, 1975; Williams et al., 1985). This induction of FMO2 coincides with increased plasma progesterone and cortisol levels. The sub-cutaneous treatment of rabbits with progesterone leads to an up-regulation of FMO2 in the lung (Lee et al., 1995).

To summarise, in mice testosterone is a negative regulator of FMO3 in the liver, whereas in rats it is a positive regulator of hepatic FMO3. Estradiol is a negative regulator of FMO1 in female rat liver but in female rat kidney FMO1 is not repressed. FMO2 appears to be under some regulation by progesterone in rabbit lung. In humans sex-dependent differences in FMO expression are not observed. Subsequently the FMO profile across sex, species, age and tissue is perplexing.

1.9 The effects of growth hormone on FMO expression

It is thought that the secretion of sex hormones is under the control of the hypothalamic pituitary axis. Growth hormone has ultimate control over sex-differences in P450 expression. Hence the expectation would be that FMOs, given the degree of hormonal regulation they are under, would be receptive to changes in growth hormone levels. As it is there is little demonstration of this.

In cultured rat hepatocytes growth hormone had no effect on the levels of FMO1 (Coecke et al., 1998). In the Mini:Nts mouse, a transgenic mouse showing lower circulating levels of growth hormone, FMO1 expression in the liver was changed little from that of a WT mouse (Tani et al., 1999).

HNF1α and HNF4α enhanced *FMO1* promoter activity (Luo and Hines, 2001). In the embryonic liver of the HNF4α null mouse, the expression of both *Fmo1* and *Fmo5* are completely repressed (Battle et al., 2006). The upstream-stimulatory factor and Sp1 have been shown able to bind to the promoter of human growth hormone (Lemaigre et al., 1989). C/EBPα has also been shown to be under direct control of growth hormone (Rastegar et al., 2000), and C/EBPα in turn regulates *Hnf3β* which controls *Hnf4* (Samadani et al., 1995).

1.10 FMOs in diabetes

The increased activity of FMOs in drug-induced diabetes was first described in 1987 when the *N*-oxidation of imipramine (an FMO1 substrate) was increased in streptozotocin-induced mouse liver (Rouer et al., 1988). Following this thiobenzamide metabolism was observed to be two-fold higher in streptozotocin-induced rats and mice (Rouer et al., 1988) and a two-fold increase in activity specifically of FMO1 was described in streptozotocin-induced rats (Wang et al., 2000). In liver biopsies of type II diabetics, *FMO5* is repressed with the implication of its involvement in stress-response (Takamura et al., 2004).

Obviously any changes in the level of metabolising enzymes is important in many pathologies as patients respond differently to therapies, with the possibility of adverse drug reactions. Hence this change in FMO level could be important in drug therapy in diabetics.

A more recent study showed that FMO activity was again induced 2-fold in streptozotocin-induced rats, but also that FMO activity became equivalent of the control on addition of insulin (Borbas et al., 2006), insulin alone had no effect. The activity of FMO correlated closely with glucose levels and the level of cytochrome b5. Cytochrome b5 has long been associated as an electron transfer component in oxidative reactions in the metabolism of fats, steroids and xenobiotics (Schenkman and Jansson, 2003).

1.11 FMOs role in iron homeostasis

Iron salts in the diet are absorbed and bound to intraluminal mucin in the duodenum. To cross the cell membrane, the iron is released from mucin and associated with integrins on the luminal surface of the cell membrane (Conrad and Umbreit, 1993). The iron is then transferred to mobilferrin and also a larger complex called parraferritin (Conrad et al., 1990). This large 520 kDa iron-binding protein is made up of mobilferrin, integrin and FMO (Umbreit et al., 1996). Mobilferrin and calreticulin are highly homologous (Conrad, 1993) and FMO was found bound to calreticulin in rabbit lung (Guan et al., 1991; Rojiani et al., 1991). The parraferitin complex has ferrireductase activity, reducing Fe (III) to Fe (II) using NADPH. The FMO portion of parraferritin is implicated in an ability to act as the ferrireductase, since the complex was also able to metabolise methimazole, a classic FMO substrate (Umbreit et al., 1996).

In two patients with sideroblastic anaemia there was a marked reduction in ferriductase activity along with a reduction in FMO protein in lymphocyte extracts and an increase in mobilferrin. This could imply that a disruption in FMO and mobilferrin concentrations could cause sideroblastic anaemia (Barber et al., 2000).

Haemochromatosis is a disorder where the duodenum hyperabsorbs iron. In mice with transgenic haemochromatosis, surprisingly haem-oxygenase was lowered, whereas CYP oxidoreductase was induced. *Fmo3* was up-regulated in the liver, but in haemochromatosis mice and WT mice treated with iron-dextran, *Fmo3* was down-regulated (Muckenthaler et al., 2003).

1.12 Instances of FMO induction

Cytochrome P450s are classically thought of as inducible, i.e. P450 gene transcription is increased in response to environmental or toxic insult. FMOs do not appear to be modulated environmentally; hence FMOs are described as refractory to dietary or chemical induction.

Although FMOs are not thought inducible by xenobiotics there is limited evidence of this. In rat liver, *FMO1* was induced over three-fold upon the addition of the

polycyclic aromatic hydrocarbon 3-methylcholanthrene, an aryl hydrocarbon receptor (AhR) ligand. The level of thiobenzamide *S*-oxidation (an FMO1 catalysed reaction) was also seen to increase (Chung et al., 1997).

In another AhR-mediated example, a microarray studying the gene expression changes in AhR (+/+) versus AhR (-/-) male mouse liver, found that on addition of the AhR ligand, TCDD, *Fmo2* and *Fmo3* were induced 4-fold and over 6-fold respectively (Tijet et al., 2006).

Hyperforin is the active component of St John's Wort, a dietary supplement used for the alleviation of depression (Muller et al., 1998). Hyperforin is a potent pregnane-x-receptor (PXR) ligand and therefore its use has implication in drug-diet interactions (Moore et al., 2000; Wentworth et al., 2000). In a microarray where HepG2 cells were dosed for 24 hours with 1 μM hyperforin, *FMO5* was induced about 3-fold, this observation was confirmed with RT-PCR (Krusekopf and Roots, 2005).

In a microarray using RNA from primary human hepatocytes dosed with 33 μM rifampicin (a PXR ligand) for 3 days, both *FMO4* and *FMO5* were induced over 3-fold (Rae et al., 2001), along with other metabolising enzymes such as *CYP2A6, CYP2B5, CYP2C9* and non metabolising enzymes such as UDP glycosyltransferase 1A, monoamine oxidase B, and glutathione-*S*-transferase P1. *CYP3A4* had the greatest fold induction, over 55 times.

FMO2 in rabbit lung and liver were induced by dexamethasone and progesterone correlating with increased plasma steroid levels during pregnancy (Lee et al., 1993). FMO1 mRNA was increased four-fold upon treatment with dexamethasone in rabbit liver (Lee et al., 1995).

1.13 FMOs and dietary components

Guinea pigs fed an ascorbic acid-deficient diet had 61% hepatic FMO activity of the controls, whilst guinea-pigs on ascorbic acid-deficient and reduced diet had 17% of the activity of a guinea-pig on a normal diet (Brodfuehrer and Zannoni, 1987). One of the first papers indicating that FMOs could be influenced by diet found that rats fed on total parental nutrition for 7 days had a 75-80% decrease in FMO activity (Kaderlik, 1991). In

rats fed a semi-synthetic diet, there was a smaller decrease in FMO activity, which was induced on addition of rat chow extract. Ziegler surmised that FMO is already maximally induced on a normal chow diet by the components of plants (Cashman et al., 1995). Kaderlik found in un-published observations that rat chow contains 290 nmoles/gram of FMO substrates.

Dietary indole-3-carbinol, a naturally occurring component of cruciferous vegetables, when dosed to male rats results in an 8-fold reduction of FMO1 in liver and almost total inhibition of FMO1 expression in the small intestine (Larsen-Su and Williams, 1996).

In plants there are 26 FMOs, and like plant P450s they have evolved to be highly-substrate specific and are involved in the synthesis of biologically active secondary metabolites. Whereas in animals, both FMOs and P450s are less specific and have a much wider substrate specificity in xenobiotic metabolism (Donaldson and Luster, 1991). One of the substrates that plant FMOs biosynthesise are glucosinolates (Hansen et al., 2007). The glucosinolates give cruciferous vegetables (eg broccoli) their distinctive flavour by the release of isothiocyanates (Halkier and Gershenzon, 2006).

Isomers of conjugated linoleic acid are found naturally in dairy products and ruminant meats. Synthetic isomers of conjugated linoleic acid are currently being touted as fat loss and insulin-sensitivity improvement pills, of which there is some evidence (Gaullier et al., 2007; Syvertsen et al., 2007). Female mice fed dietary trans 10, cis 12-conjugated linoleic acid develop fatty livers and show reduced expression of fatty acid oxidation genes such as carnitine palmitoyl transferase Ia (77%), acetyl CoA oxidase (50%) and PPARα (65 %). *Fmo3* was grouped in with these genes, and was reduced 97%, although there is no evidence for FMO3 being a fatty acid oxidation gene. The mouse liver microsomal activity of FMO was also reduced (40%) as was overall P450 activity (67%). The treatment with cis 9, trans 11-conjugated linoleic acid also decreased *Fmo3* and *P450* expression 61% and 38% respectively (Rasooly et al., 2007).

1.14 FMO, endogenous substrates and redox state

Trimethylaminuria, often referred to as 'fish-odour syndrome', is caused by a missense mutation in FMO3 (Dolphin et al., 1997). Trimethylamine is an endogenous compound which is also present in the diet. It is predominantly found in fish as the trimethylamine-*N*-oxide which is reduced by gut bacteria to the amine. Endogenous trimethylamine is formed from the break-down of choline by gut bacteria (Lowis et al., 1985) and is metabolised to the *N*-oxide, predominantly by FMO3 (Lang et al., 1998). Trimethylamine is extremely odorous whereas the *N*-oxide has little or no odour. This is the best-characterised 'endogenous' substrate for an FMO isoform. There are also a handful of other endogenous substrates.

It has been suggested that methionine is the most toxic amino acid (Benevenga, 1974) and it is metabolised to an *S*-oxide by FMO1, 2 and 3 in rabbit liver and kidney microsomes (Duescher et al., 1994) in rat liver and kidney microsomes (Krause et al., 1996) and human liver microsomes (Ripp et al., 1999). Whether the metabolism by FMOs to methionine sulfoxide represents a detoxification reaction is unknown given that the toxicity of methionine sulfoxide is also unknown. However given that methionine sulfoxide is probably more water soluble than methionine itself it may be more readily excreted. However the K_M for methionine is quite high, rabbit cDNA-expressed FMO1, 2 and 3 gave a K_M of 48, 30, and 6.5 mM, respectively (Duescher et al., 1994). Whereas the human liver microsomal K_M ranged from 0.03 to 5 mM (Ripp et al., 1999). The free plasma methionine concentration in healthy humans has been shown to be approximately 23 μM (Potgieter et al., 1997) so it is unlikely that the ability of FMOs to metabolise methionine is physiologically relevant.

Cysteamine is *S*-oxygenated by FMOs to cystamine. This may be a detoxification mechanism, since cysteamine at concentrations as low as 39 μM, is toxic to cells possibly by the production of hydrogen peroxide (Jeitner and Lawrence, 2001). Cysteamine is transported into cells as a mixed disulfide with cysteine, which is needed to maintain high cellular glutathione levels. Thus in an indirect way FMO may control hydrogen peroxide levels within the cell as well as genes regulated by H_2O_2 because cysteamine increases

hypoxia induced factor-1 (HIF-1) expression, which in turn increases redox-sensitive transcription factors and thus the general redox state (Khomenko et al., 2004).

Lipoic acid is a vital cofactor for α-ketoglutarate and pyruvate dehydrogenases. It is also taken as a supplement because of its antioxidant properties (Bustamante et al., 1998) and as a therapeutic agent (Smith et al., 2004b). FMO1 metabolises lipoic acid and lipoamide through *S*-oxygenation with a K_M of 2μM (Taylor and Ziegler, 1987).

It is interesting that the two previous examples of endogenous substrate have some sort of relationship with reactive oxygen species (ROS) or anti-oxidant ability. Since FMO is present at such high concentrations in the endoplasmic reticulum (up to 10% of total protein in rabbit lung (Williams et al., 1985), it seems that the production of ROS as a side-effect of the FMO catalytic cycle could be important. Hydrogen peroxide production by purified rabbit lung FMO (FMO2) was 41% of the total NADPH oxidised (Tynes et al., 1986). Superoxide anion radical production has been measured in purified pig liver FMO (FMO1) the level being about 4% of the total NADPH oxidised (Rauckman et al., 1979). The impact of this ROS production by FMO has never been elucidated. Of course the previous experiments were all done *in vitro*, so the measurements obtained may bear no resemblance at all to the *in vivo* situation. Interestingly in a microarray of ob/ob mice, *Fmo5* was reduced 1.4 fold and was grouped in with redox-sensitive genes (Liang and Tall, 2001).

1.15 FMO5 and its limited substrate portfolio

With regard to transcription, FMO5 mRNA has recently been shown to be expressed in the human liver to a higher extent than FMO3 mRNA, FMO3 is the enzyme predominantly involved in human hepatic xenobiotic metabolism (Zhang and Cashman, 2006). Equivalent levels of FMO3 mRNA to FMO5 mRNA have also been seen in the female mouse liver (Janmohamed et al., 2004). What is unclear is FMO5's contribution to xenobiotic metabolism. This is due to a lack of suitable substrate with which to measure FMO5 activity. FMO5 shows little or no activity towards classic FMO substrates such as trimethylamine (FMO3), imipramine (FMO1) and methimazole (FMO1 and FMO3). The known substrates of FMO5 are shown in Figure 1.15.1. A

recent paper has delved more deeply into the mouse FMO5 metabolising capabilities (Zhang et al., 2007). FMO5 metabolised phenothiazine analogs 5-DPT and 8-DPT, which are tertiary amines (as were FMO1 and FMO3). The catalytic activity of FMO5 for 8-DPT was nearly 50 times and 6 times lower than FMO1 and FMO3 respectively. *S*-methyl-esonarimod was also a substrate for mouse FMO5 which has been described previously for human FMO5 (Ohmi et al., 2003). Mouse FMO1 was also a substrate for *S*-methyl-esonarimod with a similar K_M to that of FMO5 (3.82 and 3.23 μM respectively).

FMO5 has been reported to metabolise methimazole with a very low efficiency (Overby et al., 1995), as well as to catalyse benzydamine *N*-oxidation with a K_M of 2 mM (Lang and Rettie, 2000). *N*-oxidation of *N*-octylamine has also been shown and is able to reach an activity of 26 nMol of NADPH oxidised min^{-1} nMol FMO^{-1} by human recombinant FMO5 (Overby et al., 1995). Ranitidine is also a substrate of human recombinant FMO5 (as are FMO1 and FMO3) but is not an efficient producer of the *N*- and *S*-oxides (Chung et al., 2000).

Substrates

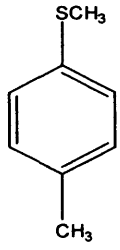

methyl-p-tolyl sulphide

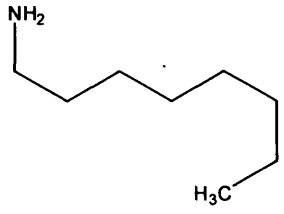

n-octylamine

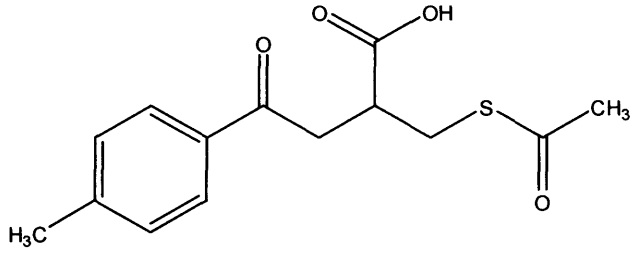

s-methy-esonarimod

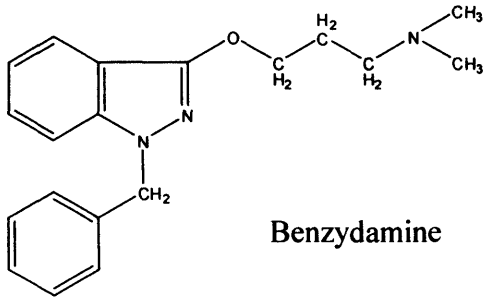

Benzydamine

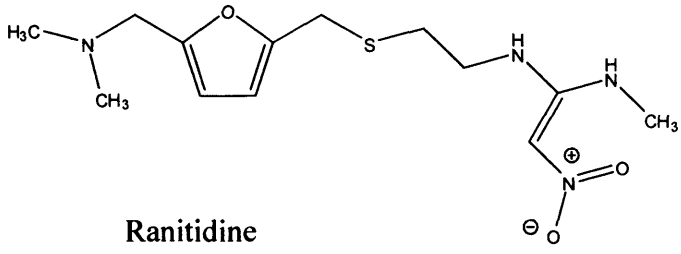

Ranitidine

Inducers

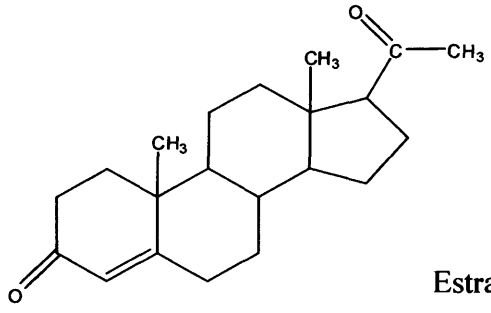

Estradiol

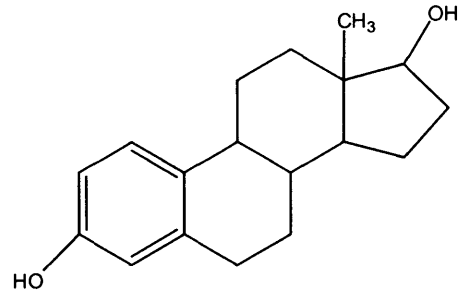

Progesterone

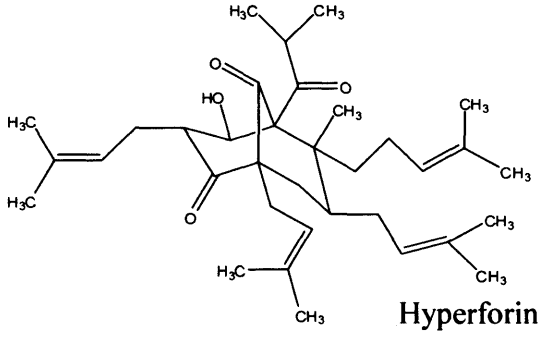

Hyperforin

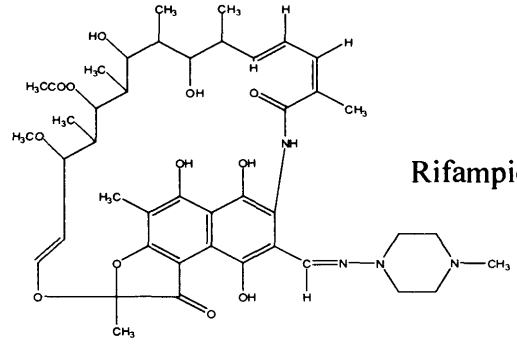

Rifampicin

1.15.1 Substrates and inducers of FMO5

1.16 FMO5 regulation by hormones

FMO5 is often thought of as gender-independent, but there is evidence of hormonal regulation of FMO5 in the literature. Apart from the example mentioned previously where FMO5 mRNA is expressed to a much higher degree in male rather than female mouse kidney (Janmohamed et al., 2004), there are several other examples of hormonal regulation.

A breast cancer cell line stably expressing progesterone A or B receptors was dosed for 18 hours with 20 nM progestin. FMO5 was induced 9-10 fold only in progesterone B receptor cells (Miller et al., 1997). Both forms of the receptor mediate the effects of progesterone, but the B receptor to a higher degree.

In human breast cancer tissue using RT-PCR, FMO5 was induced in estrogen receptor-α (ERα) positive cancers (Bieche et al., 2004). Breast cancer growth is regulated by estrogen, mediated through the ERα receptor. Patients that have ERα in their breast tumours may respond to anti-endocrine drugs such as tamoxifen. Interestingly patients who had FMO5-overexpressing tumours had a longer relapse-free survival, although this didn't retain significance when a more rigorous statistical regression analysis was used.

1.17 Orphan Nuclear Receptors

Orphan nuclear receptors are ligand-activated transcription factors. Their ligands are small and lipophillic, describing a large proportion of xenobiotics. Several orphan nuclear receptors mediate the induction and repression of P450 enzymes.

In the absence of a substrate, P450s are expressed at quite a low level basally but their expression is increased in the presence of their substrate or other inducers. The members of the CYP1A, CYP2B, CYP2C, CYP3A and CYP4A gene subfamilies are highly inducible. Initially, phenobarbital (PB) was seen to increase total P450 concentration in rats (Conney et al., 1960). This was later attributed to the transcriptional induction of P450 genes by PB (Adesnik et al., 1981). Other inducers (PB-like inducers) were found able to up-regulate transcription of CYP2A, CYP2B, CYP2C and CYP3A genes (Waxman and Azaroff, 1992) this is now attributed to the nuclear receptors who

mediate enzyme induction. Drugs do not only induce drug-metabolising enzymes or transporters, there is a pleiotrophic response, including the up- and down-regulation of many genes and systems (Okey, 1990; Waxman and Azaroff, 1992).

Cytochrome P450 induction in response to xenobiotics is mediated by four main transcription factors: the aryl hydrocarbon receptor (AhR), the constitutive androstane receptor (CAR), the pregnane-x-receptor (PXR) and the peroxisome proliferator-activated receptor (PPAR). The most important of these four is the PXR, which is described in detail below; PPAR, CAR and AhR are discussed briefly.

1.18 AhR, CAR and PPAR

Polycyclic and halogenated aromatic hydrocarbons, as well as various organochlorinated compounds, are able to cause immunosuppression, tumorogenesis and cardiovascular disease in humans. These effects are thought to be mediated via the AhR. The AhR is a basic ligand-dependant helix-loop-helix transcription factor. Ligand activation results in the cytosolic AhR relocating to the nucleus to dimerise with AhR nuclear translocator (AhRNT). Together they are able to transcriptionally activate the genes *CYP1A1, CYP1A2, CYP2B1* as well as the phase II enzymes glutathione *S*-transferase (*GST*) and UDP-glucuronyl transferase (*UDPGT*).

CAR is the 'constitutive' receptor because it is able to transactivate response elements in the absence of ligand (Baes et al., 1994). CAR forms a heterodimer with the retinoid X receptor (RXR) (RXR is also able to form a heterodimer with PXR and PPAR). CAR predominantly mediates the activation of CYP2B genes. CAR is able to mediate the expression of CYP2B1 and CYP3A1 in rat primary hepatocytes and *in vivo* in the liver (Smirlis et al., 2001). It is also able to transactivate the PXR-responsive response elements in CYP3A4 (Goodwin et al., 2002). Phenobarbital is a well-known inducer of drug metabolism in mammals including man. The phenobarbital responsive element module (PBREM) was found upstream of the rat CYP2B. Only CAR was able to activate the PBREM-dependant reporter gene (Honkakoski et al., 1998).

The PPAR also forms a heterodimer with RXR. Its ligands include clofibrate the cholesterol-reducing drug and other peroxisome proliferators. So-called because they

were observed to cause peroxisome proliferation in rodents, although not in humans. PPAR is thought to be involved in the regulation of CYP4A genes.

1.19 Pregnane X Receptor (PXR)

The *PXR* gene is expressed mainly in the liver and intestine, it plays a key role in the induction and constitutive expression of CYP3A isoforms. PXR forms a heterodimer with the retinoid X receptor (RXR) and binds the consensus motif AG(G/T)TC(A/C) in the promoters of many genes including human and rodent CYP3A genes, thus mediating *CYP3A* expression (Lehmann et al., 1998). It is also clear that PXR is able to mediate the expression of *CYP2B* genes (Goodwin et al., 2001).

Whilst pregnenolone 16α-carbonitrile is a known inducer of CYP3A in rats and mice, and activates rat and mouse PXR, rifampicin induces CYP3A and activates PXR in humans and rabbits. PXR sequence homology appears to explain the species differences regarding CYP3A induction. The DNA binding domain shares 95% homology, the ligand-binding domain shares approximately 75-80% homology between species (Jones et al., 2000). Figure 1.19.1b shows the species specificity of PXR ligands for mouse or human PXR. It has been shown that PXR is able to bind to response elements such as DR4 (direct-repeat 4, a copy of the consensus motif is repeated twice separated by 4 unspecified nucleotides) within the phenobarbital response element of the *CYP2B1* promoter as well as the DR3 site in the PXRE of *CYP3A1* (Smirlis et al., 2001). PXR is also able to mediate *CYP2B6* expression in humans (Goodwin et al., 2001) as well as that of *CYP2C8* and *CYP2C9* (Gerbal-Chaloin et al., 2002).

PXR may have a role in modulating drug metabolising enzymes in foetal liver, and requires HNF4α to do so. An HNF4α response element was found in PXR, and this was required to activate the *PXR* promoter in primary mouse foetal hepatocytes (Kamiya et al., 2003). HNF4α was also shown to have an important role in the PXR and CAR-mediated induction of *CYP3A4*. In *Hnf4α*-null mice, *CYP3A4* expression was decreased and had a reduced capacity to be induced by rifampicin (Tirona et al., 2003).

(a)

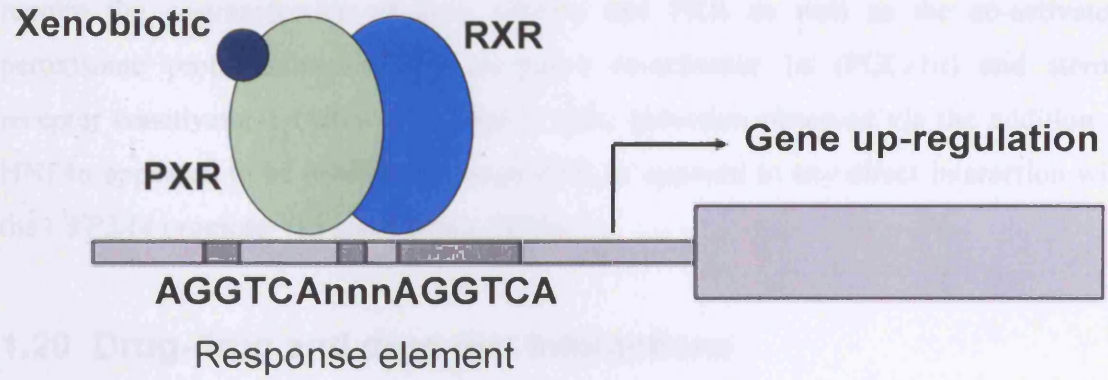

(b)

1.19.1 Nuclear receptor mode of action and PXR ligands

Part (a) shows the nuclear receptor mode of action, where PXR binds a substrate and undergoes a structural change allowing it to bind to RXR its heterodimer. Together they bind to response elements in the promoter of target genes and up-regulate transcription. Part (b) is a representation of the species specificity of PXR ligands and the substrates which are more likely to bind mouse PXR or human PXR (Kliewer et al., 1998).

More recently the maximal induction of *CYP3A4* by rifampicin was shown to require the co-transfection of both HNF4α and PXR as well as the co-activators peroxisome proliferators-activated receptor-γ co-activator 1α (PGC-1α) and steroid receptor coactivator-1 (SRC-1) in HepG2 cells. Induction observed via the addition of HNF4α appeared to be mediated through PXR as opposed to any direct interaction with the *CYP3A4* promoter (Li and Chiang, 2006).

1.20 Drug-drug and drug-diet interactions

Drug-drug interactions represent approximately 3-5% of adverse drug reactions (Leape, 1995). One drug affects the toxicity or efficacy of another. Co-administration of 2 or more drugs could mean that the combination causes an increase in efficacy of one, possibly to toxic levels. Conversely, the combination can nullify the effect of the drugs, resulting in a lack of efficacy, which can also be detrimental to a patient. As more drugs are developed and multiple drug therapies are more often used, side-effects and drug-drug interactions are bound to increase.

Drug interactions generally occur through the modulation of metabolising enzymes via induction or inhibition. Inhibition decreases metabolism of drugs and can be competitive, non-competitive or uncompetitive. Induction leads to an increase in the amount of P450 expressed, enhancing the rate of metabolism. Understanding more about the underlying causes of drug interactions may reduce the number of adverse drug reactions and result in improved therapeutic regimes.

The number of food-drug interactions is incalculable. An interesting subset of food-drug interactions on which to focus would be herbal products/complementary medicines and their associated drug interactions. The use of complementary medicines has increased a great deal over the last 20 years. Their use and production is largely unregulated, and they are promoted as 'natural' and therefore harmless. The public do not view herbals as 'drugs', although they are not exempt from interactions, since they are metabolised in the same way as prescription drugs. Problems tend to arise when a patients' use of an herbal product is not made known to their GP when going for treatment, and a severe adverse drug reaction could be the consequence.

The Dietary Supplement Health and Education Act (DSHEA) (Dietary Supplement Health and Education Act (DSHEA). 42 USC 287C–11. 1994) defines a dietary supplement as "a product (other than tobacco) that is intended to supplement the diet and that bears or contains one or more of the following dietary ingredients: a vitamin, a mineral, a herb or other botanical, an amino acid, a dietary substance for use by man to supplement the diet by increasing the total daily intake, or a concentrate, metabolite, constituent, extract or combinations of these ingredients."

Herbal products and dietary supplements are very popular. It is estimated that 20% of Americans regularly take dietary supplements, yet only a third of those inform their doctor (Kennedy, 2005). An FDA testimony puts the consumption level much higher. In the year 2000, dietary supplements, including vitamins, were consumed by 158 million Americans which is more than half the US population (US Food and Drug Administration. Statement by Joseph A. Levitt before the U.S. House of Representatives).

1.21 Liquorice

Liquorice has been used for thousands of years to treat ailments ranging from coughs and sore throats to hepatitis and stomach ulcers. Recently studies indicate that glycyrrhetinic acid (GTA) can be used to reduce the thickness of subcutaneous thigh fat (Armanini et al., 2005) and can delay the development of autoimmune disease (Horigome et al., 2001).

The main ingredient, glycyrrhizin is hydrolised to the active principal GTA by intestinal flora and absorbed by the gut. A hemi-succinate derivative carbenoxolone was synthesised and used widely in the 1950s as a treatment for stomach ulcers. A large proportion of the patients suffered from hypertension and hypokalemia, and it was thought that this was merely an 'allergic reaction' which resolved itself once the dose was reduced. It is now known that GTA is a non-specific 11β-hydroxysteroid dehydrogenase (11β-HSD) inhibitor. There are two isoforms of 11β-HSD, type 1 and type 2. Type 2 is highly expressed in the renal cortex and salivary glands and has dehydrogenase activity. It catalyses the conversion of active cortisol to inactive cortisone, protecting the mineralacorticoid receptor from cortisol and enabling it to bind aldosterone. 11β-HSD1 is mainly expressed in the liver and adipose tissue. It is a reductase and catalyses the

conversion of cortisone to cortisol. Cortisol has a variety of tissue-specific effects which may contribute to the phenotype of simple obesity, type II diabetes and the metabolic syndrome. In the liver, cortisol induces gluconeogenesis, and in adipose tissue it increases adipocyte differentiation. It impairs insulin signalling and decreases insulin secretion. If cortisol production can be turned off, as in the inhibition of 11β-HSD1, it will preserve insulin sensitivity and decrease hepatic glucose output, whilst slowing increasing adiposity.

1.22 Objectives of this project

FMOs have long been compared to P450 enzymes, but much less is known about the former than the latter. Although many of the endogenous roles of P450 enzymes have been elucidated, it is as yet unclear what the endobiotic role of FMOs are.

With the use of *Fmo1, 2, 4* (-/-) and *Fmo5* (-/-) mice the project will investigate phenotypic differences in these KO mice. These studies should give a much better understanding of the endobiotic role of FMOs and possibly indicate differences in role between the individual FMO isoforms.

Although it is well known that several P450 enzymes are inducible by xenobiotics through various nuclear hormone receptors, this has never been demonstrated in FMOs. We hope to culture primary mouse hepatocytes and use these to study more closely the effects of xenobiotics on FMOs, through the use of reporter gene asssays, and thus discover whether nuclear receptors such as PXR have a role to play in any subsequent FMO induction.

Chapter 2

Materials and Methods

2 Materials and Methods

2.1.1 Chemicals and Reagents

All chemicals used, apart from those used in tissue or cell culture, were purchased from Sigma Co. unless otherwise stated and were of analytical grade. Restriction endonucleases were purchased from NBL Gene Sciences. Reagents used for cell or tissue culture were purchased from Gibco BRL (Invitrogen) and were of tissue culture grade. Details of companies can be found in the appendix.

2.1.2 Culture of bacteria

LB medium (per L: 10g bactotryptone, 5g yeast extract, 5 g NaCl) (BIO 101, Anachem) or LB agar medium (per L: 10g bactotryptone, 5g yeast extract, 5 g NaCl, 15g agar) (BIO 101, Anachem) were made by adding capsules to water (40 capsules/L) and autoclaving. Before use, ampicillin was added at a final concentration of 50 μg/mL. The LB agar medium was left to cool until 'hand hot' and poured into 82mm Petri dishes (30mL/plate). The plates were allowed to set at room temperature and stored at 4°C. Bacteria were streaked onto the plates and incubated at 37°C overnight. A single colony was used to inoculate 5 mL of LB-ampicillin media and incubated for 6-8 hours at 37°C with shaking (300 rpm). This 'starter culture' was used immediately for small-scale isolation of DNA (see below) or used to inoculate LB-ampicillin media (25 mL) which was incubated for 12-16 hours at 37°C with shaking (300rpm).

2.1.3 Small-scale isolation of plasmid DNA from bacteria

The QIAfilter Miniprep kit (Qiagen) was used for small-scale isolation of plasmid DNA. Buffers P1, P2, N3, PB, PE and EB are all contained within the kit.

1 mL of the 5 mL starter culture from above was spun (8,000 rpm, 3 minutes) and the supernatant removed. The resulting pellet was re-suspended in buffer P1 (50mM Tris-Cl (pH 8.0), 10mM EDTA, 100 μg/mL RNase A) and the cells lysed by buffer P2 (200mM NaOH, 1%SDS). Buffer N3 was added, the tube inverted 4-6 times and the

samples centrifuged (13,000 rpm, 10 minutes). The protein layer forms the pellet and the supernatant was applied to the QIAprep Spin column. This was centrifuged (13,000 rpm, 30 seconds) and the flow-through was discarded. The spin column was washed with 0.5 mL of buffer PB and again centrifuged (13,000 rpm, 30 seconds). The spin column was washed again with buffer PE and centrifuged (13,000 rpm, 30 seconds). The flow-through was discarded and the spin column centrifuged again to remove all trace of ethanol. To elute the DNA 50 µl of buffer EB (10mM Tris, pH 8.5) was added to the filter of the column and left to stand for 1 minute, then centrifuged (13,000 rpm, 30 seconds).

2.1.4 Medium-scale isolation of plasmid DNA from bacteria

The QIAfilter Midiprep kit (Qiagen) was used for the following procedure to isolate a larger amount of plasmid DNA. Buffers P1, P2, P3, QBT, QC and QF are all contained within the kit.

The 25 mL culture obtained above was centrifuged (Sorvall, S-3000 rotor) (6000rpm, 15 minutes). The resulting bacterial pellet was thoroughly re-suspended in 4 mL of buffer P1 (50 mM Tris-Cl (pH 8.0), 10 mM EDTA, 100 µg/mL RNase A) and the cells lysed in 4 mL buffer P2 (200mM NaOH, 1%SDS). The tube was inverted 4-6 times to mix the lysate and then incubated at room temperature for 5 minutes. 4 mL of chilled buffer P3 (3M potassium acetate, pH 8.0) was added to neutralise the lysate, and the tube was inverted 4-6 times to mix. A white precipitate forms and the lysate was immediately poured onto a filter cartridge (included in the kit) and incubated (10 minutes, room temperature). During this time a QIAtip (included in the kit) was equilibrated with 4 mL buffer QBT (750mM NaCl, 50mM MOPS (pH 7.0), 15% isopropanol, 0.15% Triton® X-100).

The protein layer from the lysate naturally rises to the top of the cartridge and the cleared lysate was filtered into the equilibrated QIAtip and allowed to filter through the column. The resin in the QIAtip selectively binds plasmid DNA. The column was washed twice with 10 mL buffer QC (1M NaCl, 50mM MOPS (pH 7.0), 15% isopropanol) which removes cellular metabolites and RNA.

Plasmid DNA was eluted from the column with 2 mL buffer QF (1.25M, 50mM Tris-Cl (pH 8.5), 15% isopropanol) into a 30 mL plastic tube (Starstedt). 3.5 mL of isopropanol was added to the eluant to precipitate the plasmid DNA. The mixture was centrifuged (Sorvall, SS-34 rotor) (11,000 rpm, 30 minutes, 4°C). After removing the supernatant, 2 mL of 70% ethanol was added to wash the DNA pellet. The tube was centrifuged again (14,000 rpm, 10 minutes). The supernatant was removed and the plasmid DNA pellet was allowed to air-dry then was re- suspended in an appropriate volume of TE buffer (10 mM Tris-HCl, 1 mM EDTA, pH 8.0).

2.1.5 Quantification of DNA by UV spectrophotometry

The concentration of DNA was quantified using the NanoDrop spectrophotometer (NanoDrop). 1 µl of water was applied to the platform and used to calibrate the NanoDrop, then 1 µl of TE buffer was used to 'blank' the sample. The TE droplet was removed from the platform and a DNA solution (1 µl) was applied. The sample absorbances were measured at 260nm. An optical density (OD) of 1 at 260nm is equivalent to 50 µg of DNA.

2.1.6 Agarose gel electrophoresis of DNA fragments

1 g of agarose was melted in 100 mL of 1 x TBE (10 x TBE: 0.89M Tris-base, 0.09M Boric acid, 20mM EDTA, pH 8.0) in a microwave until the agarose was completely dissolved. Once the liquid was 'hand-hot' 5 µl of ethidium bromide (stock of 10 mg/mL, Fisher) was added. The liquid agarose was poured into a gel mould with an appropriate comb. Once set, the gel was placed into an electrophoresis tank filled with 1 x TBE. A DNA size marker, 10 µl of Hyperladder I or IV (Bioline), was pipetted into the gel and electrophoresed with any DNA samples subsequently added to the gel.

DNA samples were mixed with 1 x loading buffer (6 x loading buffer: 0.25% bromophenol blue, 0.25% xylene cyanol, 30% (v/v) glycerol) and applied to the wells of the gel. The gel was run at 100 volts until sufficient separation of DNA fragments had occurred. After electrophoresis, the gel was photographed on a UV transilluminator.

2.1.7 Gel extraction

Gel fragments were excised with a sharp scalpel from an agarose gel (1% w/v) and put into a colourless Eppendorf tube. Three volumes of buffer QG were added to 1 volume of gel (e.g. 300 µl to 100 mg of gel) and the Eppendorf tube incubated (50°C, 10 minutes) with sporadic vortexing until the gel slice melted. The buffer containing the melted gel was applied to a QIAquick spin column and centrifuged (13,000 rpm, 1 minute). To remove all trace of agarose 0.5 mL of buffer QG was added to the column and centrifuged (13,000 rpm, 1 minute) and the flow-through discarded. To wash, 0.75 mL of buffer PE was applied to the column and centrifuged (13,000 rpm, 1 minute) again discarding the flow-through. To remove any residual ethanol, the column was spun again for 1 minute. 30 µl of buffer EB was applied to the column and left to incubate for one minute. Columns were put into clean Eppendorf tubes and the DNA was eluted by centrifugation (13,000 rpm, 1 minute).

2.1.8 Polymerase Chain Reaction (PCR)

All PCR reactions were carried out in a Genius PCR machine (Techne). Primer sequences can be found in the appendix. The BIO-X-ACT™ DNA polymerase from Bioline was used.

The PCR consisted of 10 ng of template DNA, 1 x OptiBuffer buffer (a non-Tris incubation buffer, Bioline) 0.2mM dNTP mix and 0.5 µM reverse and forward primers plus 0.5 units of the BIO-X-ACT™ DNA polymerase. The volume of the reaction was made up to 50 µl with sterile water. The negative control for each reaction was made in the same way but didn't include template DNA. Amplification parameters are shown in Figure 2.1.10.1. The annealing temperatures were 65°C since the calculated Tm of each primer was much higher than this. The amplified products were viewed by agarose gel electrophoresis.

2.1.9 TOPO®/TA cloning

The TOPO®/TA cloning kit (Invitrogen) was used. The single deoxyadenosine (A) 3' overhangs on the PCR product left by the BIO-X-ACT™ DNA polymerase are used to ligate to the linearised TOPO® vector which contains 3' deoxythymidines (T) at each end. Ligation is carried out by topoisomerases that are covalently bound to the vector.

In a 0.5 mL Eppendorf, 4 μL of a freshly prepared PCR product was gently mixed with 1 μl of salt solution (contained in kit) and 1 μL of TOPO® vector. This was incubated at room temperature for 5 minutes.

2.1.10 Bacterial transformation

Mach1-T1™ or DH5α™ (both Invitrogen) competent cells were thawed on ice. 50 μL of cells were mixed with 2 μL of a ligation reaction (see sections 2.1.9 and 2.1.12). The mixture was incubated on ice for 30 minutes, then incubated at 42°C for 30 seconds, and put back on ice. Provided with the competent cells was SOC medium (Formulation per 1L: 2% tryptone, 0.5% yeast extract, 10 mM sodium chloride, 2.5 mM potassium chloride, 10 mM magnesium chloride, 10 mM magnesium sulphate, 20 mM glucose) 250 μL was added to the bacteria. Cells were incubated with shaking (1 hour, 37°C, 300 rpm). 20 μL of the bacterial culture was plated onto an LB-ampicillin plate. Plates were incubated overnight (37°C).

(a)

Programme 1	1 cycle	
	95°C	5 mins
	65°C	30 secs
	68°C	1 min/Kb
Programme 2	30 cycles	
	95°C	5 mins
	65°C	30 secs
	68°C	1 min/Kb
Programme 3	1 cycle	
	68°C	5 mins

(b)

$$Tm = 69.3 + (0.41 \times (\%G+C)) - 650/\text{length in nucleotides}$$

$$\text{Annealing temperature} = \frac{Tm1 + Tm2}{2} - 6$$

2.1.10.1 PCR parameters

The PCR programme (a) is shown. The extension temperature for BIO-X-ACT™ was 68°C. The annealing temperature was 65°C. The Tm of each primer was calculated, and Tm values for both primers were used to calculate the annealing temperature (b).

2.1.11 Restriction endonuclease digestion of DNA

Restriction endonuclease digestions were carried out in 1.5 mL Eppendorf tubes. Plasmid DNA and reaction buffer (1x) were added to the tube. The volume was made up to 25 or 50 µl with sterile water, depending on the amount of DNA to be digested. Finally the restriction endonuclease enzyme (1 unit per µg of DNA) was added to the tube, and the reaction mixture was incubated at 37°C for at least 1 hour. When two different restriction endonucleases were required, both enzymes were added to the reaction containing a compatible reaction buffer.

2.1.12 Ligation

The fragments cloned using the TOPO™ kit were cut from the TOPO™ vector and ligated into the pGL3 Basic (Promega) vector. Ligation was carried out using the Quick-Stick ligase kit (Bioline). 9 µL of a promoter fragment was added to 1 µL of the digested pGL3 Basic vector to a maximum of 100 ng, and made up to 14 µL with sterile water. Quick-stick ligase (1 µL) plus QS buffer (5 µL) (contained in kit) was added to the DNA and mixed thoroughly. The reaction mixture was incubated for 5 minutes at room temperature. The ligated fragment is now ready for bacterial transformation.

2.1.13 Preparation of glycerol stocks

For long-term storage of bacterial cultures, 0.85 mL of culture (grown overnight, 37°C) was mixed with 0.15 mL of glycerol (100%, autoclaved) in a 1.5 mL Eppendorf tube, and immediately stored at -70°C.

2.2 Isolation and maintenance of primary mouse hepatocytes

2.2.1 Sterilisation of the perfusion apparatus

The perfusion apparatus was filled with 70% ethanol and left overnight. The morning on which hepatocyte isolation was planned, the apparatus was rinsed thoroughly three times with sterile water.

2.2.2 Matrigel coating of culture plates

All well-plates were coated with Matrigel™ Basement Membrane Matrix (BD Biosciences) the morning of hepatocyte isolation. The Matrigel™ was diluted 1:9 with Williams E media then a sufficient amount of this dilution was pipetted into each well (e.g. 200 µL in a well from a 12-well plate). This solution was spread evenly over the well with a cell scraper (Corning) and left to set (1 hour, 37C). Just before the hepatocytes were plated, any Matrigel™ that hadn't set was rinsed off with Williams E media.

2.2.3 Dissection

All dissection equipment was cleaned and autoclaved before use. Hepatocytes were isolated from male C57BL-6 mice at least 6 weeks old, who had access to food *ad libitum*.

Mice were anaesthetised by combining ketamine (5.7 mg/mL) and xylazine (2.6 mg/mL) and injecting 0.1 mL/20g body weight intraperitoneally. Once the mouse failed to respond to stimuli, the abdomen was swabbed with alcohol (70% v/v ethanol) and the mouse immobilised on the dissection mat. The abdomen of the mouse was opened through a U-shaped incision and the intestines swept to the left of the torso. Using a 'vein-lifter' a ligature (size 3 Mersilk, Ethicon) was loosely tied around the inferior vena cava (IVC) below the junction to the kidney. A small hole was cut in the IVC below the ligature and the cannula (24G gavage needle, Popper and Son) filled with heparin (50U/mL) was inserted. Air bubbles in the cannula would seriously impair perfusion. The

heparin reduces clotting in the liver that may also affect perfusion. It was important not to insert the cannula too far into the vessel as this could damage the liver. The ligature was tightened and knotted. A diagram of the vasculature of the liver is shown in Figure 2.2.4.1.

2.2.4 Two-step Perfusion of the Mouse Liver

Before dissection of the mouse, approximately 50 mL of Buffer 1 (Hanks Balanced Salt Solution (without $CaCl_2$ and $MgCl_2$), containing 50 mM EGTA, 125 g glucose) with the temperature maintained at 37°C, was circulated around the perfusion apparatus. This was done to remove bubbles in the system. Buffer 1 had 95% O_2 and 5% CO_2 bubbled through it for 15 minutes prior to the perfusion. After this time the pH was re-instated to pH 7.4 with the addition of HCl (1M, sterile). Arepresentation of the apparatus is shown in Figure 2.2.4.2.

The tubing from the perfusion apparatus was connected to the cannula that was inserted into the IVC of the mouse. Buffer 1 was then pumped through the liver at a rate of 2 mL/min. As soon as the perfusion apparatus was connected to the cannula, the portal vein was snipped and the perfusion flow rate increased to 7 mL/min. To prevent the buffer perfusing the heart and hence the rest of the body, the diaphragm was cut and the IVC clamped just below the heart. The liver should bleach of colour almost immediately and take on a light beige colour. The abdomen would be rinsed with distilled water to clear out the blood. Perfusion with Buffer 1 would take approximately 7 minutes. During this time collagenase H (0.8 U of collagense/ mL, Roche) was added to pre-warmed Buffer 2 (100 mL of Hanks Balanced Salt Solution (with $CaCl_2$) plus 1.74 mM $CaCl_2$, 0.72 % w/v BSA and 125 g glucose) and mixed well.

The buffer was changed from Buffer 1 to Buffer 2, and the perfusion was continued for approximately 8-10 minutes, or until the liver became soft and had a glassy appearance. Occasionally massaging the liver very gently between thumb and fore-finger aided the digestion of the liver by preventing clot formation. Once the liver was soft it was removed from the mouse taking care not to cut through the intestines, as this could result in contamination of the cells.

2.2.4.1 Blood supply and circulation in the human liver

The cannula is inserted at the lower end of the inferior vena cava (light grey arrow). From here the perfusion buffer flows into the liver and out of the hole cut in the portal vein (dark grey arrow). To prevent the buffer flowing throughout the body, a ligature is placed around the inferior vena cava below the heart (black line, top of diagram). Excerpt from Merck.com.

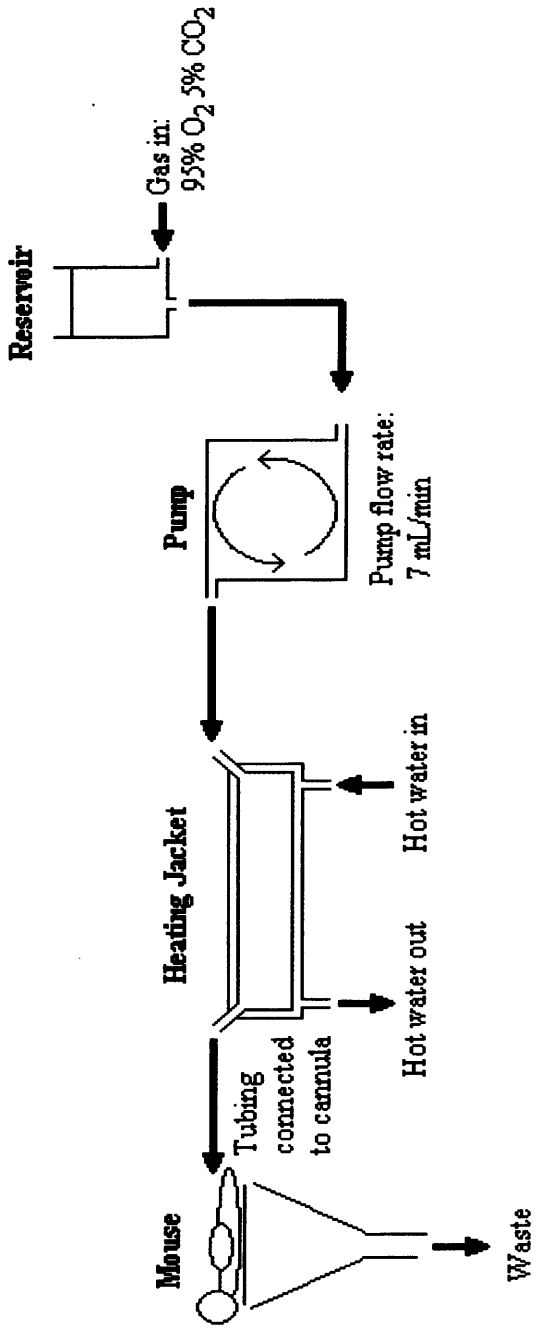

2.2.4.2 Representation of liver perfusion apparatus

Pre-warmed perfusion buffer 1 or 2 in the reservoir has gas (95% O_2, 5% CO_2) bubbled through it. It is pumped from the reservoir to the heating jacket at a flow rate of 7 mL/min, where its temperature is maintained at 37°C. From here it travels to the mouse liver through tubing connected to the cannula inserted in the mouse inferior vena cava.

2.2.5 *Purification of Mouse Hepatocytes*

The liver was transferred to ice-cold William's E (WE) media (containing 7% v/v FBS (fetal bovine serum), 10 mL/L insulin tranferrin selenium (10X), 30 mM pyruvate, 300 µg/mL gentamicin) and the cells dispersed by carefully scraping the Glissons capsule with 2 round-ended forceps. The digestion was successful if this was easily done. The cells were further dispersed through a large-bore pipette and filtered through a 70 µm nylon filter (Falcon). The remaining suspension was diluted to 20 mL with ice-cold WE (as above) and centrifuged (50 x g, 4°C, 2 minutes). The supernatant was poured away and the remaining pellet was re-suspended in 20 mL ice-cold WE (as above). Centrifugation and re-suspension was repeated twice. After the final centrifugation the pellet was re-suspended in 25 mL of WE (containing 7% FBS, 10 mL/L ITS, 30 mM pyruvate, 5nM dexamethasone, 300 µg/mL gentamicin) ready to be plated out. The suspension was kept on ice whilst the cells were counted and the viability determined using the Trypan Blue exclusion test (see below). 1 mL/well of the suspension was plated onto Matrigel™ coated 12-well culture plates (see section 2.2.2) at a density of 0.5 million cells per mL. The plates were incubated at 37°C, with 95% O_2 and 5% CO_2 for 2-3 hours depending on how well the cells had attached to the plate. After this time the media and dead cells were removed from the plates and replaced with fresh media typically omitting FBS so as not to interfere with further dosing experiments.

2.2.6 *Hepatocyte dosing regime*

After 2-3 hours incubation, the media was removed from the wells and replaced with fresh culturing media without FCS but containing the compound of interest. The plates were incubated at 37°C, with 95% O_2 and 5% CO_2 for 24 hours. Total protein lysates were isolated as described in Section 2.2.7. The isolation of total RNA was carried out as described in Section 2.3.3.

2.2.7 *Isolation of primary mouse hepatocyte lysates*

Cell lysates from primary mouse hepatocytes were isolated by scraping the cells from the plate using a cell scraper (TPP), and rinsing the plate with phosphate buffered saline (PBS, Gibco). This mixture of PBS and cells was transferred to clean Eppendorfs and centrifuged (12,000 x g, 15 minutes) to get a cell pellet. The remaining PBS was removed from the pellet and the pellet allowed to drain. It was reconstituted in 40 µL of 1 x TE, mixed well and then the cells lysed by sonication at the lowest setting for 2 seconds. These cells lysates were subsequently used for protein gels and Western blotting.

2.2.8 *Trypan Blue exclusion test*

If a cell is alive its cell membrane is intact and it is able to exclude Trypan Blue. The opposite is true for dead cells. Hence live cells appear white and dead cells, which have taken up Trypan Blue, appear blue.

200 µL of well-mixed cell suspension was added to 200 µL of Trypan Blue stain (0.4% w/v). This was mixed and applied under a cover slip on top of a haemocytometer. The cells in the large central square on the haemocytometer were counted. Cells on the top and left border were included and those on the bottom and right border were excluded. If fewer than 100 cells were counted, cells in more squares were counted. The number of squares counted was taken into account (see Figure 2.2.8.1).

(a)

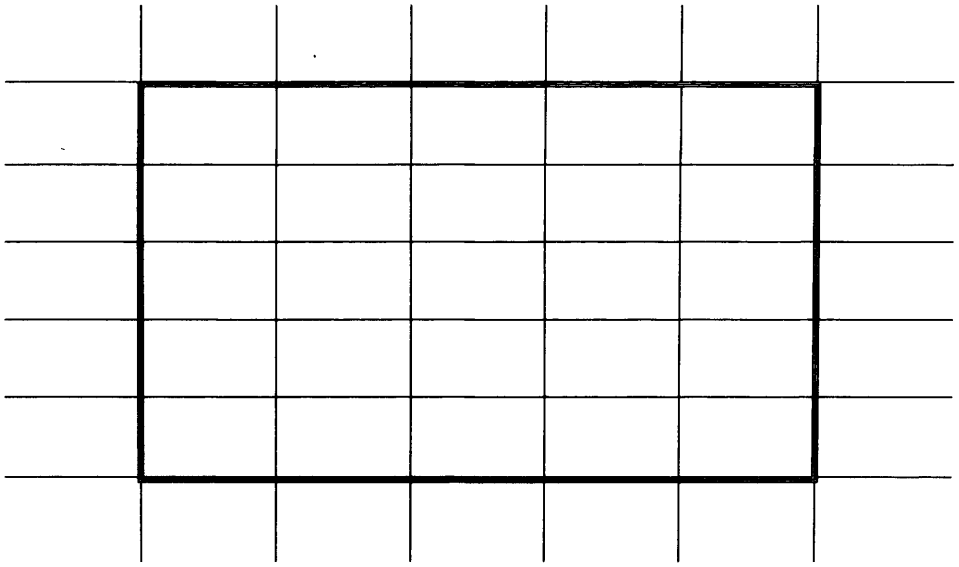

(b)

$$\text{Cell number per mL} = \frac{\text{Cell count}}{\text{No. of large squares counted}} \times 2 \times 10^4$$

For cell viability the total number of cells were counted along with the number of blue (dead) cells.

Number of live (white) cells = total number of cells – number of dead (blue) cells

$$\text{Viability} = \frac{\text{Number of white cells}}{\text{Total number of cells}} \times 100$$

2.2.8.1 Trypan Blue Exclusion Test

A picture of the grid on a haemocytometer is shown (a). The calculations to determine cell number and viability are shown in (b)

2.3 Cell culture

2.3.1 HepG2 cell culture

HepG2 cells (passage number 9 or 10) were obtained from the European Collection of Cell Culture (ECACC) and seeded onto tissue culture flasks (MG Scientific) and grown in an incubator (Heraeus®, Kendro) at 37°C with 5% CO_2 until the cells were 70-75% confluent. Cells were washed twice with PBS ((1x) 137 mM NaCl, 2.7 mM KCl, 10 mM Na_2HPO_4, 1.8mM KH_2PO_4), detached with 4 mM EDTA in 1 x PBS and pelleted by centrifugation (1900 rpm, 2 minutes, room temperature). The pellet was re-suspended in fresh complete medium and seeded onto 24-well plates (Nunc). To ensure that the cells were 70-75% confluent at the time of transfection, they were plated 48 hours beforehand. HepG2 cell culture was carried out by Dr. Mina Edwards.

2.3.2 Transient transfection of HepG2 cells

The HepG2 cells were plated into 24-well plates at a density of 4 x 10^4 per well. For transfection the cells were 70-80% confluent. For each well, 0.5 µg of DNA was diluted in 100 µL of Opti-MeM® and to this 2.5 µL of Lipofectamine LTX was added. This solution was mixed gently and incubated at room temperature for 25 minutes to form the DNA-Lipofectamine LTX complexes. The growth media from the plates was removed and to each well 0.5 mL of complete media and 100 µL of the DNA-Lipofectamine LTX complexes were added. The solutions were mixed by gently rocking the plate and the complexes were left for 24 hours before treatment with the selected xenobiotics. After a further 24 hours the cells were isolated for use with the Dual-Luciferase reporter assay (see below).

2.3.3 Isolation of total RNA from HepG2 cells or primary hepatocytes

After the cells (primary mouse hepatocytes or HepG2 cells) had been treated for 24 hours with an appropriate xenobiotic, the cell total RNA was isolated using the RiboPure™ kit

(Ambion). After removal of the media (without washing the cells) TRI™-reagent (phenol and guanathionate) (200 µl per well in a 12-well plate) was added to the cells allowed to cover the plate. TRI™-reagent completely detaches the cells, and this homogenate was removed and transferred to clean Eppendorf tubes. The tubes were frozen (-70°C) until RNA isolation could be carried out. At this time the tubes were allowed to thaw at room temperature (RT) and 100 µL of bromochloropropane was added to each mL of homogenate and vortexed for 15 seconds. The mixture was incubated (RT, 5 minutes) then centrifuged (12,000 x g, 10 minutes, 4°C). 400 µL of the upper aqueous phase was pipetted into a new centrifuge tube and 200 µL of ethanol (100%) was added and vortexed. The samples were transferred to filter cartridges and spun in collection tubes (12,000 x g, 30 seconds, RT). The flow-through was discarded and 500 µL of wash solution was added to the filter cartridge. This was centrifuged (12,000 x g, 30 seconds, RT), and the flow-through discarded. The whole washing sequence was repeated, and the filter cartridges were centrifuged a final time to remove residual wash solution. The filter cartridges were transferred to clean collection tubes and 100 µL of Elution Buffer added to the filter. They were left to incubate (RT, 2 minutes), then were centrifuged for 30 seconds. The eluant contained the RNA.

2.4 Down-stream analysis

2.4.1 Dual-Luciferase reporter assay and pGL3 vectors

The Dual-Luciferase® reporter assay kit was purchased from Promega. It utilises a Firefly and Renilla luciferases. The pRL-TK vector contains the *Renilla* (*Renilla reniformis*) luciferase reporter gene (*Rluc*) upstream of which is the herpes simplex virus thymidine kinase (HSV-TK) promoter. The pGL3 Basic vector contains a multiple cloning site upstream of the firefly (*Photinus pyralis*) luciferase reporter gene (luc^+) (See Figure 2.4.1.1). The ability of any fragments cloned into this site to drive expression of this reporter gene can be measured. The cells were simultaneously transfected with the pRL-TK vector containing *Renilla* luciferase to act as an internal control.

Luciferase Assay Reagent II (LARII) is the substrate for firefly luciferase, and its activity is measured first. Stop & Glo® Reagent is added to the same tube, this is used to measure the activity of the *Renilla* luciferase. It also quenches the luminescence produced from firefly luciferase so the two measurements do not interfere.

Cells are lysed using lysis buffer contained within the Dual-Luciferase® reporter assay kit, by adding it to the cells (200 µl per well in a 24-well plate) and rocking the plate for 15 minutes to allow for complete lysis. The lysate (20 µl) was transferred to a 96-well plate and LARII was added (100 µl) before measuring the luminescence.

The plate was read at 520 nm absorbance on a Pherastar plate reader. This first step measures the firefly luciferase then Stop and Glo reagent (100 µl) was added to the same wells and the *Renilla* luciferase is measured. Relative light units (RLU) are the values obtained when the firefly luciferase measurement is divided by the *Renilla* luciferase measurement.

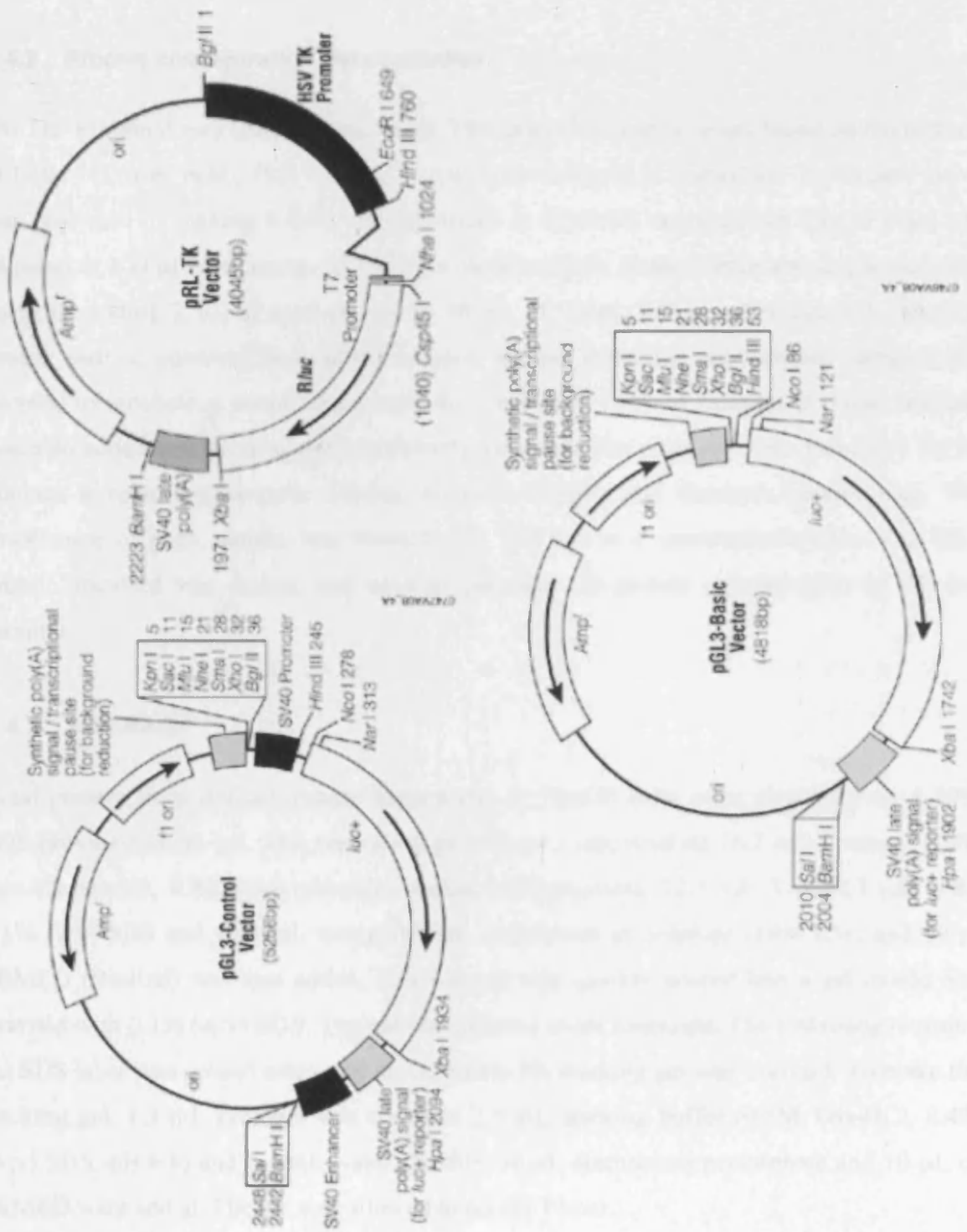

2.4.1.1 The pGL3 vectors by Promega

Promoter fragments were cloned into the pGL3-Basic vector. The pGL3-Basic vector was also used as a negative control. The pGL3-Control vector was used as the positive control. The pRL-TK vector was co-transfected with each plasmid to act as an internal standard for each transfection reaction.

2.4.2 Protein concentration determination

The DC Protein Assay (BioRad) was used. This is a colourimetric assay based on the method of Lowry (Lowry et al., 1951). BSA (1.4 mg/mL) was used as a standard. A standard curve was produced by making 6 BSA concentrations in duplicate ranging from 2µg to 20µg and adjusted to 100 µL with water. Any protein samples (cells lysates) were also duplicated, and made by adding 2 µL of total protein to 98 µL of water. 500 µL of Reagent A (alkaline copper tartrate solution) was added to each sample including the standard samples and allowed to incubate at room temperature for 5 minutes. 4 mL of Reagent B (Folin reagent) was also added to each tube and immediately vortexed. The reactions were incubated for 20 minutes at room temperature. During this time, samples and standards became blue. The absorbance of each sample was measured at 750 nm in a spectrophotometer. The BSA protein standard was drawn, and used to calculate the protein concentration of the test samples.

2.4.3 SDS-PAGE

Total protein from primary mouse hepatocytes or HepG2 cells were visualised on a 10% SDS-polyacrylamide gel. The separating gel (50 mL) consisted of 16.7 mL Protogel (30% w/v acrylamide, 0.8% bisacrylamide, National Diagnostics), 12.5 mL Tris-HCl (pH 8.8), 0.1% (v/v) SDS and 19.8 mL water. 0.5 mL ammonium persulphate (10% v/w) and 50 µl TEMED (BioRad) was also added. This mixture was quickly poured into a gel mould and overlaid with 0.1% (w/v) SDS. The gel was allowed to set overnight. The following morning the SDS layer was poured away and in its place a 3% stacking gel was overlaid. To make the stacking gel, 1.3 mL Protogel was added to 2.5 mL stacking buffer (0.5M Tris-HCl, 0.4% (w/v) SDS, pH 6.8) and 6.1 mL water. To this, 50 µL ammonium persulphate and 10 µL of TEMED were added. The gel was allowed to set for 1 hour.

Protein samples were mixed with loading buffer (6x, Invitrogen) and denatured for 3 minutes at 99°C. ß-mercaptoethanol was added to each sample to a final concentration of 20% (v/v). Samples were briefly vortexed and centrifuged, then loaded onto the gel. The gel was electrophoresed in running buffer (0.025M Trizma base, 0.192M Glycine, 0.1% w/v SDS) at 25 mA until the protein samples had moved through the stacking gel, then the voltage was increased to 35 mA until completion.

After electrophoresis the gel was stained with Coomassie Blue staining (see below) solution or a Western blot was carried out.

2.4.4 Coomassie Blue staining

The gel was placed in Coomassie Blue staining solution (0.25% w/v Coomassie brilliant blue dye, 45% methanol, 10% glacial acetic acid) until such a time that the gel was stained completely blue. The gel was put in de-staining solution (45% methanol, 10% glacial acetic acid) until protein bands stained blue could clearly be seen. The gel was transferred to 3M Whatman paper and dried using a gel dryer.

2.4.5 Western blotting

The proteins separated by SDS-PAGE were fixed to a nitrocellulose filter by western transfer. To do this the nitrocellulose filter, several 3MM Whatman papers and 4 blotting pads were pre-soaked in transfer buffer (25 mM Tris, 192 mM Glycine, 20% v/v methanol). The SDS-PAGE gel was placed on the nitrocellulose filter, and sandwiched between the Whatman papers and blotting pads and put into a blotting cassette. The cassette was put in a transfer tank filler with transfer buffer. A constant current of 100 mA was run through the tank overnight (room temperature) to transfer the proteins to the nitrocellulose filter. The following morning the current was increased to 200 mA for 1 hour to ensure the transfer of proteins.

For immunoblotting the filter was soaked for 1 hour in blocking solution (0.2 % w/v milk protein, 20 mM Tris-HCl (pH 7.5), 0.15 M NaCl). The filter was washed in TTBS (20 mM Tris-HCl, 150 mM NaCl, 0.1 % v/v Tween-20) 3 times for 5 minutes each time. The primary antibody (Santa Cruz) was diluted 500-5000 times (depending on the original titre of the antibody) in a solution containing 0.2 % w/v milk protein, 20 mM Tris-HCl (pH 7.5) and 150 mM NaCl. The filter was soaked in the primary antibody for 1 hour then the antibody was removed and the filter washed again in TTBS (3 x 5 minutes). The secondary antibody, which recognises the primary antibody is alkaline phosphatase conjugated. It was diluted in the blocking solution at 1:1000. The filter was incubated in the secondary antibody for 1 hour then rinsed in TTBS (3 x 5 minutes).

To visualise the amount of primary antibody bound to the nitrocellulose filter, the Alkaline Phosphatase Conjugate Substrate kit (BioRad) was used. Briefly, for 25 mL of solution, 24 mL water, 1 mL of AP development buffer, 0.25 mL of AP colour reagent A, and 0.25 mL colour reagent B was combined. The nitrocellulose filter was immersed in the solution and agitated gently for 10 minutes or until the colour development was complete.

2.5 Microarray

2.5.1 Cell treatment and preparation of RNA for microarray

12-well plates of hepatocytes were dosed. Half of the wells on each plate were treated with glycyrrhetinic acid (10 μM), half with the vehicle, 70% ethanol. The plates were incubated at 37°C, with 95% O_2 and 5% CO_2 for 24 hours. The media was removed and 200 μL of TRI-reagent from the RiboPure kit (Ambion) was added to each well as explained in Section 2.2.7.

The RNA concentration was measured and 5 μL run on a 1% agarose gel to confirm RNA integrity. The samples were then sent away to the MRC Microarray Facility at the MRC Mammalian Genetics Unit at Harwell. I visited the facility and carried out the following procedures.

2.5.2 Microarray procedure

The microarray slides used were the RNG-MRC Mouse set 25k, printed by MRC Microarray Facility at Harwell.

The Roche cDNA Synthesis kit was used to produce the first and second strand cDNA. 10μg of total RNA were added to 2μL of T7 Oligo [dT] 24 primer (100 pmol/μL) and made up to 21.5 μL with double-distilled water. This mixture was incubated at 70°C for 10 minutes then placed immediately on ice. To this tube, 8 μL of Reverse Transcriptase buffer, 4 μL DTT, 2.5 μL Reverse Transcriptase Enzyme mix and 4 μL dNTP mix were added. This was incubated for 1 hour at 42°C then put on ice. To generate the second strand, the first strand cDNA (40 μL) was added to second strand synthesis buffer (30 μL), dNTP mix (1.5 μL), second strand synthesis enzyme mix (6.5 μL) and distilled water (72 μL). This mixture

was incubated at 16°C for 2 hours. Then T4 DNA Polymerase (20 µL) was added to this mixture and incubated (5 minutes, 16°C). The reaction was stopped by adding 17 µL EDTA (0.2 M, pH 8.0). The cDNA was then applied to a Qiaquick PCR purification column and eluted in 50 µL of water. The cDNA is run on a 1% agarose gel for quality control and then labeled by randomly primed Cy incorporation using Klenow fragment of DNA polymerase 1.

Klenow Labelling was carried out using random primers and klenow from Bioprime kit (Invitrogen). The sample cDNA (20 µl) was added to Random primer/Reaction buffer mix (20 µL). This is boiled for 5 minutes and cooled on ice. While on ice the following was added [10x] dNTP mix (low dC) (5 µL); 1 mM Cy5-dCTP or Cy3-dCTP (2 µL); Klenow (high conc.) (1.5 µL); H_2O (1 µL). The reaction mixture was incubated at 37 °C for between 1 and 18 hours and the reaction stopped with 0.5 M EDTA (pH 8.0)(5 µL). Each labeling reaction was applied to a Sephadex G50 spin column to remove 90% of the unincorporated nucleotide. The eluents from Cy-3 & Cy-5 tubes are combined and read on the NanoDrop to determine incorporation of labelling. The blocking agent Cot1 (1µg/µL, 10-20 µL) was added and Poly(dA) (8 µg/µL, 2 µL) is added as a "packer" to increase the concentration in the hybridisation solution. The sample was evaporated to dryness in a speedvac, then re-suspended in 50 µL microarray hybridization solution. This was incubated at 85°C for 5 minutes then at 42°C for 30 - 60 minutes prior to placing on the array. Meanwhile the array slide is placed into a hybridisation cassette (Corning) and 15 µL of water is put in each end of the chamber to ensure humidity. The chamber is sealed and placed in an oven at 42°C for 30-60 minutes.

The samples were spun for 2 minutes at 13000 rpm then labelled mixture carefully added onto the slide (avoiding picking up any solid matter). The coverslip & cassette lid were added and hybridised at 48°C overnight.

The slides were washed by placing slides (in rack) in a container with 1 L of Wash solution A ([2x] SSC) until the cover slip falls off. The rack was transferred rapidly to a container with 1L Wash solution B ([0.1x] SSC, 0.1% SDS) & mixed vigorously for 5 minutes. Again the rack was transferred rapidly to a container with 1L Wash solution C ([0.1x] SSC) and mixed vigorously for 2 minutes. The slides were quickly moved into a 50 mL Falcon tube using forceps whilst taking care not to touch the surface of the array. The slides were placed in a tube with the labelled end in the bottom of the falcon tube (this means

that any debris is spun away from the array, not over it) and spun for 5 minutes at 600 rpm at room temperature. The array was then scanned using the Perkin Elmer ProScanArray HT confocal scanner, and the data extracted using the Imagene version 6.0 software from Biodiscovery.

2.5.3 Real-time RT PCR

Having isolated the RNA as described in Section 2.3.3, using the Ambion RNAeasy kit the RNA concentration was measured using the NanoDrop (Section 2.1.5). To accurately measure the RNA within the samples real time RT-PCR was carried out. This procedure varies little from RT-PCR but a fluorescent probe, SYBR green is incorporated into the double stranded DNA as it is amplified. The fluorescence is measured and plotted at the end of each cycle, this is the cDNA copy number, those that rise above the background fluorescence are recorded and known as the threshold cycle (Ct). This value is used in an equation to calculate the quantity of cDNA taking the original quantity into account.

Firstly cDNA must be made from total RNA using Superscript First-strand cDNA Synthesis System for RT-PCR (Invitrogen). Oligonucleotide primers are used to bind to a complementary sequence in the RNA. A recombinant reverse-transcriptase enzyme recognises the primer-RNA hybrid and synthesises a complimentary strand of DNA along the RNA template, resulting in a double stranded RNA-DNA molecule. To yield the RNA, high-temperature separates the two and the RNA template is degraded at a lower temperature with RNAse. Oligo(dT) primer was used for the reverse transcription because Oligo(dT) selects only RNA transcripts carrying a polyadenylation signal of at least 16 adenine nucleotides. This reduces the likelihood of amplifying any genomic DNA that might be present.

Solution A contains total RNA (1μg), Oligo(dT) (0.5 μg), dNTPs (1mM), DEPC-H_2O (up to 9 μL), this was incubated (65°C for 5 minutes) and then put on ice (5 minutes). Solution B contained RT-buffer (1X), $MgCl_2$ (5mM), DTT (10mM) and RNAse OUT (RNAse inhibitor 40 units). 9 μL of Solution B was added to Solution A and incubated (42°C for 2 minutes). 1 μL (50 units) of Superscript II reverse transcriptase enzyme was added and the reaction mixture was incubated (42°C for 50 minutes), then 70°C for 15 minutes. The mixture was left on ice for 5 minutes then 1 μL (2 units) of RNAse H was added and the

mixture was incubated at 37°C for 20 minutes. The yield of cDNA was determined by spectrophotometry using a NanoDrop (Section 2.1.5).

The real time RT-PCR reactions carried out in this study were done on a Stratagene Mx3000P machine using the Quantace Sensimix dT Kit with SYBR Green. The reactions were prepared in a total volume of 25 µL. cDNA (0.5 µg), gene-specific forward primer (500 nM), gene-specific reverse primer (500 nM), SYBR Green solution (1X), Sensimix solution (1X) (containing Taq DNA polymerase, dNTPs, and 3mM $MgCl_2$) and water (to 25 µL).

Below are the PCR conditions:

Condition	**Temp**	**Time**	
Initial denaturation	94°C	10 minutes	
Denaturation	94°C	30 seconds	40 cycles
Annealing	63°C	30 seconds	
Extension	72°C	30 seconds	

A melting curve analysis was carried out after the completion of each PCR run in order to detect the presence of non-specific products which might themselves contribute fluorescence. If fluorescence from non-specific products was above the background level it might interfere with proper interpretation of the expression level of the target gene. The melting curve analysis consisted of heating the PCR products to 94°C and immediately measuring the fluorescence emitted from the sample. The temperature was then lowered by 1°C and the fluorescence measured again. This process was repeated until the temperature reached 55°C. Typically amplified PCR product melted between 70-90°C and primer dimers melted between 55-60°C. Real time RT-PCR data was interpreted from the raw data plots by the method of Liu and Saint using an internal reference gene (Liu and Saint, 2002).

2.6 Animal Husbandry

Fmo1, 2, 4 (-/-), *Fmo5* (-/-) mice and C57BL/6 (wild-type) mice were housed according to Home Office regulations in a 12 hour light/dark cycle in cages of two or more mice. They were fed on a normal chow diet and water *ad libitum* unless otherwise stated. Animals were

weaned at 3 weeks and kept in male or female only cages, unless the animals were to be used for breeding, when they were kept one male to two females.

2.6.1 Mouse weighing

The ages of the mice were calculated so that their ages would correspond to each other. Animals were weighed twice a week for up to 20 weeks from the age of weaning. The mice were weighed individually on a Heraeus balance at 11am (+/- one hour) on the appropriate day.

2.6.2 Mouse diets

Mice were fed a standard chow diet unless otherwise stated. Standard chow diet was obtained from Harlan Teklad Global 18% total protein rodent diet, containing 18% protein, 5% fat and 56% carbohydrate. At 14 weeks of age, 6 WT males, 7 WT females, 3 *Fmo5* (-/-) males, 3 *Fmo5* (-/-) females, 5 *Fmo1, 2, 4* (-/-) males and 6 *Fmo1, 2, 4* (-/-) females were placed on a high-fat diet for 7 weeks. After this period of time the mice were culled and dissected (see below). The high-fat diet was obtained from Special Diet Services UK SDS DIO 35% kcal FAT diet containing 35% of calories from fat.

At 6 weeks of age 6 WT males, 5 *Fmo1, 2, 4* (-/-) males and 3 *Fmo5* (-/-) males were placed on a normal chow diet containing 0.1% (w/w) α lipoic acid. Every effort was made to make the feed in a sterile manner. Any apparatus used was swabbed with 70% ethanol and rinsed with autoclaved de-ionised water. Typically 100g of feed was made by grinding 99.9 g of normal chow pellets in a coffee grinder, adding 0.1g of lipoic acid powder (Sigma) and mixing well. Pellets were re-formed by adding 20 mL of autoclaved de-ionised water and mixing to form a pulp. Pellet shapes were made by rolling the feed pulp in the palm of the hand. The pellets were left to harden by heating in an oven at 35°C overnight.

2.6.3 Dissection

At an appropriate age, male and female *Fmo1, 2, 4* (-/-), *Fmo5* (-/-) mice and C57BL/6 (wild-type) mice were killed by CO. The mice were then weighed, their length measured, then they were dissected and major organs were removed. These were the liver, kidneys, spleen, heart,

gonadal fat and brown adipose which were also weighed, and aliquots stored both at -70°C and in RNAlater™ at -20°C. The frozen tissues were initially snap frozen in a dry ice-ethanol bath and the liver and gonadal fat used later for histological analysis (Section 2.6.6), whilst the RNAlater stored tissues were used to generate RNA and study the expression levels of the FMOs using real-time RT-PCR (Section 2.5.3).

2.6.4 Blood collection

The blood was collected from the mice between 9.30am and 12.00 midday to minimise the effects of circadian rhythm. The mice were then incubated for 10 minutes at 37°C to make it easier to collect the blood. After this time the mice were put in a restrainer and the tail tip snipped at a 45° angle, from this the blood was collected in Starstedt heparin-coated tubes. The blood was spun (8000rpm, 10 mins, 4°C) and the upper plasma layer removed into clean tubes and frozen (-70°C).

2.6.5 Blood plasma biochemical tests

The blood plasma was sent to the MRC Mammalian Genomics Unit, Harwell in Oxfordshire. The samples were analysed using an ion selective electrode contained within an Olympus Diagnostic Systems AU400 Automated Clinical Chemistry Analyzer. The samples were measured as described by Hough (Hough et al., 2002).

2.6.6 Liver histology

Small amounts of liver from the WT, *Fmo1, 2, 4* (-/-) and *Fmo5* (-/-) mice were cut from frozen tissue and left to freeze at -70°C for 20 minutes in a cryo-mould filled with TissueTech (Samura). During this time the cryostat (Leica CM1850) was brought up to temperature. For liver and heart this was -16°C. After being frozen, the tissues in TissueTech were put into the cryostat at -16°C to bring the tissues up to temperature also. The tissue frozen in TissueTech is now taken out of its mould and fixed onto a platform that is inserted into the cryostat. The section thickness was selected (12 μM) and the tissue was cut into these 12 μM sections which are immediately 'fixed' onto slides by the process of attraction.

To stain for total lipids, liver sections were stained in Oil Red O. This was made by dissolving Oil Red O (Sigma) in isopropanol overnight, then adding to a 1% w/v solution of dextran and filtering through a Whattmann filter Size 2. Slides were put into the Oil Red O stain for 15 minutes, rinsed in tap water then stained in Hematoxylin (Gil's type 1, Sigma) for 30 seconds then rinsed in tap water until the nuclei turned blue (approximately 1 minute). Photographs were taken with an Orbit micropublisher colour digital camera using an Axioskop 2 plus-Zeiss confocal microscope.

2.6.7 Adipose histology

Paraffin embedded tissue sectioning was employed for the investigation of the cellular structure of white adipose tissue in the *Fmo1, 2, 4* (-/-) mice as cryo-sectioning is not cold enough to maintain the structure of fat. Adipose was first fixed in neutral buffered formalin (NBF) containing formaldehyde 40% (v/v) (100 mL), sodium phosphate (4g), sodium chloride (6g) and water to 1 L, and stored at 4°C until used.

Tissue samples that were to be paraffin embedded were first dehydrated through a series of alcohols. This ensures that the hydrophobic paraffin can infiltrate the tissue properly. An approximately 50 mg tissue portion was incubated with 5 mL of room temperature alcohol as follows:

Distilled Water	30 minutes
50% Ethanol	45 minutes
70% Ethanol	45 minutes
90% Ethanol	45 minutes
100% Ethanol	1 hour
100% Ethanol	1 hour
Xylene	15 minutes
Xylene	15 minutes

Following dehydration the tissue samples were incubated in liquid paraffin (58°C overnight). The following day the tissues were transferred to clean liquid paraffin and incubated (1 hour at 58°C). Tissues were then embedded in liquid paraffin set into blocks at room temperature where they set. The blocks were sectioned (10 μM) using a Leica 2325

microtome and floated on 37°C water to remove wrinkles, and then transferred to slides. The sections were allowed to dry and stored at room temperature until staining.

Haematoxylin stains nuclei a deep blue colour and Eosin stains the cytoplasm a light pink colour. The Haematoxylin-Eosin staining procedure employed was a modification of the method of Culling (Culling et al., 1974). The staining procedure involves three steps; the hydration of the tissue, the staining, and finally dehydration of the tissue.

Hydration		**Staining**		**Dehydration**	
Xylene	5 mins	Haematoxylin (Gil's)	5 mins	50% Ethanol	30 secs
Xylene	5 mins	Water (running tap)	5 mins	70% Ethanol	30 secs
100% Ethanol	5 mins	70% Ethanol	30 secs	90% Ethanol	30 secs
100% Ethanol	5 mins	Eosin Y alcoholic	2 mins	100% Ethanol	1 min
90% Ethanol	5 mins	Water (running tap)	10 secs	100% Ethanol	1 min
70% Ethanol	5 mins			Xylene	1 min
Water (tap)	5 mins			Xylene	1 min

The slides were mounted in DPX, a xylene based mounting medium and cover-slipped.

Chapter 3

Results and Discussion

FMO5 promoter cloning, analysis and effects of xenobiotics

3 FMO5 promoter cloning and analysis

3.1 Identification of *FMO5* leader sequence

Sequence information for the full human genome is freely available from the Ensembl.org website. From here four clones of the human *FMO5* promoter were designed. The start site of transcription was confirmed by using the DBTSS website (http://dbtss.hgc.jp). This information was checked by aligning all available FMO5 cDNA clones to find any differences to the published sequence such as alternative splice sites (Figure 3.2.1), none of which were found.

The human *FMO5* gene lies on chromosome 1 region 1q21.1. It is 39,084 bp long and is located between chromodomain helicase DNA binding protein 1-like (CHD1L) and the 5'-AMP-activated protein kinase subunit beta-2 (PRKAB2) gene. The mouse *Fmo5* gene is between the same two genes on chromosome 3 region F2.2, and is 23,679 bp in length.

3.2 Amplification of the *FMO5* promoter region

Sequences were amplified by PCR using primers designed from the published sequence (see Appendix). To influence the choice of primers and the position of the resulting constructs, the *FMO5* promoter was analysed for possible transcription factor binding sites (see Section 3.4).

The PCR-amplified sequences were cloned into TOPO™ vectors. The insert was then removed using restriction enzymes *Bgl II* and *Kpn I* and ligated into the pGL3 Basic vector (Promega) which had been digested with the same two enzymes. The pGL3 Basic vector contains a firefly luciferase gene, and the *FMO5* promoter fragments were cloned upstream of this. The four *FMO5* clones, -531, -1031, -1723 and -2443 were named by the length of the fragment, each clone starting at the same point within exon 1 (See Figure 3.5.1 for cloning strategy). The resulting clones were analysed by restriction enzyme digestion and agarose gel electrophoresis to ensure that the promoter fragments were the correct sizes (Figure 3.2.2). The clones were further analysed by determining their DNA sequence. No differences from the published sequence were found.

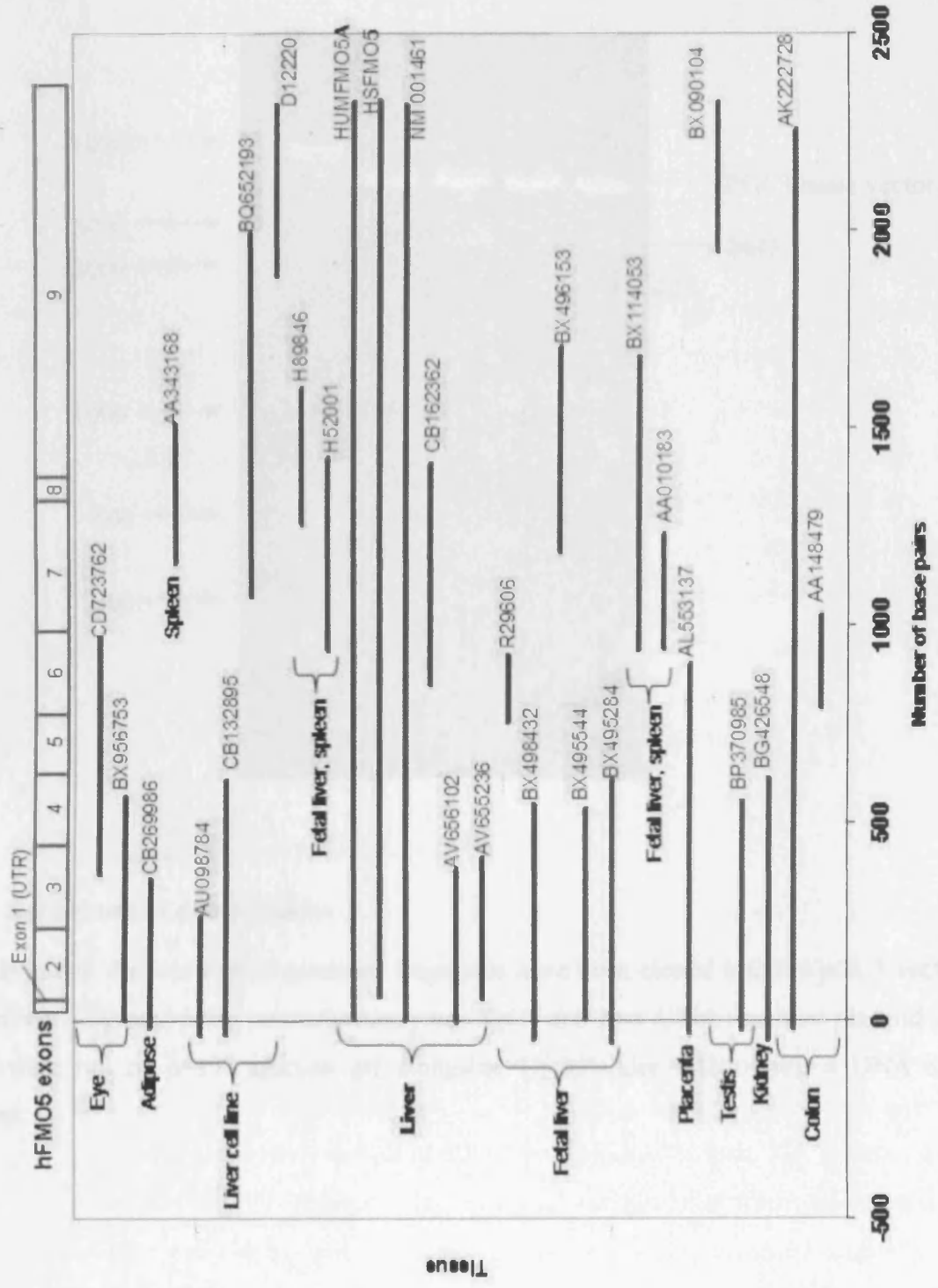

3.2.1 *FMO5* cDNAs

FMO5 cDNAs from various tissues plotted alongside each other and the exon structure of *FMO5*.

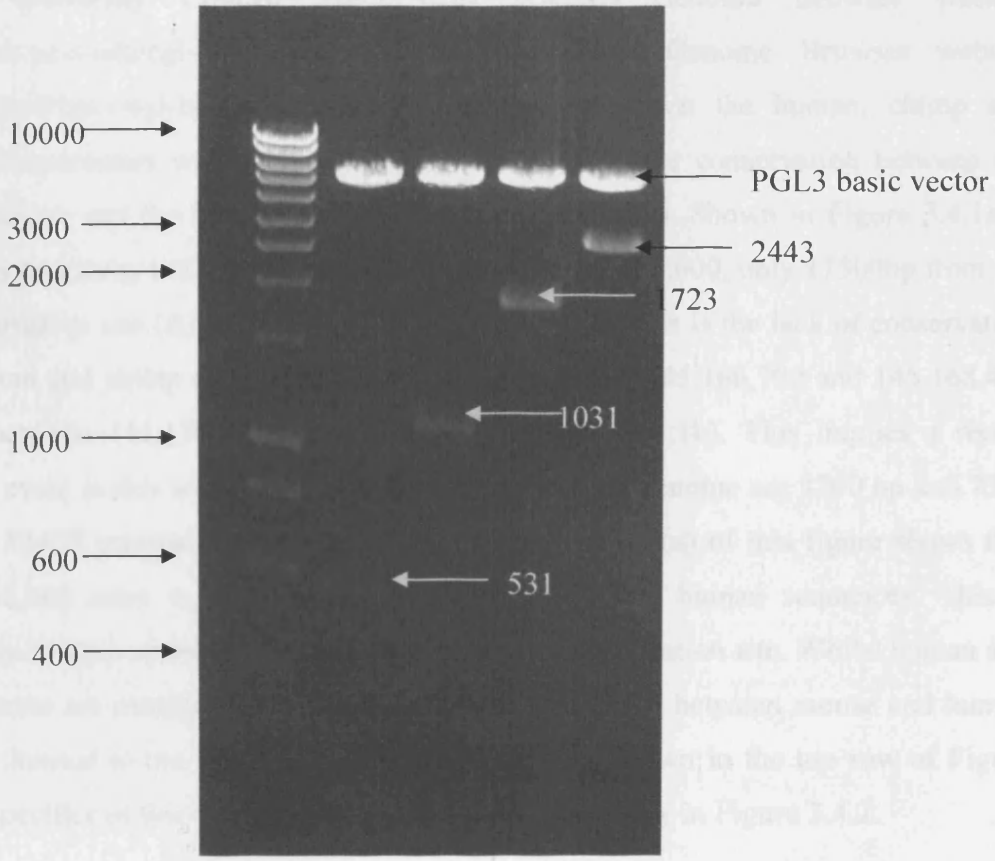

3.2.2 Gel picture of clone inserts

To confirm that the four FMO5 promoter fragments have been cloned into the pGL3 vector, the clones are digested using restriction enzymes *Bgl II* and *Kpn I*. The resultant plasmid and inserts were run on a 1% agarose gel alongside Hyperladder I (Bioline), a DNA size indicator.

3.3 Conservation of the human *FMO5* promoter region

Using the University College Santa Cruz (UCSC) Genome Browser website (http://genome.ucsc.edu/cgi-bin/hgGateway) and the Vista Genome Browser website (http://pipeline.lbl.gov/cgi-bin/gateway2), the similarity between the human, chimp and mouse *FMO5* promoters was analysed. Figure 3.4.1 shows the conservation between the human and mouse and the human and chimp *FMO5* promoters. Shown in Figure 3.4.1a is *FMO5* and its proximity to CHD1L, which starts at base 145,181,000, only 17500bp from the translation initiation site (ATG) of *FMO5*. What can also be seen is the lack of conservation between human and chimp sequences in two places, between 145,166,700 and 145,168,400 as well as between 145,170,835 and 145,171,945 (Figure 3.4.1b). This implies a recent evolutionary event in this area. These insertions in the human genome are 3200 bp and 7335 bp from the *FMO5* translation initiation site respectively. Part (a) of this figure shows that from 145,166,060 there is no similarity between rodent and human sequences. This is approximately 2500bp upstream from the *FMO5* translation initiation site. Whilst human and chimp sequences are mostly highly conserved, the conservation between mouse and human sequences is limited to the first 500bp of the promoter, as shown in the top row of Figure 3.4.1c. The specifics of this conservation are studied more closely in Figure 3.4.2.

3.4 *FMO5* promoter sequence analysis

As shown in Figure 3.4.1 there is a lack of conservation between the rodent and human *FMO5* promoter sequences beyond the first 2500 bp, upstream from the translation initiation site. This 2500 bp of sequence was analysed using the Match program (http://sdmc.lit.org.sg/ERE-V2/index) (Matys et al., 2003). Both human and mouse promoters were examined, and in Figure 3.4.2 some of the possible regulatory sequences have been annotated. As was observed using the Vista program (Section 3.3), conservation between the two promoters is limited to the first 500 bp upstream from the translation initiation site. These conserved areas focus around key regulatory elements such as Sp1 sites/GC boxes and TATA boxes. Within the first 500 bp are two Sp1 sites situated at -150 bp and -194 bp from the translation initiation site. Both are conserved in the human and mouse. The core sequence is GGGCG the so-called GC box. Sp1 recognises and binds to GC

(a) Human compared to mouse

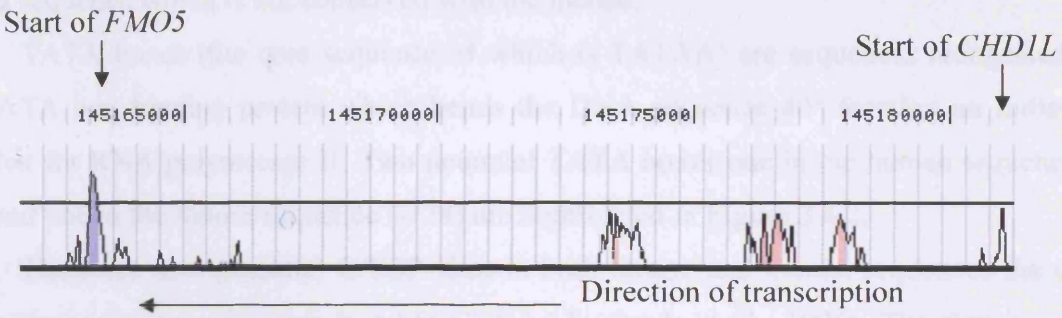

(b) Human compared to chimp

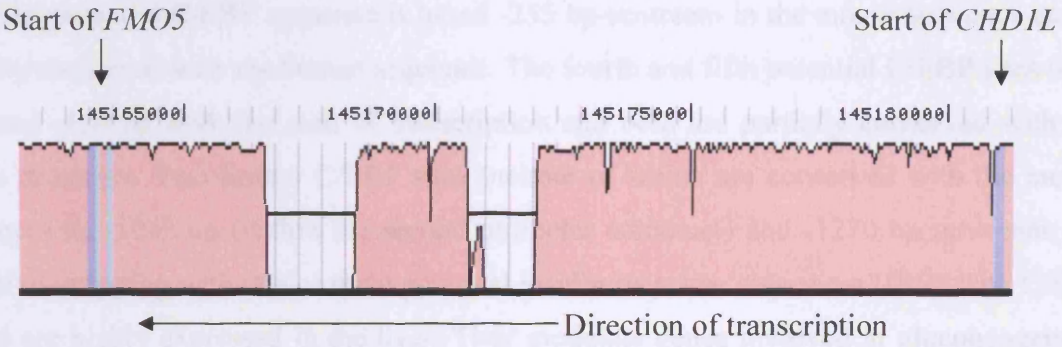

(c) Mouse and chimp compared to human-the first 1500bp of the promoter

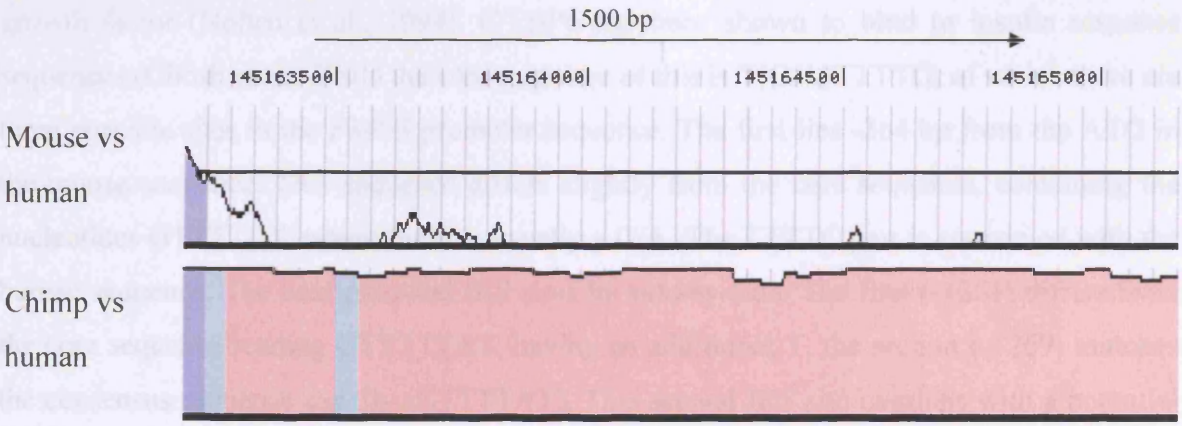

3.4.1 Human FMO5 promoter compared to the mouse and chimp promoters

The promoter sequences are compared using Vista Genome Browser. The peaks indicate similarity to human sequence, the more and higher the peaks the greater similarity. Numbers above the peaks indicate the position in the chromosome. Parts (a) and (b) show the proximity of *FMO5* and *CHD1L*. Part (c) compares the first 1500 bp of human *FMO5* promoter to the mouse and chimp sequences.

boxes, initiating transcription. A third Sp1 site is found much further upstream (-1007) in the human sequence which is not conserved with the mouse.

TATA boxes (the core sequence of which is TATAA) are sequences recognised by the TATA box binding protein which bends the DNA sequence 80° forming an initiation complex for RNA polymerase II. Two potential TATA boxes one in the human sequence (-116) and one in the mouse sequence (-128) are highlighted in Figure 3.4.2.

There are also potential C/EBP sites in both mouse and human sequences the core recognition sequence of which is ATTCGGCAAT (Osada et al., 1996). The first possible C/EBP site (-100 bp) is not conserved with the mouse sequence, but the second (-134 bp) is. The third potential C/EBP sequence is based -255 bp upstream in the mouse sequence and is partially conserved with the human sequence. The fourth and fifth potential C/EBP sites lie at -413 and -454 bp from the start of transcription and both are partially conserved with the mouse promoter. Two further C/EBP sites (neither of which are conserved with the mouse sequence) lie -1043 bp (within the second promoter construct) and -1270 bp upstream, the second overlapping with one of three potential insulin response sequences (IRS). The C/EBP factors are highly expressed in the liver. They modulate genes involved in gluconeogenesis and response to insulin as well as factors in control of liver-function such as insulin-like growth factor (Nolten et al., 1994). C/EBPα has been shown to bind to insulin response sequences (Ghosh et al., 2001) the core sequence of this is T(G/A)TTTTG, of which there are three possible sites in the *FMO5* promoter sequence. The first lies -264 bp from the ATG in the mouse sequence. This sequence differs slightly from the core sequence, containing the nucleotides GTTTTCT, where the C is usually a G/A. The TTTTC part is conserved with the human sequence. The next potential IRS sites lie side-by-side. The first (-1261) differs from the core sequence reading GTTTTTAT, having an additional T, the second (-1269) matches the consensus sequence exactly (GTTTTAT). This second IRS site overlaps with a potential C/EBP site (-1270). Neither IRS sequence shows conservation with the mouse sequence. The similarity between the consensus sequences is presumably the reason why C/EBPα has been shown to bind to the IRS. Two other potential IRS sequences lie much further upstream (-2218 and -2304), neither of which are conserved with the mouse sequence.

There are also potential hepatic nuclear factor-3 (HNF-3) and HNF-4 binding sites within the mouse *Fmo5* upstream sequence. It has recently been shown that HNF4α is essential for the induction of CYP3A4 (Tirona et al., 2003) and CYP2C9 (Chen et al., 2005)

via PXR and CAR. HNF3 has been shown to control genes implicated in glucose-induced insulin release (Wang et al., 2002). The consensus sequence for HNF3 is TATTGAC/TTTA/TG, whilst that for HNF4 is A/GTGA/GC/ACT/CTT/AGGC/A (Carter et al., 1993).

Another potential regulatory sequence present in the *FMO5* promoter is that of upstream stimulatory factor (USF). This consensus sequence consists of an E-box (CANNTG) followed by AC (Vostrov et al., 1995). There are two possible USF consensus sequences in the human *FMO5* promoter (-490 and -680) and one in the mouse sequence (-490) which reads AGAGCACCTGCTTG, and is conserved with the human sequence.

A recombination signal (CCCACCC) repeated four times is just within the first construct (-531) of the promoter sequence, lying -591 from the ATG. A recombination event may be the reason for the lack of similarity between human and mouse sequences beyond this point in the promoter.

Many half-sites for the pregnane-x-receptor (PXR) (yellow) and estrogen receptor (ER) (green) have been highlighted in Figure 3.4.2. The ER consensus sequence is GGTCAnnnTGACC, but no full sites were found in the *FMO5* promoter. The same applies to full PXR consensus sequences, but there are several half-sites (highlighted). The glucocorticoid receptor (GCR) binds to the glucocorticoid responsive element (GRE) (consensus: GGTACANNNTGTTCT) which consists of two GRE 'half-sites' (TGTTCT). There is a possible GRE located in the mouse *Fmo5* promoter -510bp from the translation initiation site. The sequence is partly conserved with the human sequence. As well as the main role of GCR to sense changes in circulating steroid levels, it has been shown that GCR and CAR are able to modulate cytochrome P450 gene expression together (Pascussi et al., 2003).

3.4.2 *Analysis of mouse and human FM05 promoter*

Pregnane-x-receptor half sites — Other regulatory sequences are in pink or blue or highlighted

Estrogen receptor half sites — Primers and exon 1 in grey — * shows nucleotide conservation between sequences

```
HUMAN FMO5 -2475 GTCTAGTAATAGCATGAGTAACTGAGTTGAGTCTGTATATTAATTTGGATGTATCAAGTTATTTTTCAATGAA      -2402
MOUSE FMO5       TTTGATATTAGAATGCCTACTCCAGCTTGTTTCTTAGGACCATTTTCTTGAAAAATTGTTTTCCAACTGTTTA
                  * *                 *    ***  ***    *  * ***          *** *    *  *  *

GAAATTGACTTACTTGCAAATTGTCAGCTAGGCAAGAGAGAGAACATTTGAGTCAAGGTTTAAAACATTGTATAAGTAATTTTAATACAA      -2312
CTCTGAGGTAGTGTCTGCCTTTGTCACTGAGGTGGTTTTACTGTATGCAGCAACATGCTGGGGCCTGTTTATGTATCCAGCCTGTTAGTT
      *      *      ******   ***                  *   ** * *       **     *   *   *  **

  IRS
CACAAAACATATTTGCTATATTCAAAAGCAATTAATTATAAGACACAATTGAAGTAGGGGGACATTAAAATAAAATTACATTGTTAACTA      -2222
TATGTCTTTTGGGGGAAATTGAGTCCATTGATGTTACTTCCTGTTATTTTTGTTGTTAGAGTCTGAATTATGTTTGTGTGGCTATCTTAT
 *       *    *  **       *   **      *         **        * * *   *  *      *       *

IRS
CATTTTAAAAGTAATTCTTGCATTATTTGTAAAACTGATTCAGTAGGAGGAAATTAATACTCAGTTTATAAAAGTATTCATGTTTTCCTT      -2132
TTTGGATTATTTGAAAGATTACTTTCTTGCTTTTTCAGTGTCCATGATGTATCTTCCTGTGTCCTTTCCCTCCTCCTTCTCTGTGGAACT
  *     *  * *              ***          *      *  * *  **  *      ***          ***    *     *

TAGGCATTTCTTCTAGCGCATTCAAA-ATTATCCAATTTACAA-GTAATTCATTTTAAGTTAACTTCTAGCATATAAAATGGTTGTG-TT      -2042
TAGGTACCTACAACATGGCAGACATGCAATAGGTATTGTGCTGTGTGTATGACCCCTGAATTACTCACGACTGTTACAAACTTTACGATT
**** *  *     *  ***  **   * **   * * * *   **   * *        * ***     *   ** **   **  * **

                                                  TATA box     TATA box
GAAACA--CTGTCTTCAGAATTTTATTTTTAAAAGATACTATT-TTAGTATAAATTCACATTTATAGTTGAATGCTTTTGTGAAAGATAT      -1952
GTAGCAAATAAGTTTCCCAATGGTAAGTCCGTTTCTATCACTATCAGTTTACACGTGGGGCAGCTGGCTTCCACTGCTATCCTTCAGCC
* * **       ***  ***  **  *       ***  *   * *** ** *              *       **  * *     *

TAGTCTTTAAAATATTTTACAGGCTGGCCTTGTTGGCTCATGCCTGTAATCCCAGCACTTTGGGAGGCCAAG-GCAGGTGGATCAC--TT      -1862
AAGACTCAAGTTGGTCCAATTACAAGACGTGGCCTCCTAAGAGAGATAGTTATTGAATGTACGTAAGCAAAATGCAGACTTAGCAAAATA
 ** **  *     *   *      * * * *    ** *      ** *    * *  *  * * ** **  ****    * **   *

                  Primer -1723
GAGCCCAGGAGTTCAAGACCAGCTTGAGCAACATAGTGAAACCTCATTTCTACAAAAAATACAAAAATT----ACCAGGTGTGGTGGCAC      -1772
AAATTAGGAAATAAGAAAACATAATAGGATCCAGAGAGATGACTCAGACGTCAAGAACACTGCCTGCTCCTGCAGAAGACCTGGGTTCAG
 *     * * *   * * **   *  *   ** ** **   ****    *  * ** *       *     *  **   ***   **

ACAGCTGTAGTCCCTACTCAGAAGGCTGAGGTGGGAGGGTAGATTGAGCCCAGGAGATAGAGGCTGCAGTGAGCCATGATTGCACCACTG      -1682
GTTGCTGGTAACCCAACGGCAACTATACAAATAGAAATACAAAGAGAACCATCTTGAACTCCAGCTCCAGGAGATCAGGCATAGTCTCCTG
   ****    *** **    *      *  * * *    * *  ** **      *     *** ***     ** *  *   *  ***
```


-1592
-1502
Ap-1
-1412
-1322
C/EBP
IRS
IRS
-1232
-1142
Primer -1031
-1052
C/EBP
GC box
Sp1
-962
-872
-782

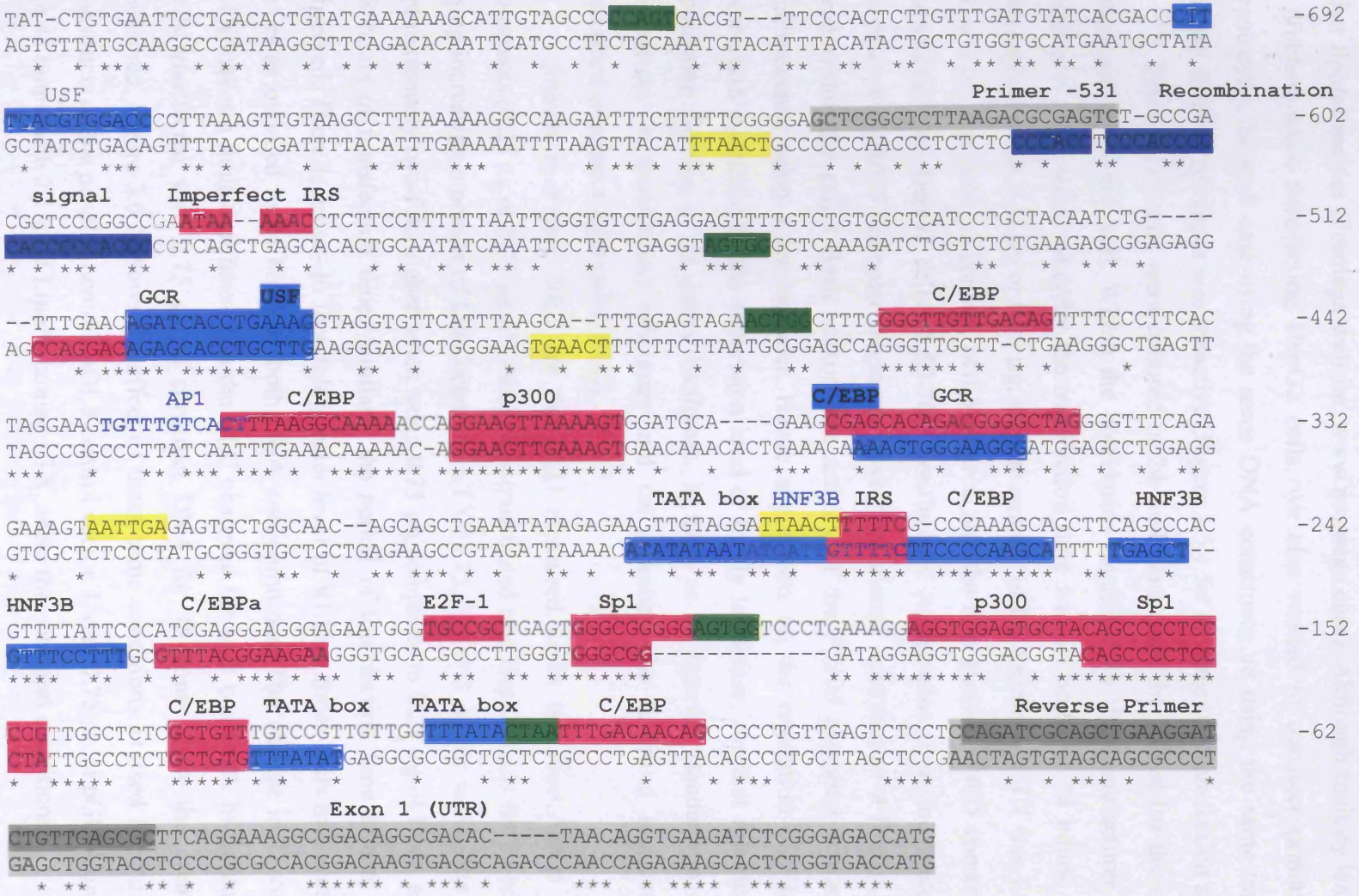
USF
Primer -531
Recombination
signal
Imperfect IRS
GCR
USF
C/EBP
AP1
C/EBP
p300
C/EBP
GCR
TATA box
HNF3B IRS
C/EBP
HNF3B
HNF3B
C/EBPa
E2F-1
Sp1
p300
Sp1
C/EBP
TATA box
TATA box
C/EBP
Reverse Primer
Exon 1 (UTR)
-692
-602
-512
-442
-332
-242
-152
-62

3.5 Transfecting HepG2 cells

Lipofectamine LTX was chosen as a transfection reagent as it is purportedly less toxic than other lipofectamines (Promega website, www.promega.com). Although toxicity isn't usually a problem when transfecting HepG2 cells, we also wanted to transfect primary mouse hepatocytes. In each case using the same DNA constructs, so using the same transfection reagent for both cell types was attractive (Figure 3.5.1 for cloning and transfection strategy).

The HepG2 cells were cultured in 24-well plates and the values for the conditions below are stated per well. Within the boundaries suggested by the manufacturer, different conditions were tested whereby the transfection time was 24 hours or 48 hours; the DNA concentration was 0.25 μg or 0.75 μg; and the amount of lipofectamine LTX was 1.75 μl, 2.5 μl or 3 μl. The positive control, pGL3 control, and the four human *FMO5* constructs were transfected into HepG2 cells at 50-70% confluency. As mentioned in the Materials and Methods the *FMO5* promoter fragments have been cloned upstream of a firefly luciferase gene within the pGL3 Basic vector. The activity of the *FMO5* promoter is measured as luminescence using a luminometer. Hence any effects on the regulation of *FMO5* gene expression is defined by the expression level of firefly luciferase. Another reporter plasmid containing *Renilla*, a sea pansy luciferase, is used as an internal standard to allow for differences in transfection efficiency and cell number, the resulting luminescence is described as relative light units (RLU).

Shown in Figure 3.6.1 are the RLU measured when the four *FMO5* promoter constructs (0.25 μg or 0.75 μg of DNA) were transfected into HepG2 cells for 24 or 48 hours using increasing amounts of Lipofectamine LTX (1.75, 2.5 or 3 μl per well). The RLU are approximately two-fold higher when using 0.75 μg compared to 0.25 μg of DNA after 24 or 48 hours of transfection time. Similarly the period of transfection time affects the RLU observed. There is a two- to four-fold greater level of RLU in those cells transfected for 48 hours as opposed to 24 hours at both DNA concentrations. The change in Lipofectamine LTX makes a limited difference to the RLU observed for each construct. In summary those cells transfected with 0.75 μg of construct DNA for 48 hours show the greatest RLU measured. Figure 3.6.2 shows the effect of those same conditions as used for the promoter constructs on the positive control, pGL3-control vector. Using 0.75 μg of pGL3-control DNA for 48 hours with 2.5 μl of Lipofectamine LTX, seem the optimum conditions.

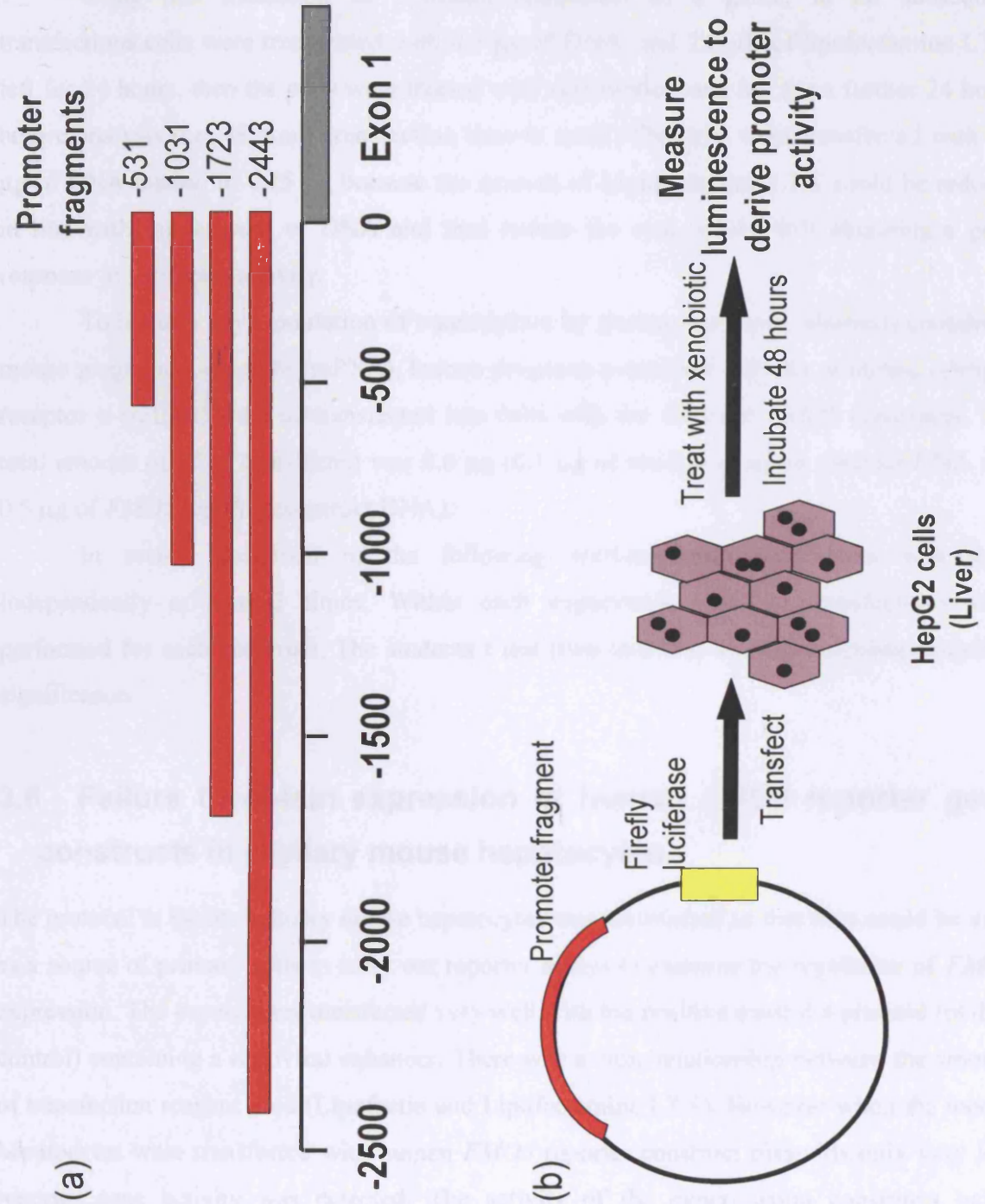

3.5.1 *The promoter cloning and transfection strategy*

The promoter fragments as they sit in relation to each other and exon 1 of *FMO5* (a). A promoter fragment is cloned into pGL3-Basic and transfected into HepG2 cells with a xenobiotic and incubated for 48 hours before measurement of luciferase (b).

Using this indication of optimum conditions as a guide, in all subsequent transfections cells were transfected with 0.5 μg of DNA, and 2.0 μL of lipofectamine LTX, left for 24 hours, then the cells were treated with xenobiotics, and left for a further 24 hours before analysis (i.e. 48 hours transfection time in total). The cells were transfected with 0.5 μg of DNA instead of 0.75 μg because the amount of Lipofectamine LTX could be reduced in line with this amount of DNA and thus reduce the cost, whilst still obtaining a good response in luciferase activity.

To identify any modulation of transcription by nuclear receptors, plasmids containing mouse pregnane-x-receptor (mPXR), human pregnane-x-receptor (hPXR) or mouse estrogen receptor α (mERα) were co-transfected into cells with the different *FMO5* constructs. The total amount of DNA transfected was 0.6 μg (0.1 μg of nuclear receptor plasmid DNA and 0.5 μg of *FMO5* reporter construct DNA).

In results described in the following sections each experiment was done independently at least 3 times. Within each experiment triplicate transfections were performed for each construct. The students t test (two-tail) was used to calculate statistical significance.

3.6 Failure to obtain expression of human *FMO5* reporter gene constructs in primary mouse hepatocytes

The protocol to isolate primary mouse hepatocytes was established so that they could be used as a source of primary cells to carry out reporter assays to examine the regulation of *FMO5* expression. The hepatocytes transfected very well with the positive control a plasmid (pGL3-control) containing a retroviral enhancer. There was a clear relationship between the amount of transfection reagent used (Lipofectin and Lipofectamine LTX). However when the mouse hepatocytes were transfected with human *FMO5* reporter construct plasmids only very low reporter gene activity was detected. The activity of the experimental constructs being equivalent to cells transfected with a negative control plasmid, pGL3-Basic.

The lack of reporter activity in mouse hepatocytes transfected with human *FMO5* constructs may be due to species-specific differences in the promoter regions of the gene.

As discussed in Section 3.3 the mouse and human 5' flanking sequence of the *FMO5* gene have little sequence similarity beyond the first 500 bp.

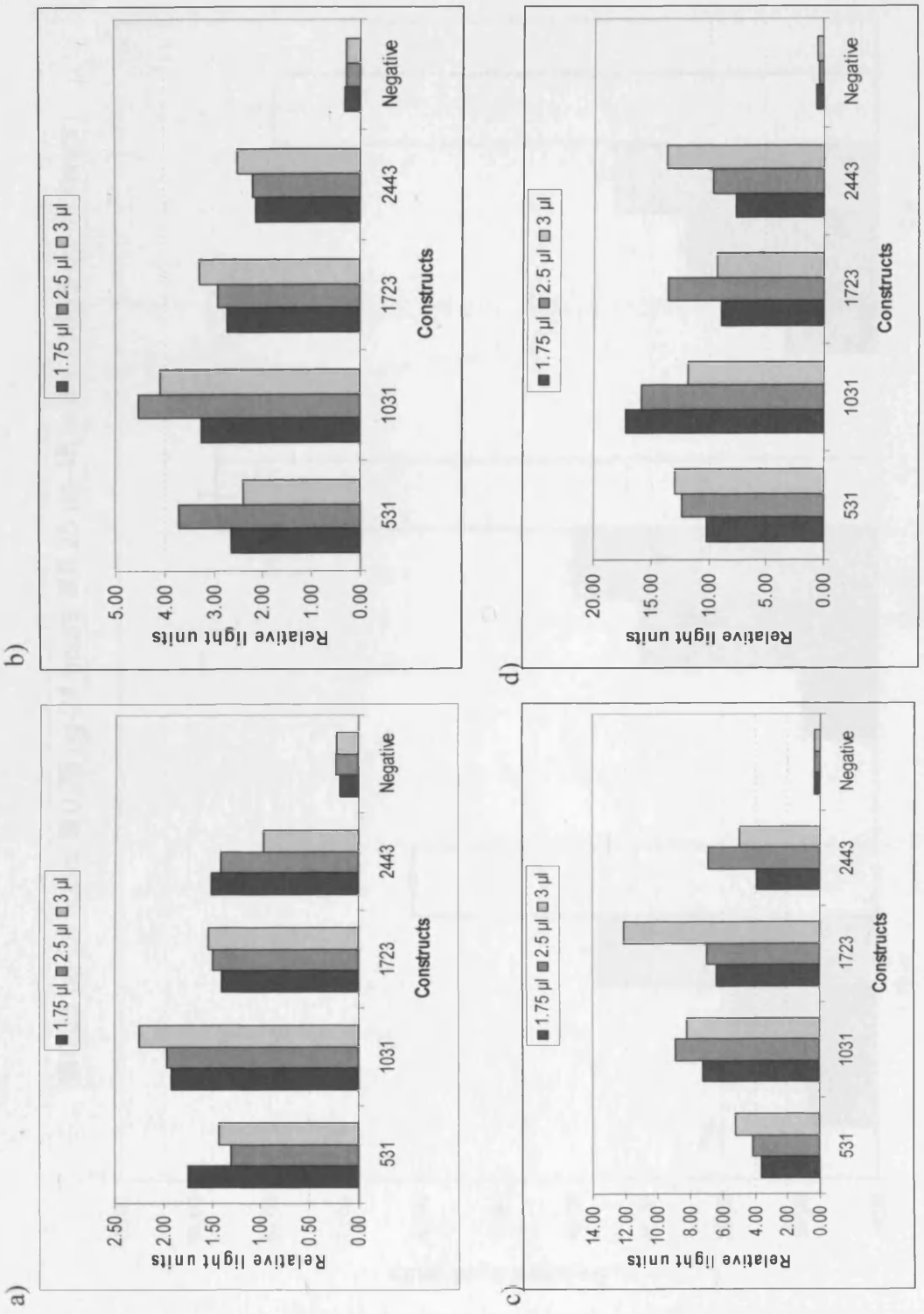

3.6.1 Luciferase assay development-constructs at 24 and 48 hours

The *FMO5* constructs were transfected into HepG2 cells with varying amounts of Lipofectamine LTX (1.75, 2.5 or 3 µL) for 24 hours with 0.25 µg DNA in a) and 0.75 µg DNA in b) and for 48 hours with 0.25 µg DNA in c) and 0.75 µg DNA in d).

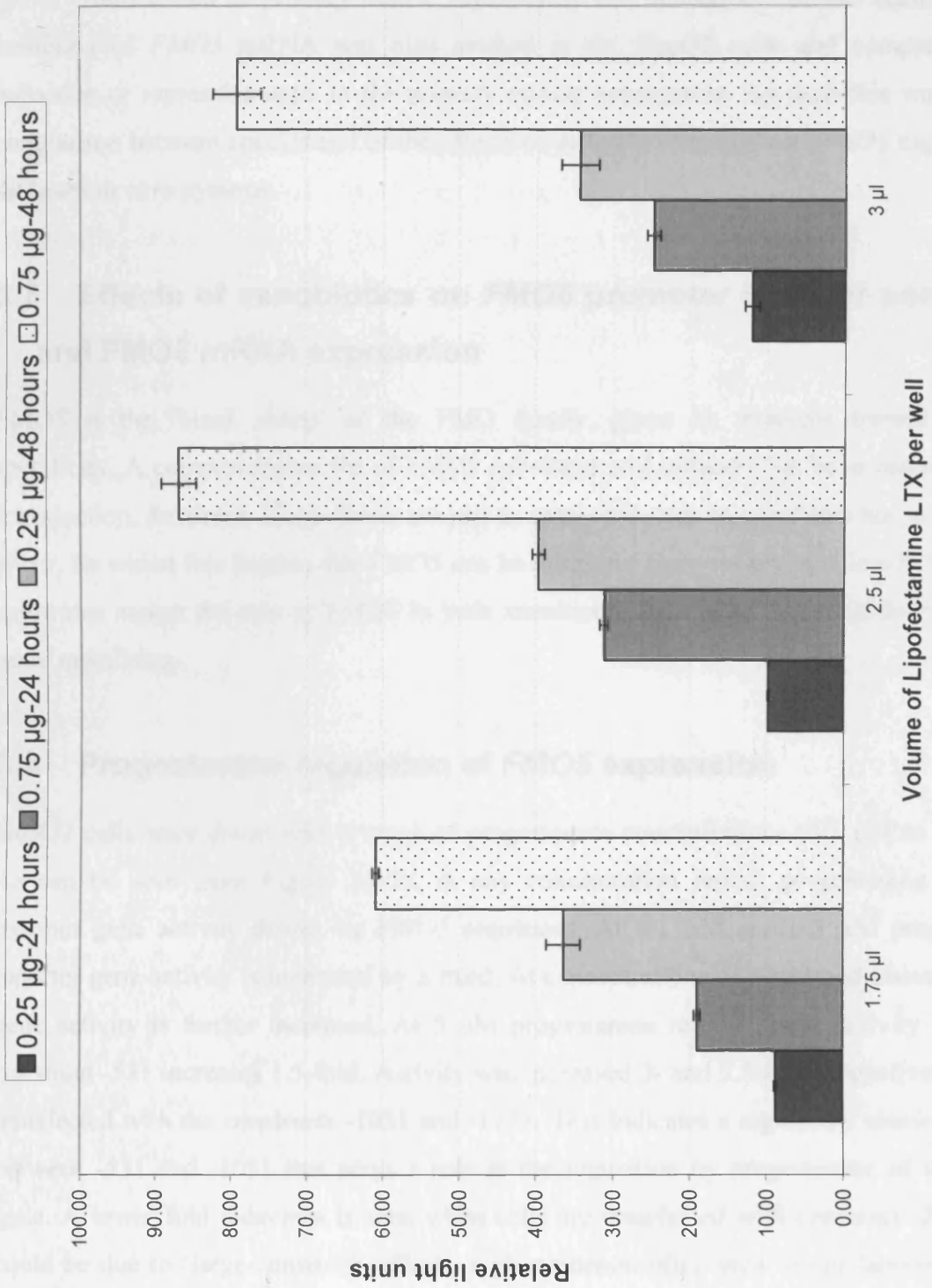

3.6.2 Luciferase assay development-pGL3 control

The expression of the positive control (pGL3 Control) in HepG2 cells after 24 and 48 hours of transfection, with 0.25 µg or 0.75 µg of DNA and with three different volumes of Lipofectamine LTX.

Transfection of primary mouse hepatocytes was abandoned for this reason, but the induction of *FMO5* mRNA was also studied in the HepG2 cells and compared to the induction or repression seen in the primary mouse hepatocytes. As such this was a useful comparison between species and of the effects of different chemicals on *FMO5* expression in different *in vitro* systems.

3.7 Effects of xenobiotics on *FMO5* promoter reporter constructs and FMO5 mRNA expression

FMO5 is the 'black sheep' of the FMO family, given its apparent limited substrate specificity. A comprehensive list of FMO5 substrates and inducers has been assembled (see Introduction, Section 1.15.1). There are just as many inducers as substrates but not many of either. So whilst this implies that FMO5 can be refractive to environmental insult, the lack of substrates makes the role of FMO5 in both xenobiotic and endogenous metabolism all the more tantalising.

3.8 Progesterone regulation of *FMO5* expression

HepG2 cells were dosed with a range of progesterone concentrations (0.1 μM to 100 μM). As can be seen from Figure 3.8.1a, at any concentration tested, progesterone increases reporter gene activity driven by *FMO5* sequences. At 0.1 μM and 0.5 μM progesterone, reporter gene activity is increased by a third. At concentrations of 5 μM and above, reporter gene activity is further increased. At 5 μM progesterone reporter gene activity driven by construct -531 increases 1.5-fold. Activity was increased 3- and 2.5-fold respectively in cells transfected with the constructs -1031 and -1723. This indicates a regulatory element located between -531 and -1031 that plays a role in the regulation by progesterone of the *FMO5* gene. A lower fold induction is seen when cells are transfected with construct -2443. This could be due to 'large-construct' effects, a phenomenon often seen in our laboratory when the size of an inserted fragment gets beyond an optimum point. At higher concentrations of progesterone (50 and 100 μM) the increase in reporter gene activity in cells transfected with the three larger constructs (-1031, -1723, -2443) is less than that seen at 5 μM. Reporter gene

activity of cells transfected with the -531 construct (the shortest construct tested) is about two-fold higher at 50 and 100 μM than that observed with just the vehicle.

The lowest concentration of progesterone (0.1 μM) tested was selected for co-transfection experiments. Each reporter gene construct was co-transfected with hPXR or mPXR (both 0.1 μg). Only hPXR increases reporter gene activity above that seen with progesterone alone (Figure 3.8.1b). This is probably because HepG2 cells are human cells in origin, and the constructs are derived from the human *FMO5* sequence. As well as having its own receptor, progesterone is a PXR ligand (Kliewer et al., 1998), and is able to induce PXR up to fifty times during pregnancy (Masuyama et al., 2001). Here we see that progesterone is able to increase *FMO5* reporter gene activity through hPXR.

As mentioned in the introduction section, mPXR and hPXR show only 80% similarity in their ligand-binding domains, this accounts for some of the differences in xenobiotic induction of CYP3A4 between the species. The two receptors however share about 96% amino acid sequence similarity in their DNA-binding domains (Lehmann et al., 1998). Progesterone is a ligand of mouse PXR (Kliewer et al., 1998), as well as human PXR which induced CYP3A4 four-fold (Lehmann et al., 1998).

The changes in FMO5 mRNA expression were measured using real-time RT-PCR. When HepG2 cells were treated with progesterone, FMO5 mRNA increased 165 % and 222% at concentrations 0.5 μM and 5.0 μM respectively (Figure 3.8.2a) (FMO5 mRNA expression from cells treated with the vehicle are zero percent). This increase in mRNA is similar to the increases observed in the reporter gene luciferase assays. For example, in cells transfected with the *FMO5* construct -2443, and treated with 0.5 μM and 5.0 μM progesterone, luciferase activity increased 98% and 289% respectively. When FMO5 mRNA is measured in progesterone-treated primary female mouse hepatocytes (Figure 3.8.3), there is a dose-dependent increase in mRNA of 108%, 141% and 203% (i.e. 2-fold, 2.4-fold and 3-fold) at the concentrations of 0.1 μM, 0.5 μM and 1.0 μM respectively. The same does not apply with progesterone-treated primary male mouse hepatocytes, where FMO5 mRNA amounts are decreased by 27% and 7%, at concentrations of 0.1 μM and 0.5 μM respectively (Figure 3.8.2b). The physiological concentration of progesterone is approximately 13-79 nM in the luteal phase of pre-menopausal women (Dabrosin, 2005) and in pregnant mice the concentration is 30-50 nM (Milligan and Finn, 1997). At 0.1 μM, the progesterone concentration is on the upper limits of the physiological range for women and at least twice

as much for female mice. Lehmann et al., (1998) surmise therefore that progesterone is unlikely to be a natural ligand of hPXR as the accompanying EC_{50} values are >10 μM.

As explained in the introduction progesterone has already been shown to have modulating effects on the FMOs. This is particularly obvious during pregnancy in rabbits (Lee et al., 1995) where *FMO1* is induced in the liver and *FMO2* in the lung. *FMO5* has been shown to be induced in a progesterone receptor-dependant manner in a breast cancer cell line (Miller et al., 1997). Perhaps progesterone is acting through its own receptor and this may be the pathway through which *FMO5* expression is increased. Although progesterone is thought of as the hormone of pregnancy it has many other roles, such as neuroendocrine control and mediation of sexual behaviour (Andersen and Tufik, 2006). The difference in response to progesterone by the male and female hepatocytes is interesting and could be due to differential expression of progesterone receptor isoforms (A or B) in males and females. Progesterone receptor B was found to be the predominant form in female rat brain (Guerra-Araiza et al., 2000), and progesterone receptor A was the predominant form in male rat brain (Guerra-Araiza et al., 2001). Given that there is a different response to progesterone by these two isoforms (B is inductive, A is able to repress the B isoform (Vegeto et al., 1993)), it is possible that this is the reason for the differential response in male and female mouse hepatocytes. This could be the reason for the limited repression of FMO5 mRNA via progesterone observed in male mouse hepatocytes. Estrogen is also able to induce progesterone receptors in female rat brain (Parsons et al., 1980; Scott et al., 2002), as well as inducing the B isoform in human breast cancer cells in culture (Graham et al., 1995). Although the induction of *FMO5* expression has already been described in a progesterone receptor B-dependent manner (Guerra-Araiza and Camacho-Arroyo, 2000) , the progesterone receptor is expressed in low amounts in the liver (Perrot-Applanat et al., 1985). So although the effect of different concentrations of progesterone receptor is a credible reason for the differential induction of *FMO5*, the mediation by a receptor that is highly expressed in the liver cannot be dismissed. But this does not explain the differential induction between the sexes, since PXR (and CAR) (both highly expressed in the liver (Kliewer et al., 2000)) is described as sex-independent (Honkakoski et al., 2003; Waxman, 1999).

In summary it is probable that there are male-female differences in response to progesterone generally, as seen behaviorally in rats (Heinsbroek et al., 1987) but a difference in progesterone metabolism could be the underlying cause (Kato et al., 1971).

(a)

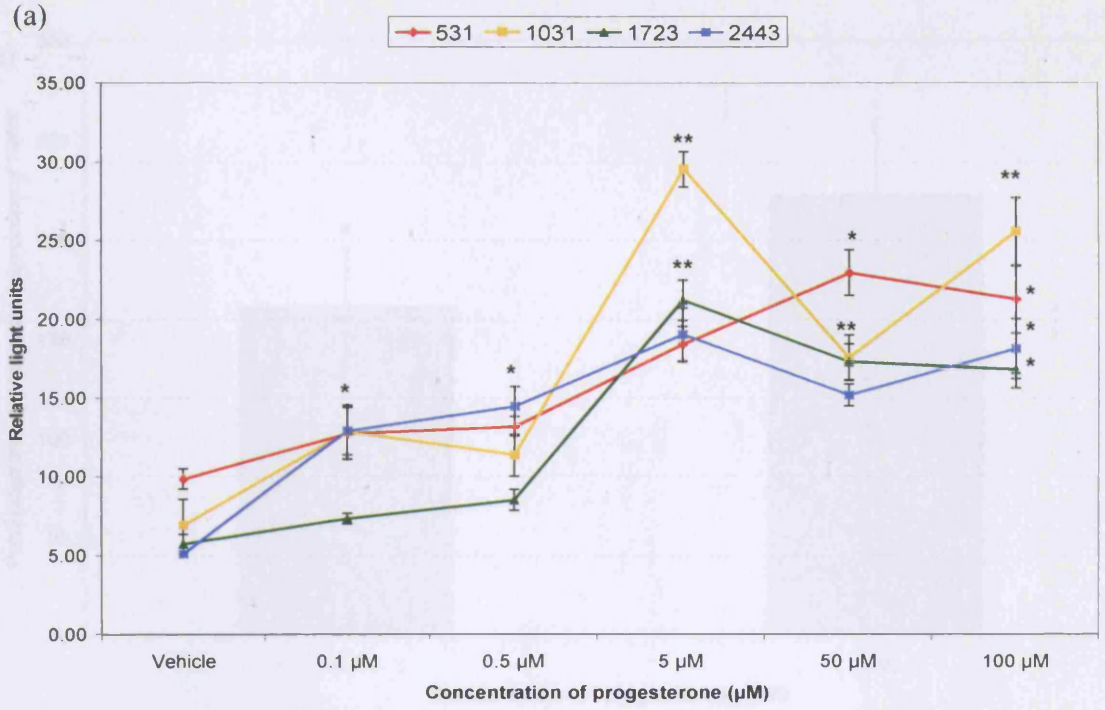

(b)

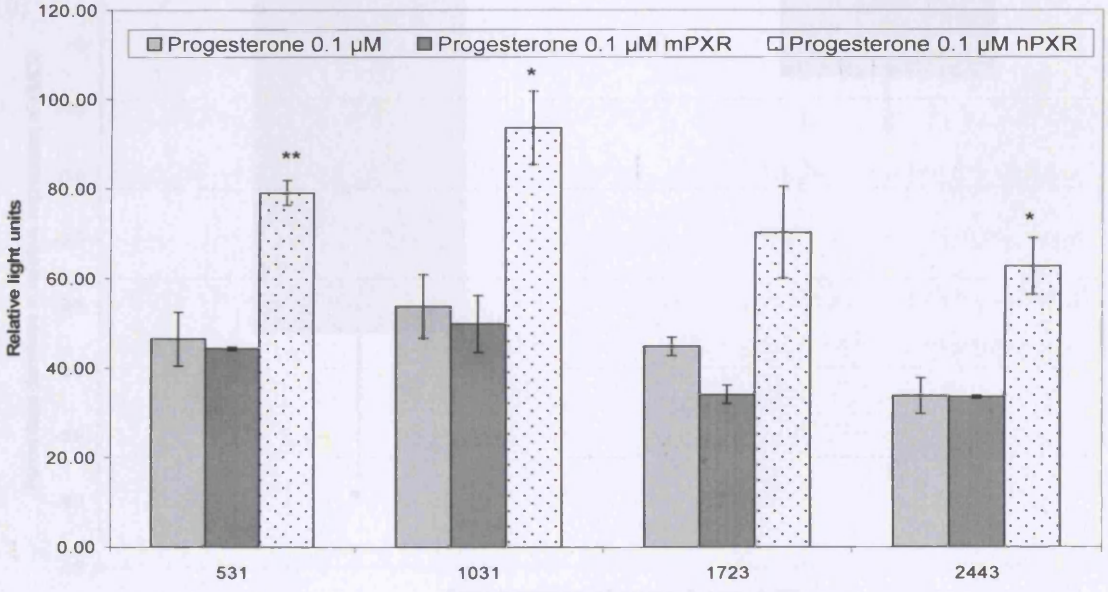

3.8.1 *Progesterone effects on FMO5 promoter constructs in HepG2 cells*

HepG2 cells were transfected with *FMO5* constructs and dosed with various concentrations of progesterone (a). HepG2 cells were co-transfected with *FMO5* constructs and mPXR or hPXR, the cells were then dosed with 0.1 µM progesterone (b). Significance is calculated from the vehicle where * is $p<0.05$ and ** is $p<0.005$. Error bars are SEM.

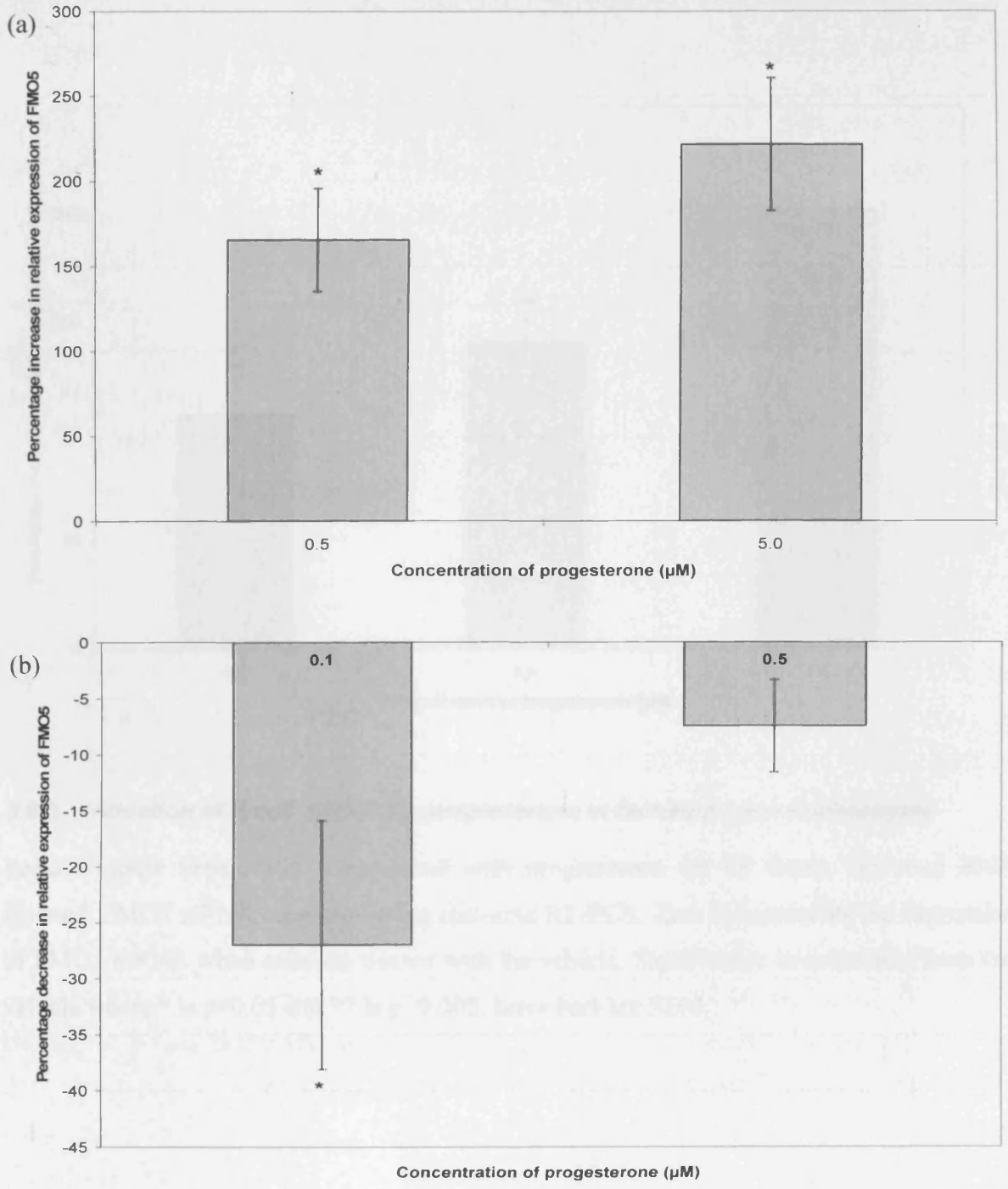

3.8.2 Progesterone effects on FMO5 mRNA in HepG2 and male mouse hepatocytes

HepG2 cells (a) and male mouse hepatocytes (b) were dosed with progesterone for 24 hours, the total RNA isolated; FMO5 mRNA measured using real-time RT-PCR. Zero % represents the expression of FMO5 mRNA when cells are treated with the vehicle. Significance is calculated from the vehicle where * is $p<0.05$ and ** is $p<0.005$. Error bars are SEM.

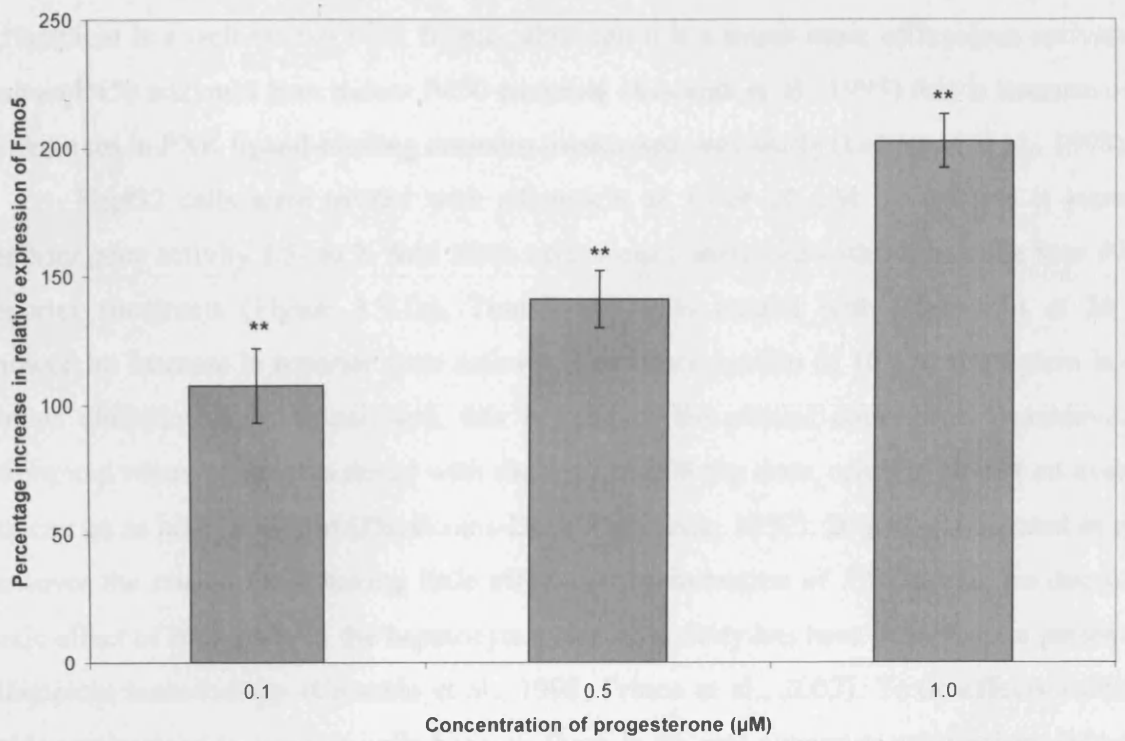

3.8.3 *Induction of Fmo5 mRNA by progesterone in female mouse hepatocytes*

Female mouse hepatocytes were dosed with progesterone for 24 hours, the total RNA isolated; FMO5 mRNA measured using real-time RT-PCR. Zero % represents the expression of FMO5 mRNA when cells are treated with the vehicle. Significance is calculated from the vehicle where * is $p<0.05$ and ** is $p<0.005$. Error bars are SEM.

3.9 Rifampicin induces *FMO5* expression, and FMO5 mRNA in both human and mouse

Rifampicin is a well-known PXR ligand, although it is a much more efficacious activator of human P450 enzymes than rodent P450 enzymes (Kocarek et al., 1995) this is because of the differences in PXR ligand-binding domains mentioned previously (Lehmann et al., 1998).

HepG2 cells were treated with rifampicin at 10 or 20 μM. At 10 μM it increases reporter gene activity 1.5- to 2- fold when cells were transfected with each of the four *FMO5* reporter constructs (Figure 3.9.1a). Transfected cells treated with rifampicin at 20 μM showed no increase in reporter gene activity. The concentration of 10 μM rifampicin is used almost ubiquitously by researchers, this is because the plasma concentration achieved by rifampicin when a patient is dosed with the typical 600 mg dose, reaches 10 μM on average, but can go as high as 40 μM (Physicians-Desk-Reference, 1992). 20 μM is also used *in vitro*, however the reason for it having little effect on the induction of *FMO5* may be due to the toxic effect of rifampicin in the hepatocytes. Hepatotoxicity has been described in patients on rifampicin monotherapy (Cancado et al., 1998; Prince et al., 2002). Toxic effects would be more pronounced in isolated cells because there is no real excretory mechanism. Although the cells appeared healthy, they were only dosed for 24 hours, had treatment continued, any toxic effects would have been observed in the morphology of the hepatocytes.

HepG2 cells were co-transfected with the *FMO5* reporter constructs and hPXR or mPXR and dosed with 0.5 μM or 10 μM rifampicin (Figure 3.9.1b). Both 0.5 and 10 μM rifampicin induce reporter gene activity in all four constructs. The two PXR homologs increase reporter gene activity even further, with mPXR inducing as much as hPXR. This is interesting given rifampicin is supposed to have very little effect on the induction of CYP3A4 through PXR in mice (Jones et al., 2000). There is a clear response to PXR in cells transfected with *FMO5* reporter gene constructs and most-importantly the increase in activity is via rifampicin, which is one of the most potent and specific PXR ligands (Kocarek et al., 1995), with an EC50 value of ~800 nM (Lehmann et al., 1998).

FMO5 mRNA isolated from rifampicin-treated (10 μM) female mouse hepatocytes and HepG2 cells was induced 206% and 231% respectively (Figure 3.9.2a). FMO5 mRNA is increased only 35% in male hepatocytes treated with 10 μM rifampicin. Given the apparent lack of induction of CYP3A4 through PXR in mice with rifampicin (Jones et al., 2000), this

profound increase in FMO5 mRNA observed in female mouse hepatocytes is surprising. However, there are examples of induction of the PXR responsive p-glycoprotein in mice after treatment with rifampicin (Schuetz et al., 1996; Wrighton et al., 1985). CYP3A11 and CYP3A13 are also induced in mouse liver after rifampicin treatment (Yanagimoto et al., 1997).

PXR as explained is expressed in a sex-independent manner. The difference in xenobiotic metabolism between the sexes is complex, but overall the expression of metabolising enzymes can be mediated by growth hormone (Waxman and O'Connor, 2006). A greater induction of CYP3A4 has been observed in female human liver than in male (Gorski et al., 2003) which could account for the higher rate of clearance for some drugs often seen in female patients (Hulst et al., 1994; Kahan et al., 1986). Interestingly in the same study CYP3A4 was induced to a greater extent in male intestine rather than female, further complicating the sex-dependent dichotomy of xenobiotic metabolism.

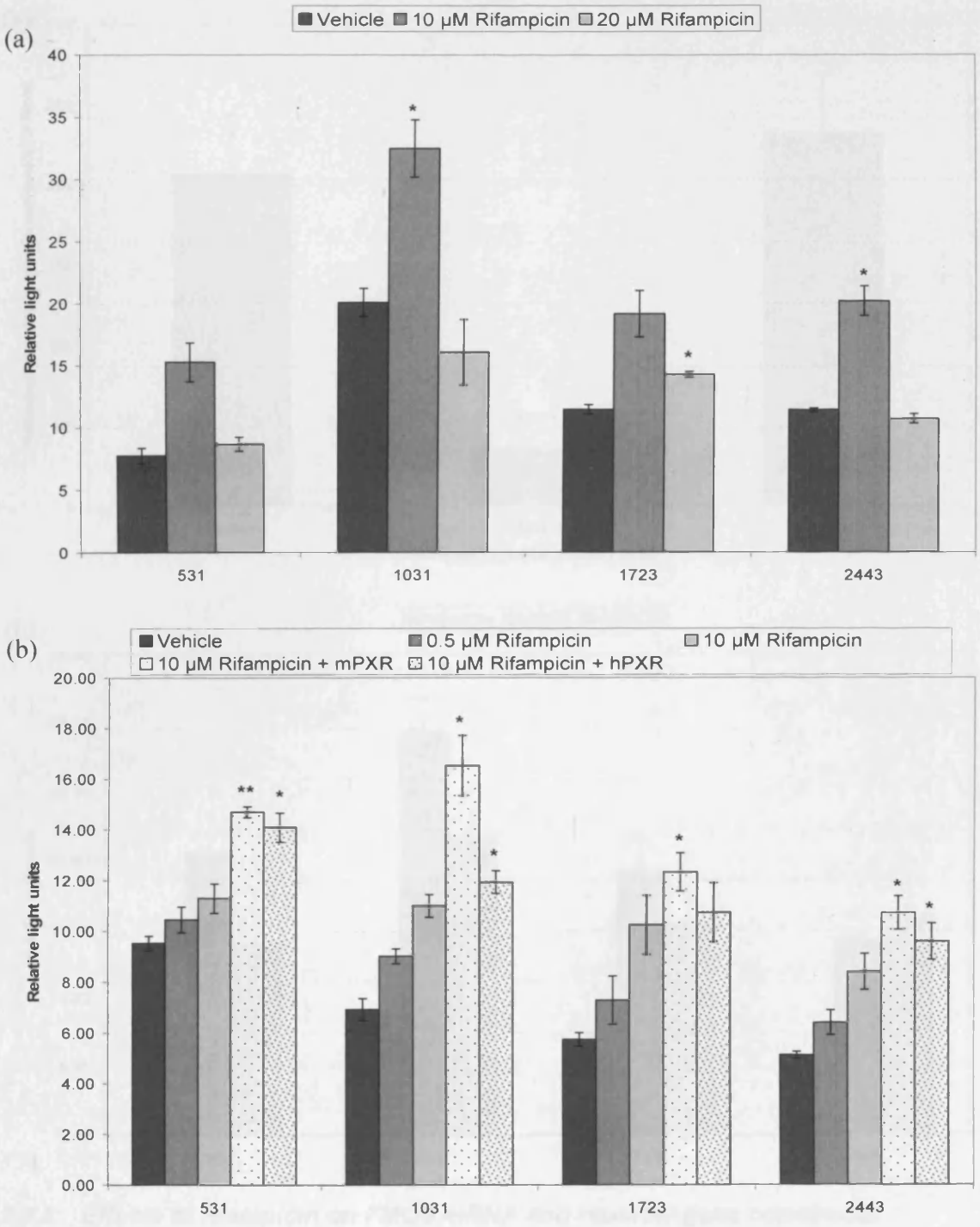

3.9.1 *Effects of rifampicin on FMO5 promoter constructs in HepG2 cells*

HepG2 cells were transfected with *FMO5* constructs, and dosed with rifampicin (10 µM or 20 µM) (a). HepG2 cells were transfected with *FMO5* constructs alone or with 0.1 µg hPXR or 0.1 µg mPXR, then dosed with 0.5 µM or 10 µM rifampicin (b). Significance is calculated from the vehicle where * is $p<0.05$ and ** is $p<0.005$. Error bars are SEM.

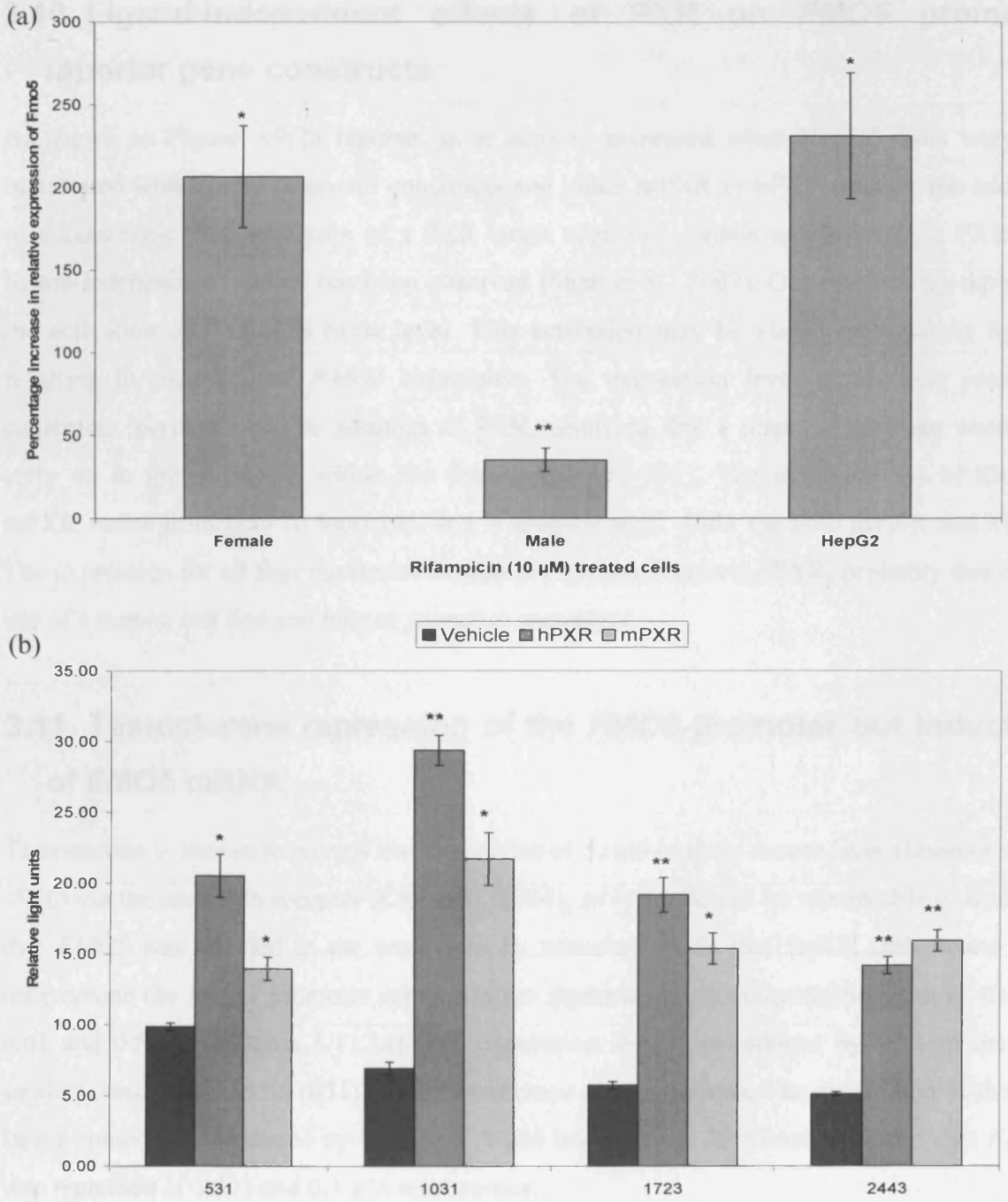

3.9.2 Effects of rifampicin on FMO5 mRNA and reporter gene constructs

HepG2 cells, female and male hepatocytes were dosed with rifampicin for 24 hours, the total RNA isolated; FMO5 mRNA measured using real-time RT-PCR. Zero % represents the expression of FMO5 mRNA when cells are treated with the vehicle (a). HepG2 cells were co-transfected with *FMO5* constructs and hPXR or mPXR (b). Significance is calculated from the vehicle where * is $p<0.05$ and ** is $p<0.005$. Error bars are SEM.

3.10 Ligand-independent effects of PXR on *FMO5* promoter reporter gene constructs

As shown in Figure 3.9.2b reporter gene activity increased when HepG2 cells were co-transfected with *FMO5* promoter constructs and either mPXR or hPXR without the addition of a xenobiotic. The induction of a PXR target sequence-containing plasmid via PXR in a ligand-independent manner has been observed (Shah et al., 2007). Our results may represent the activation of PXR at a basal level. This activation may be via an endogenous ligand, resulting in induction of *FMO5* expression. The expression level of all four promoter constructs increase with the addition of PXR, implying that a response element would lie early on in the sequence, within the first construct (-531). The induction via hPXR and mPXR varies from two- to four-fold, and is greatest with -1031 via both mPXR and hPXR. The expression for all four constructs is seen at a greater level via hPXR, probably due to the use of a human cell line and human promoter sequences.

3.11 Testosterone repression of the *FMO5* promoter but induction of FMO5 mRNA

Testosterone is known to repress the expression of *Fmo3* in male mouse liver (Dannan et al., 1986) via the androgen receptor (Chanden, 2004), so it would not be remarkable to discover that *FMO5* was affected in the same way by testosterone. In the HepG2 cells dosed with testosterone the *FMO5* promoter constructs are repressed at all concentrations tested (0.001, 0.01 and 0.5 μM) (Figure 3.11.1a). The expression levels are reduced by 50% in the two smaller constructs (-531, -1031) by all testosterone concentrations. The expression of the two larger constructs is reduced by 75% by 0.5 μM testosterone. Dr Chandan found that *FMO3* was repressed at 0.001 and 0.1 μM testosterone.

The repression of FMO5 by testosterone is seen also when the mRNA is measured from HepG2 cells (Figure 3.11.2a). At the concentrations of 0.01 μM and 1.0 μM, *FMO5* expression is repressed 26% and 16% respectively. Comparing these values to those observed using the promoter assay, at 0.01 μM and 0.5 μM the *FMO5* promoter fragments were repressed to a greater extent, 40-50% and 50-80% respectively.

Dosing primary mouse hepatocytes with testosterone had the opposite effect to the HepG2 cells with regard to *FMO5* expression. Mouse FMO5 mRNA was induced 78%, 70% and 210% from the vehicle at 0.001 μM, 0.01 μM and 0.5 μM testosterone respectively in male hepatocytes (Figure 3.11.2b) and induced 96% at 0.01 μM in female hepatocytes (Figure 3.11.1b). Clearly there is a great deal of difference in the response to testosterone in the human cell line and in the mouse *ex vivo* system. Testosterone is repressing *FMO5* reporter gene activity and FMO5 mRNA in the human cell line (HepG2), but testosterone is inducing FMO5 mRNA in the primary mouse hepatocytes. These differences could be explained by differences in human versus mouse or cell line versus tissue culture. The different availability of liver-specific transcription factors to mediate this response by testosterone could be pertinent, the mouse hepatocytes being more closely related to an *in vivo* liver and therefore having a greater availability of these factors than the HepG2 cells (Wilkening et al., 2003).

Androgens are known to be able to repress mRNA levels of genes such as the transforming growth factor β (Kyprianou and Isaacs, 1989) and the testosterone-repressed prostate message TRPM-2 (Leger et al., 1987) as well as *Cyp17* in mouse MA-10 tumor Leydig cells (Burgos-Trinidad et al., 1997). The mechanism by which the androgen receptor is able to repress genes is unclear, but the binding of the receptor to the promoter is required for the repression, certainly in the case of *Cyp17*, in order to prevent cAMP associated up-regulation.

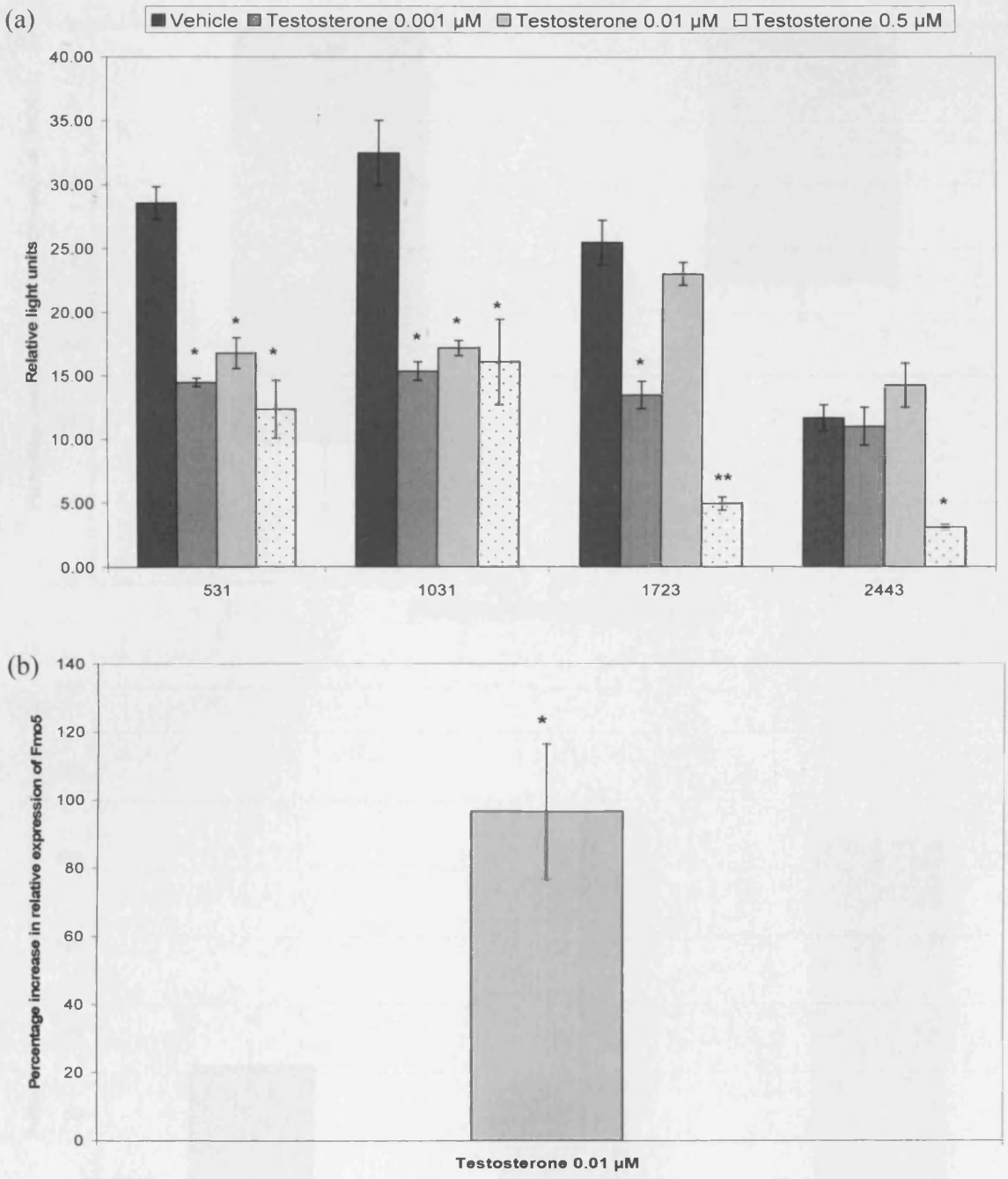

3.11.1 Effects of testosterone on the FMO5 promoter and on Fmo5 mRNA

HepG2 cells were transfected with *FMO5* constructs, then dosed with 0.001 µM, 0.01 µM or 0.5 µM testosterone (a). Female mouse hepatocytes dosed with testosterone for 24 hours, the total RNA isolated; FMO5 mRNA measured using real-time RT-PCR (b). Zero % represents the expression of FMO5 mRNA when cells are treated with the vehicle. Significance is calculated from the vehicle where * is $p<0.05$ and ** is $p<0.005$. Error bars are SEM.

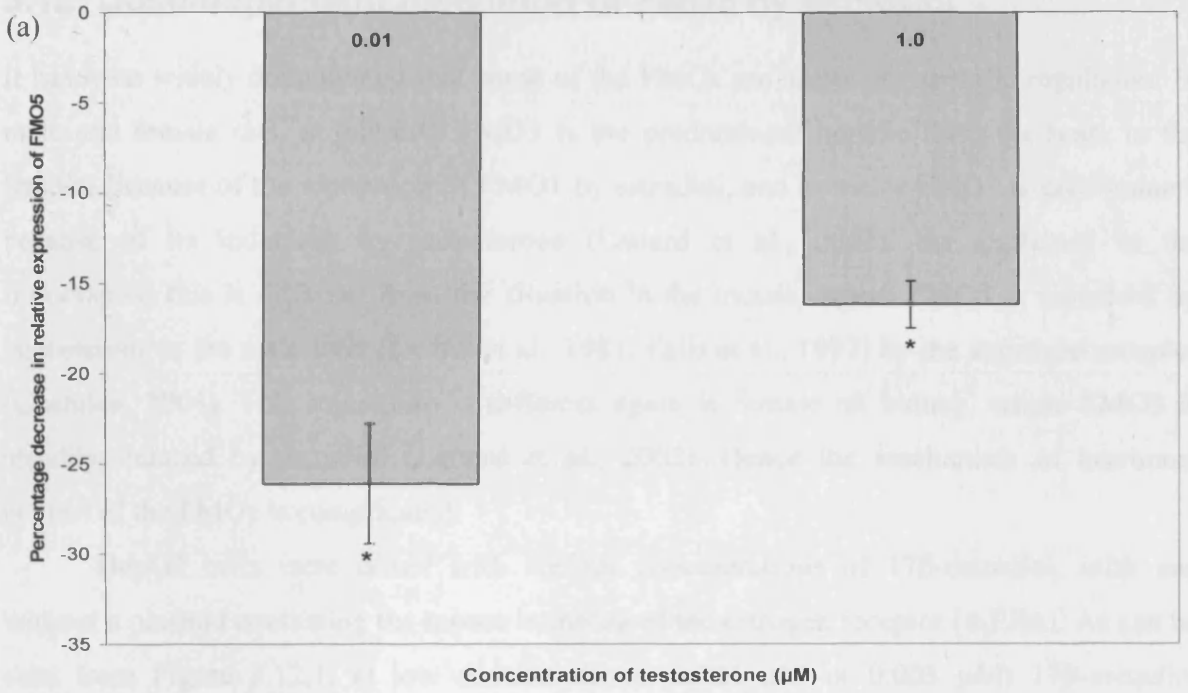

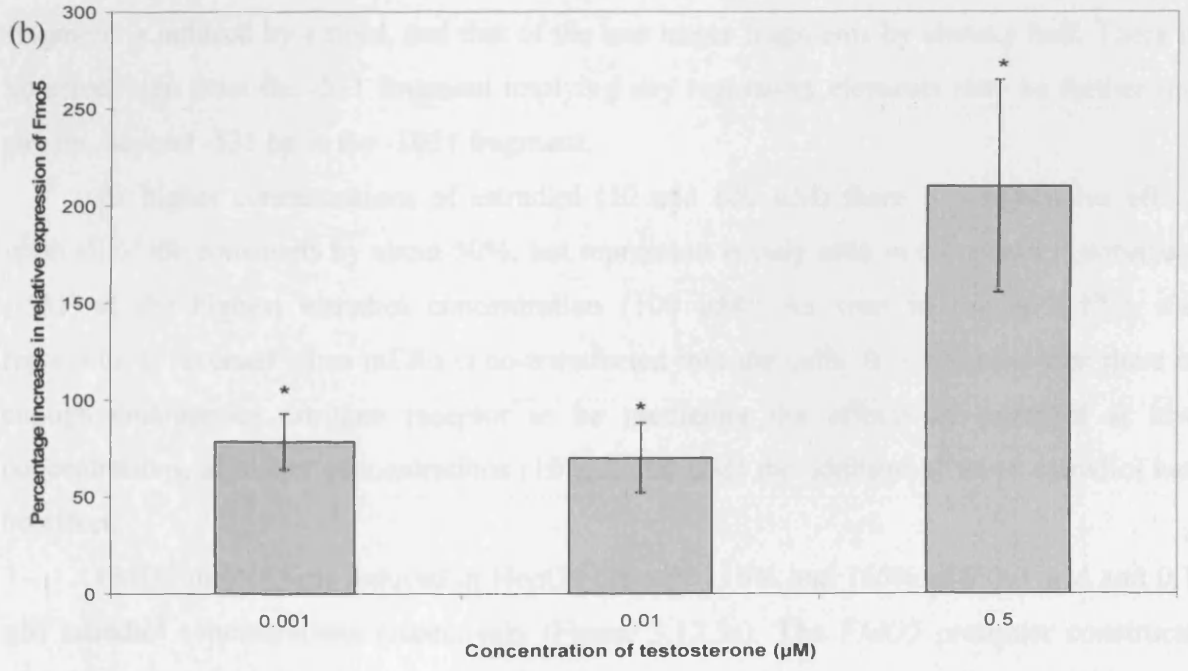

3.11.2 Testosterone effects on FMO5 mRNA in HepG2 and male mouse hepatocytes

HepG2 cells (a) and male mouse hepatocytes (b) were dosed with testosterone for 24 hours, the total RNA isolated; FMO5 mRNA measured using real-time RT-PCR. Zero % represents the expression of FMO5 mRNA when cells are treated with the vehicle. Significance is calculated from the vehicle where * is $p<0.05$ and ** is $p<0.005$. Error bars are SEM.

3.12 Dose-dependent mediation of *FMO5* by estradiol

It has been widely documented that some of the FMOs are under sex specific regulation. In male and female rats, at maturity FMO3 is the predominant hepatic form for both, in the females because of the repression of FMO1 by estradiol, and in males FMO3 is predominant because of its induction by testosterone (Lattard et al., 2002). As explained in the introduction this is different from the situation in the mouse, where FMO3 is repressed by testosterone in the male liver (Duffel et al., 1981; Falls et al., 1997) by the androgen receptor (Chanden, 2004). This regulation is different again in female rat kidney, where FMO3 is steadily induced by estradiol (Lattard et al., 2002). Hence the mechanism of hormonal control of the FMOs is complicated.

HepG2 cells were dosed with various concentrations of 17β-estradiol, with and without a plasmid containing the mouse homolog of the estrogen receptor (mERα). As can be seen from Figure 3.12.1, at low concentrations (0.001 μM or 0.003 μM) 17β-estradiol induces the expression of *FMO5*. At 0.003 μM estradiol the construct containing the -1031 fragment is induced by a third, and that of the two larger fragments by about a half. There is no effect seen from the -531 fragment implying any regulatory elements may be further up-stream, beyond -531 bp in the -1031 fragment.

At higher concentrations of estradiol (10 and 100 μM) there is a repressive effect upon all of the constructs by about 50%, but repression is only seen in the smallest construct (-531) at the highest estradiol concentration (100 μM). As seen in Figure 3.12.2, the repression is reversed when mERα is co-transfected into the cells. It is probable that there is enough endogenous estrogen receptor to be mediating the effects of estradiol at low concentrations, at higher concentrations (10 and 100 μM) the addition of more estradiol has no effect.

FMO5 mRNA was induced in HepG2 cells by 116% and 165% at 0.001 μM and 0.1 μM estradiol concentrations respectively (Figure 3.12.3a). The *FMO5* promoter constructs are also induced in HepG2 cells by 22-85% and 46-129% at 0.001 μM and 0.003 μM respectively. In male hepatocytes FMO5 mRNA was induced 52%, 25%, 55% and 140% at 0.001 μM and 0.01 μM, 0.5 μM and 1.0 μM estradiol respectively (Figure 3.12.3b). The FMO5 mRNA from female hepatocytes was induced 126 % but only at 0.003 μM. At the higher concentrations of 0.03 μM and 0.5 μM the mRNA is repressed 37% and 13%

respectively (Figure 3.12.4). The promoter constructs were also repressed at the higher concentration of 0.1 μM. So in comparison, 0.5 μM estradiol represses *Fmo5* in females, but induced *Fmo5* expression in males. It is likely that this is due to the total levels of estradiol already within each male and female liver. In rats the circulating level of estradiol is nearly twice as much in females than in males (Rahimian et al., 1997). So the addition of estradiol to female hepatocytes could result in an increased total concentration of estradiol when compared to the males, leading to repression in females.

The estrogen receptor is able to repress transcription but its repressive effect has not been widely studied and is not fully understood. ER represses tumor-necrosis factor-α (TNFα) by binding to an AP-1 like site (TGTTTGT) in the TNFα promoter with co-activators such as the glucocorticoid receptor interacting protein-1 (An et al., 1999).

With regard to ER consensus sites in the *FMO5* promoter, there are several half-sites (see Section 3.1.4). Although they are not complete sites this may not be a concern with regard to the promoter analysis, since it has been reported that ER will bind and meditate transcription of genes through Sp1 sites (Saville et al., 2000), of which there are two within the first 200 bp, conserved between the mouse and human (Section 3.1.4). A third is approximately 1000 bp from the *FMO5* start site. Since any inductive response to estrogen is only seen in the larger three constructs this third Sp1 site would be the prime candidate. Although no inductive response is seen from the smallest fragment (-531), repression is observed in this fragment in cells dosed with a higher concentration of estradiol (50 or 100 μM). Implying the mediation by estradiol is through two different mechanisms.

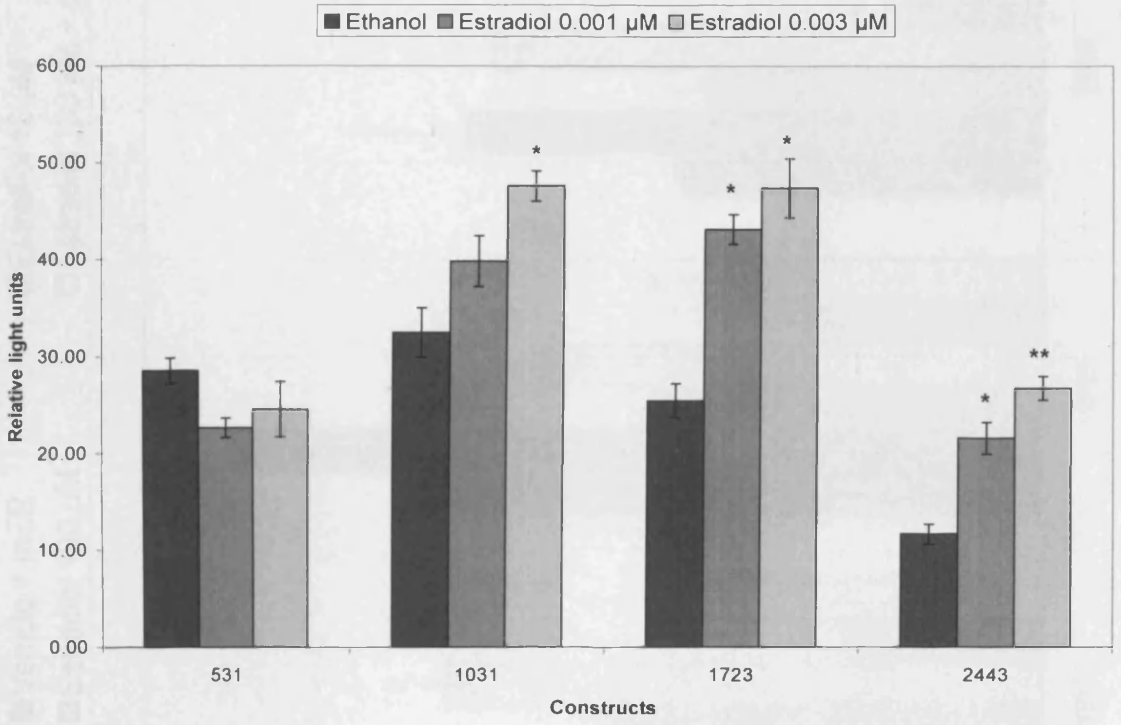

3.12.1 Effects of 17β-estradiol on FMO5 promoter constructs in HepG2 cells

HepG2 cells were transfected with *FMO5* constructs and dosed with 0.001 µM or 0.003 µM 17β-estradiol. Significance is calculated from the vehicle where * is $p<0.05$. Error bars are SEM.

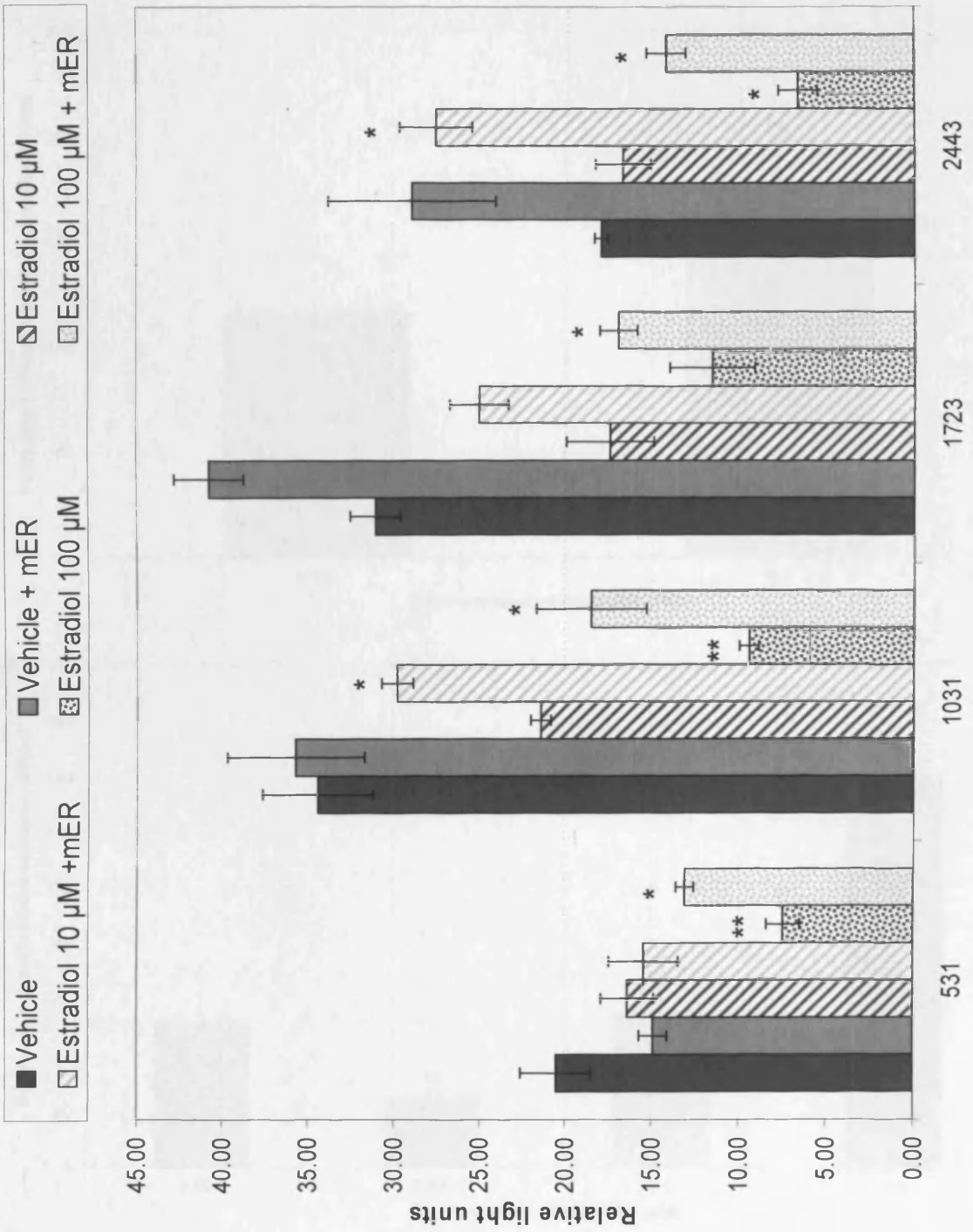

3.12.2 Effects of estradiol on FMO5 promoter constructs in HepG2 cells co-transfected with mERα

HepG2 cells were co-transfected with *FMO5* constructs with and without mERα, then dosed with 10 µM or 100 µM 17β-estradiol. Significance is calculated from the vehicle where * is $p<0.05$ and ** is $p<0.005$. Error bars are SEM.

(a)

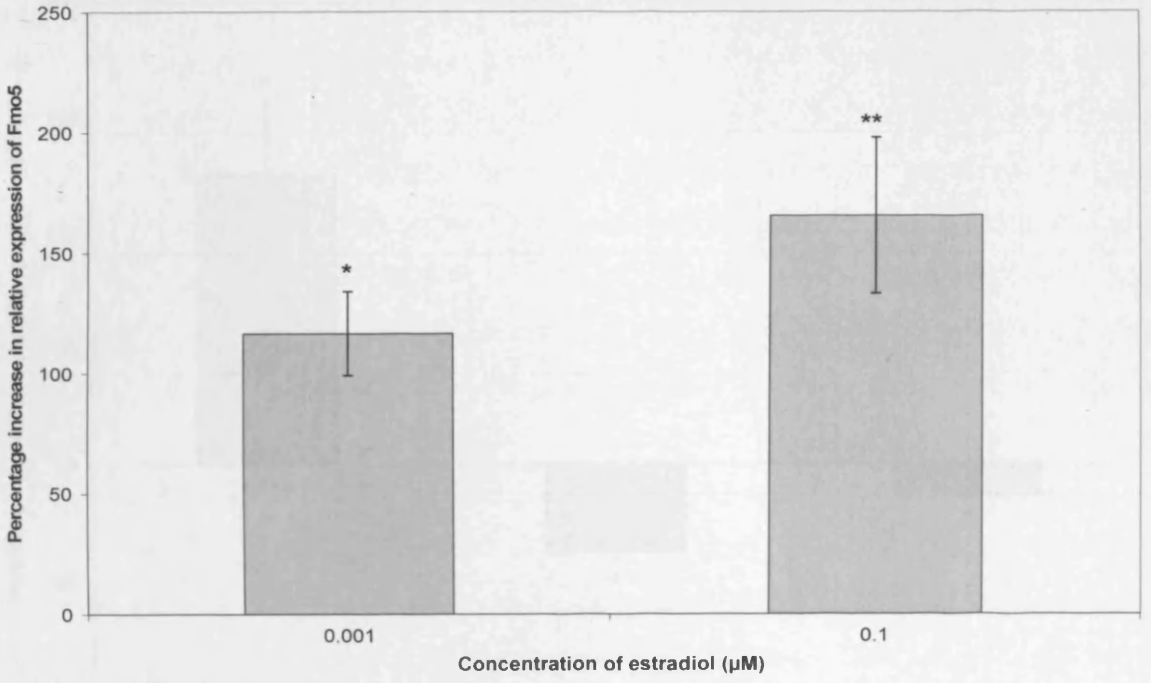

(b)

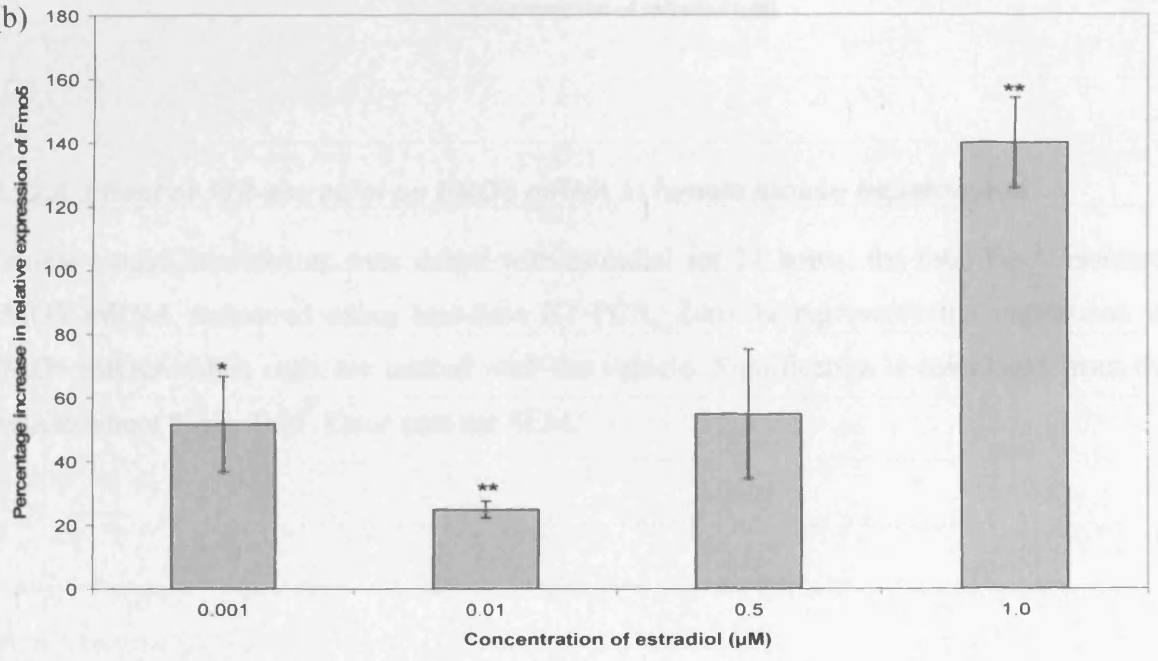

3.12.3 17β-estradiol effects on FMO5 mRNA in HepG2 and male mouse hepatocytes

HepG2 cells (a) and male mouse hepatocytes (b) were dosed with estradiol for 24 hours, total RNA isolated. FMO5 mRNA measured using real-time RT-PCR. Zero % represents the expression of FMO5 mRNA when cells are treated with the vehicle. Significance is calculated from the vehicle where * is $p<0.05$ and ** is $p<0.005$. Error bars are SEM.

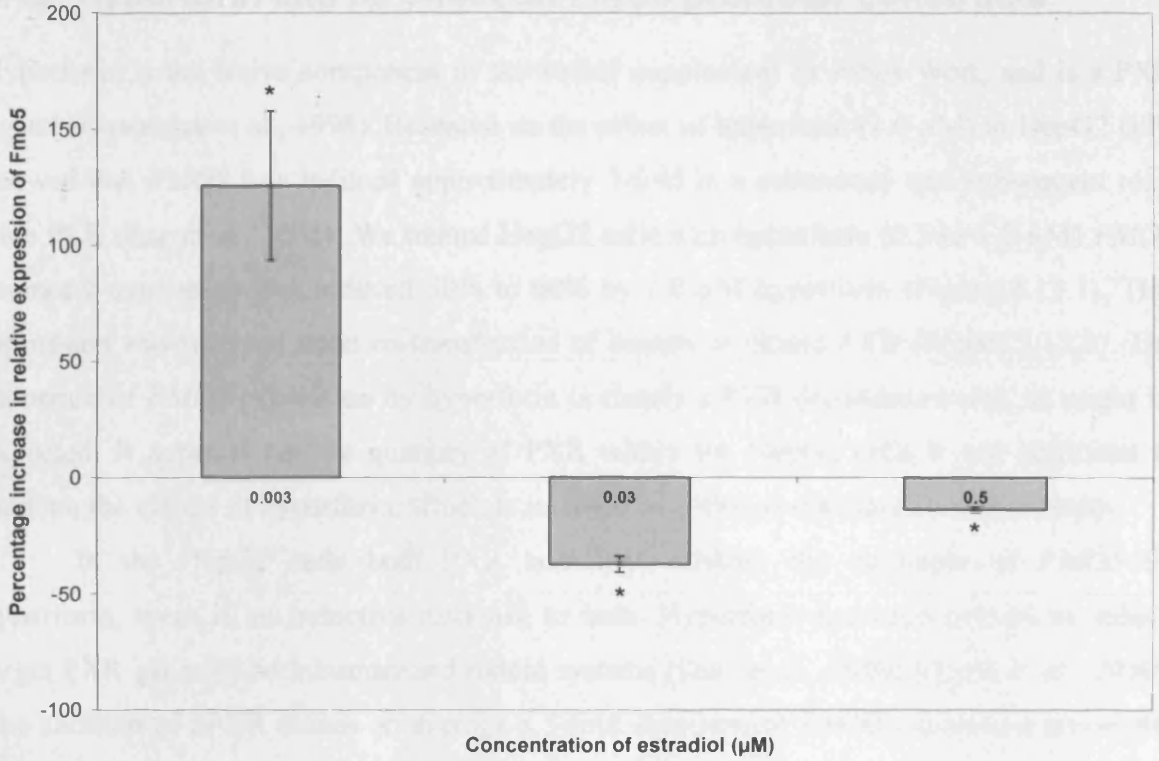

3.12.4 Effect of 17β-estradiol on FMO5 mRNA in female mouse hepatocytes

Female mouse hepatocytes were dosed with estradiol for 24 hours, the total RNA isolated; FMO5 mRNA measured using real-time RT-PCR. Zero % represents the expression of FMO5 mRNA when cells are treated with the vehicle. Significance is calculated from the vehicle where * is $p<0.05$. Error bars are SEM.

3.13 Hyperforin and its effect on *FMO5* promoter constructs

Hyperforin is the active component of the herbal supplement St Johns Wort, and is a PXR ligand (Chatterjee et al., 1998). Research on the effect of hyperforin (1.0 μM) in HepG2 cells showed that *FMO5* was induced approximately 3-fold in a microarray and subsequent real-time PCR (Rae et al., 2001). We treated HepG2 cells with hyperforin (0.5 or 1.0 μM) *FMO5* promoter expression was reduced 30% to 60% by 1.0 μM hyperforin (Figure 3.13.1). This repression was reversed upon co-transfection of human or mouse PXR (Figure 3.13.2). The induction of *FMO5* expression by hyperforin is clearly a PXR-dependent event, as might be expected. It appears that the quantity of PXR within the HepG2 cells is not sufficient to mediate the effects of hyperforin, which is rectified with the co-transfection experiments.

In the HepG2 cells both PXR homologs mediate the induction of *FMO5* by hyperforin, there is an inductive response to both. Hyperforin has been proven to induce target PXR genes in both human and rodent systems (Durr et al., 2000; Moore et al., 2000). The addition of hPXR causes on average a 3-fold induction of *FMO5* expression across the promoter fragments whereas mPXR induces 2-fold across the fragments. The potency of hyperforin for hPXR over mPXR has been described (Vignati et al., 2004).

The treatment of HepG2 cells or primary mouse hepatocytes resulted in no induction of *FMO5* mRNA. It is possible that a longer treatment time is required to see a response. This has been described in mice treated with St John's Wort, where an effect was only seen after three weeks of treatment (Bray et al., 2002), the original study saw an induction of CYP3A after two weeks of treatment (Durr et al., 2000). In an *in vitro* setting however, hyperforin was found to be a potent activator of hPXR (more so than mPXR) in HepG2 cells (Vignati et al., 2004) only after 24 hours at 1 μM.

It is likely then that because an induction of *FMO5* reporter constructs by hyperforin is only observed when hPXR and mPXR is added that the amount of PXR in the HepG2 cells and hepatocytes is the cause of this lack of induction of mRNA.

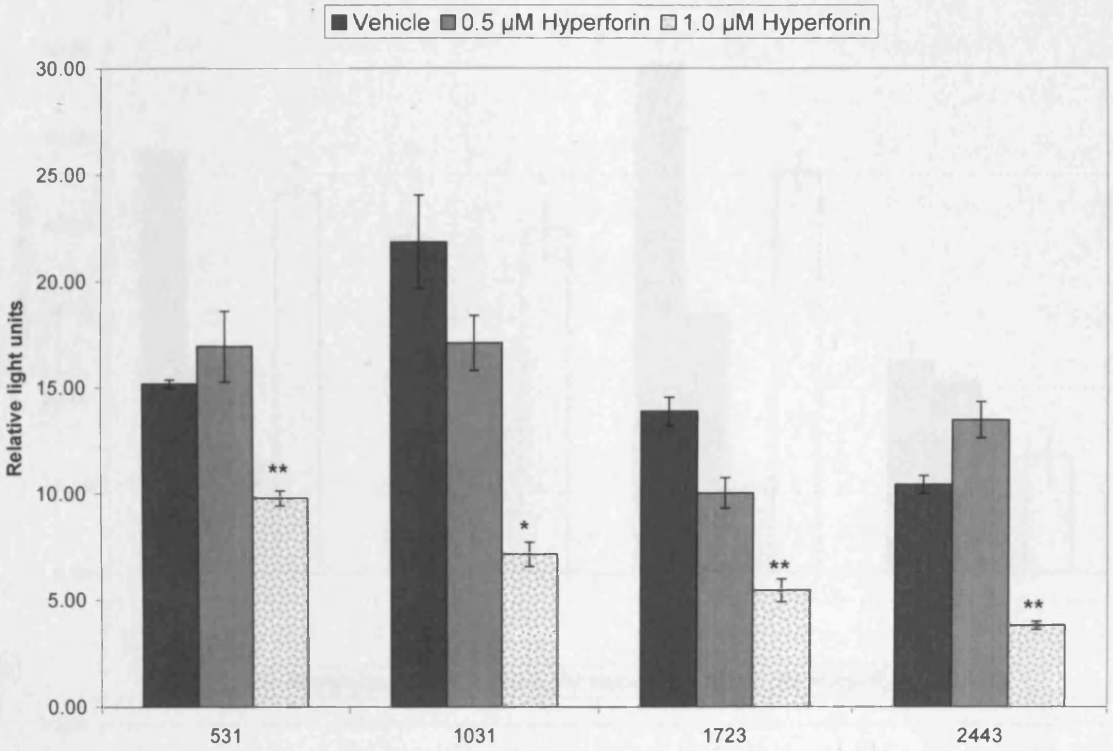

3.13.1 The repression of FMO5 promoter constructs by hyperforin in HepG2 cells

HepG2 cells were transfected with *FMO5* constructs, then dosed with 0.5 µM or 1 µM hyperforin. Significance is calculated from the vehicle where * is $p<0.05$ and ** is $p<0.005$. Error bars are SEM.

(a)

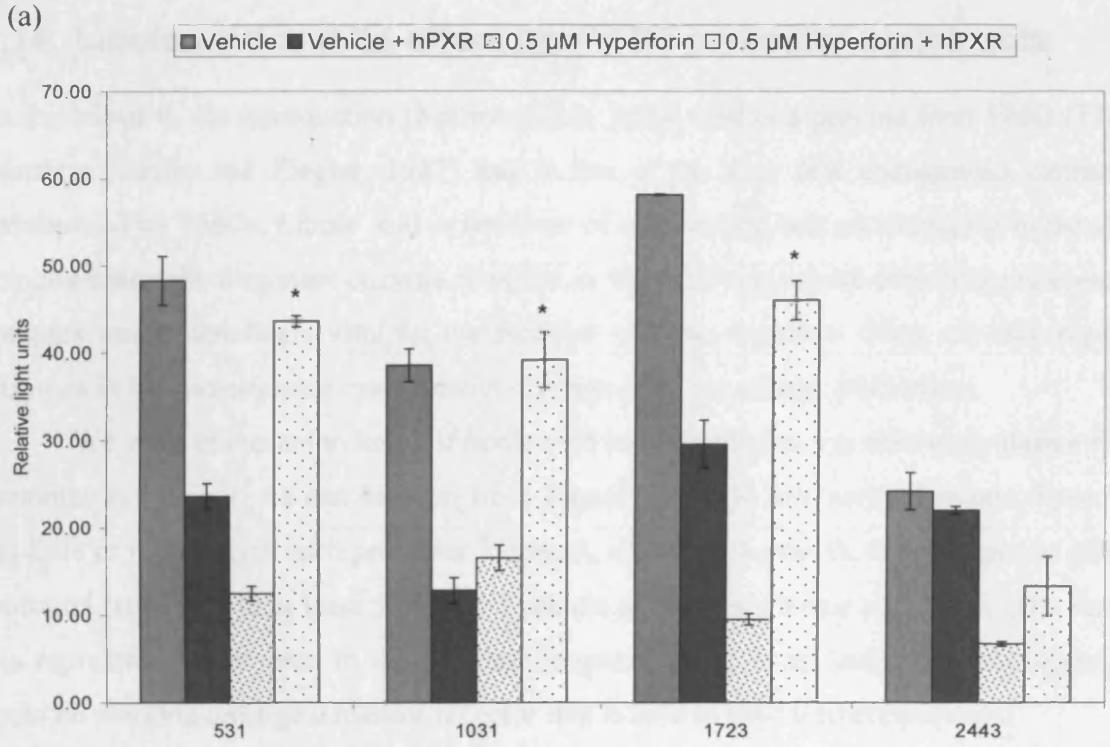

(b)

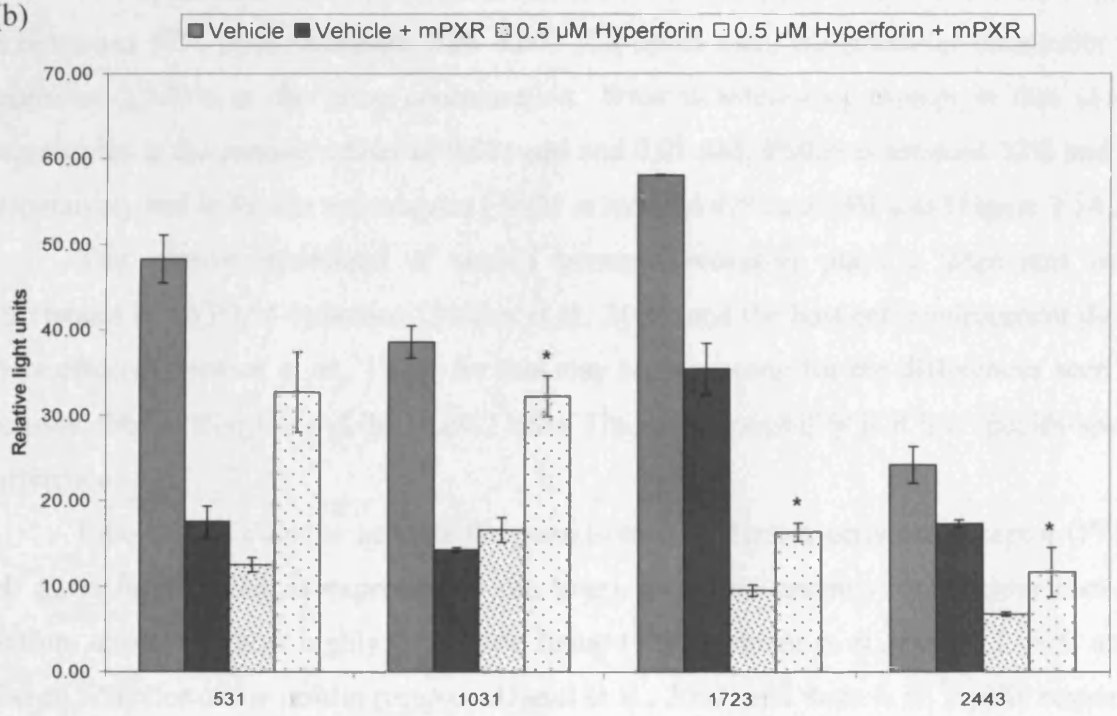

3.13.2 The effect of hyperforin and hPXR or mPXR on the FMO5 promoter

HepG2 cells were co-transfected with *FMO5* constructs with or without hPXR (a) or mPXR (b) and dosed with 0.5 µM hyperforin. Significance is calculated from the vehicle where * is $p<0.05$. Error bars are SEM.

3.14 Lipoic acid and its effect on *FMO5* promoter constructs

As explained in the introduction (Section 1.14), lipoic acid is a porcine liver FMO (FMO1) substrate (Taylor and Ziegler, 1987) and is one of the very few endogenous compounds metabolised by FMOs. Lipoic acid in the form of a lipoamide acts as a cofactor in the alpha-ketoglutarate dehydrogenase enzyme complex as well as the pyruvate dehydrogenase enzyme complex and is absolutely vital for the function of these enzymes. They are two important enzymes in the oxaloacetate cycle, obviously important for energy production.

We were interested to know if lipoic acid in its free form was able to modulate *FMO5* promoter expression. As can be seen from Figure 3.14.1 at low concentrations, lipoic acid has little or no effect on each promoter fragment, at 0.5 μM however, it does have an effect, a profound repression to at least 50% of the vehicle on the three larger constructs. The fact that this repression is not seen in the smallest fragment (531) is an indication that lipoic acid could be working through a nuclear receptor that is able to bind further upstream.

In HepG2 cells the mRNA reflects the results from the promoter assay. FMO5 mRNA is repressed 57% upon treatment with 0.001 μM lipoic acid, the promoter constructs were repressed 22-40% at the same concentration. What is interesting though is that in male hepatocytes at the concentrations of 0.001 μM and 0.01 μM, FMO5 is induced 72% and 33% respectively and in female hepatocytes FMO5 is induced 92% at 0.001 μM (Figure 3.14.2).

The relative abundance of steroid hormone receptors plays a large part in any differences in CYP3A4 induction (Swales et al., 2003) and the host cell environment dictates these effects (Barwick et al., 1996). So this may be the reason for the differences seen here between the hepatocytes and the HepG2 cells. The other possibility is it is a species-specific difference.

Lipoic acid is able to activate the peroxisome proliferator-activated receptor (PPAR), the alpha form (which is expressed in the liver), but more potently the gamma form, the isoform expressed most highly in adipose tissue (Venkatraman et al., 2004). Lipoic acid is also an activator of the insulin receptor (Diesel et al., 2007) and there is an insulin responsive sequence in the mouse *Fmo5* promoter (Section 3.1.4).

(a)

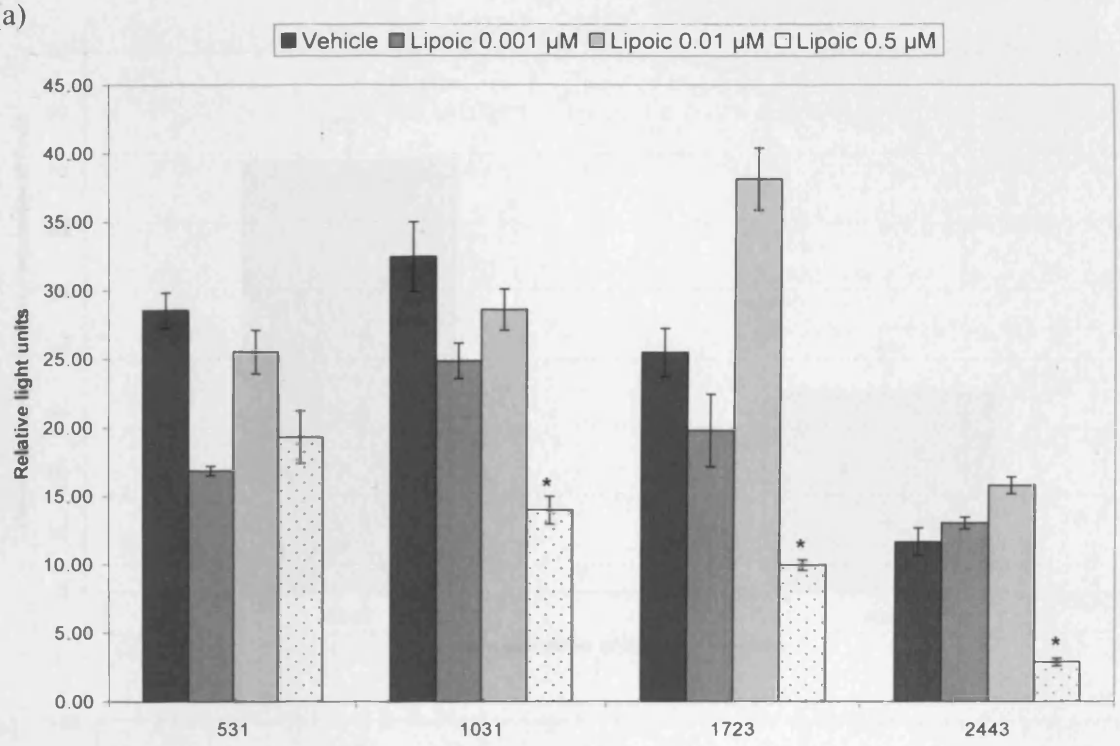

(b)

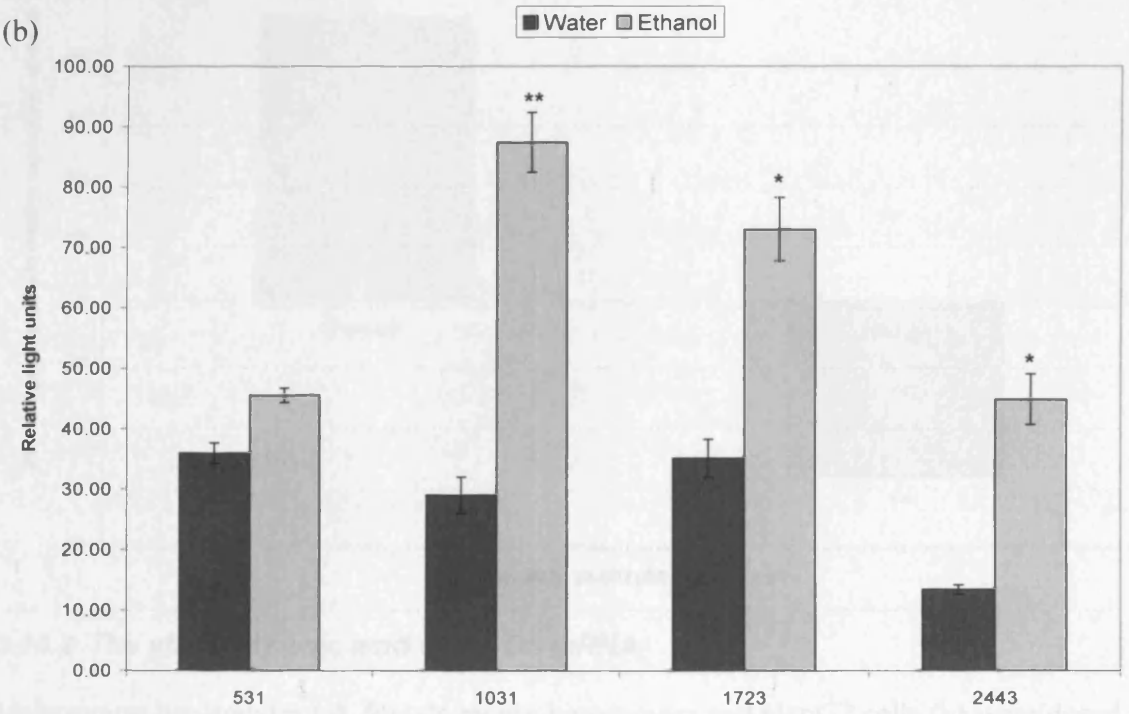

3.14.1 The effect of lipoic acid or ethanol on the FMO5 promoter

HepG2 cells were transfected with *FMO5* constructs and dosed with 0.001 µM or 0.01 µM lipoic acid (a) or ethanol (b) for 24 hours. Significance is calculated from the vehicle where * is $p<0.05$. Error bars are SEM.

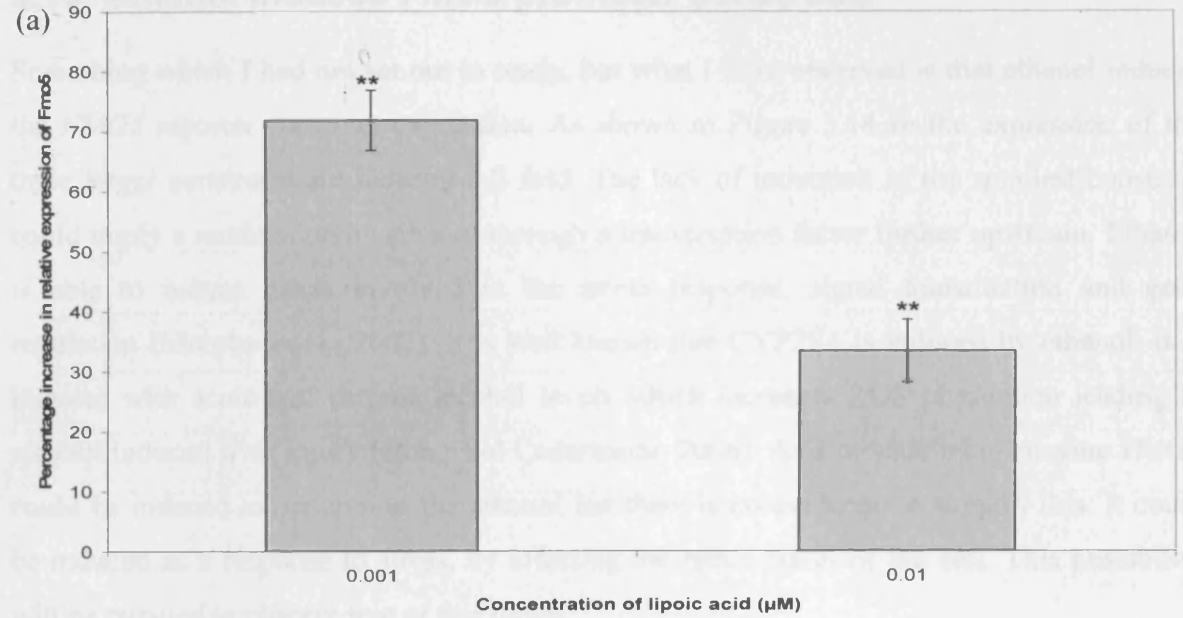

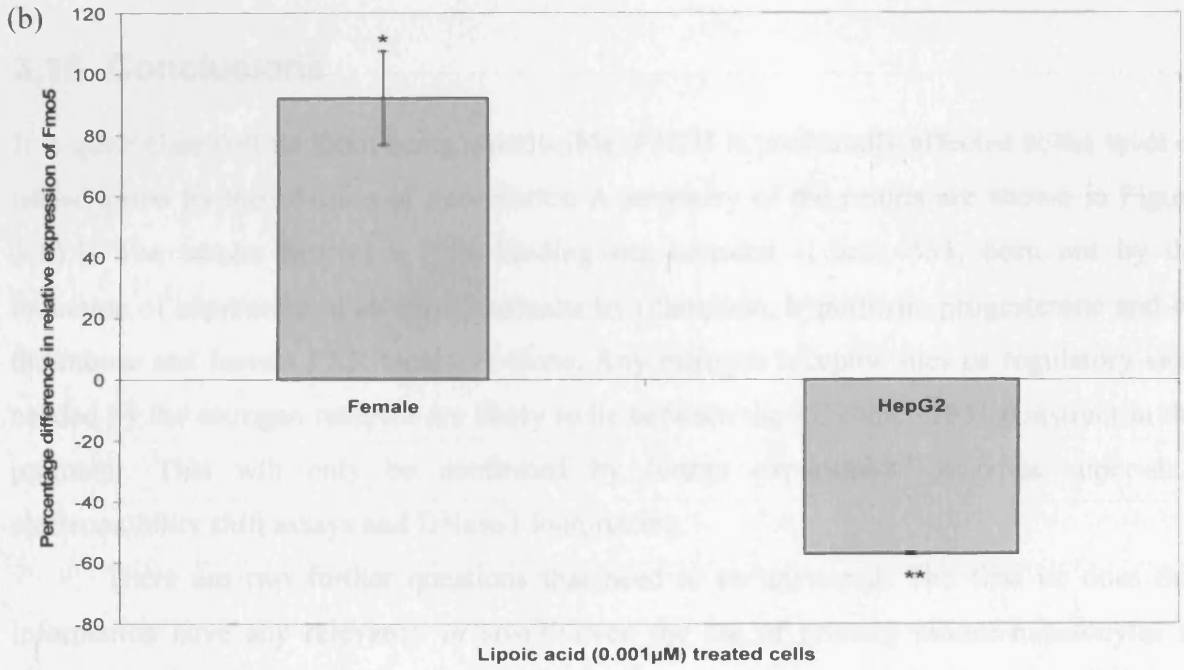

3.14.2 The effect of lipoic acid on FMO5 mRNA

Male mouse hepatocytes (a), female mouse hepatocytes and HepG2 cells (b) were dosed with lipoic acid for 24 hours, the total RNA isolated; FMO5 mRNA measured using real-time RT-PCR. Zero % represents the expression of FMO5 mRNA when cells are treated with the vehicle. Significance is calculated from the vehicle where * is $p<0.05$ and ** is $p<0.005$. Error bars are SEM.

3.15 Ethanol induces *FMO5* promoter constructs

Something which I had not set out to study, but what I have observed is that ethanol induces the *FMO5* reporter construct expression. As shown in Figure 3.14.1b the expression of the three larger constructs are induced 2-3 fold. The lack of induction of the smallest construct could imply a modulation by ethanol through a transcription factor further upstream. Ethanol is able to induce genes involved in the stress response, signal transduction and gene regulation (Murphy et al., 2002). It is well known that CYP2E1 is induced by ethanol. It is induced with acute and chronic alcohol levels which increases ROS production leading to alcohol induced liver injury (Gong and Cederbaum, 2006). As a metabolising enzyme FMO5 could be induced to metabolise the ethanol but there is no evidence to support this. It could be induced as a response to stress, by affecting the redox status of the cell. This possibility will be pursued in chapter five of this thesis.

3.16 Conclusions

It is quite clear that far from being uninducible, *FMO5* is profoundly affected at the level of transcription by the addition of xenobiotics. A summary of the results are shown in Figure 3.16.1. The results support a PXR binding site between -1 and -531, born out by the induction of expression of all four constructs by rifampicin, hyperforin, progesterone and by the mouse and human PXR receptors alone. Any estrogen receptor sites or regulatory sites needed by the estrogen receptor are likely to lie between the -531 and -1031 construct in the promoter. This will only be confirmed by further experiments such as super-shift electromobility shift assays and DNase I footprinting.

There are two further questions that need to be answered. The first is: does this information have any relevancy *in vivo*? Given the use of primary mouse hepatocytes in determining some of the effects by the xenobiotics, it seems that the information gleaned is more relevant than that obtained from an immortalised cell line. Although the hepatocytes are a good *in vitro* model, they are only a model of mouse liver, not human and not any other tissue. As explained, the FMOs are subject to tissue-specific regulation, as well as hormonal control. But the use of human sequences and HepG2 cells, a human cell line, does provide a human slant to the information.

The second question, and one which will not be answered fully by this thesis, is, what is the endogenous role of FMO5?

FMO5 is clearly under the control of PXR ligands, it is induced by rifampicin, progesterone, hyperforin and estradiol. Until an electromobility shift assay is carried out however, it is difficult to say whether *FMO5* is being mediated by PXR exclusively. The maintenance of luciferase activity by the addition of mERα seems to imply that at least one other receptor, as well as PXR, has some control over *FMO5* transcription.

PXR is renowned for its control over important xenobiotic metabolising enzymes, but it does have endogenous compounds as its ligands, and is able to regulate the metabolism of these as well as the exogenous drugs. PXR does have an important role in blocking bile acid production from cholesterol when cholesterol metabolism is in disarray or when bile acids accumulate. Bile acid metabolism and transport mechanisms are induced to clear the build-up (Goodwin et al., 2003). The farnesoid-x-receptor (FXR) is able to induce the transcription of PXR (Jung et al., 2006) thus FXR which blocks the synthesis of bile up-regulates PXR which increases the metabolism of bile, thereby protecting the liver.

PXR also appears to have some cross-talk with the glucocorticoid receptor (GCR) (Pascussi et al., 2000) in the role of inducing PXR-target genes. There are two GCR consensus sites in the *FMO5* promoter. GCR and C/EBPα also have some cross-over. Glucocorticoids are able to induce G_1 cell cycle arrest in hepatoma cells, and C/EBPα is required for this arrest (Ramos et al., 1996). C/EBPα consensus sites are also found in the *FMO5* promoter. C/EBPα probably has a role in normal liver epithelial cell function, and appears to be required for normal differentiation of hepatocytes (Diehl et al., 1994).

Testosterone induces *Fmo5* in primary male and female mouse hepatocytes, which is the opposite effect it has on *Fmo3* in male mice. There are many examples of testosterone-regulated gene induction but its role in the induction of lipogenic genes such as fatty acid synthase and acetyl-coA-carboxylase in androgen target tissues (Heemers et al., 2003) is especially pertinent to the status of the knock-out *Fmo* mice. The positive regulation by testosterone of *Fmo5* has already been observed; it is expressed six-times more highly in male mouse kidney than in female (Janmohamed et al., 2004).

As mentioned testosterone has a role in lipid homeostasis, similarly estrogen has a role in glucose homeostasis. It seems to do this via the activation of ERα by changing the insulin sensitivity of hepatocytes. ERα knockout mice have higher fasting blood glucose and

plasma insulin levels. The suppression of glucose production by insulin was reduced and hepatic lipid biosynthesis genes were up-regulated (Bryzgalova et al., 2006). In ob/ob mice the treatment with estrogen led to a reduced insulin resistance and reduced plasma triglyceride levels. Lipid biosynthesis genes were down-regulated, an opposite effect to that seen in the ERαKO mice. Estrogen also induced signal transducer and activator of transcription 3 (*Stat3*) mRNA (Gao et al., 2006). STAT3 is required for normal glucose homeostasis in the liver (Inoue et al., 2004). FMO5 could have a role in these homeostatic functions, especially given the lower plasma cholesterol levels in the *Fmo5* (-/-) mice. This will be explored further in chapter five of this thesis.

The *FMO5* promoter contains many possible regulatory sequences which have not previously been associated with FMO gene transcription. As described in Section 3.1.4, potential C/EBPα sequences are found. In the C/EBPα knockout mouse, the animals died very early on due to their impaired energy homeostasis (Wang et al., 1995), this was overcome using Cre/lox-P technology to create a C/EBPα conditional knockout, where C/EBPα expression is inactivated only in the liver. The animals had impaired bilirubin detoxification due to the repression of bilirubin UDP glucuronosyltransferase expression (Lee et al., 1997). C/EBPα also appears to have a major role in adipocyte differentiation (Lin and Lane, 1994) and the C/EBPα (-/-) mice have severely impaired adipose generation (Flodby et al., 1996).

This has two notable involvements that may be pertinent to the role of FMOs in general. Two possible USF sequences have been found in the *FMO5* promoter (Section 3.4). USF binds to the promoter of haem-oxygenase (HO) and regulates its transcription in human renal proximal tubular epithelial cells (Hock et al., 2004). FMO5 and FMO1 are both expressed in the human (Dolphin 1996, Janmohamed 2001) and mouse (Janmohammed 2004) kidney. HO breaks down haem, in addition it can be seen as cytoprotective whereby it shifts the redox state to a more antioxidant status (Applegate et al., 1991) and increases iron efflux (Ferris et al., 1999). Interestingly *Fmo3* has been shown to respond to iron levels. *Fmo3* was induced in transgenic mice with haemachromatosis, (HO was repressed in this mouse), but on addition of iron-dextran, *Fmo3* was repressed (Muckenthaler et al., 2003). That perhaps is even more intriguing given the lower plasma iron concentration in the *Fmo5* (-/-) mice (see Section 5.18). Also lipoic acid induces the expression of HO (Cheng et al., 2006; Ogborne et

al., 2005), part of lipoic acid's antioxidant effect. The plasma iron concentration then increases on lipoic acid treatment in *Fmo5* (-/-) mice (Section 5.19).

This is an interesting coincidence, given that porcine FMO1 is able to metabolise lipoic acid (Taylor and Ziegler, 1987). Also, during the insulin regulation of the fatty acid synthase (FAS) gene, upstream stimulatory factor (USF) is required to bind to the promoter of the FAS gene for insulin regulation to have an effect (Wang and Sul, 1997). Clearly the transcriptional regulation of FMO5 has some intriguing similarities with the possible mechanisms involved in both of the *Fmo* knock-out mice, given the *Fmo1, 2, 4* (-/-) mice and their lack of fat, as well as the *Fmo5* (-/-) mice and their intriguing low plasma lipid profile which is covered in Chapter 5 of this thesis.

	Dual-reporter assay	**mRNA levels using real-time RT-PCR**		
	HepG2	HepG2	Male mouse hepatocytes	Female mouse hepatocytes
Progesterone	Increased 0.3 to 3-fold over concentrations 0.1, 0.5, 5.0, 50 and 100 μM	Increased at 0.5 and 5.0 μM, 1.5-2 fold	Decreased at 0.1 and 0.5 μM by 75%	Increased at 0.1, 0.5 and 1.0 μM, 1 to 2-fold
Estradiol	Increased 0.5-fold at 0.001 and 0.003 μM. Decreased 50% at 10 μM	Increased 1 to 1.5-fold at 0.001 and 0.1 μM	Increased 0.2 to 1.5-fold at 0.001, 0.01, 0.5 and 1.0 μM	Increased 1.5-fold at 0.003 μM & decreased 50% at 0.03 & 0.5 μM
Testosterone	Decreased 50% at 0.001, 0.01 and 0.5 μM	Decreased at 0.01 and 1.0 μM	Increased 1 to 2-fold at 0.001, 0.01 and 0.5 μM	Increased 1-fold at 0.01 μM
Rifampicin	Increased by 0.5 to 2 fold at 10 μM	Increased 2-fold at 10 μM	Increased 0.5-fold at 10 μM	Increased 2-fold at 10 μM
Hyperforin	Decreased 50% at 0.5 and 1.0 μM	ND	ND	ND
Lipoic-acid	Decreased 50% at 0.5 μM	Decreased 50% at 0.001 μM	Increased 0.5 to 1-fold at 0.001 and 0.01 μM	Increased 1-fold at 0.001 μM
Ethanol	Increased 2-fold	ND	ND	ND
Ligand-independent	Increased 1 to 2-fold with hPXR and mPXR	ND	ND	ND

Figure 3.16.1 Summary of results involving FMO5 promoter studies and changes in mRNA levels using various xenobiotics

Chapter 4

Results and Discussion

Isolation and maintenance of primary mouse hepatocytes and their use to elucidate the genomic effects of liquorice

4 Isolation and maintenance of primary mouse hepatocytes

The major organ involved in the metabolism and detoxification of xenobiotics is the liver and therefore it has the highest expression of metabolising enzymes in the body. Hence, the liver is an attractive site of study to learn more about the effects of xenobiotics, including nutritional supplements, upon these metabolising enzymes.

We required primary hepatocytes for the study of the promoter of *FMO5* using gene-reporter assays, as explained in the previous chapter this was unsuccessful due to the stark differences between the human and mouse promoters; and human *FMO5* promoter constructs were never successfully expressed in primary mouse hepatocytes. The hepatocytes were used instead to examine the gene expression level, using real-time RT-PCR, of mouse *Fmo5* after the addition of xenobiotics. Although cell lines derived from liver hepatomas (e.g. HepG2) may be employed, the gene expression levels observed may differ from the *in vivo* situation. For the study of *FMO5* regulation these cells are very useful, as their inductive response appears similar to primary hepatocytes (Wilkening et al., 2003).

Primary hepatocytes can be termed 'ex vivo' and the functional capabilities of freshly isolated hepatocytes more closely mirror the capacities of a normal *in vivo* liver (Wilkening et al., 2003). HepG2 cells are representative of cancerous cells, a de-differentiated system, and so have less association with a normal healthy liver. For example in a recent study, researchers found, using genetic probe sets, that primary human hepatocytes (cultured in a sandwich system to increase the similarity to an actual liver) retained 77% similarity to liver biopsies, whereas HepG2 cells displayed less than 48% similarity (Olsavsky et al., 2007). Primary hepatocytes are also much better at biotransformation reactions than HepG2 cells, with increased levels of oxidation (phase I metabolism) as well as sulphation and glucuronidation (phase II metabolism) (Nyberg et al., 1994). Primary hepatocytes are not wholly representative of a normal liver given that the cells are wrenched from their *in vivo* situation and forced to grow *in vitro*. The expression of enzymes involved in xenobiotic metabolism, as well as those involved in gluconeogenesis or glycolysis are greatly reduced over the first three days of culture (Guguen-Guillouzo and Guillouzo, 1983; Sirica et al., 1979; Steward et al., 1985) and even when supplemented with glucocorticoids and insulin the

transcription of certain genes falls 3-10% in comparison to that *in vivo* (Jefferson et al., 1984).

Primary hepatocytes nonetheless are a useful model in which to study changes in gene expression. Their use requires fewer animals than would be required to carry out a full *in vivo* study, as well as being more closely related to a normal liver than cell lines.

4.1 Isolation of primary hepatocytes from mice

There is no standard procedure for isolating primary hepatocytes. There is much variation in the perfusion media used, the time taken to perfuse and the type of collagenase. The method involves perfusion of the liver with collagenase through the vena porta (antegrade method; the portal vein to the hepatic vein) or the inferior vena cava, the so-called retrograde (reverse) way. Most methods are based on Seglen (Seglen, 1976) who perfused the liver in two steps. The liver is perfused *in situ* with dissociating agents to get a viable suspension of liver parenchymal cells. The first perfusion medium contains EGTA to chelate the calcium. Calcium is contained within desmosomes which form part of the junctional complexes between cells. To isolate the hepatocytes chelating calcium irreversibly cleaves the desmosomes. This doesn't happen immediately, so if calcium is restored too quickly the desmosomes will re-form. The second perfusion buffer contains collagenase which digests the collagen matrix between the cells. Collagenase requires calcium to function, so calcium must be re-introduced into the liver in the second perfusion buffer. Hence the requirement of two steps.

The isolation of primary hepatocytes is a very difficult procedure to master, since it is essentially microsurgery. The number of different factors to consider in the method, compounds this issue. Myself and Dr Edwards went through each aspect of the method and made changes. In this way we discovered the parts of the procedure that were vital to its success, and which were less so.

Several methods were tried and the final protocol is an amalgamation of these. The first method (A in Table 1) was one used in our lab 10 years ago for the isolation of primary hepatocytes from transgenic mice by Dr. K Kramer. It in turn was based on the procedures used in the laboratories of Dr. P. Maurel (INSERM, Montpellier, France) who isolated rabbit hepatocytes and Prof. V. Rogiers (Vrije Universiteit Brussels, Belgium) who isolated rat

hepatocytes. These methods had to be adapted due to the sheer size difference of the animals. For example whilst Prof. Rogiers favoured a glass cannula for the rat, the same device would be too fragile in a mouse. Dr. Kramer, who honed the method in the mouse, favoured a fine plastic pipette tip. When we began we used Dr. Kramer's method and found that we had to make many more changes for the procedure to be reproducible.

4.2 Cannulation

To cannulate the portal vein, you must tie a loose ligature around it, make a small incision then insert the cannula. When we tried to cannulate the portal vein with a tip, it was prone to slip out of the ligature, or tear the fragile vessel. Cannulating the portal vein holds another problem. The vessel is so fine, that once it is cut, it collapses; making the procedure to insert the cannula almost impossible. It occurred so often that we moved on to an intravenous (I.V.) catheter for neonates. The very fine needle is sheathed in a thin plastic. The needle and its sheath are inserted into the portal vein and then the needle is removed, abolishing the need to cut the vessel. The problem with this instrument was that when the ligature was tightened, the plastic sheath would collapse and block the method of perfusion. The needle being so fine and the plastic so thin, it held very little physical strength. It became clear that perfusing the portal vein was too prone to failure to be of use. Many researchers, who I assume have come to the same conclusion, perfuse via the inferior vena cava (IVC) (Aiken et al., 1990; Bajt et al., 2004). Perivenous hepatocytes appear to contain a higher level of metabolising enzymes (Bengtsson et al., 1987; Suolinna et al., 1989; Vaananen, 1986) so perfusing via the IVC may obtain hepatocytes more resembling the *in vivo* situation. After the advice from Dr. Rick Moore (NIEHS, North Carolina, USA) (Method B in Table 1) we purchased a 24 gauge, ball-tipped gavage needle (Popper and Son). Because the IVC is a much larger and robust vessel, cutting it does not result in its complete collapse, and we were able to cannulate and ligate the needle much more easily. The gavage needle is metal, so it doesn't collapse when the ligature is tightened and the ball-tip keeps the needle above the ligature and stops it slipping out of the vein. However, this method was still prone to failure. The cutting of the IVC would flood the abdomen with blood and make inserting the cannula into the hole cut for it very difficult. Although we had more successes than failures, we considered going back to IV cannulas, but this time for use in the IVC. We acquired IV catheters of a larger gauge to

insert into the IVC. Although the plastic sheath could withstand the tightened ligature, the cannula was still prone to slip out. This is because IV catheter plastic is designed to be entirely inert, so nothing will prevent the smooth removal of the catheter from the vein. Finally we found that securely taping this sturdier cannula to the mouse kept it in place. But because the catheter plastic is flexible, the cannula is much more difficult to place in the IVC. We have found that small movements of the cannula can help or hinder the perfusion of the liver. When the cannula is placed deep in the IVC close to the liver, the blood flow backs-up and bursts the IVC, or damages liver cells due to the proximity of the flow. It is difficult to place the cannula further from the liver, since it becomes difficult to get the cannula to lie in a flat position so that it can be secured. The plastic cannula therefore is harder to get into the correct position and apt to coming out of the incision entirely. Once this happens it is very difficult to replace the cannula, as by this time the IVC has collapsed and all blood in it has been perfused away, making the incision very difficult to find again. It was for this reason that we began using the ball-tipped gavage needle again and contented ourselves with a securer perfusion and a better than average success rate, which improved with practice.

4.2.1 Hepatocyte methods

The methods used to isolate primary mouse hepatocytes. A is from Dr K Kramer (Ph. D. thesis); B is from Dr R Moore, NIEHS (personal communication); and C is from Dr. Bajhat (Bajat, et al., 2000).

	Buffer Solutions		Collagenase	Cannula	Liver disruption method	Culture media	Culture media after 3 hours	Collagen, plates and plating density	Additional Information
	1	2							
A	EBSS (Ca and Mg^{2+} free) 10 mM HEPES 0.5 mM EGTA Total: 25 mL	EBSS alone (50 mL) followed by EBSS 5mM $CaCl_2$ (100 mL)	0.25% collagenase H (Roche)	Plastic catheter	Use of curved forceps to scrape cells from Glissons capsule	Dispersed in EBSS plus 2% (w/v) BSA then plate in WE plus 5% (w/v) FBS	WE and Glutamax I with 10 µg/mL insulin, 0.1µM DEX, 10 µg/mL transferrin, 25 µg/mL ascorbic acid, 10 U/mL nystatin, 50 µg/mL gentamycin	1×10^6 on 60mm plates (Iwaki) coated in collagen Type I (Sigma)	Cells were grown at 33°C.
B	HBSS (Ca^{2+} and Mg^{2+} free) plus 0.3 mM EDTA 1 µM insulin 10 mM	HBSS (with Ca^{2+} and Mg^{2+}) 1 µM insulin 10 mM HEPES Total: 100 mL	Collagenase H (Roche)	Ball-tipped gavage needle, 22G (Poppin and son)	Metal comb (48 x 48 mm, teeth 2mm length)	Disperse in WE, then plate in WE plus 7% FBS, 10 mL/L ITS, 30 mM	WE plus 7% FBS, 10 mL/L ITS, 30 mM pyruvate, 5 nM DEX, penicillin	1×10^5/ well on 12-well plates (Nunc) no collagen	Time from cannula insertion to perfusion should be 70 secs. Collagenase

	HEPES Total: 100 mL at 5 mL/min	at 5 mL/min				pyruvate, penicillin			digestion should take max 4 mins
C	Krebs Ringer with glucose, 0.1 mM EGTA Total: 50 mL at 2 mL/min increase to 7 mL/min	Krebs Ringer with glucose, 1.37 mM $CaCl_2$ Total: 50 mL at 7 mL/min	Blendzyme Type I (Roche)	22G x 1" catheter IV type	Cut liver through capsule, disperse cells with large-bore pippette	DMEM with 10% FCS 1% ABAM	DMEM with 10% FCS 1% ABAM	Collagen Type III (calf skin, Sigma) on Corning plates	Cover liver with moistened gauze and place lamp over mouse for warmth
Final	HBSS (without CaCl2 and MgCl2), containing 50 mM EGTA, 0.75 g glucose Total: 50 mL at 2 mL/min increase to 7 mL/min	HBSS plus 1.74 mM CaCl2 0.72% w/v BSA and 1.25 g glucose Total: 100 mL at 7 mL/min until digestion is good (10 mins)	Collagenase H (Roche) 0.08 U/mL	Ball-tipped gavage needle, 24G (Popper and son)	Use of curved forceps to scrape cells from Glissons capsule	Disperse cells and plate in WE plus 7% FBS, 10 mL/L ITS, 30 mM pyruvate, 300 µg/ ml gentamicin	Plate cells in WE plus 7% FBS, 10 mL/L ITS, 30 mM pyruvate, 5nM DEX, 300 µg/mL gentamicin	1 x 10^5/ well on 12/24-well Nunc plates coated with Matrigel (BD Bio-sciences)	Fill the cannula with 50U/mL of heparin before insertion into IVC

All methods require the buffer solutions to be pH 7.4, at 37°C and have O_2 and CO_2 bubbled through them. All media is at pH 7.4 and filtered.

Abbreviations: ABAM-Anti-biotic Antimycotic; BSA-Bovine Serum Albumin; DEX-Dexamethasone; EBSS-Earl's Balanced Salt Solution; FBS-Foetal Bovine Serum; HBSS-Hanks Balanced Salt Solution; ITS-Insulin Transferrin Selenium; WE -Willam's E medium

The methods used to isolate primary mouse hepatocytes. A is from Dr K Kramer (thesis); B is from Dr R Moore, NIEHS (personal communication); and C is from Dr. Bajhat (Bajat, et al., 2000).

4.3 Liver removal

The initial method from Dr. Kramer involved removing the liver from the animal before perfusion began. We found this very cumbersome. The cannula is in such a fragile position that it became folly to then cut around the liver while the blood within it begins to clot. Cell viability seemed to improve the quicker we moved through the procedure. Clearly the cells need nourishing media as soon as possible. The two subsequent protocols we used (method C (Bahjat et al., 2000); method B kindly provided by Dr R Moore) advocated 'whole body' perfusion of the liver. The cannula was inserted the same way, via the IVC, but the liver was left where it was, giving the cannula a much sturdier base. Merely clamping the superior vena cava below the heart negated the problem of disturbing the cannula. It also limited the path of the perfusion buffer so it was directed at the liver and not the whole body.

4.4 Perfusion buffers

Few detailed methods on mouse hepatocyte isolation are available. Many isolation procedures are based on the rat, and a particular worry that the media used for rat would not be suitable for mouse hepatocytes. The two available detailed methods were tested by us. Dr. Bajhat (Method C in Table 1) provided great detail specifically about mouse hepatocyte isolation. She used Krebs Ringer solution as her perfusion buffer and DMEM as her dispersal buffer and culture medium. In contrast Dr. Moore uses HBSS to perfuse then Williams E medium to disperse and culture the hepatocytes. We tried out both methods. The use of different perfusion buffers seems to make no difference to the perfusion or the culturing of the cells. But pH appears to be very important. Gao et al. found that the viability of the hepatocytes at pH 6.4 was about 63%, whereas at pH 7.2 it was 75% (Gao et al., 2005). Maintaining a physiological pH is obviously important so the pH indicator in HBSS enabled us to check the pH and re-adjust it to pH 7.4 once 95% O_2 and 5% CO_2 was bubbled through the buffer.

4.5 Perfusion flow rate

Initially we tried to perfuse the liver via gravity. Having measured the flow rate, the buffer was running at about 2 to 3 mL/min. This pressure was insufficient to exclude the blood from the mouse liver. This method works in rats where the flow rate is inevitably higher because the cannula is much larger. However, the fine cannula used in mice precludes the use of gravity flow. We therefore connected the cannula to a peristaltic pump and initially used a flow rate of 15 mL/min. Our cell viability was 50%. A flow rate of 7 mL/min was used by Bajhat (2001) and when we reduced the flow rate to 7 mL/min viability improved to 60%. It is clear that flow rate is important. Perhaps the mechanical (sheer) stress of such a high rate reduces the viability.

4.6 Collagenase

I would say that finding the correct collagenase is the most important factor to get right in hepatocyte isolation. Once we found a batch that worked for us, the method was consistently successful and viability was maintained at at-least 65%. Collagenase is made up of a crude preparation of a bacterial culture from *Clostridium histolyticum*. Other proteases in this preparation include clostripain, trypsin, neutral protease and aminopeptidase. Hence collagenase activity varies from batch to batch. We purchased collagenase H and Blendzyme 3 both from Roche and collagenase I from Sigma. The collagenase from Sigma looked very crude and the procedure resulted in low viability even at a low collagenase activity. Blendzymes from Roche are produced to have no lot to lot variability. They are much less crude. However, again the viability was very low with Blendzyme 3 at 0.1 U/mL. The procedure would probably have benefited from some method development, but Blendzymes are very expensive, and by this time we had found collagenase H to give a good viability and cell number. We found that using 0.08 U/mL of collagenase H (Roche) was the ideal activity for our procedure although we tried several batches to get this right. We typically achieved 65-70% viability and 65 - 75 x 10^6 cells per liver.

4.7 Maintenance of mouse primary hepatocytes-use of media

Williams and Gunn (1974) investigated the long-term culture of adult epithelial cells and developed Williams' Medium E. We tried DMEM and Williams' E media. The type of media used did not appear to improve or hinder the culturing of the cells. Guguen-Guillouzo (1983) also found that few differences resulted from the choice of medium.

4.8 Plate coatings

Dr Moore's protocol specifies he uses uncoated plates on which to culture the hepatocytes. When we tried this the cells did not attach onto the plate very well, and they lived for only a day or so. So we coated the plates with collagen Type I (Sigma) as used by Dr Kramer. This worked very well; the cells attached onto the plate at a greater density and maintained their pavement-like morphology. The cells also have a rounded healthy-looking shape when they initially attach, which is very pleasing. Although collagen was an excellent base for the hepatocytes, the cells have a short life span of only a couple of days (Figure 4.9.1). To improve their survival we plated the cells onto Matrigel™-coated plates. It is a biomatrix extracted from the Engelbreth-Holm-Swarm mouse sarcoma. Matrigel™ is a mixture of collagens, designed to give a support structure more like that *in vivo*. Various matrix components are found in the liver including collagens I, III, IV, V and VI, noncollagenous glycoproteins such as laminin and fibronectin (Clement et al., 1986). Indeed the cells cultured on Matrigel™ attached very well, and survived for at least 5 days when cultured on this substratum. Although it is difficult to be definitive purely on microscopic observations, the cells appeared to have a less flattened and a more "polygonal" morphology. However, even so we found that the concentration of Matrigel to layer onto the plates required some method development. The protocol provided by the supplier of Matrigel specifies using it at a 3:1 concentration, the greater part made up from the culture media, such as Williams E. When used at this concentration however, the cells were inclined to get too entrenched in the Matrigel™, not change their morphology or make contacts with their neighbours (Figure 4.9.2). Subsequently we found that a 9:1 dilution combined a longer survival time with a liver-like morphology.

4.9 Plating density

We tried plating cells at several densities on 12-well plates, from 1 million cells per well (per mL) down to 0.1 million cells per well. At the level of 1 million, the cells did not attach at all to the plate. They appear to crowd each other out and die in suspension. But at 0.5 million cells per well, the cells attach to the plate immediately. We plated 0.4, 0.3, 0.2, 0.1 million cells per well also. The cells also attach at these lower densities. However after 24 hours, when plated below 0.3 million cells, the hepatocytes appear to be stretched beyond their means, (Figure 4.9.3), and hepatocyte characteristics are no longer like those of an intact liver in which cells are in contact with other cells (Koji et al., 1988).

(a)

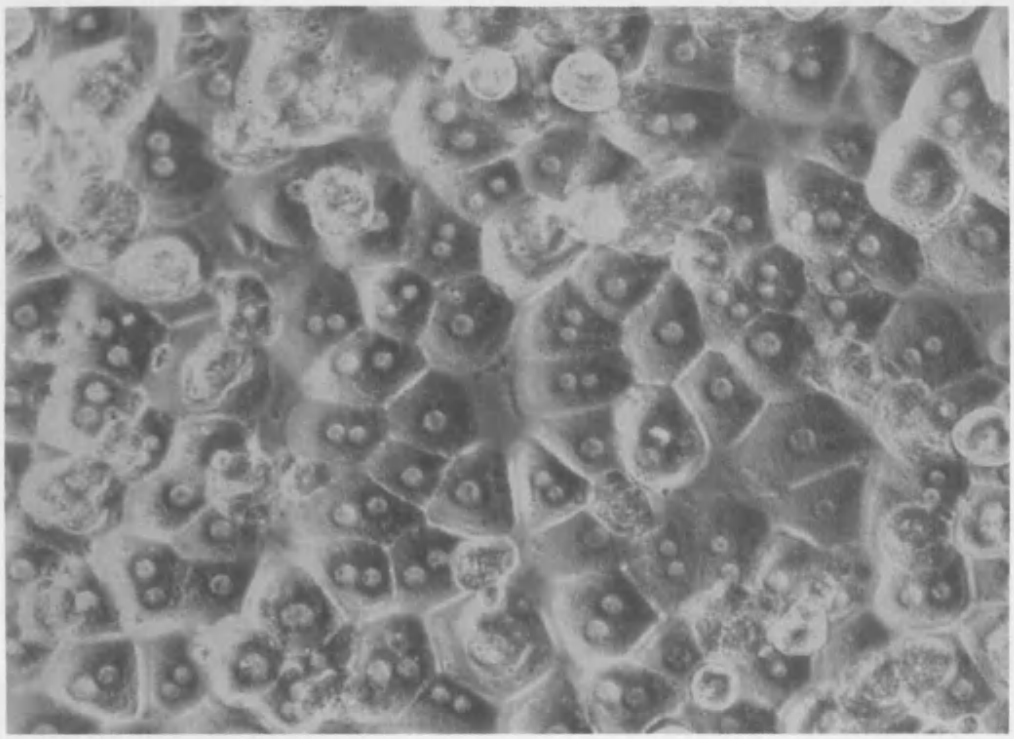

(b)

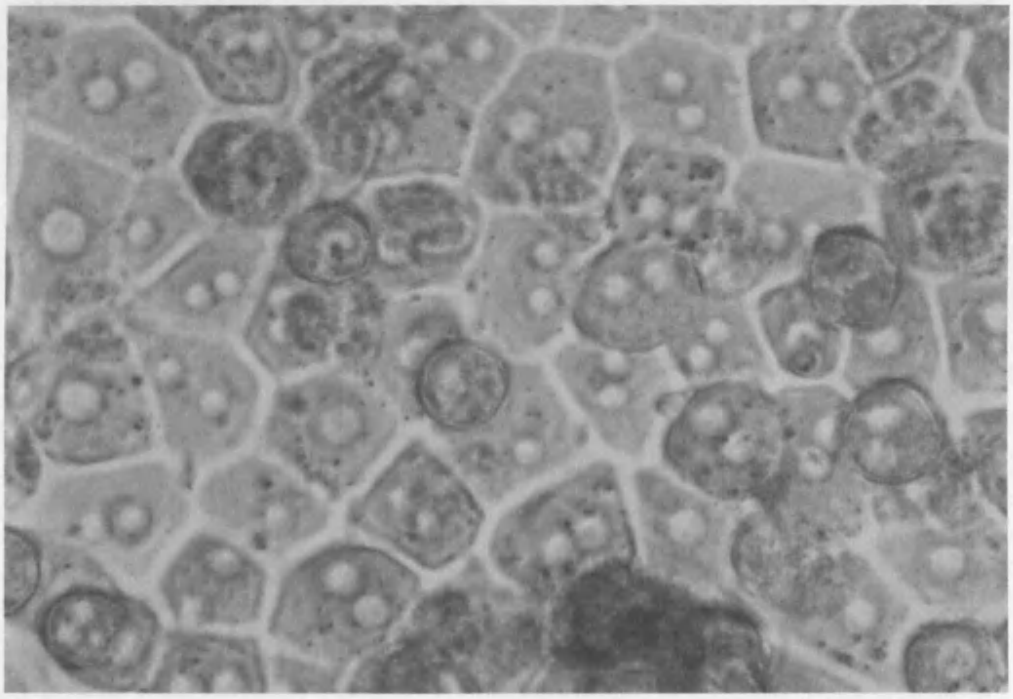

4.9.1 Primary mouse hepatocytes plated onto collagen

Primary male mouse hepatocytes plated on collagen, hepatocytes after 20 hours, X20 magnification (a), hepatocytes plated for 40 hours, X40 magnification (b).

(a)

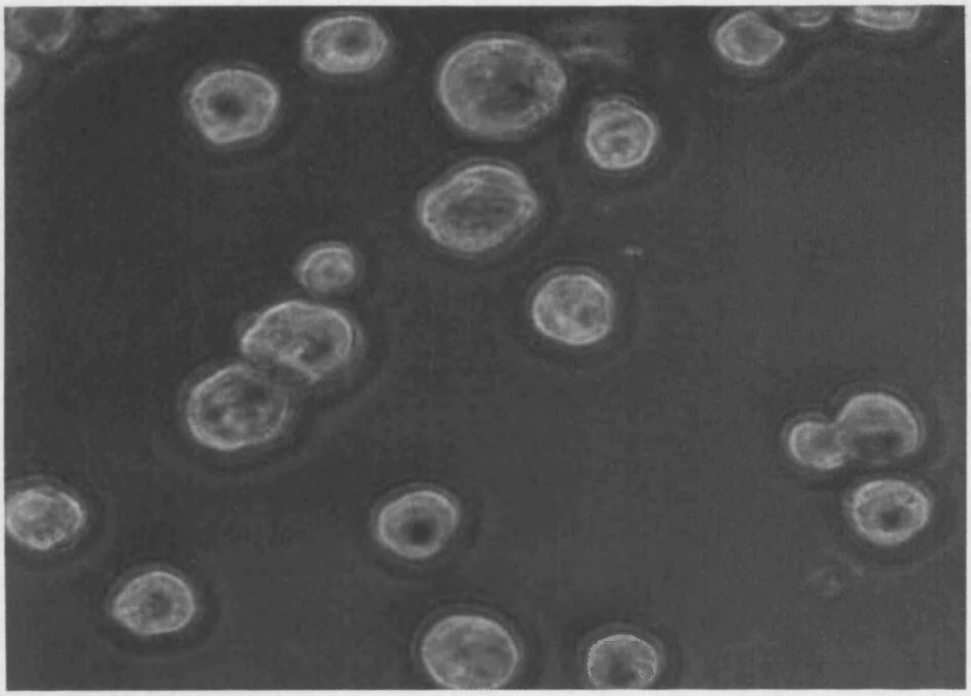

(b)

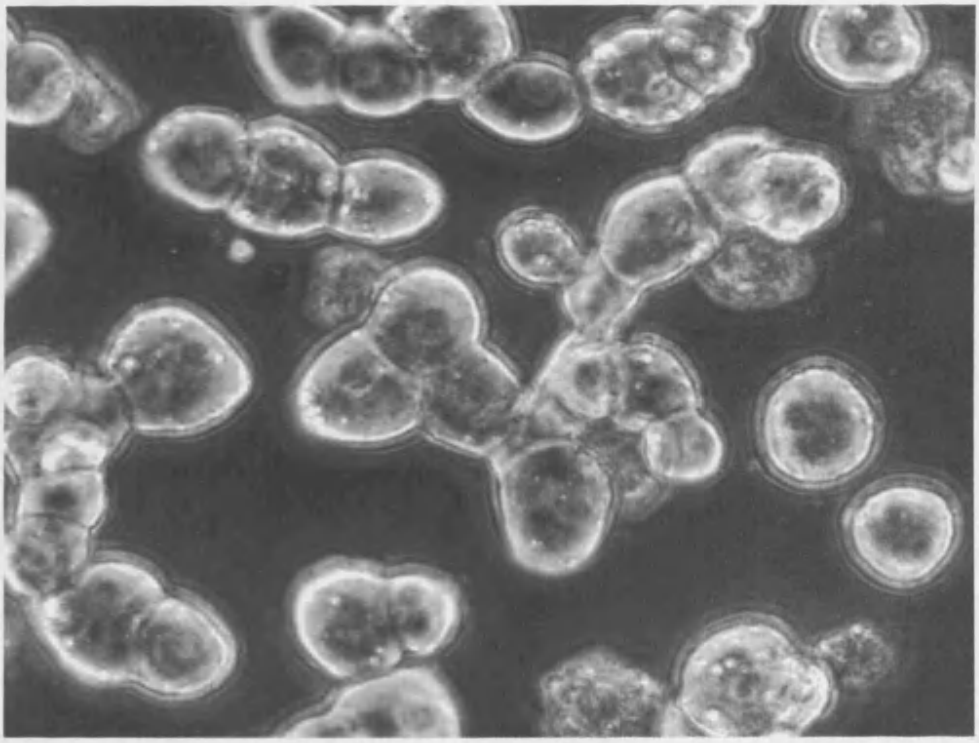

4.9.2 Primary male mouse hepatocytes plated on Matrigel™

Hepatocytes plated on Matrigel™ diluted 1:3 (a); Cells plated on Matrigel™ diluted 1:5 (b) (X20 magnification)

(a)

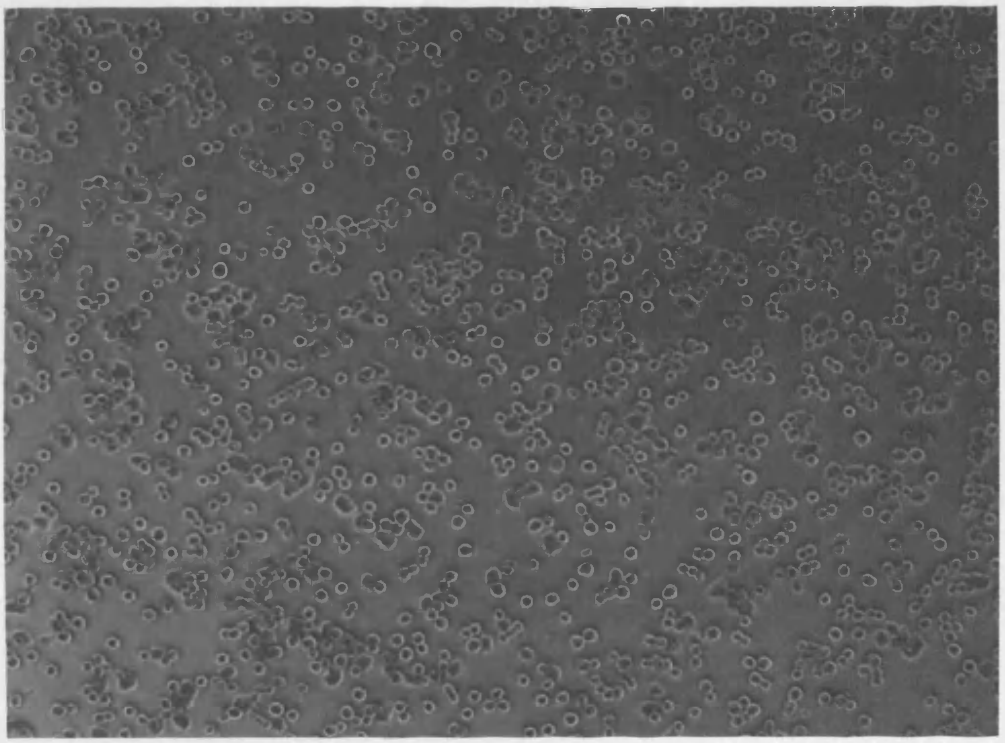

(b)

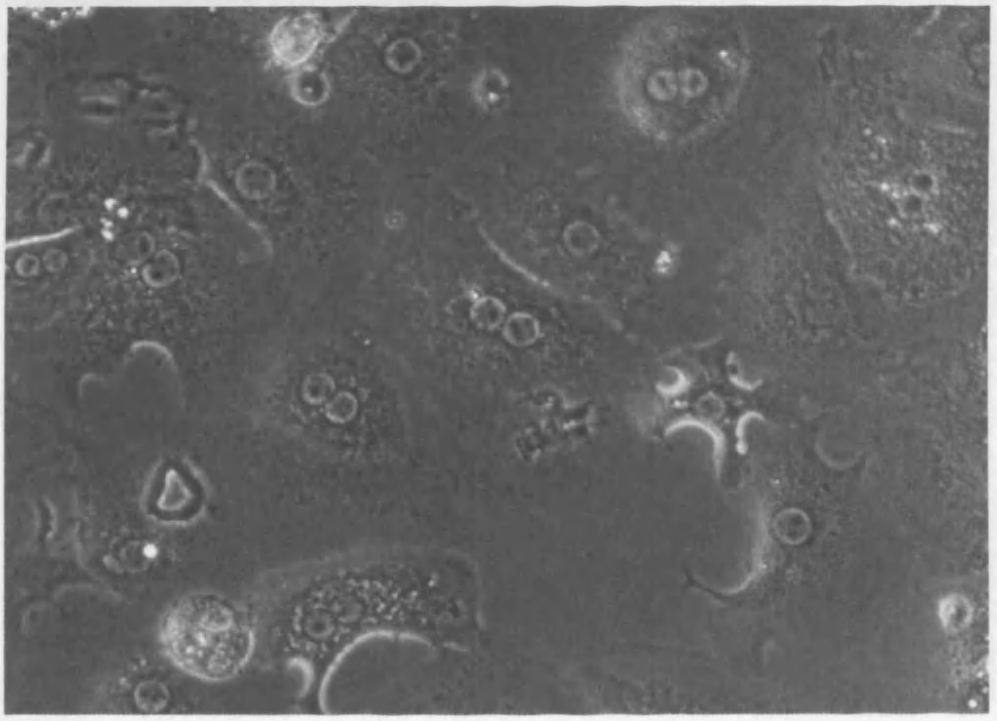

4.9.3 *Primary male mouse hepatocytes plated onto Matrigel™ and cell density*

Primary male mouse hepatocytes plated onto Matrigel™ 1:5 (X10 magnification) (a). Cells plated at 0.2 million cells per mL (X 20 magnification) (b).

(a)

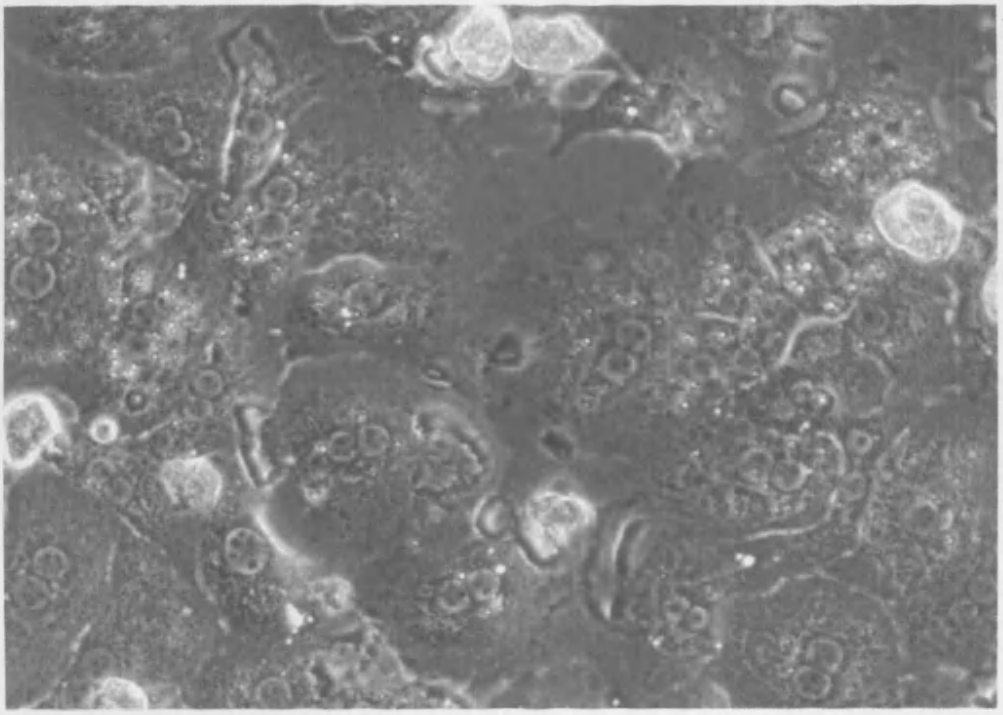

(b)

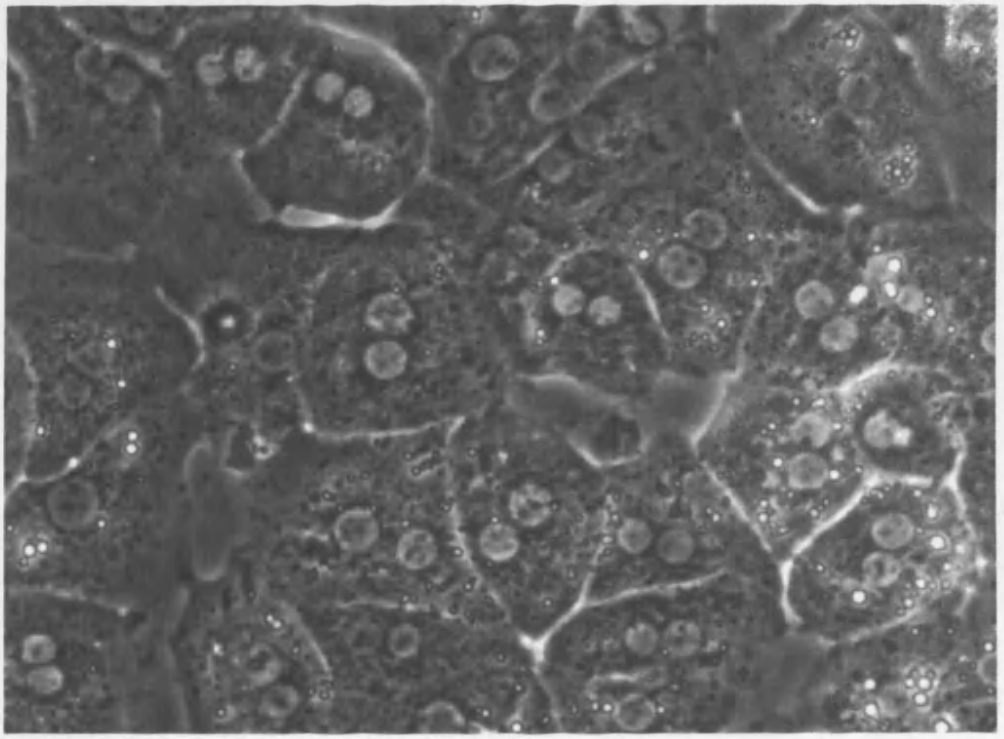

4.9.4 Primary male mouse hepatocytes-plating density

Primary male mouse hepatocytes plated at 0.3 million cells per mL (a). Cells plated at 0.5 million cells per mL(b) (x 20 magnification).

4.10 Defining a differentiated system-examples of healthy cultured mouse hepatocytes

Mouse hepatocytes were cultured as described in the methods section. In Figure 4.10.1 I have chosen to display the same cells, but the photographs are taken with a different light source to show the rounded morphology of the cells. This is important; because as the cells become de-differentiated, they lose their shape and become flatter. You can also see that the majority of the cells are bi-nucleate. This is also indicative of a differentiated system, implying the cells are healthy. Similarly the defined junctions between cells and the pavement-like shape they acquire show the cells are well. Unhealthy or de-differentiating cells will expel pseudopodia and the barriers between cells become less-well defined.

(a)

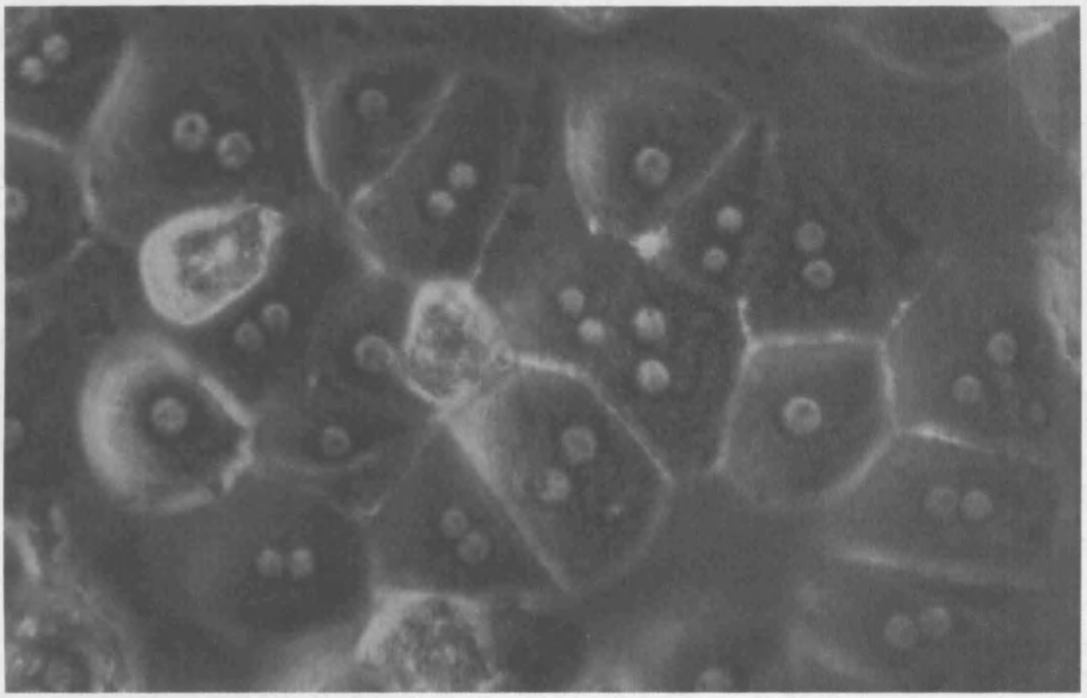

(b)

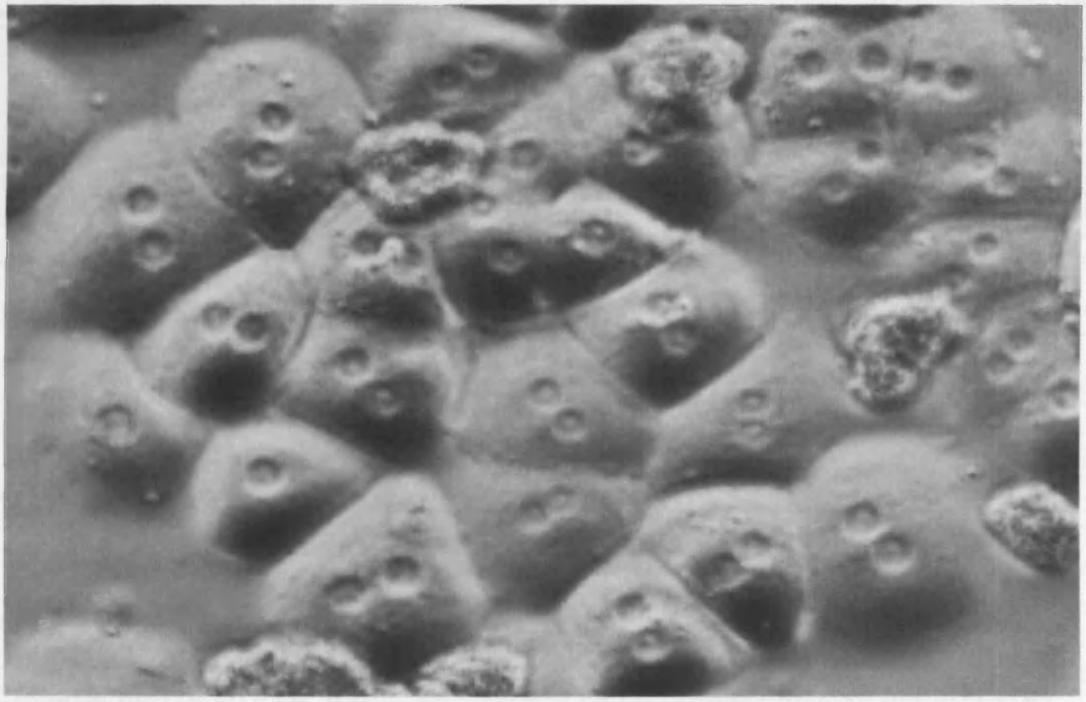

4.10.1 Demonstration of healthy morphology

Cells are shown with the light source from below (a) to demonstrate defined gap junctions and pavement morphology, and a light source from above (b) to show the rounded and therefore healthy morphology.

4.11 Confirmation of a P450 response using phenobarbital

To confirm that the hepatocytes maintained healthy responses to stimuli and maintained transcriptional activity, they were dosed with PB. In healthy cells CYP2B should be induced. As shown in Figure 4.11.1 CYP2B1/2 is inducible in the mouse hepatocytes and that they have therefore maintained crucial factors required for induction of the mouse CYP2B gene. A concentration of 1mM phenobarbital was found to give the highest induction. Previous studies also show that induction of CYP2B by phenobarbital is greatest at similar concentrations (0.75-1mM) (Kocarek et al., 1990).

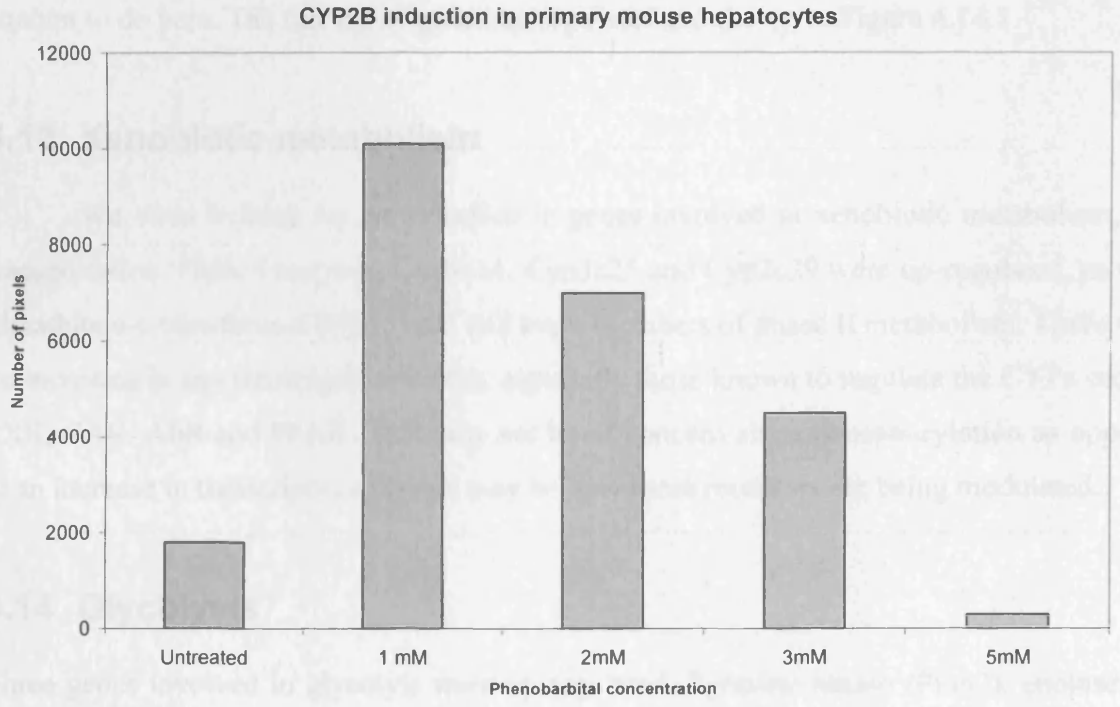

4.11.1 Induction of CYP2B in phenobarbital-treated primary mouse hepatocytes

Hepatocytes were treated with phenobarbital for 24 hours. Cells were scraped from the plates and protein concentration measured. The graph is a quantitation of the resulting bands from a Western blot using an anti-CYP2B1/2 antibody. This is a representative result from three different cultured male mouse livers and their western blots.

4.12 Investigating hepatocyte genetic response to glycyrrhetinic acid using microarray

Microarray enables the investigator to look at the up- or down-regulation of genes in a whole organism in response to a treatment or environmental condition. Two discrete cell populations are used and the experiment is usually carried out using triplicate microarray slides.

Hepatocytes were treated with a component of liquorice, glycyrrhetinic acid (10μM) for 24 hours. 56 genes were up-regulated in total, but only two were above the two-fold cut off, in all 3 slides. The rest of the 'up-regulated' genes were increased above 2-fold but in only 2 out of 3 slides, or above 1.5-fold and in 3 or 2 out of 3 slides. No genes were down-regulated. The 'upregulated' genes can be split into general functions and this is what I will attempt to do here. The full list of genes up-regulated are shown in Figure 4.14.1.

4.13 Xenobiotic metabolism

We were looking for an induction in genes involved in xenobiotic metabolism, and transportation. Phase I enzymes Cyp3a11, Cyp3a25 and Cyp2c29 were up-regulated, as were glutathione-s-transferases (GST) mu3 and mu4, members of phase II metabolism. There were no increases in any transcription factors, especially those known to regulate the CYPs such as PXR, CAR, AhR and PPAR. This may not be of concern since phosphorylation as opposed to an increase in transcriptional levels may be how these receptors are being modulated.

4.14 Glycolysis

Three genes involved in glycolyis were up-regulated. Pyruvate kinase (Pkm2), enolase and glyceraldehyde-3-phosphate dehydrogenase (Gapdh).

Pyruvate kinase was up-regulated more than 2-fold in all 3 slides and converts phosphoenolpyruvate (PEP) to pyruvate. Enolase is the enzyme that produces PEP from 2-phosphoglycerate. Gapdh is involved in an earlier step of glycolysis, converting glyceraldehyde-3-phosphate to 1,3-bisphosphoglycerate. Clearly glycolysis in this system is being up-regulated. The reaction catalysed by pyruvate kinase produces ATP by direct phosphorylation of ADP.

Function/ Process	Common Name	Name	Fold Increase
Glycolysis	Pkm2	pyruvate kinase, muscle	2.06
	Gapdh	glyceraldehyde-3-phosphate dehydrogenase	1.42
	Eno1	enolase 1, alpha non-neuron	1.66
Xenobiotic metabolism	Cyp3a11	cytochrome P450, family 3, subfamily a, polypeptide 11	2.11
	Cyp3a25	cytochrome P450, family 3, subfamily a, polypeptide 25	1.91
	Cyp2c29	cytochrome P450, family 2, subfamily c, polypeptide 29	1.60
	Gstm3	glutathione S-transferase, mu 3	4.07
	Gstm4	glutathione S-transferase, mu 4	1.49
Apoptosis	Bnip3	BCL2/ adenovirus E1B 19kDa-interacting protein 1, NIP3	1.69
	Ddit4	DNA-damage-inducible transcript 4	1.75
	Itm2b	integral membrane protein 2B	1.62
Stress response	Rnase4	ribonuclease, RNase A family 4	1.55
	Ndrg1	N-myc downstream regulated gene 1	2.34
	Hig1	hypoxia induced gene 1	1.51
	Hspa8	heat shock protein 8	1.67
	Egln3	EGL nine homolog 3	1.79
Signalling	Bmp8a	bone morphogenetic protein 8a	3.14
Protein binding	Lgals3	lectin, galactose binding, soluble 3	1.72
	nebulin	nebulin	1.75
Amine transporter	Slc30a1	solute carrier family 30 (zinc transporter), member 1	1.63
Hormone	Prl	prolactin	1.98
Glycosylation	Pmm1	Phosphomanno-mutase 1	1.47
Blood coagulation	Fgg	fibrinogen, gamma polypeptide	1.56

Metal ion binding	Loxl2	lysyl oxidase-like 2	1.44
	Mt2	metallothionein 2	1.98
	Plekhe1	pleckstrin homology domain containing, family E (with leucine rich repeats) member 1	1.92
Calcium ion binding	Gsn	gelsolin	1.77
	Calb2	calbindin 2	1.48
	Nell2	nel-like 2 homolog (chicken)	1.70
Interleukin receptor	Il17rb	interleukin 17 receptor B	1.58
G-protein coupled receptor	Olfr821	olfactory receptor 821	1.46
Transport	Fabp1	fatty acid binding protein 1, liver	1.46
	Crabp1	cellular retinoic acid binding protein I	1.43
Unknown	MGC54-896	similar to CTCL tumor antigen se57-1	1.37
	Attp	signaling molecule ATTP	1.54
	Sca10	spinocerebellar ataxia 10 homolog	1.31
	9230109-N16	hypothetical protein 9230109N16	1.46
DNA-binding (stress)	Nupr1	nuclear protein 1	1.66
Mitosis	Mapre2	microtubule-associated protein, RP/EB family, member 2	1.43
Angiogenesis	Vegfa	vascular endothelial growth factor A	1.64
	Serpine1	serine (or cysteine) proteinase inhibitor, clade E, member 1	1.73
Protein biosynthesis	Rpl12	ribosomal protein L12	1.83
	Rpl23a	ribosomal protein L23a	1.79
Differentiation	Sprrl7	small proline rich-like 7	2.73

4.14.1 Table of the genes up-regulated in glycyrrhetinic acid-treated hepatocytes

This table contains the genes up-regulated when primary male mouse hepatocytes were dosed with 10 μM glycyrrhetinic acid for 24 hours. The total RNA was isolated, and mRNA was analysed using microarray.

This is substrate-level phosphorylation and is especially important for providing energy for a tissue when they are lacking oxygen (Salway, 1999). Pkm2 is the only pk isozyme detectable in early fetal tissues. The other isoforms, L-, R-, and M1-type gradually replace M2 as development progresses. However, when tissues are de-differentiated or are developing a neoplasm, M2 is reactivated or increased (Asai et al., 2003). It also appears that during increased cell proliferation pkm2 increases energy production.

This is a key point when elucidating the consequences of dosing GTA to hepatocytes, especially when it is known that all three enzymes are under transcriptional control of hypoxia-inducible factor 1 (HIF-1α).

4.15 Hypoxia and apoptosis

As well as glycolysis, other genes are up-regulated in these treated hepatocytes that are acutely related to hypoxia. HIF-1α is the transcription factor that mediates hypoxia and modulates the transcription of genes involved in angiogenesis, glucose transport and metabolism, inflammation, apoptosis and cellular stress. As part of a cell's response to hypoxia, HIF-1α is stabilised, it forms a heterodimer with HIF-1β and the pair target hypoxia response elements in a plethora of genes. It is clear that HIF-1α has a large part to play in the fate of these glycyrrhetinic-dosed cells, although HIF-1α wasn't induced in the microarray.

HIF-1α's role is to prepare the cell for survival against hypoxia, as cells are able to grow and proliferate normally in hypoxia. This perhaps is especially true in solid-tumours, where the growth tissue often becomes hypoxic, and what is often observed associated with these cancers is angiogenesis. A normal or cancerous cell increases the blood flow to that tissue to increase the flow of oxygen, the first step of which is to up-regulate vascular endothelial growth factor (VEGF), directly under the control of HIF-1α. VEGF is up-regulated in this system, and is obviously part of a normal cell's response to hypoxia. Prolactin is also induced in this system and has also been implicated in angiogenesis (Jackson et al., 1994).

Another gene under the control of HIF-1α is Ddit4 (DNA-damage-inducible transcript 4) it was induced and is activated in response to cellular stresses such as DNA damage and hypoxia (Lin et al., 2005). It activates the mTOR signalling pathway which in turn also activates HIF-1α, and ultimately up-regulates angiogenesis. Already there are

control mechanisms in place whereby hypoxia induces HIF-1α and then Ddit4, but also Ddit4 itself responds to hypoxia, giving two levels of control. The inactivation of HIF-1α is also being regulated in the form of EGL nine homolog 3 (Egln3). HIF-1α contains independent oxygen degradation domains, which Egln3 targets, flagging HIF-1α for proteasomal degradation (Villar et al., 2007). Egln3 catalyses oxygen-dependent hydroxylation of HIF-1α and is up-regulated by hypoxia at the mRNA level and appears to be involved in the negative feedback of HIF-1α (Epstein et al., 2001).

Heat shock protein 70 (HSP70/Hsp8a) is increased in hypoxic hepatocytes at an early stage (Tokyol et al., 2005) and Hsp70 was also induced in this system. Heat shock proteins have a cytoprotective effect, an example being the inhibition of lipopolysaccharide-mediated apoptosis in cultured sheep pulmonary artery endothelial cells over-expressing Hsp70 (Wong et al., 1996). Cultured murine lung epithelial cells under thermal stress were protected by Hsp70 from oxidant-mediated injury (Wang et al., 1996).

Higl (hypoxia-induced gene 1) was characterised in hypoxic cervical epithelial cells, and could be involved in pro-apoptotic signalling (Bedo et al., 2005). Ndrg1 (N-myc down-regulated gene 1) was also up-regulated in this system and is regulated during cell proliferation, differentiation, and in response to stress. It modulates the response to hypoxic injury in human trophoblasts (Chen et al., 2006). The RNase4 level was increased, it is as yet unclear what RNase4's role is, but its promoter is dependent on an intact HIF-1α consensus binding site (Dyer and Rosenberg, 2005). Bone morphogenic 8a (Bmp8a) is an intracellular signaling molecule that is released when there are changes in cell proliferation, cell survival, differentiation and cell fate (Zhao et al., 1998). The up-regulation of Hsp70, Higl, Ndrg1 and RNase4, Itm2b and Bmp8a is perhaps indicative of the cell adapting to hypoxia, but also in preparation for apoptosis. This is because there is another side to HIF-1α, whilst it is able to protect against hypoxia it can also prepare the cell for destruction and be pro-apoptotic. BNIP3 (BCL2/adenovirus E1B 19kDa-interacting protein 1, NIP3) was induced and is under direct control of HIF-1α. BNIP3 is a pro-apoptotic mediator and is important in hypoxia-induced death in normal as well as malignant cells (Lee and Paik, 2006). Bnip3 binds to Bcl-2/Bcl-XL, repressing them and inducing cell death. Integral membrane protein 2B (Itmb2) is also able to inhibit Bcl-2, and is up-regulated in this system. Itm2b appears to have a p53-independent apoptotic role (Fleischer and Rebollo, 2004).

Clearly the cells are under some stress. In an hypoxic environment, where the lack of oxygen means less ATP will be obtained from oxidative phosphorylation, glycolysis is up-regulated to try to compensate. Cell proliferation is increased to produce more ATP-providing units in an effort to maintain the energy level, and in whole systems, genes to increase angiogenesis are transcribed to increase the flow of oxygen. If these measures fail to lift the cells out of an hypoxic environment, then pro-apoptotic mediators are up-regulated in preparation for cell suicide. This appears to be the environment the hepatocytes are in. The question as to why the cells are becoming hypoxic seems to be resolved by Salvi (Salvi et al., 2003) who investigated the effects of glycyrrhetinic acid (10μM), on rat liver microsomal mitochondria. They found that glycyrrhetinic acid caused swelling of the mitochondria, enhanced oxygen uptake and mitochondrial membrane potential collapse. To uncover the reasons for this, in their follow-up paper (Salvi et al., 2005), they used carbenoxolone, the glycyrrhetinic acid derivative, which has been used more widely in the past clinically. They found that carbenoxolone produced oxidative stress which opens up the transition pore in mitochondria. The possible mechanism being that carbenoxolone produces H_2O_2 which reacts with thiol groups that are critical in opening the mitochondrial pore. The increased uptake in oxygen leads to a greater production of H_2O_2 and more thiol group oxidation. This could explain the hypoxic conditions we observe in the GTA-treated hepatocytes. Carbenoxolone causes an increase in the permeability of mitochondrial membrane which can result in the release of critical proapoptotic intermembrane space effectors into the cytosol such as cytochrome c.

In a more recent paper Pivato (Pivato et al., 2006) found that carbenoxolone stimulated state IV respiration, which led to the uncoupling of oxidative phosphorylation and the induction of membrane pore transition.

The system may not be descending into apoptosis just yet, as the interplay of signals to decide the cell's fate is not clear-cut. Interestingly there is up-regulation of the anti-oxidant glutathione (GSH) by the hepatocytes to try to minimise the damage, as well as up-regulating gelsolin, a protein that appears to be involved in closing the transition pore (Kusano et al., 2000). The up-regulation of Egln3 may also be in preparation for a normoxic environment where HIF-1α can be degraded.

There is also no sign of up-regulation of the 'executioner caspases' -3, -6 and -7 which are typically required for full-blown apoptosis. So although the cells are under a

condition of stress, it may not be too severe, given that the level of induction of the genes involved is fairly slight, only just over the two-fold cut-off. The cells also weren't obviously morphologically different otherwise the RNA wouldn't have been isolated.

Unfortunately I was unaware of the mitochondrial effects of carbenoxolone and hence glycyrrhetinic acid before the cells were dosed at 10 μM, which incidentally is a similar concentration to the plasma concentration derived after liquorice ingestion (de Groot et al., 1988), the reason for the hepatocytes being dosed at that concentration in the first place. This mitochondrial action may also explain some of the beneficial effects observed when people take liquorice for inflammation and cancer, promoting the safety mechanism of the body, apoptosis, to dispose of the damaged cells.

Although the microarray doesn't tell us any more about the control of xenobiotic metabolism when glycyrrhetinic acid is applied, it does show what can be inferred from the induction of genes and the 'cross-talk' between transcription factors and effector genes that may ensue.

These results do show rather elegantly however, what does happen at a genomic level when the cell is under a condition of stress and if nothing else, this experiment does validate the process of microarray.

4.15.1 Diagram 1: The response of genes and their inter-relationship when primary male mouse hepatocytes are treated with glycyrrhetinic acid

On the next page is a diagram showing the relationship of genes induced by glycyrrhetinic acid (10 μM) in primary male mouse hepatocytes. The blue genes are those induced by the microarray. Black arrows indicate an inductive effect of one gene on another, or upon a process. Red arrows are inhibitive.

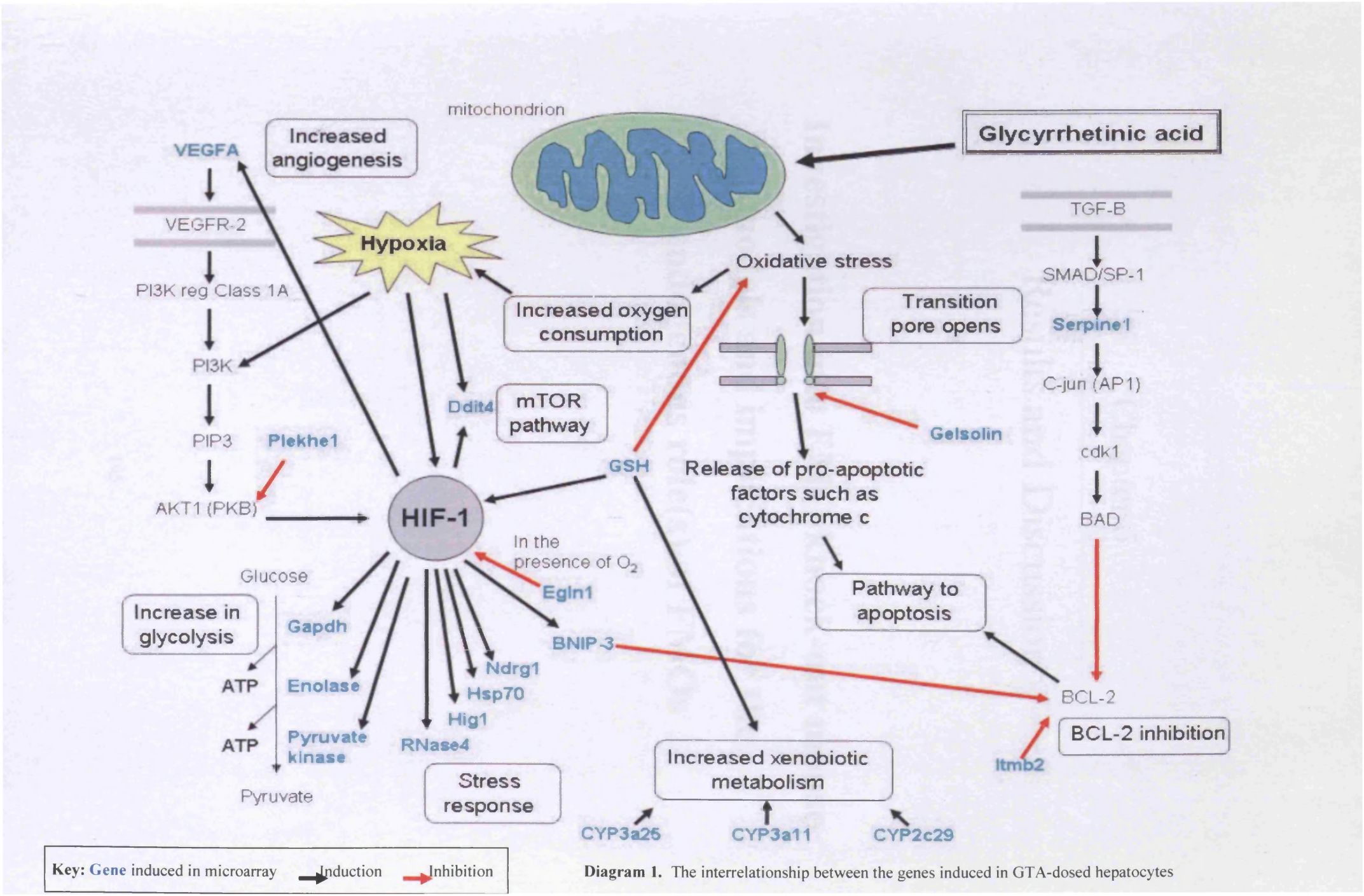

Diagram 1. The interrelationship between the genes induced in GTA-dosed hepatocytes

Chapter 5

Results and Discussion

Investigation into FMO knock-out mouse models and implications for the endogenous role(s) of FMOs

5 Investigation into FMO knock-out mouse models and implications for the endogenous role(s) of FMOs

FMOs are drug-metabolising enzymes, but presumably they originally had an endobiotic role and have evolved to metabolise xenobiotics. Their possible endogenous role has to this day remained elusive. To study the likely endogenous function(s) of FMOs two knock-out mouse models had previously been created by the laboratory of Professor Elizabeth Shephard. The first mouse to be made was the *Fmo1, 2, 4* (-/-) mouse (also referred to as the 'cluster' knock-out) which was created according to Hernandez et al., (2006). The second was an *Fmo5* (-/-) mouse, created by removing exon two of the transcript, resulting in a non-functional enzyme. Using these two models we have undertaken extensive study to uncover the endogenous role of FMOs.

In the following chapter I will describe the research into these two knock-out (KO) mouse models separately. The interesting results seen with the *Fmo1, 2, 4* (-/-) mice will be described first; the investigations into the *Fmo5* (-/-) mice will be set out in the second half of the chapter.

5.1 Weight analysis of male *Fmo1, 2, 4* (-/-) knock-out mice

Once homozygous knock-outs had been produced, it was observed that the body weight of the male *Fmo1, 2, 4* (-/-) mice was less than that of wild-type (WT) males of the same age (Figure 5.1.1). The body weight of these animals was measured for 15 weeks from 4 weeks of age (Figures 5.3.1). At 4 weeks of age the WT male weight (16g) is less than that of the *Fmo1, 2, 4* (-/-) males, being about 23g. This is clearly a large difference, but the WT mice gain 5g in weight on average and the *Fmo1, 2, 4* (-/-) lose 2g to become the same weight as each other from 5.5 to 6.5 weeks of age. Between 6.5 and 7 weeks of age the WT males on average put on 1.5g in weight, whilst the *Fmo1, 2, 4* (-/-) males gain no weight. Shown in Figure 5.3.3 are the percentage weight gains over periods of time for comparison between male *Fmo1, 2, 4* (-/-) mice and male WT mice. From 4.5 to 6 weeks the WT males gain 38% in weight, whilst the *Fmo1, 2, 4* (-/-) males gain 7.5% weight over the same time. From 6 to 10 weeks, the WT males gain 32% in weight, but the *Fmo1, 2, 4* (-/-) males gain only 14%.

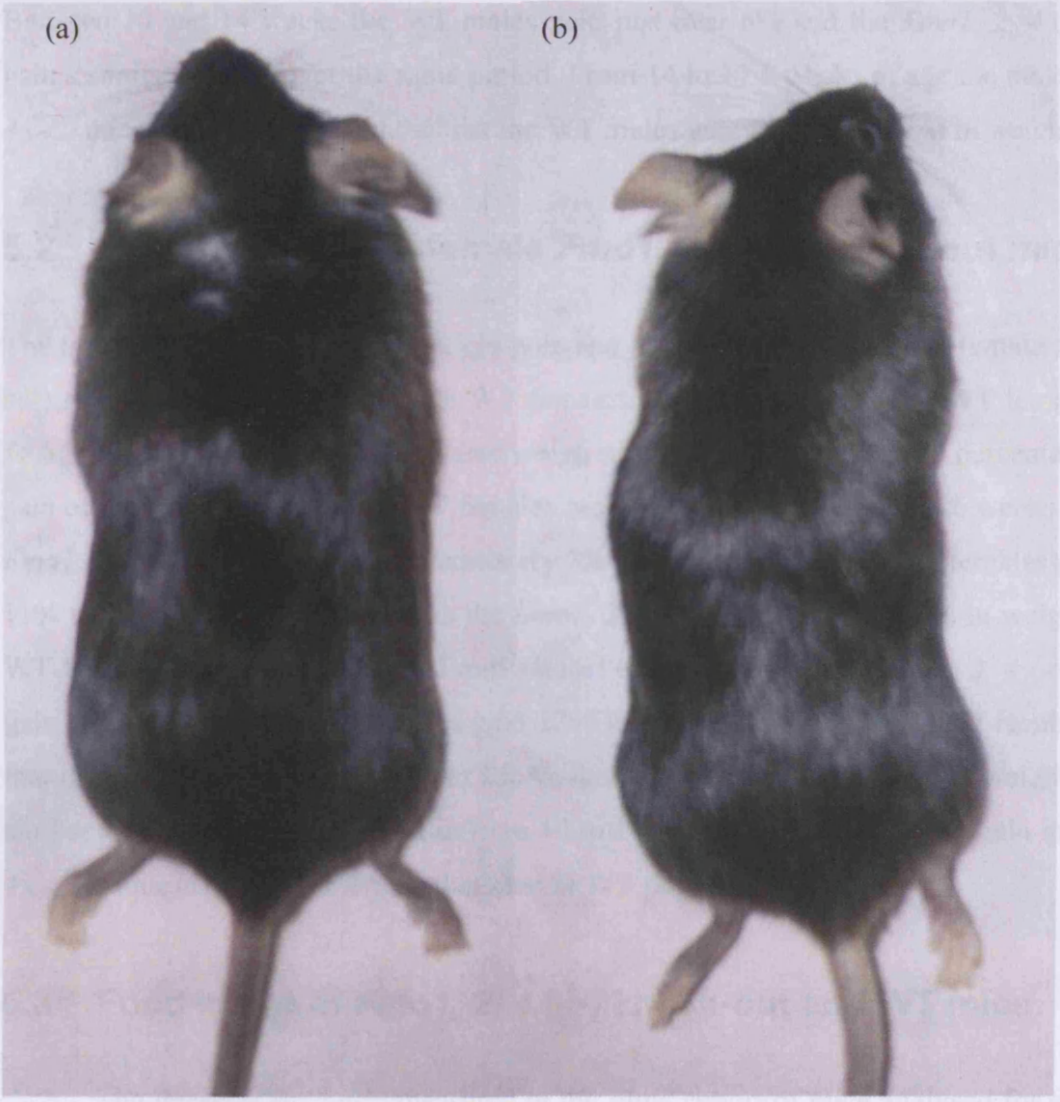

5.1.1 Picture of Fmo1, 2, 4 (-/-) male mouse and WT male mouse

Photographs of a representative WT male mouse (a) and a male *Fmo1, 2, 4* (-/-) mouse (b) are shown.

Between 10 and 14 weeks the WT males gain just over 6% and the *Fmo1, 2, 4* (-/-) males gain a similar amount over the same period. From 14 to 17.5 weeks of age the male *Fmo1, 2, 4* (-/-) mice gain 2.5% in weight whilst the WT males gain twice that (5%) in weight.

5.2 Weight analysis of female *Fmo1, 2, 4* (-/-) knock-out mice

The influence of gender in FMO weight gain and phenotype is observed in female *Fmo1, 2, 4* (-/-) mice who weigh more than the WT females. At 5 weeks of age the WT females weigh 15.8g, but the *Fmo1, 2, 4* (-/-) females weigh nearly 3 grams more. The percentage weight gain of the *Fmo1, 2, 4* (-/-) and WT females are quite similar. From 4.5 to 6 weeks of age the *Fmo1, 2, 4* (-/-) females gain approximately 7% in weight, whilst the WT females gain about 11% in weight. From 6 to 10 weeks the *Fmo1, 2, 4* (-/-) females gain 18% in weight and the WT females gain 20% in weight. From 10 to 14 weeks of age the *Fmo1, 2, 4* (-/-) females gain only 7.5% and the WT females gain 12% in weight (Figure 5.3.3). Our results indicate that the *Fmo1, 2, 4* (-/-) females start life weighing more, then maintain the weight gain at a similar level to the WT females. But from 10 to 14 weeks of age the weight gain in *Fmo1, 2, 4* (-/-) females is slightly less than that seen in WT females.

5.3 Food intake of *Fmo1, 2, 4* (-/-) knock-out and WT mice

The intake of food was measured in the same cohort of mice analysed for changes in bodyweight. The feed put into cages was weighed and the remaining feed was measured twice a week. This value was divided by the number of mice in the cage.

All mice ate a similar amount of food (Figure 5.3.2). Thus the lower bodyweight in the *Fmo1, 2, 4* (-/-) males is not due to decreased food consumption compared to WT males. Similarly the increased bodyweight observed in the *Fmo1, 2, 4* (-/-) females compared to WT females is not due to an increased consumption of food.

(a)

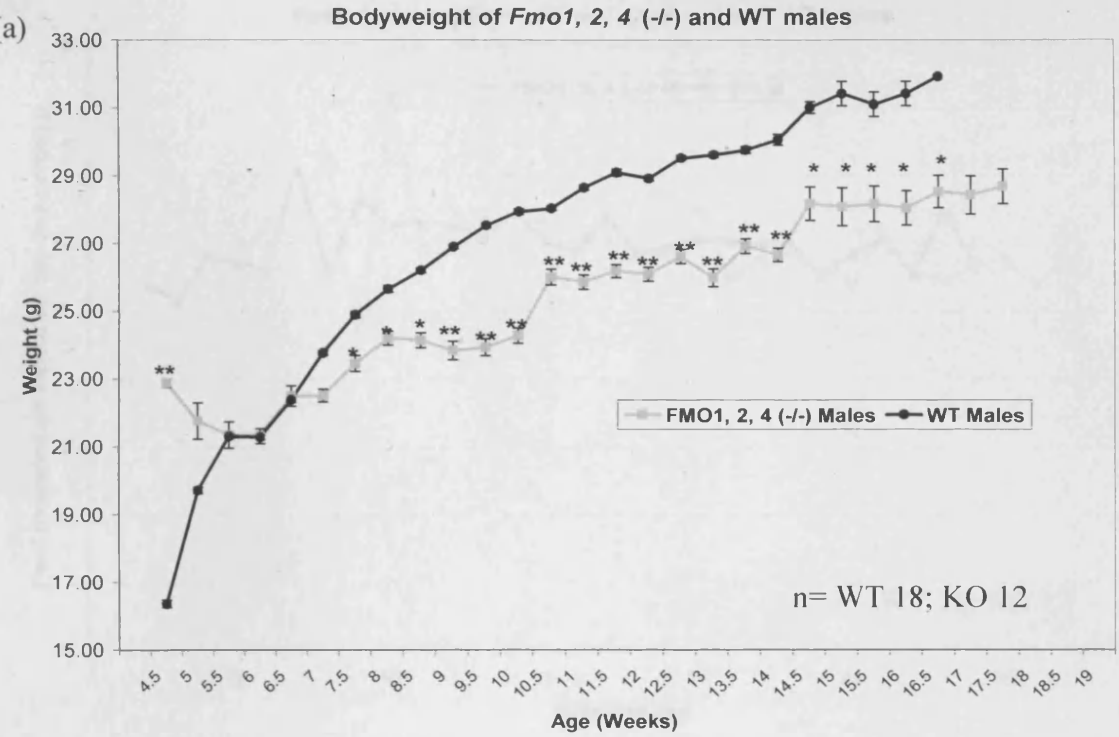

(b)

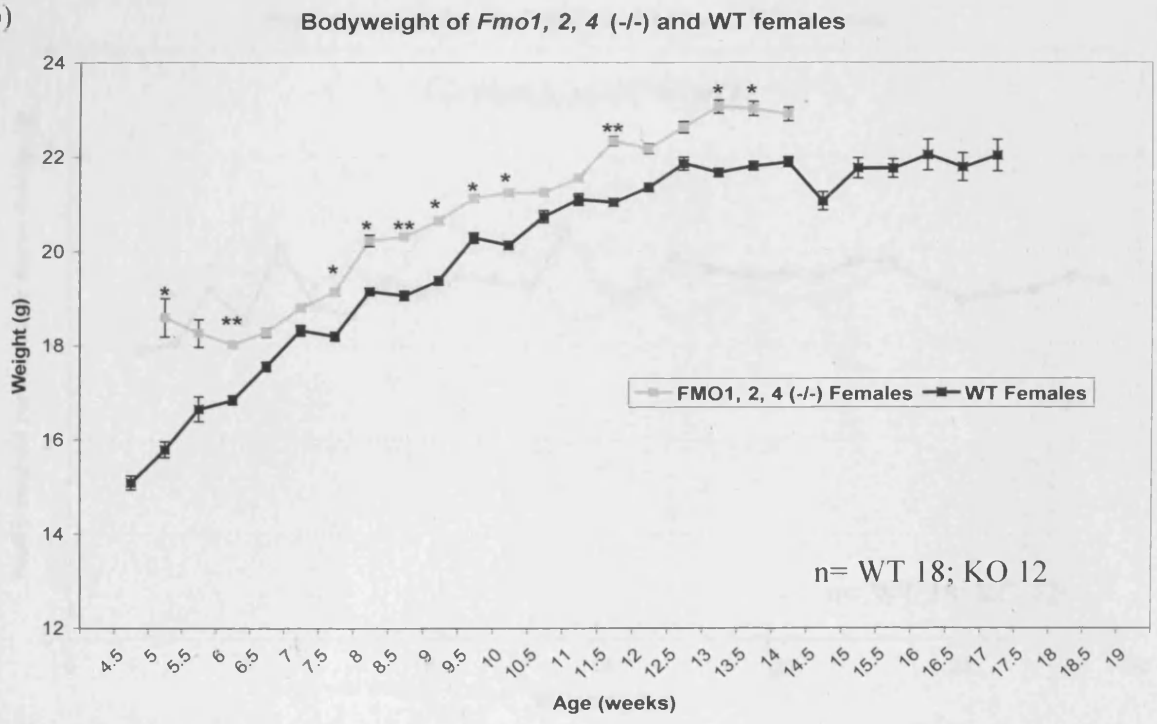

5.3.1 *Bodyweights of Fmo1, 2, 4 (-/-) and WT mice*

The bodyweight of *Fmo1, 2, 4* (-/-) and WT males (a) and females (b) on a normal chow diet from 4 to 18 weeks of age. * is $p<0.05$, ** is $p<0.005$. Error bars are SEM.

(a)

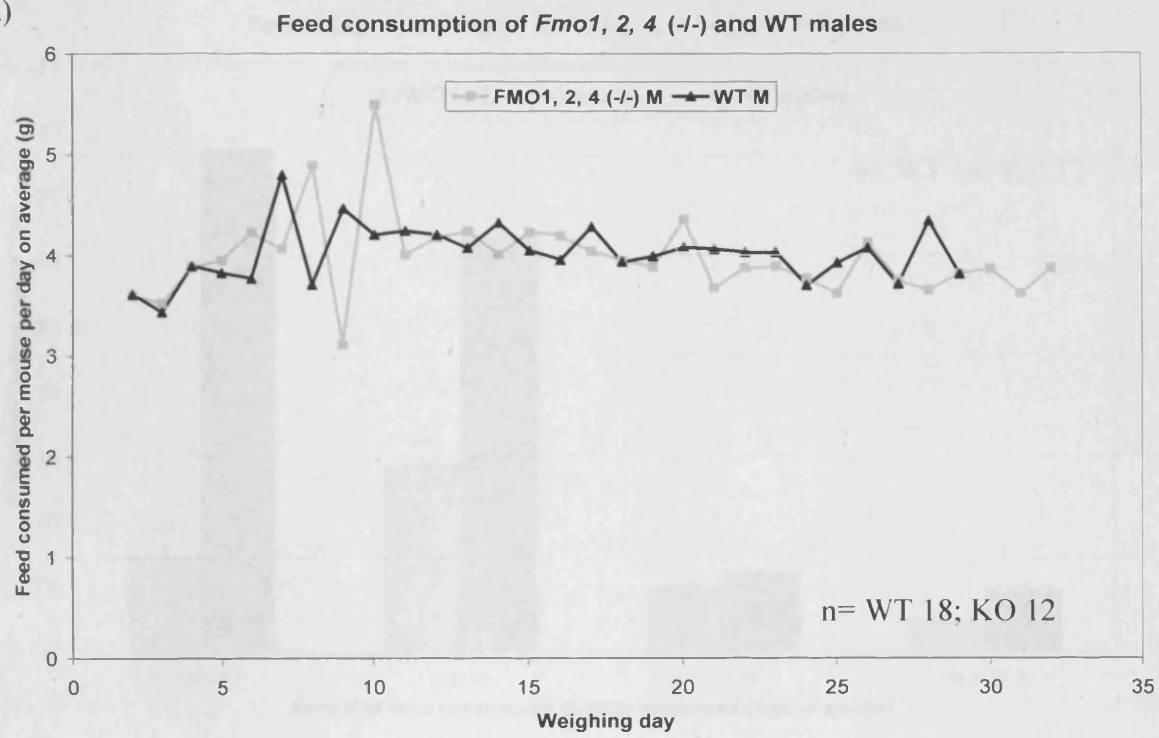

(b)

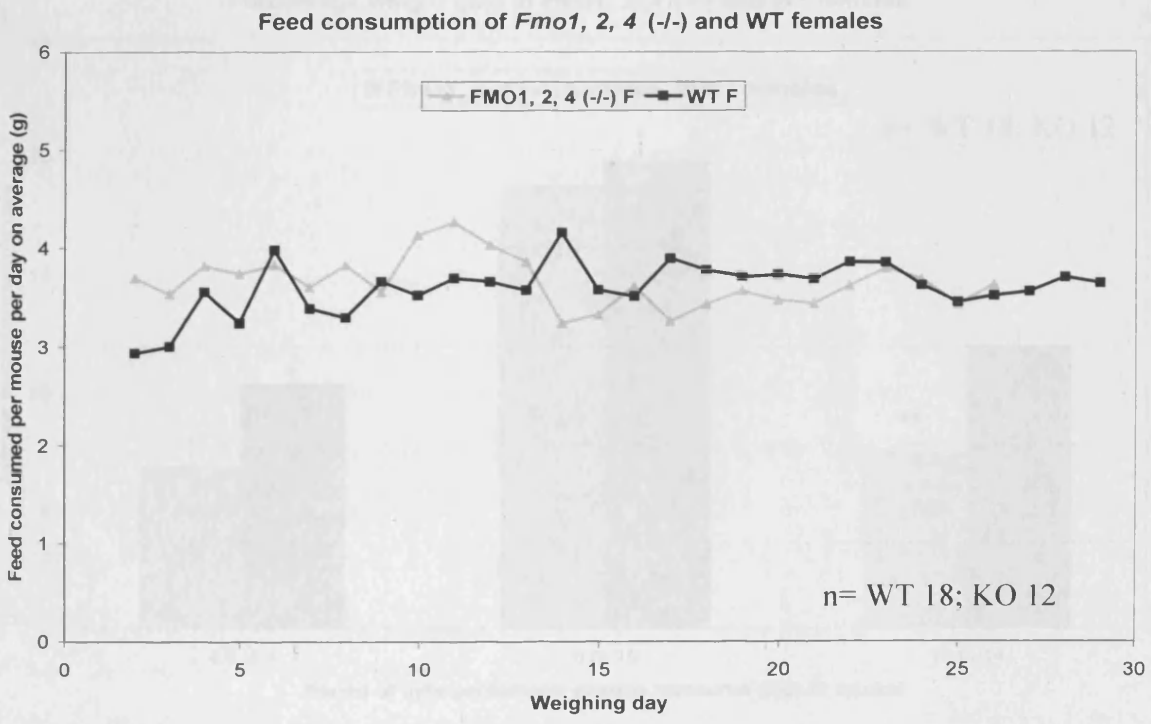

5.3.2 *Food consumption of Fmo1, 2, 4 (-/-) and WT mice*

Food consumption per mouse per day of *Fmo1, 2, 4* (-/-) and WT males (a) and females (b) on a normal chow diet.

(a)

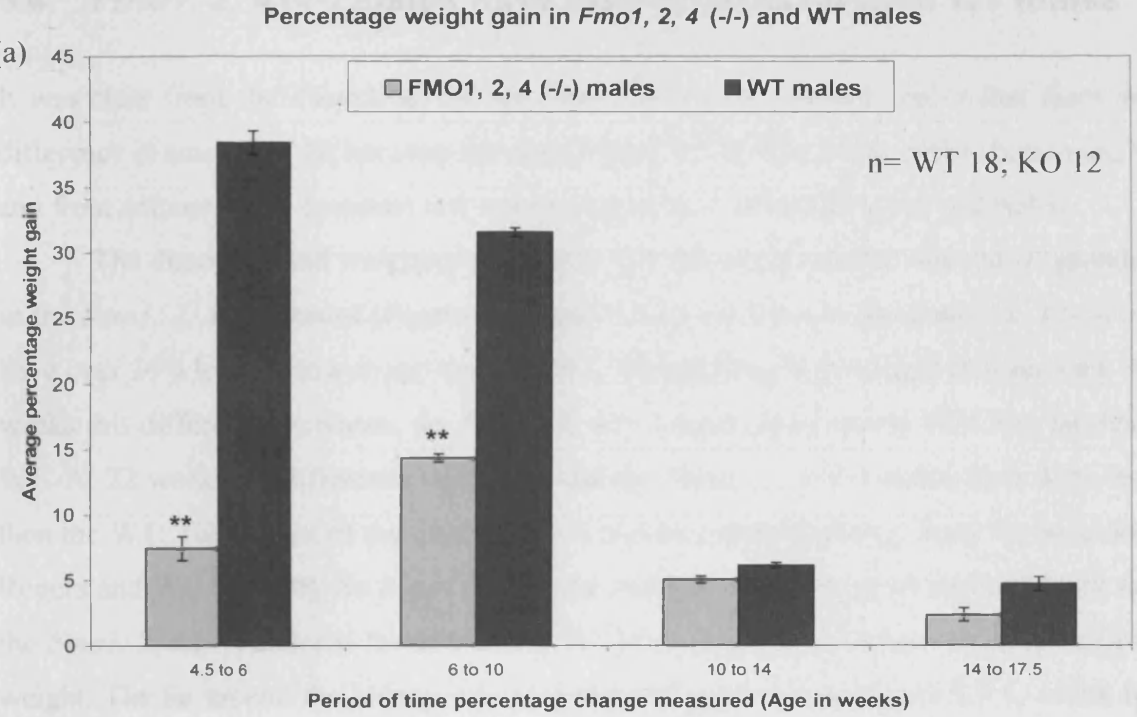

(b)

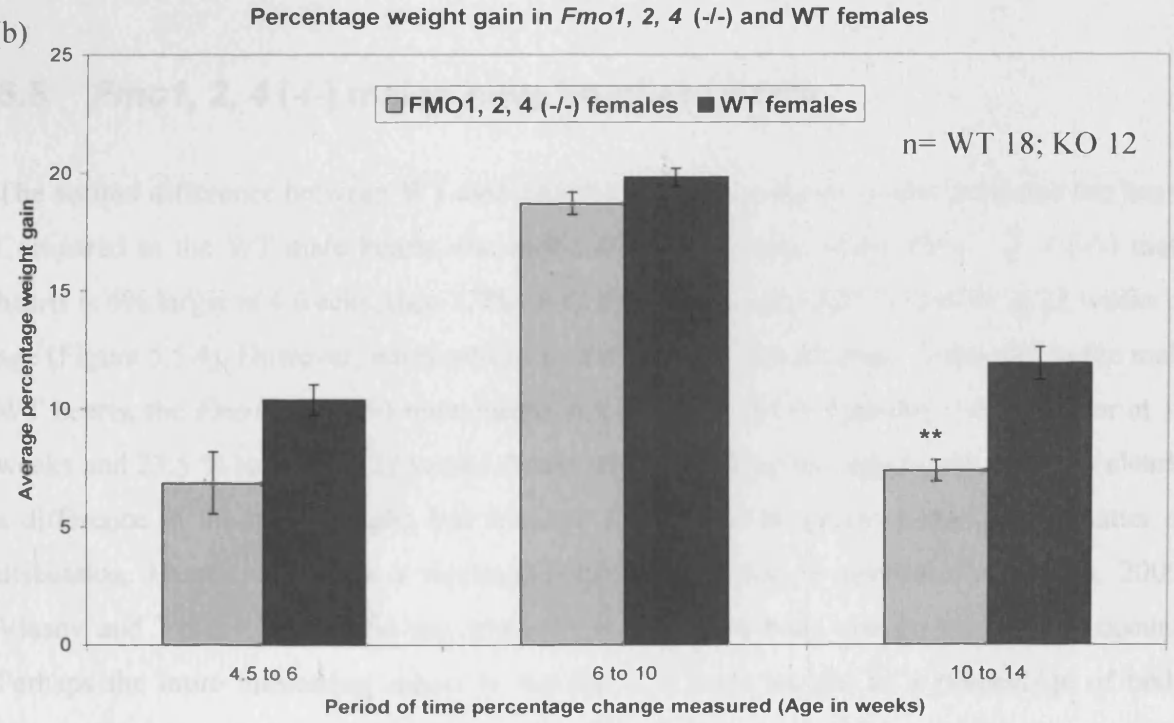

5.3.3 Percentage weight gain of Fmo1, 2, 4 (-/-) and WT mice

The percentage weight gain of *Fmo1, 2, 4* (-/-) and WT males (a) and females (b) on a normal chow diet. * is $p<0.05$, ** is $p<0.005$. Error bars are SEM.

5.4 *Fmo1, 2, 4* (-/-) males have less gonadal fat than WT males

It was clear from the dissections of the *Fmo1, 2, 4* (-/-) and WT males that there was a difference in amount of fat between the two (Figure 5.5.1). The liver, spleen, brown fat, heart and front adipose tissue (gonadal fat) were weighed in 4, 10 and 22 week old males.

The dissection and weighing confirmed that there is a reduced amount of gonadal fat in the *Fmo1, 2, 4* (-/-) males (Figure 5.5.2 and 5.5.3). At 4 weeks the *Fmo1, 2, 4* (-/-) males have over 26% less fat on average than the WT, when taking body weight into account. At 10 weeks this difference increases, the *Fmo1, 2, 4* (-/-) males have nearly 47% less fat than the WT. At 22 weeks the difference continues and the *Fmo1, 2, 4* (-/-) males have 43% less fat then the WT. The weight of the gonadal fat is a good estimate of total body fat according to Rogers and Webb (1980). So it can perhaps be assumed that in general the total body fat for the *Fmo1, 2, 4* (-/-) males is lower than the WT mice, leading to a mouse with reduced body weight. The fat around the kidney was also reduced as shown in Figure 5.5.1, which backs this theory up.

5.5 *Fmo1, 2, 4* (-/-) males have smaller hearts

The second difference between WT and cluster KO mice in organ weight concerns the heart. Compared to the WT male hearts, the absolute organ weight of the *Fmo1, 2, 4* (-/-) male hearts is 6% larger at 4 weeks, then 17% smaller at 10 weeks and 21% smaller at 22 weeks of age (Figure 5.5.4). However, when you take body weight into account, compared to the male WT hearts, the *Fmo1, 2, 4* (-/-) male hearts are 16.5% larger at 4 weeks, 7.8% smaller at 10 weeks and 23.5 % smaller at 22 weeks. None of these values are significant. There is clearly a difference in the heart weight, but whether this should be given credence is a matter of discussion. Hearts tend to be a representation of body size in general (Janz et al., 2000; Vlasov and Volkov, 2004). So any changes should have body weight taken into account. Perhaps the more interesting aspect is that the KO heart weight as a percentage of body weight plummets at 22 weeks, whereas the WT hearts remain fairly consistent across the ages.

WT male

Fmo1, 2, 4 (-/-) male

5.5.1 Abdominal and kidney photos from Fmo1, 2, 4 (-/-) and WT male mice

Representative photographs of the in situ gonadal fat (a) and the kidney with associated fat (b). The WT images on the left of the page, *Fmo1, 2, 4* (-/-) images on the right.

(a)

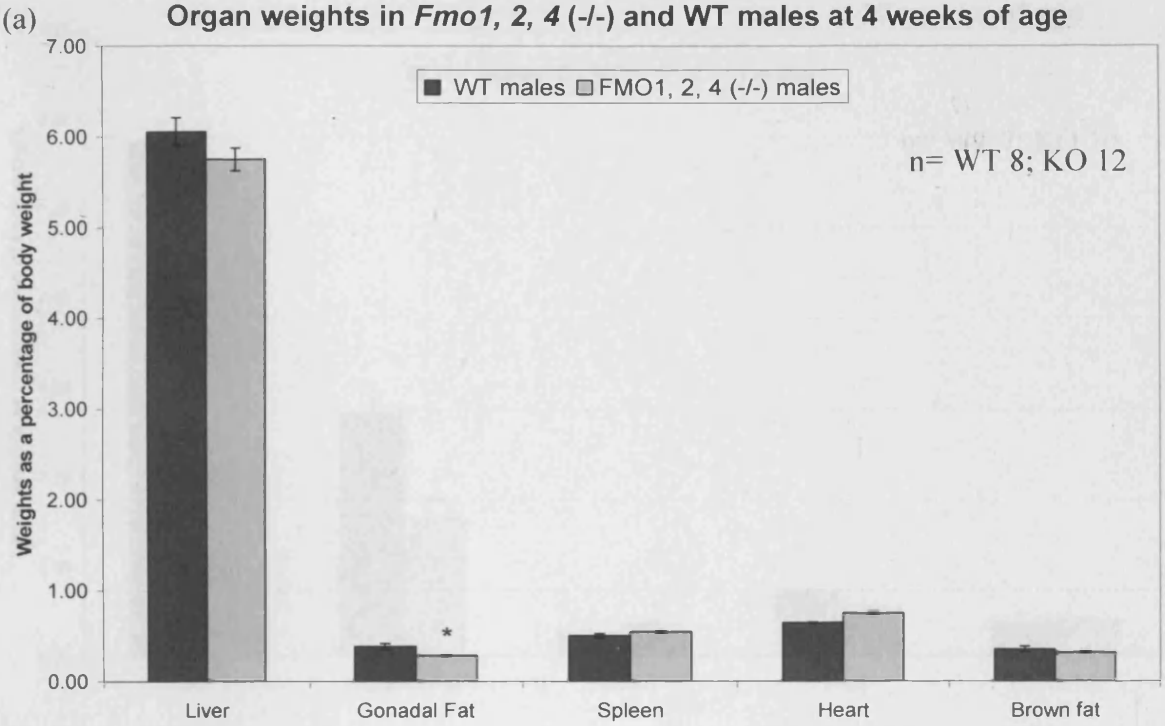

(b)

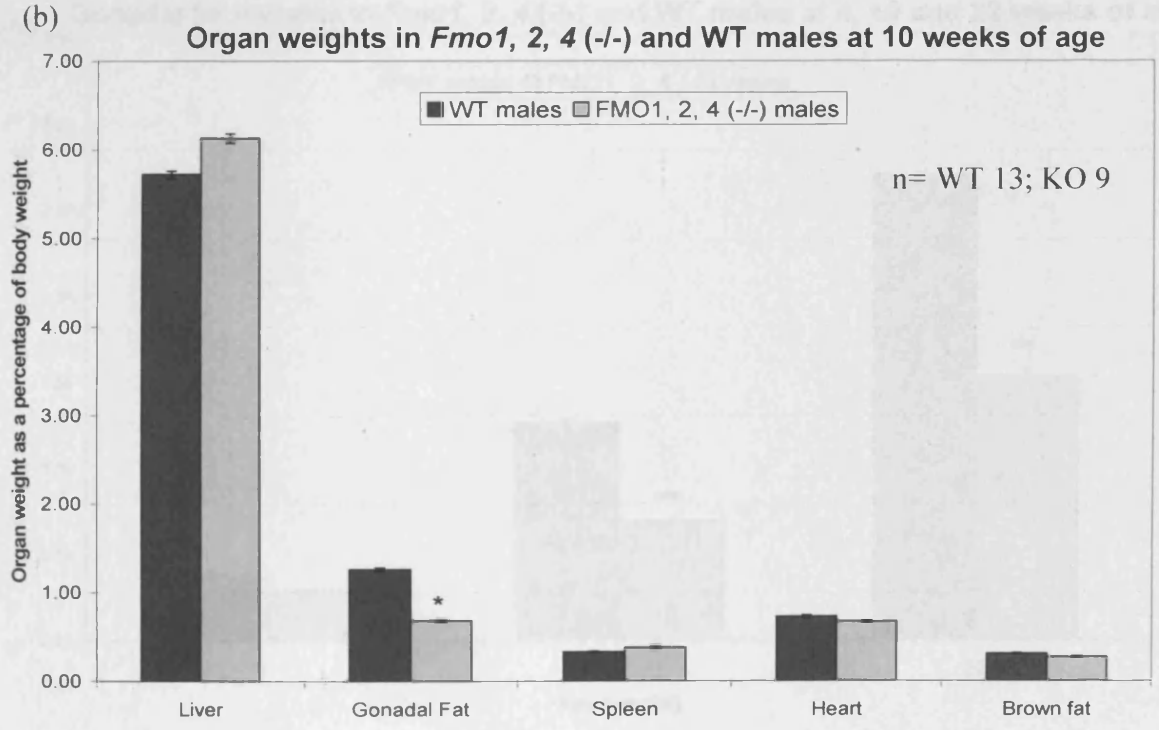

5.5.2 Organ weights at 4 and 10 weeks of age-Fmo1, 2, 4 (-/-) males

The organ weights as a percentage of body weight of *Fmo1, 2, 4* (-/-) and WT males on a normal diet at 4 weeks of age (a) and 10 weeks of age (b). * is $p<0.05$. Error bars are SEM.

(a)

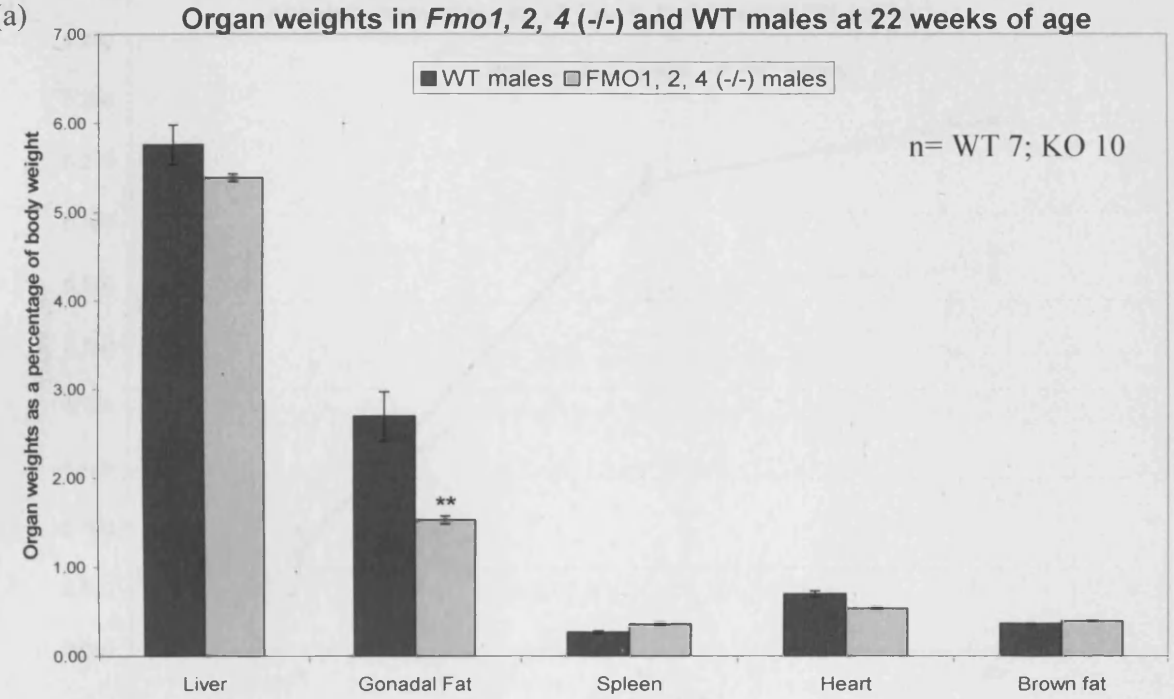

(b)

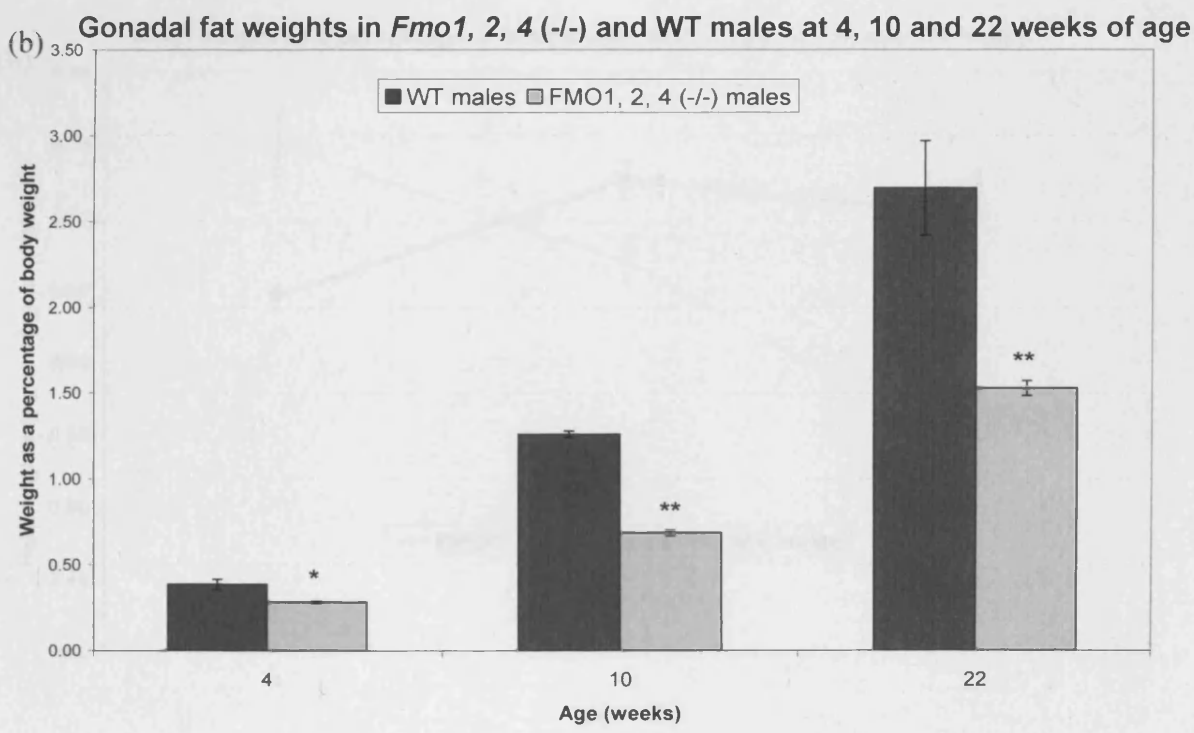

5.5.3 Organ weights and gonadal fat weight

Organ weights at 22 weeks of age (a) and gonadal fat weight at 4, 10 and 22 weeks of age (b) in *Fmo1, 2, 4* (-/-) and WT males. * is $p<0.05$, ** is $p<0.005$.

(a)

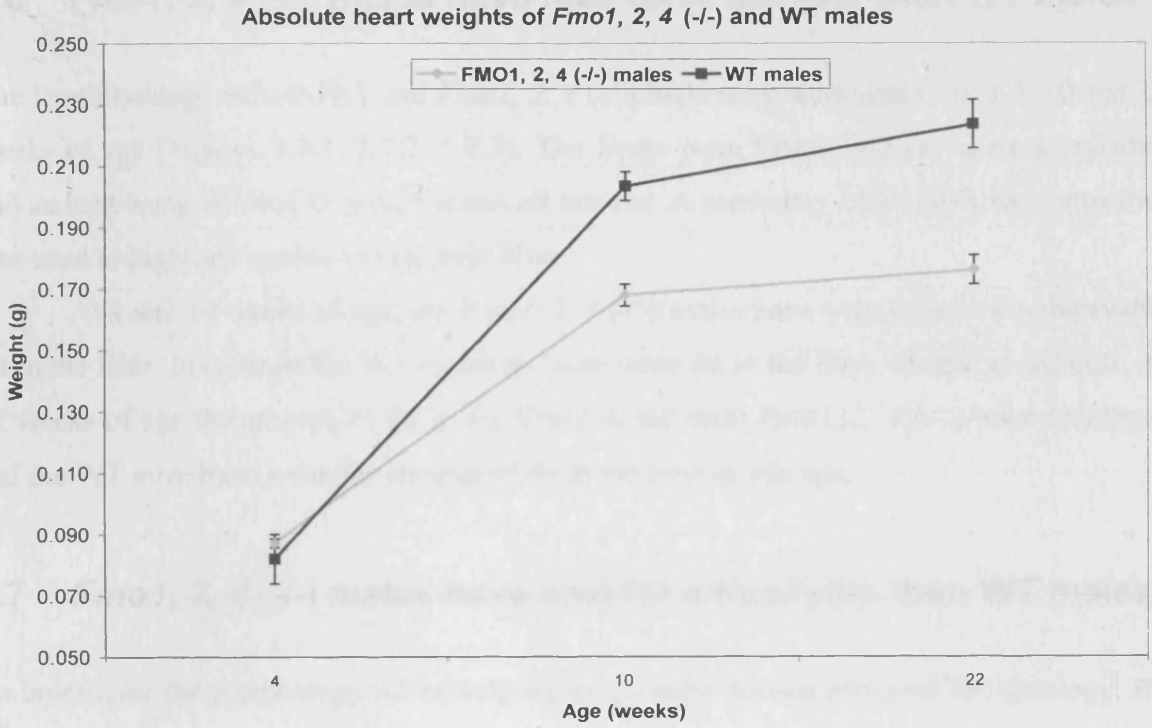

(b)

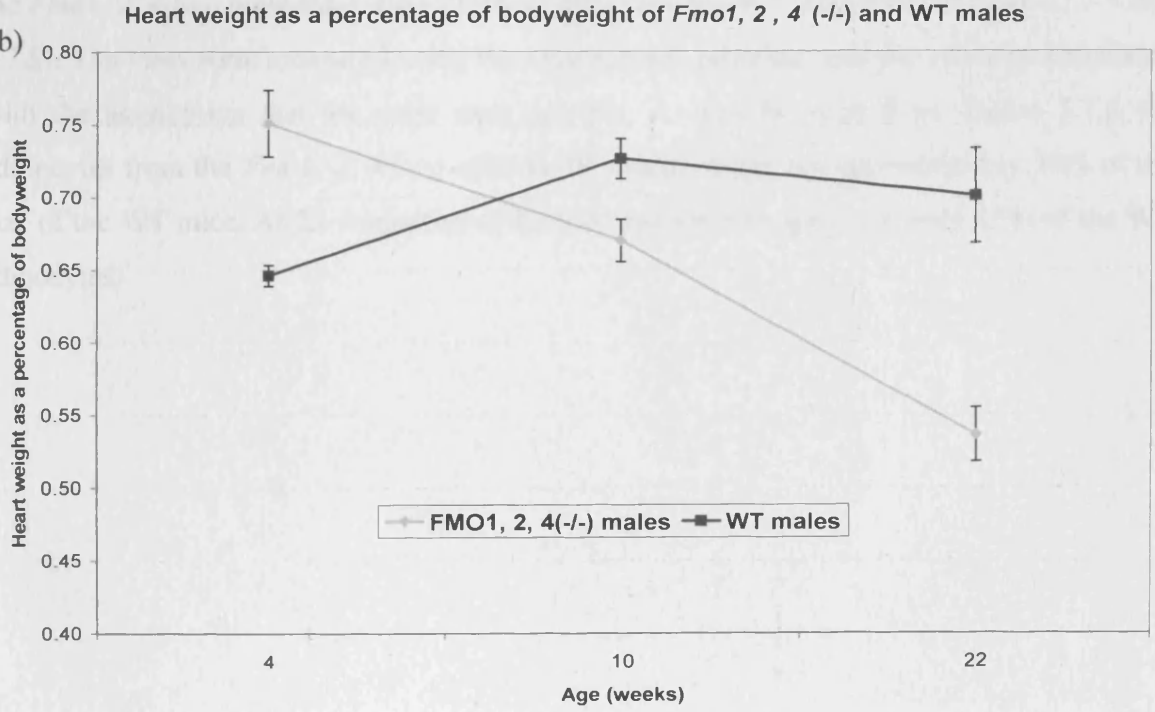

5.5.4 *Heart weights*

Absolute heart weight (a) and heart weight as a percentage of body weight (b) in *Fmo1, 2, 4* (-/-) and WT males at 4, 10 and 22 weeks of age. Error bars are SEM.

5.6 *Fmo1, 2, 4* (-/-) males have less fat in the liver than WT males

The liver histology of both WT and *Fmo1, 2, 4* (-/-) male mice were analysed at 4, 10 and 22 weeks of age (Figures 5.7.1, 5.7.2, 5.7.3). The livers were frozen and cut using a cryostat, and stained using Oil Red O, which stains all fats red. A secondary stain, Gil's haematoxylin, was used to highlight nuclei, which stain blue.

At 4 and 10 weeks of age, the *Fmo1, 2, 4* (-/-) males have very little or no observable fat in the liver. In contrast the WT males do have some fat in the liver, visible as red dots. At 22 weeks of age the amount of fat in the livers of the male *Fmo1, 2, 4* (-/-) mice increases, and the WT mice have a similar amount of fat in the liver at this age.

5.7 *Fmo1, 2, 4* (-/-) males have smaller adipocytes than WT males

To investigate the morphology of the adipocytes, gonadal fat was removed for histology. All adipose fixing and staining was done by Mr Omar. It became clear that the adipocytes from the *Fmo1, 2, 4* (-/-) male mice were much smaller than the WT adipocytes (Figures 5.7.4 and 5.7.5). The sizes were measured using the Openlab 6.0 program, and the volumes calculated with the assumption that the cells were spheres. As can be seen from Figure 5.7.6 the adipocytes from the *Fmo1, 2, 4* (-/-) mice at 10 weeks of age are approximately 50% of the size of the WT mice. At 22 weeks this difference increases to approximately 25% of the WT adipocytes.

(a)

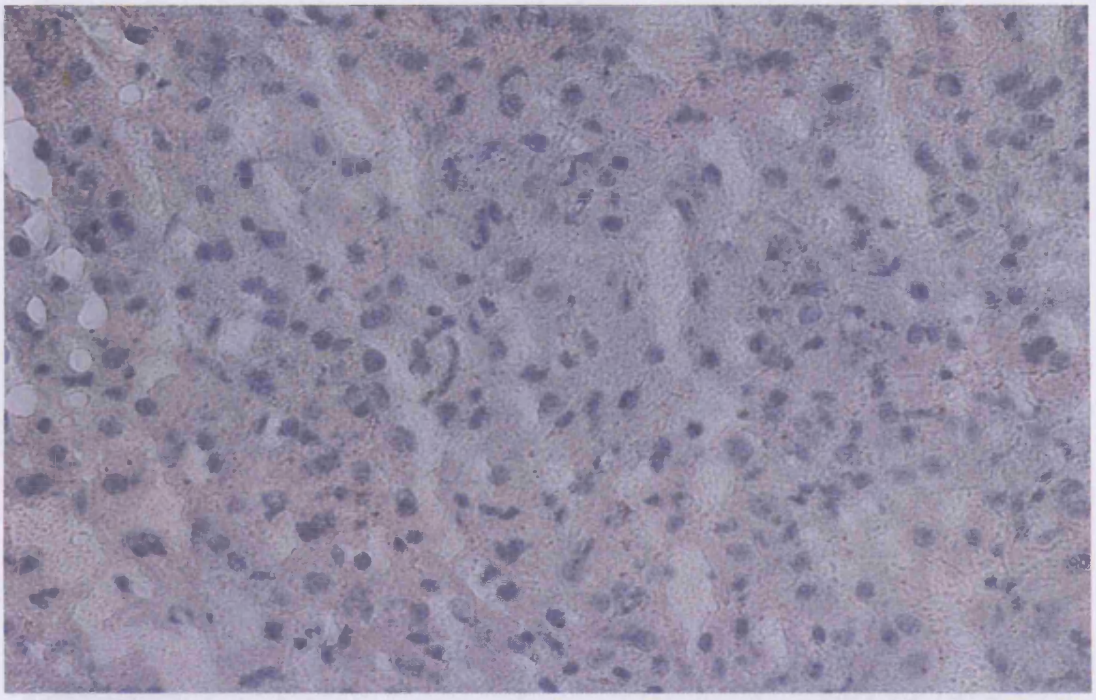

(b)

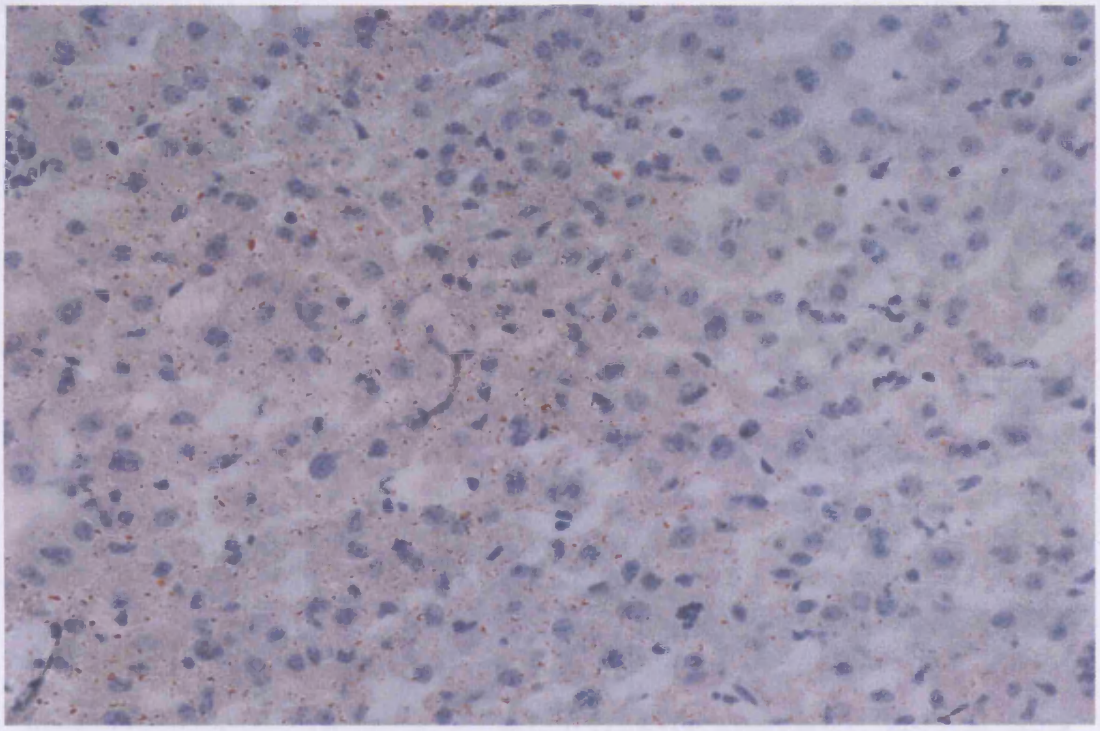

5.7.1 Liver histology in Fmo1, 2, 4 (-/-) and WT males at 4 weeks of age

A representative photograph of the liver histology in *Fmo1, 2, 4* (-/-) males (a) and WT males (b) at 4 weeks of age.

(a)

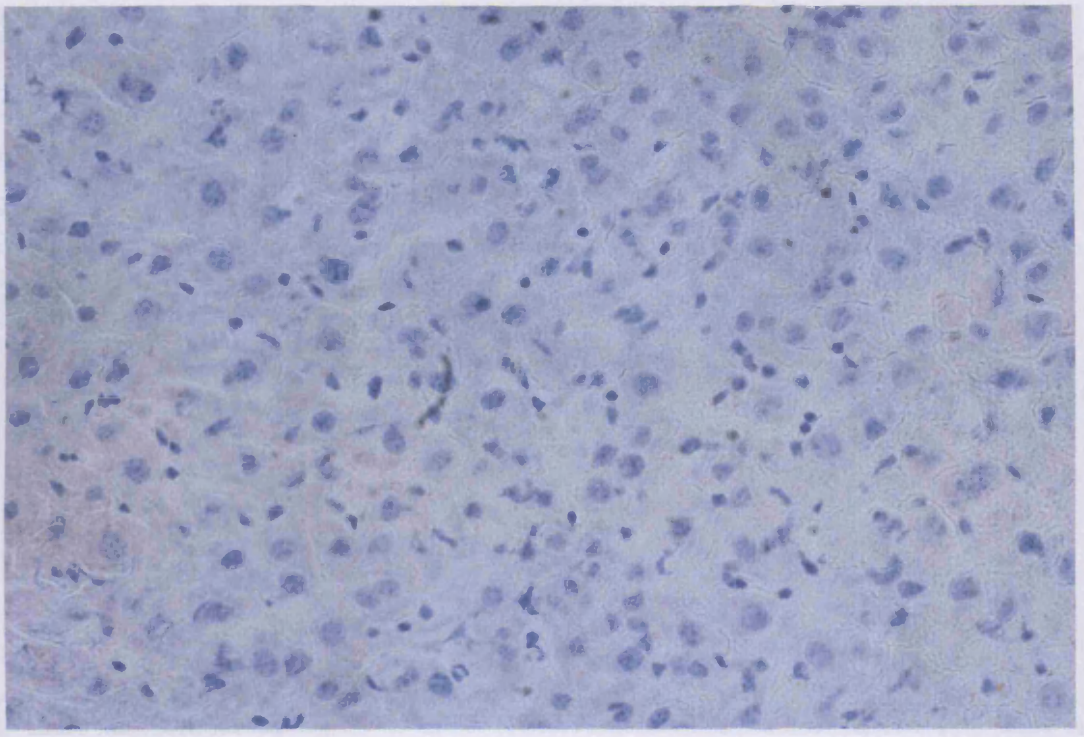

(b)

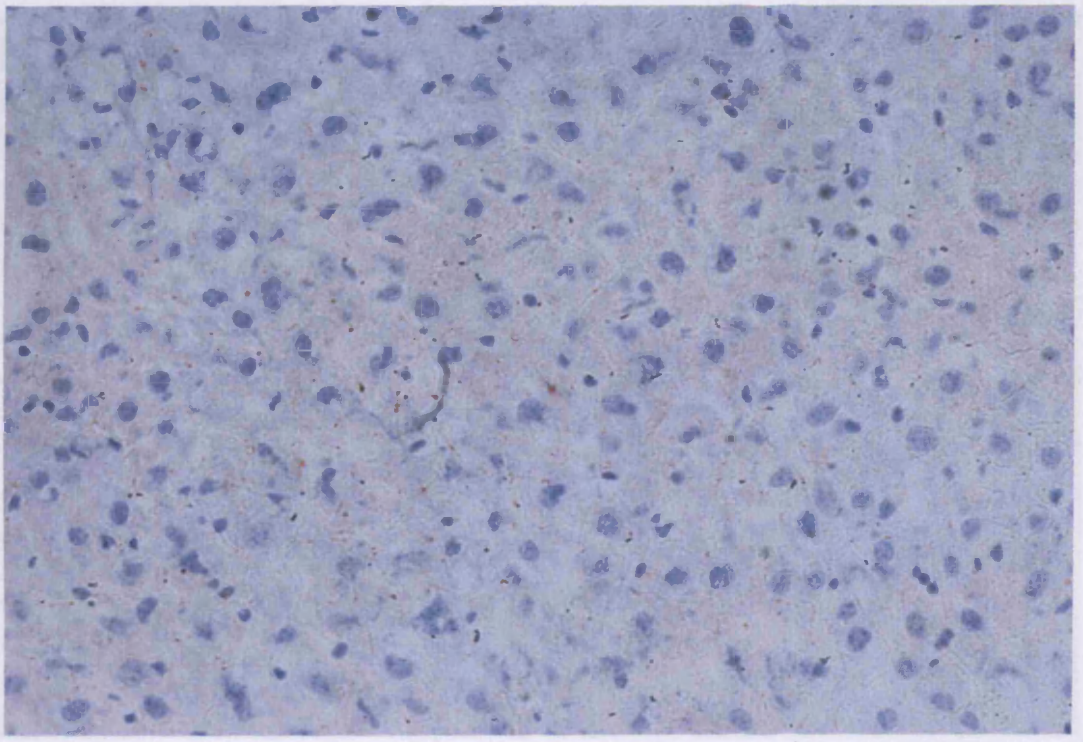

5.7.2 *Liver histology in Fmo1, 2, 4 (-/-) and WT males at 10 weeks of age*

A representative photograph of the liver histology in *Fmo1, 2, 4* (-/-) males (a) and WT males (b) at 10 weeks of age.

(a)

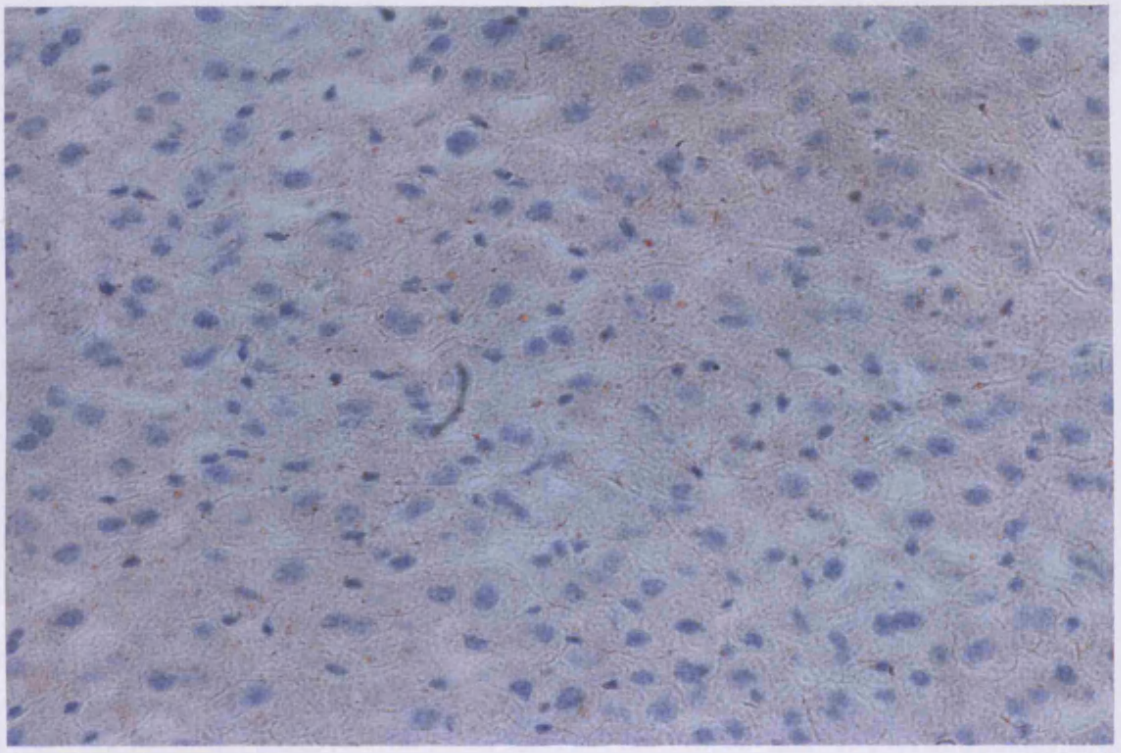

(b)

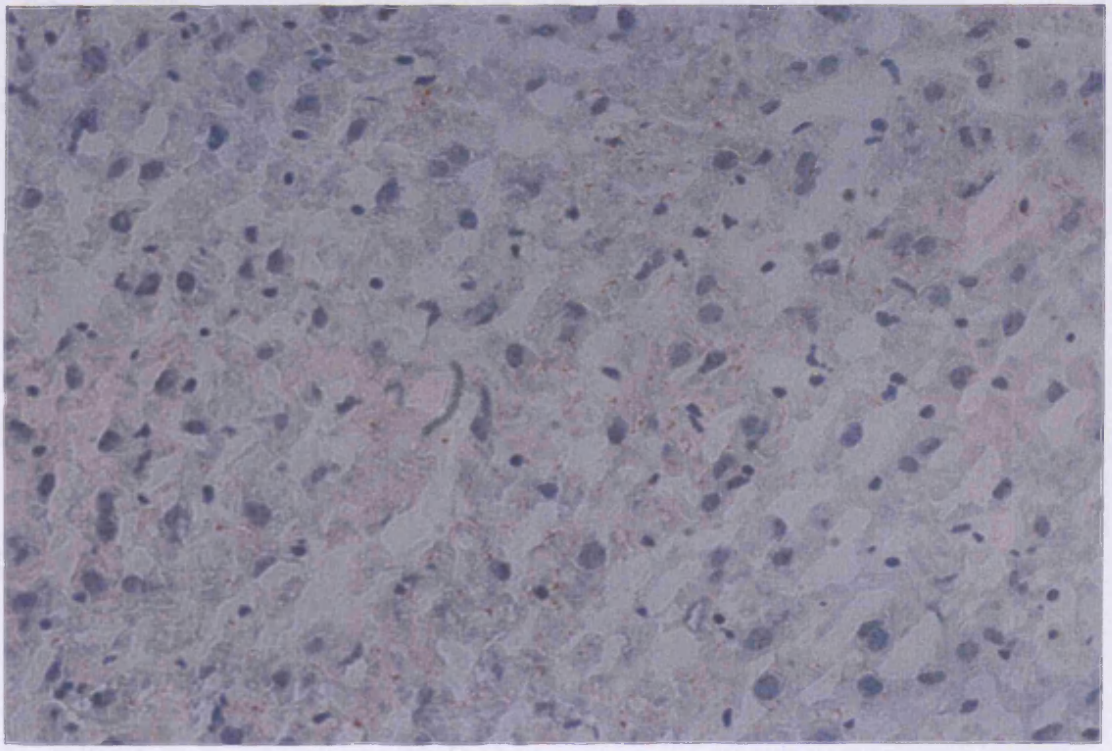

5.7.3 Liver histology in Fmo1, 2, 4 (-/-) and WT males at 22 weeks of age

A representative photograph of the liver histology in *Fmo1, 2, 4* (-/-) males (a) and WT males (b) at 22 weeks of age.

(a)

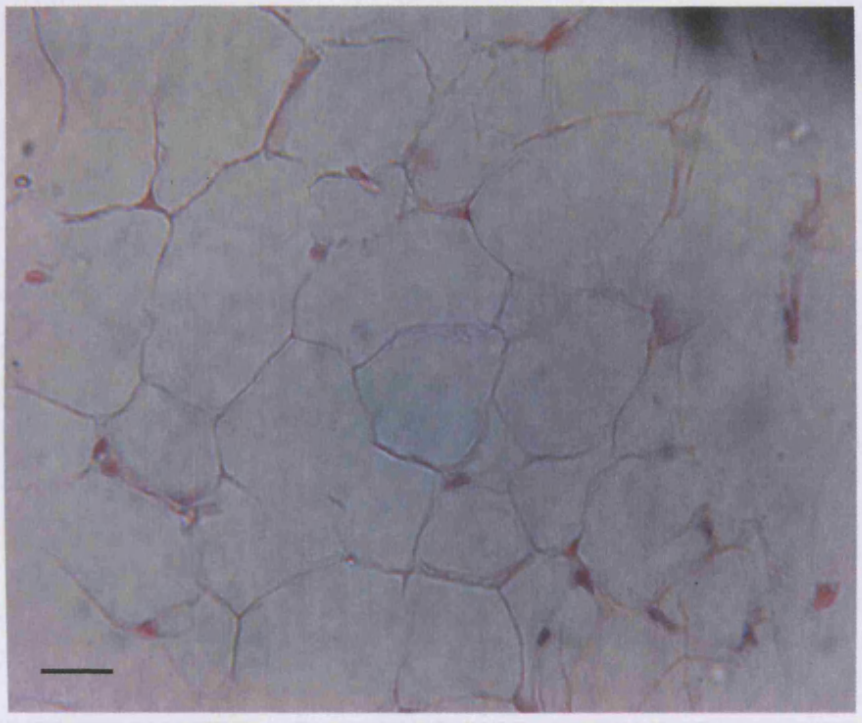

(b)

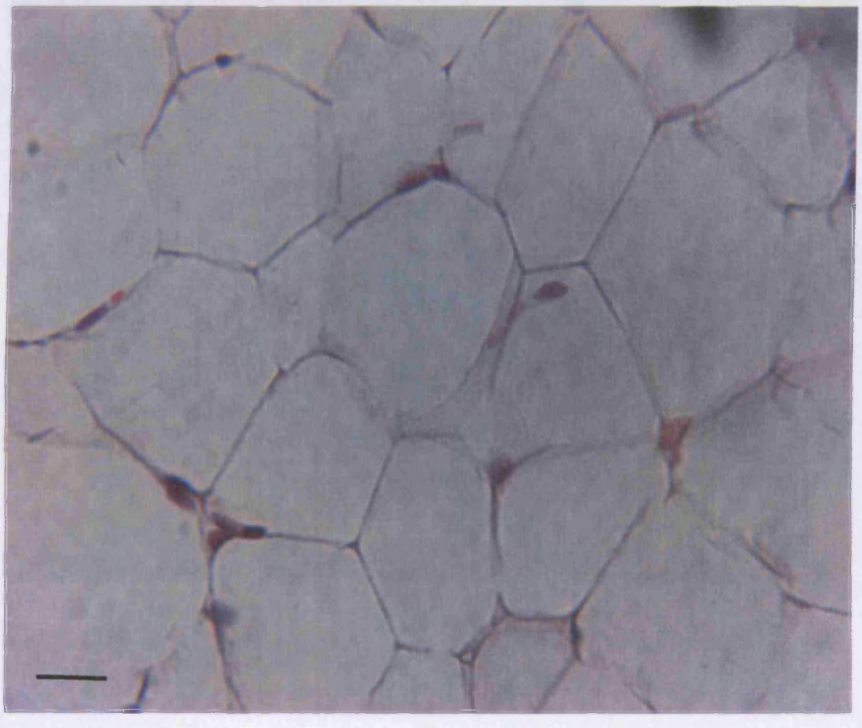

5.7.4 *Adipocyte histology-10 week males*

Representative images of the adipocyte histology of 10-week old male mice, *Fmo1, 2, 4* (-/-) (a), and WT (b), both on a normal chow diet. Scale bar represents 75 μm.

(a)

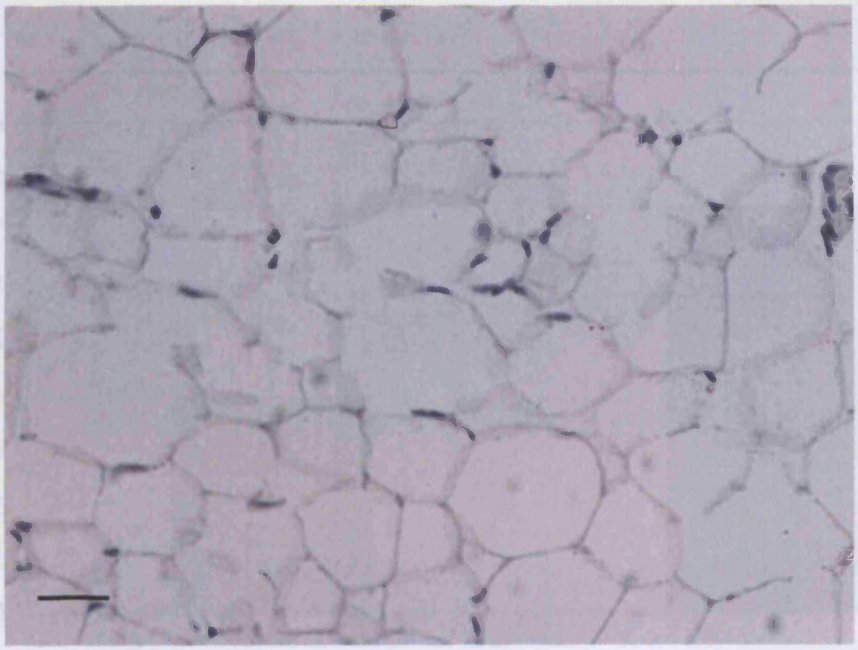

(b)

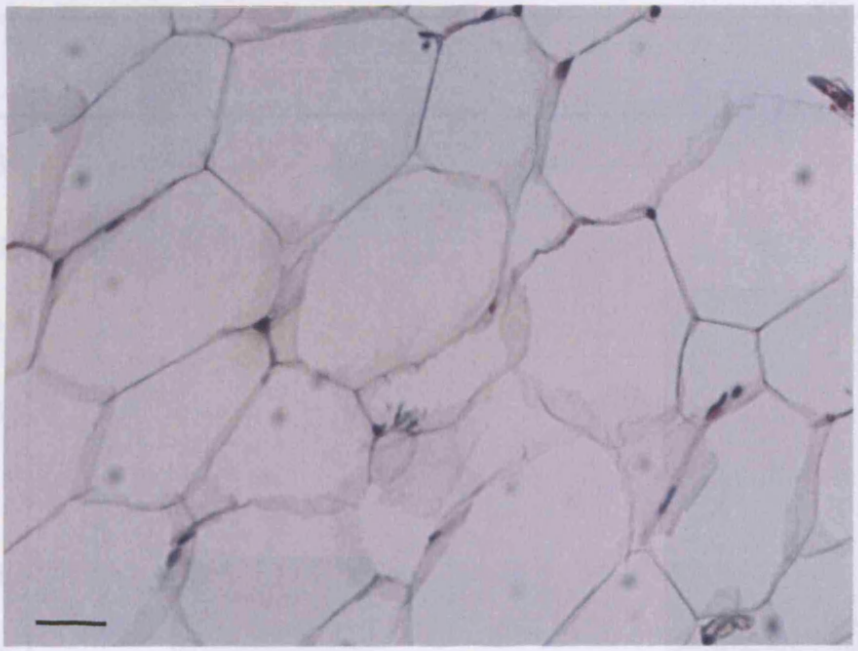

5.7.5 *Adipocyte histology-22 week males*

Representative images of the adipocyte histology of 22-week old male mice, *Fmo1, 2, 4* (-/-) (a), and WT (b), both on a normal chow diet. Scale bar represents 75 μm.

(a)

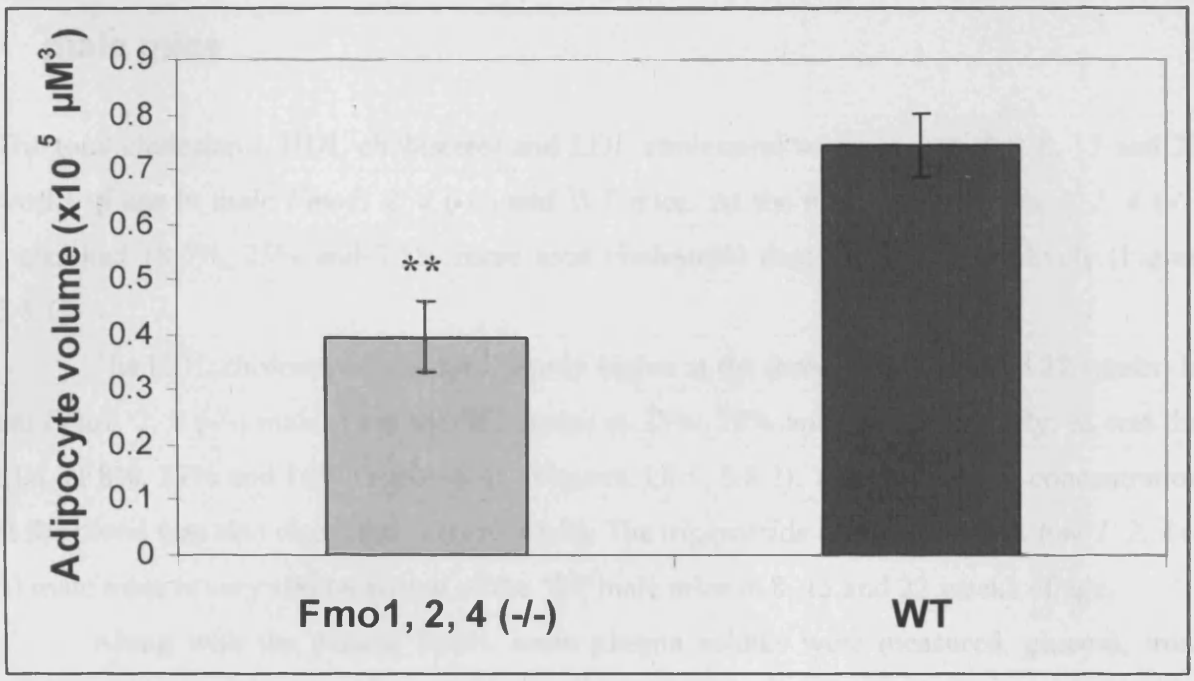

(b)

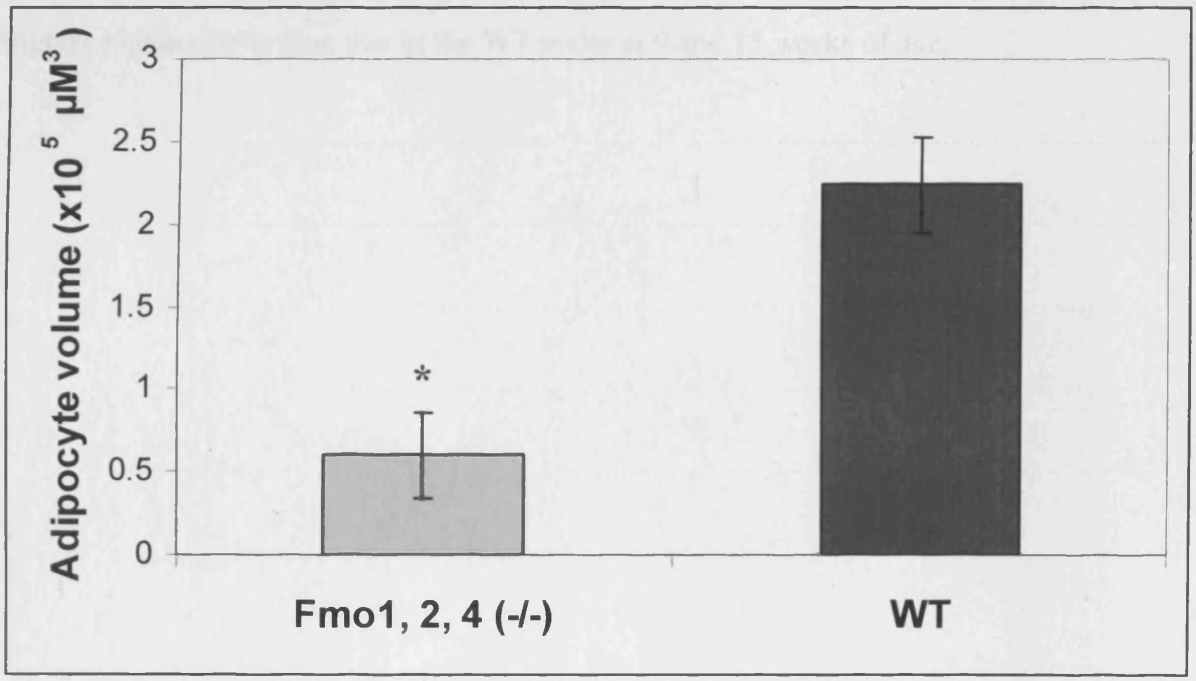

5.7.6 Adipocyte volumes-normal diet

The adipocyte volumes of 10-week (a) and 22-week (b) old male *Fmo1, 2, 4* (-/-) and WT mice, both on a normal chow diet. * is $p<0.05$, ** is $p<0.005$. Error bars are SEM.

5.8 Analysis of blood plasma lipids and solutes in *Fmo1, 2, 4* (-/-) male mice

The total cholesterol, HDL cholesterol and LDL cholesterol were measured at 8, 15 and 22 weeks of age in male *Fmo1, 2, 4* (-/-) and WT mice. At the three ages the *Fmo1, 2, 4* (-/-) males had 18.5%, 25% and 7.5% more total cholesterol than the WT respectively (Figure 5.8.1).

The HDL cholesterol was consistently higher at the three ages (8, 15 and 22 weeks) in the *Fmo1, 2, 4* (-/-) males than the WT males at 23%, 28% and 9% respectively; as was the LDL at 8%, 27% and 16% respectively (Figures 5.8.1, 5.8.2). The triglyceride concentration in the blood was also measured (Figure 5.8.2). The triglyceride concentration in *Fmo1, 2, 4* (-/-) male mice is very similar to that of the WT male mice at 8, 15 and 22 weeks of age.

Along with the plasma lipids, some plasma solutes were measured, glucose, iron, calcium and urea. There were no significant changes in plasma solutes observed in the *Fmo1, 2, 4* (-/-) male mice (Figures 5.8.3 and 5.8.4), although the level of iron in the plasma is slightly higher (20%) than that in the WT males at 9 and 15 weeks of age.

(a)

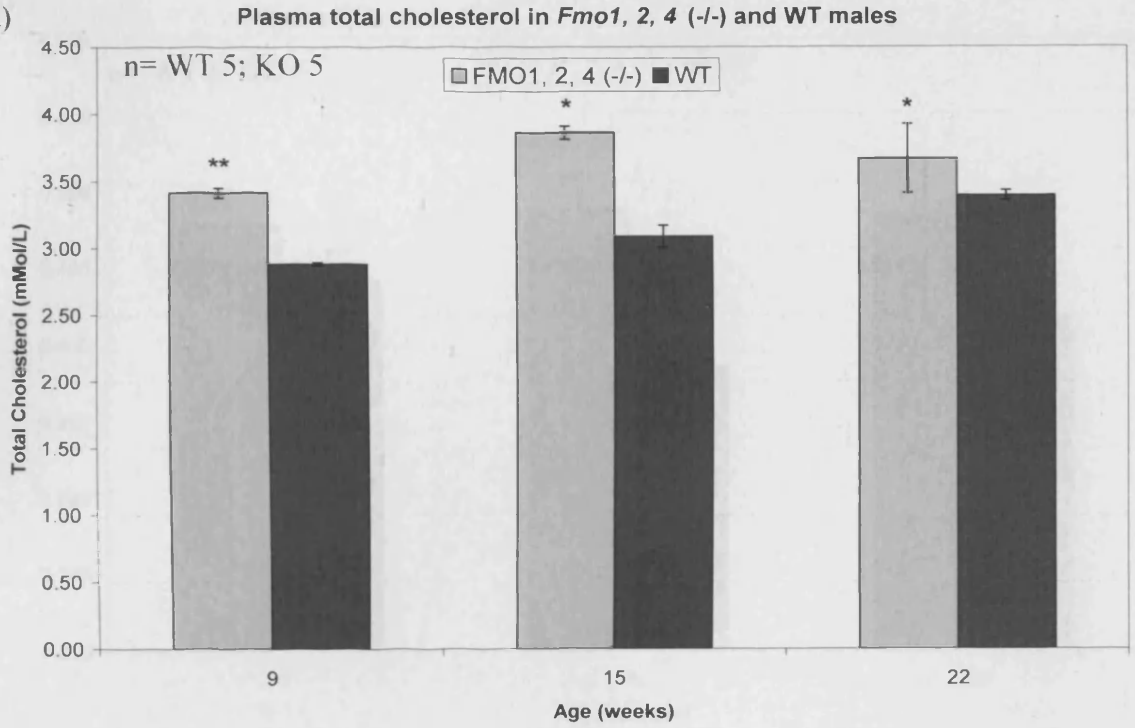

(b)

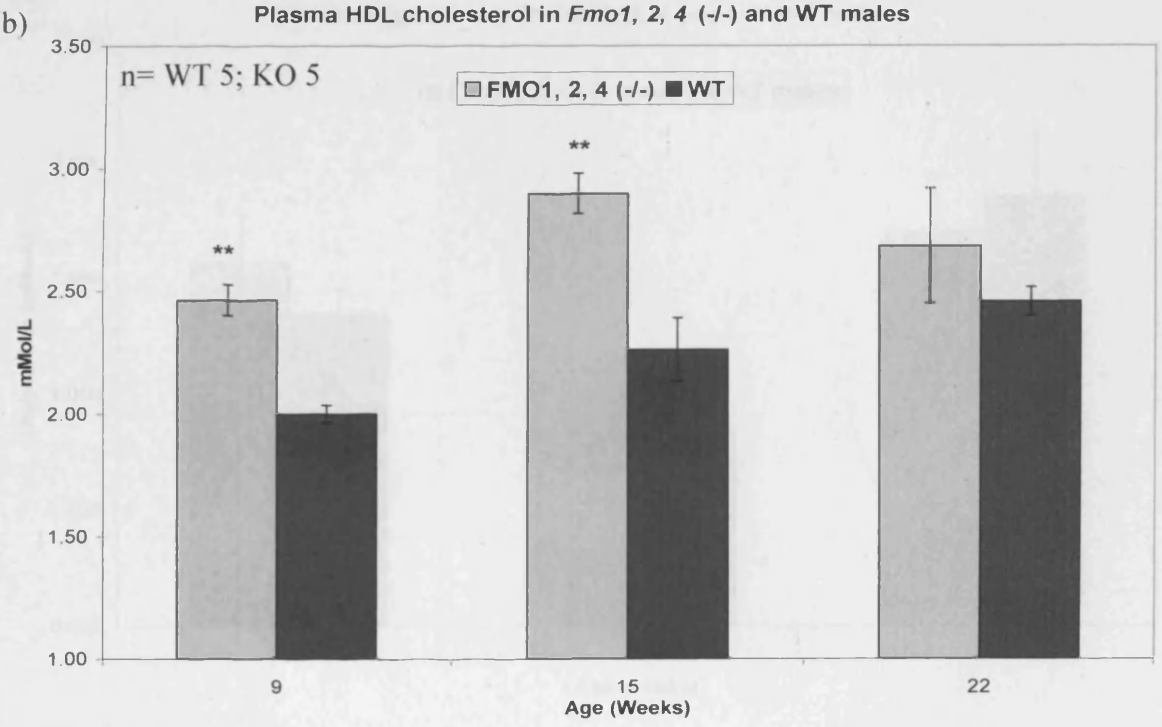

5.8.1 *Total cholesterol and HDL cholesterol*

The blood plasma lipids in *Fmo1, 2, 4* (-/-) and WT males, total cholesterol (a) and HDL cholesterol (b) at 8, 15 and 22 weeks of age. * is $p<0.05$, ** is $p<0.005$. Error bars are SEM.

(a)

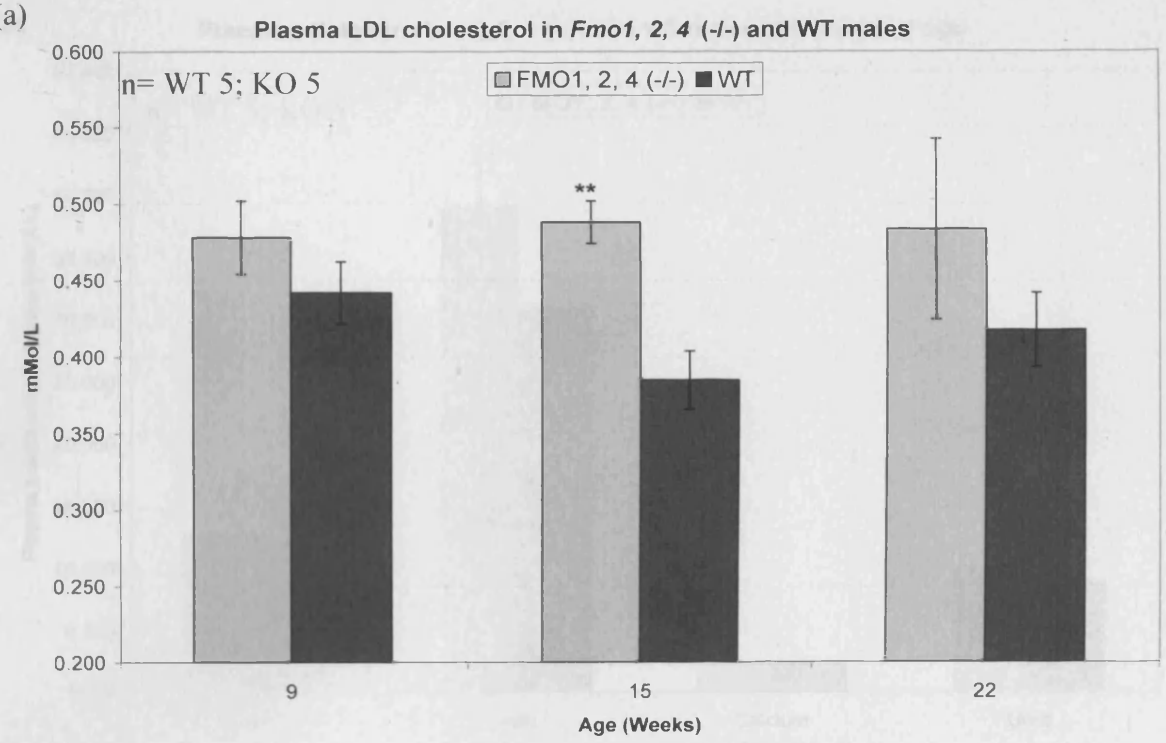

(b)

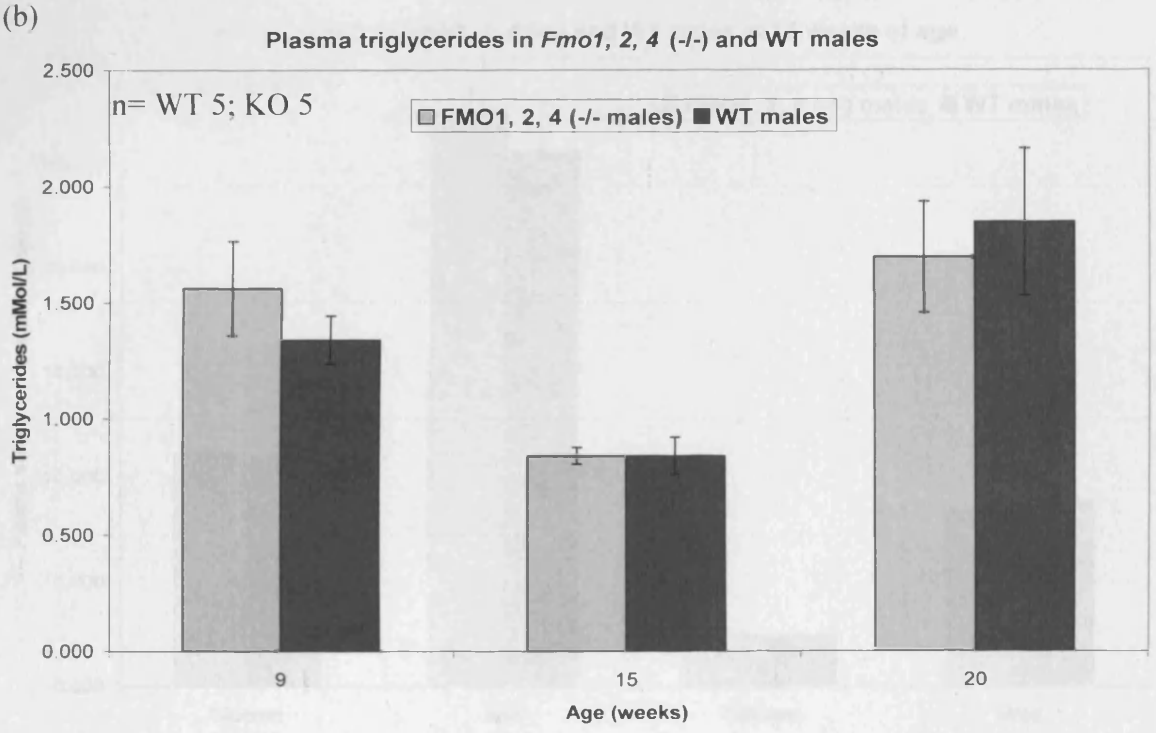

5.8.2 LDL cholesterol and triglycerides

The blood plasma lipids in *Fmo1, 2, 4* (-/-) and WT males. LDL cholesterol (a) and triglycerides (b) at 8, 15 and 22 weeks of age.* is $p<0.05$, ** is $p<0.005$. Error bars are SEM.

(a)

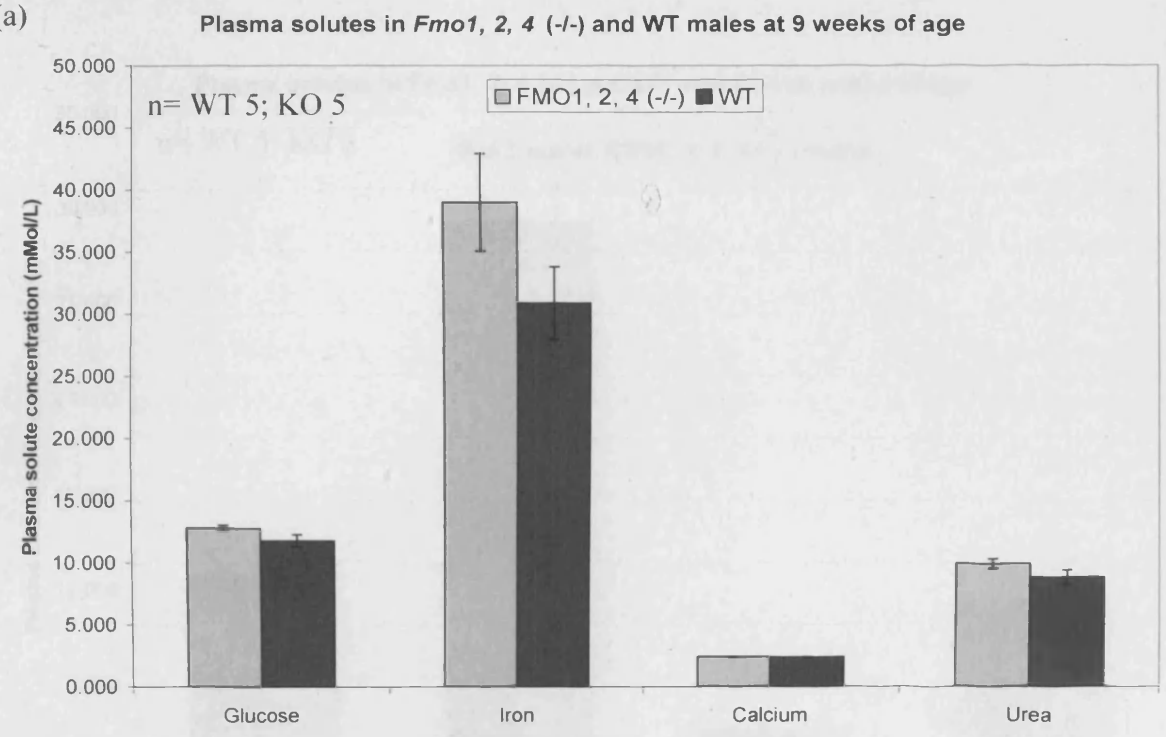

(b)

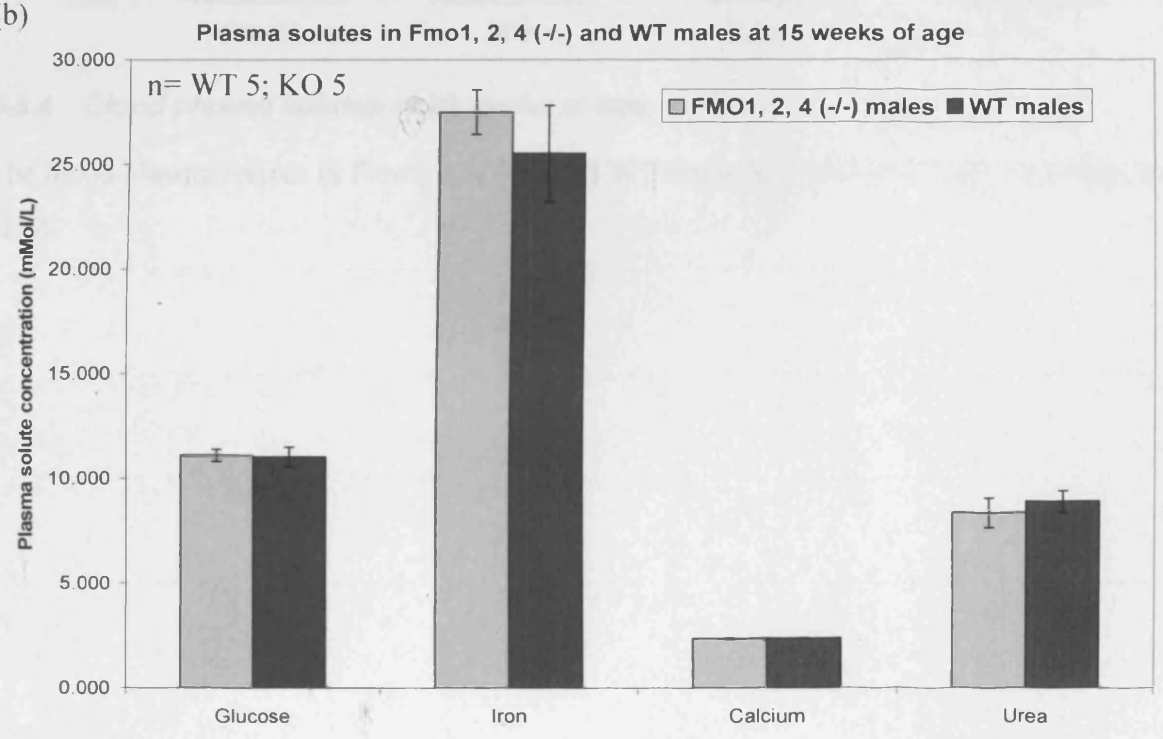

5.8.3 Blood plasma solutes at 9 and 15 weeks of age

The blood plasma solutes in *Fmo1, 2, 4* (-/-) and WT males at 9 weeks of age (a) and 15 weeks of age (b). Error bars are SEM.

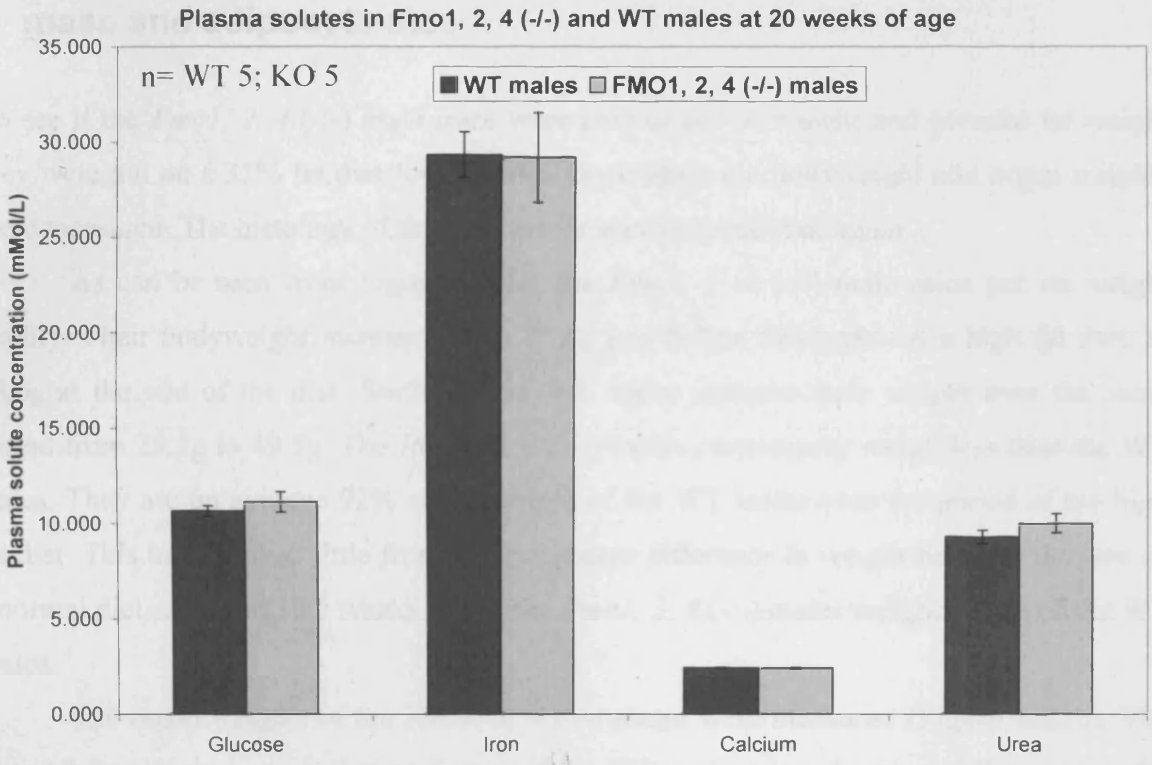

5.8.4 Blood plasma solutes at 20 weeks of age

The blood plasma solutes in *Fmo1, 2, 4* (-/-) and WT males at 20 weeks of age. Error bars are SEM.

5.9 On a high-fat diet *Fmo1, 2, 4* (-/-) mice gain body weight, fat mass and adipocyte size

To see if the *Fmo1, 2, 4* (-/-) male mice were able to put on weight and gonadal fat weight they were put on a 35% fat diet for 7 weeks. Once again the bodyweight and organ weights were measured. The histology of the gonadal fat was also analysed again.

As can be seen from Figure 5.9.1a, the *Fmo1, 2, 4* (-/-) male mice put on weight readily. Their bodyweight increases from 25.8g just before being put on a high fat diet, to 38.6g at the end of the diet. Similarly the WT males increase their weight over the same period from 29.1g to 49.5g. The *Fmo1, 2, 4* (-/-) males consistently weigh less than the WT males. They are on average 92% of the weight of the WT males over the period of the high fat diet. This has changed little from the percentage difference in weight between the two on a normal diet, where at 16.5 weeks of age the *Fmo1, 2, 4* (-/-) males weighed 89% of the WT males.

The organ weights of the *Fmo1, 2, 4* (-/-) males were measured (Figure 5.9.1b). The gonadal fat weight is now similar to that of the WT male mice. Another difference on the high-fat diet is seen in the liver weights, where the in the *Fmo1, 2, 4* (-/-) males the livers weigh 14% less than those of WT males. The spleens of the *Fmo1, 2, 4* (-/-) males were slightly larger (35%) than the WT male spleens on a high-fat diet.

The histology of the *Fmo1, 2, 4* (-/-) male adipocytes was checked, this time the cells were a similar size to the WT cells (Figure 5.9.2). So the *Fmo1, 2, 4* (-/-) male mouse adipocytes are not incapable of gaining size and storing fat. Perhaps putting these animals on a high-fat diet has made them more like the WT mice, similar body weight and a similar adipocyte size.

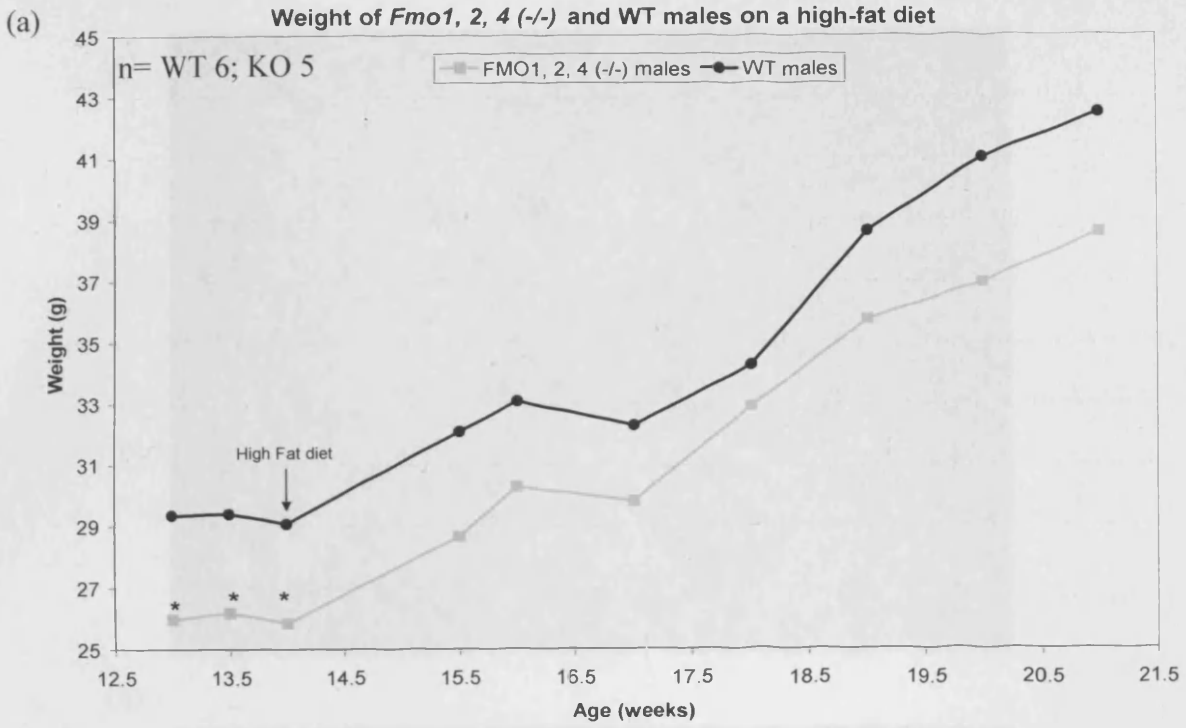

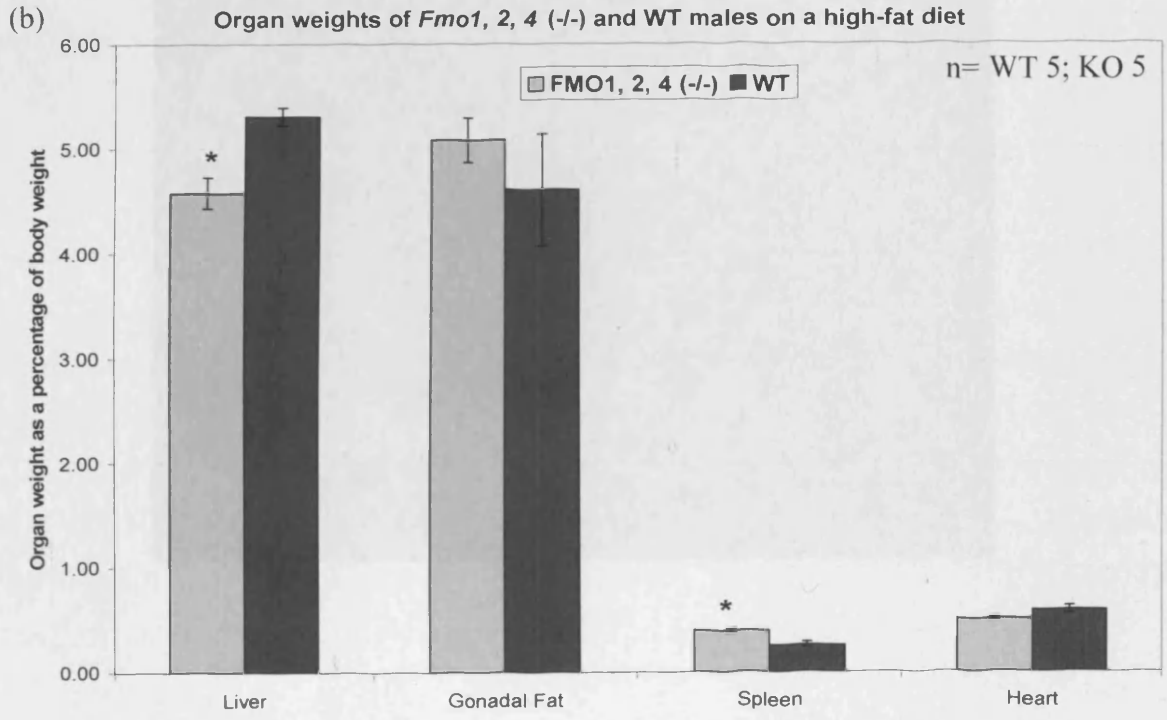

5.9.1 Bodyweight and organ weights on a high-fat diet

Bodyweight (a) and organ weights (at 21 weeks of age) (b) of *Fmo1, 2, 4* (-/-) and WT males on a high-fat diet. * is $p<0.05$. Error bars are SEM.

(a)

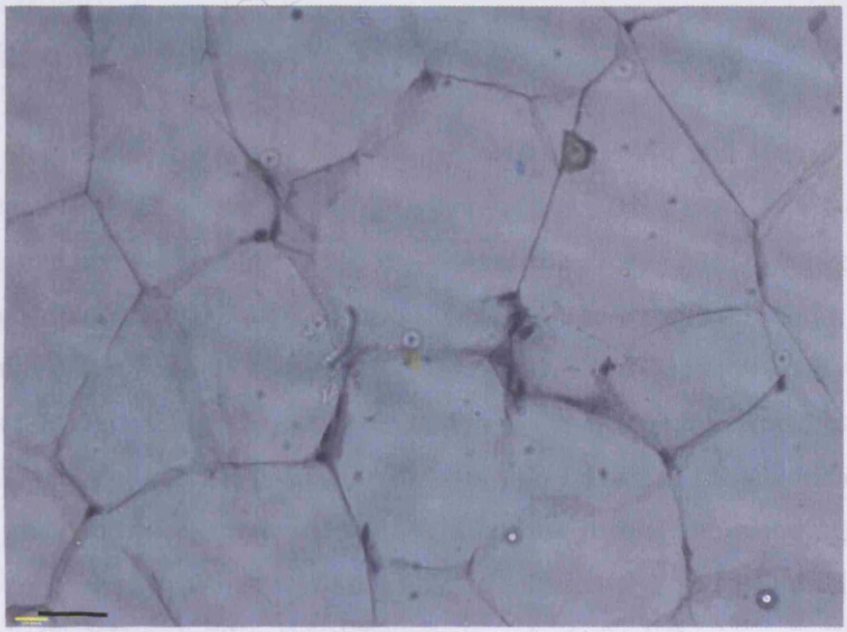

(b)

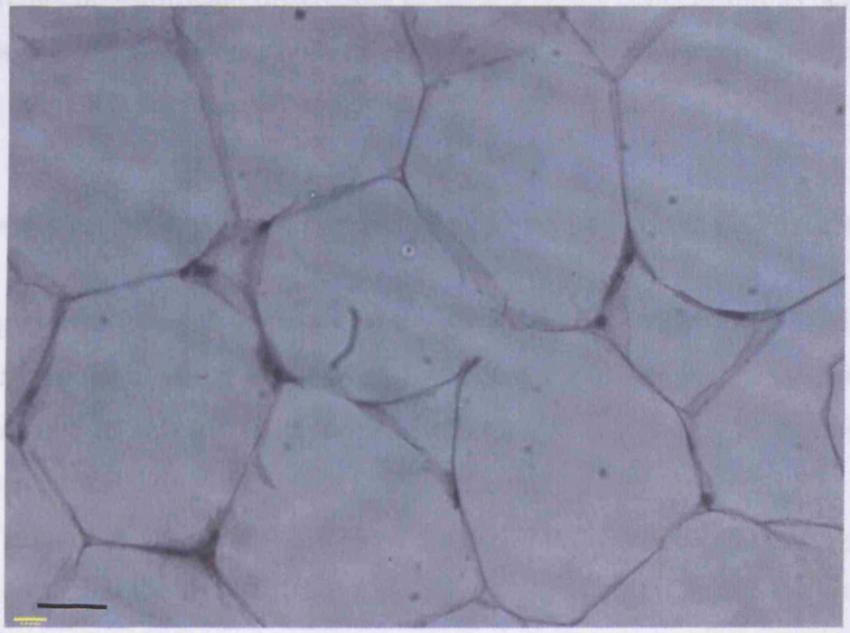

5.9.2 *Adipocyte histology-high fat diet*

The adipocyte histology of *Fmo1, 2, 4* (-/-) (a) and WT males (b) at 22 weeks of age on a high-fat diet. Scale bar represents 75 μm.

5.10 Plasma lipid and solute analysis in *Fmo1, 2, 4* (-/-) males on a high-fat diet

The plasma lipid concentration was measured in the WT and *Fmo1, 2, 4* (-/-) males on a high-fat diet at 22 weeks of age (Figures 5.11.1). The *Fmo1, 2, 4* (-/-) males have increased plasma lipids compared to the WT males. The *Fmo1, 2, 4* (-/-) males on a high fat diet have higher plasma total cholesterol (39%), HDL cholesterol (34%) and LDL cholesterol (53%) than the WT males on a high fat diet. The *Fmo1, 2, 4* (-/-) males have reduced plasma triglycerides (-40%) on a high fat diet compared to WT males on the same diet.

At 22 weeks of age, the plasma lipids on a high-fat diet in the KO males are all much higher than the WT mice, more so than on a normal diet at the same age. The plasma triglyceride concentration which was very similar between WT and KO on a normal diet is much lower in the KO males than the WT males on a high-fat diet.

There are no significant differences in plasma solute concentrations between *Fmo1, 2, 4* (-/-) males and WT males on a high-fat diet. Although the iron concentration on average is 20% higher in the KO than the WT males.

5.11 Liver histology on a high-fat diet in WT and KO mice

The histology of the livers from males on a high-fat diet was examined. As shown in Figure 5.11.2, there is much more fat in the livers of both WT and *Fmo1, 2, 4* (-/-) mice on a high-fat diet, compared to animals on a normal diet at 22 weeks of age, as demonstrated by the markedly increased staining of Oil Red O in both samples.

The amount of fat in the WT males on a high-fat diet appears to be slightly more than that contained within the livers of the *Fmo1, 2, 4* (-/-) males. Clearly the trend of reduced hepatic fat in the *Fmo1, 2, 4* (-/-) males is continued. This may account for the lower liver weight in *Fmo1, 2, 4* (-/-) males compared to WT males on a high-fat diet.

(a)

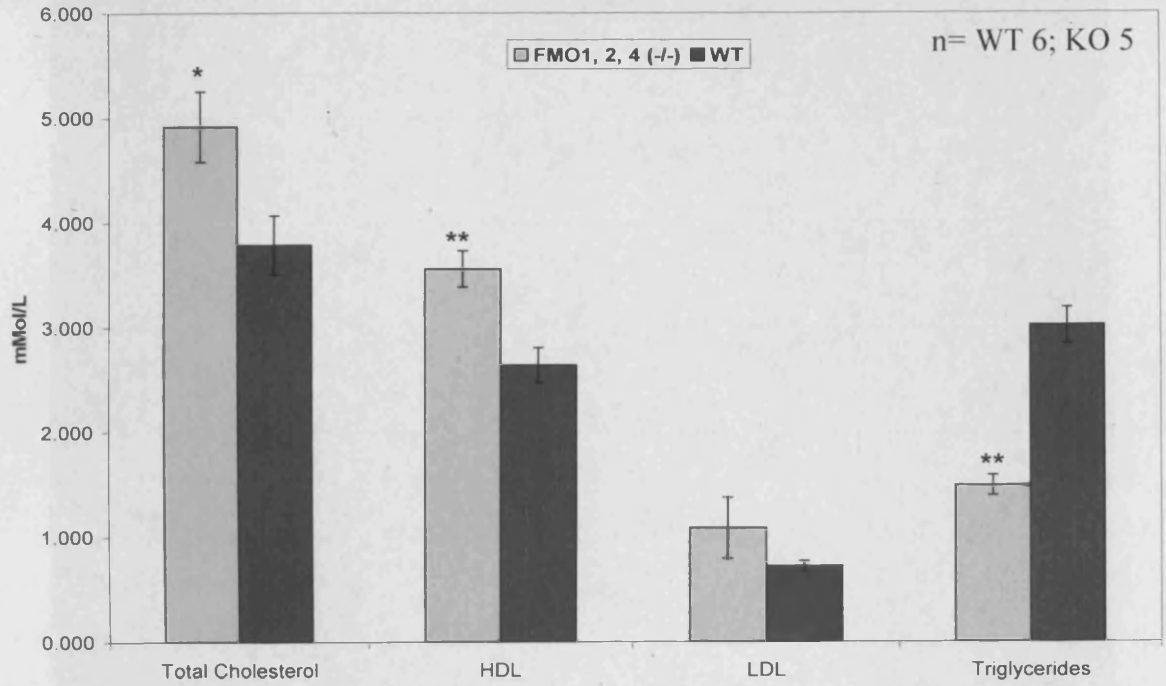

(b)

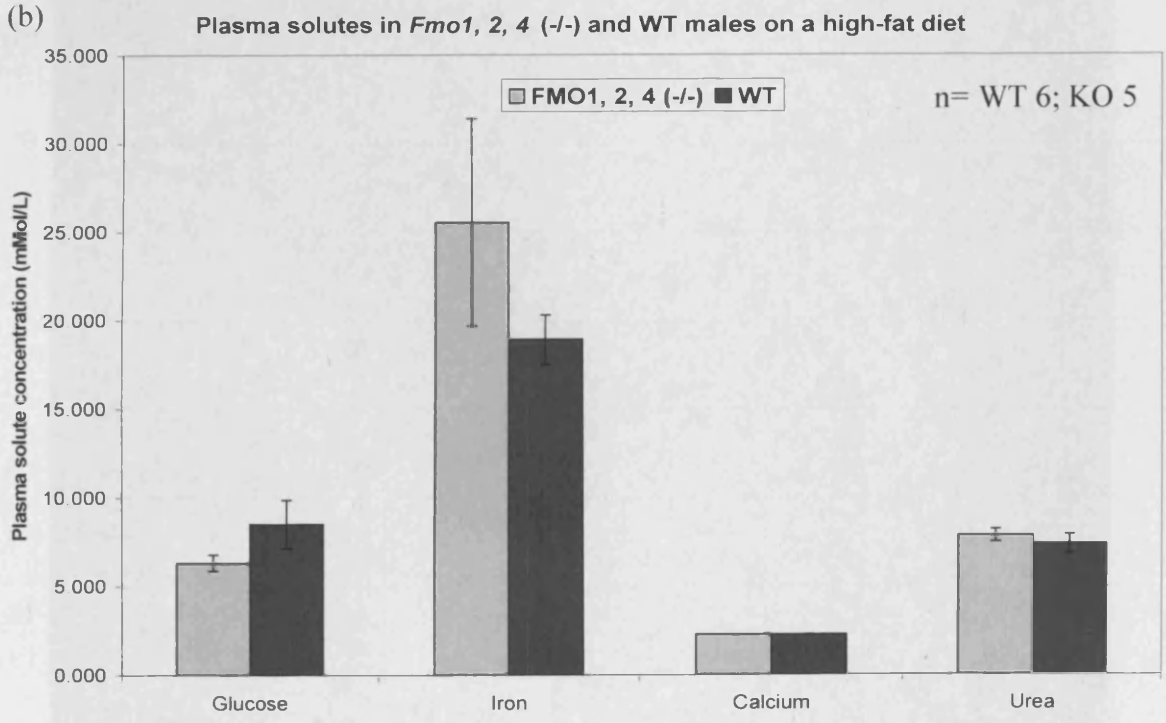

5.11.1 Plasma lipid and solutes on a high-fat diet

The plasma lipids (a) and plasma solutes (b) were measured in *Fmo1, 2, 4* (-/-) and WT males on a high-fat diet. * is $p<0.05$, ** is $p<0.005$. Error bars are SEM.

(a)

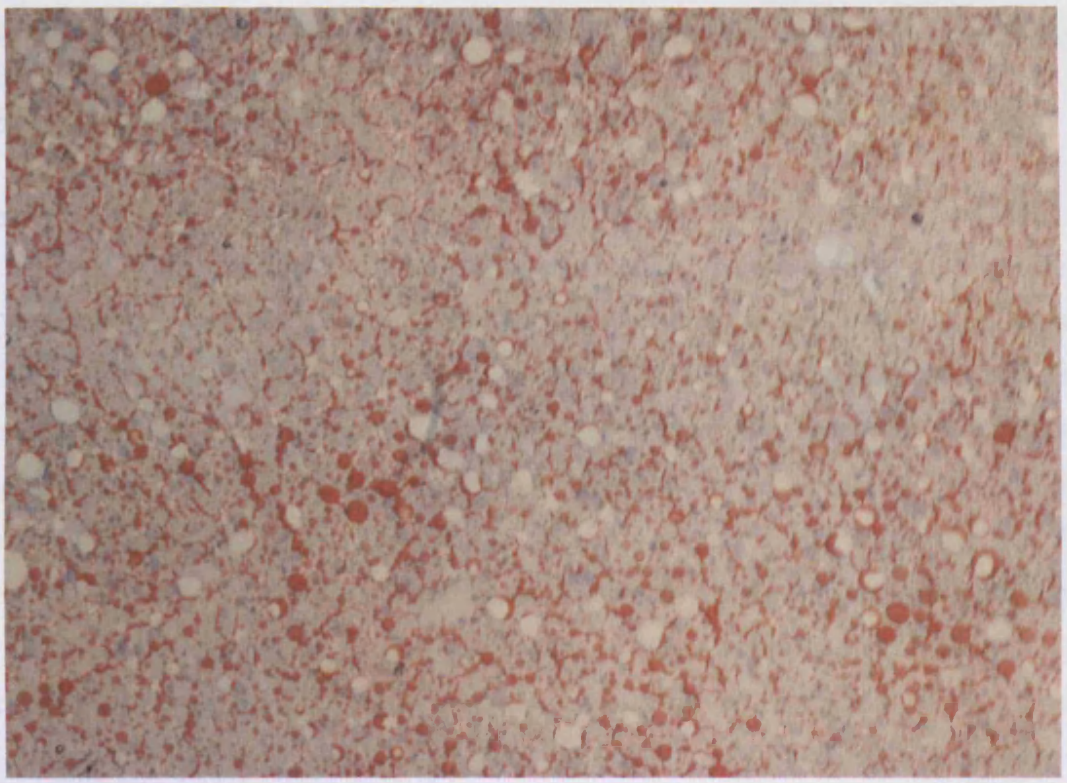

(b)

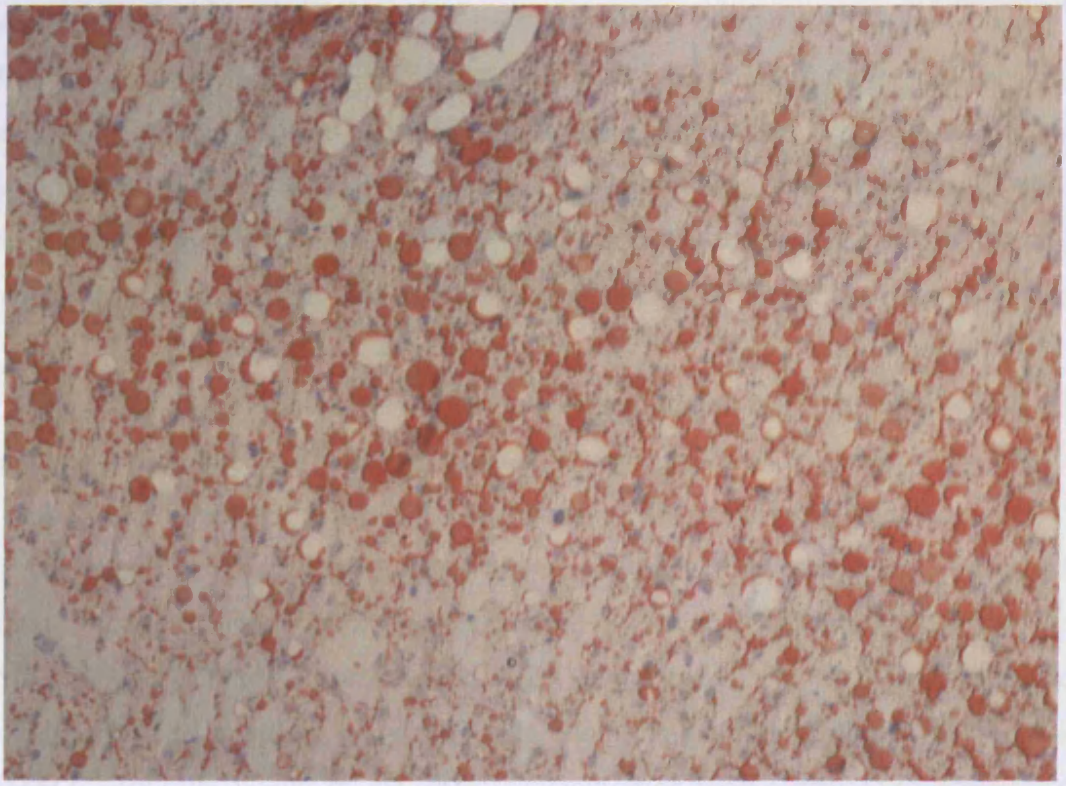

5.11.2 Liver histology in Fmo1, 2, 4 (-/-) and WT males on a high-fat diet

A representative photograph of the liver histology in *Fmo1, 2, 4* (-/-) males (a) and WT males (b) at 22 weeks of age on a high-fat diet.

5.12 Analysis of bodyweight, organ weight, plasma lipids and plasma solutes in *Fmo1, 2, 4* (-/-) males on a lipoic acid diet

To try to narrow down the possible reasons for the observed weight reduction in male *Fmo1, 2, 4* (-/-) mice, we turned to the known endogenous substrates of the FMOs. Lipoic acid has been shown to be a substrate for porcine FMO1 (Taylor and Ziegler, 1987). In its lipoamide form it is an important cofactor for enzymes of the Krebs cycle. Mice fed lipoic acid show a reduction in weight via an increase in energy expenditure and reduction in food intake. Lipoic acid does this by reducing the activity of AMP-activated protein kinase (AMPK) an important fuel-sensor in the cell (Kim et al., 2004). Our hypothesis was that without FMO1 to metabolise lipoic acid, any weight reduction in the animals would be more pronounced in the *Fmo1, 2, 4* (-/-) mice as any lipoic acid would not be metabolised as efficiently. Hence that could be the underlying cause of the phenotype observed of the male *Fmo1, 2, 4* (-/-) mice. To see if any differences could be seen, the *Fmo1, 2, 4* (-/-) and WT male mice were put on a 0.1% lipoic acid diet for 4 weeks (from 7 weeks of age to 11 weeks of age). Their weight was measured over this time. Shown in Figure 5.12.1a are the weights of the animals on the lipoic acid diet compared to their weights on a normal chow diet. All of the animals lose weight compared to what they weighed on a normal chow diet. At the beginning of the diet the *Fmo1, 2, 4* (-/-) mice weigh 9% less than they did at the same time on a normal chow diet. At the end of the diet they weigh 2.3% less than they did at the same time on a normal diet.

The organ weights of the 0.1% lipoic acid-treated mice were also measured at the end of the 4 weeks (Figure 5.10.3). There was a slight reduction in liver weight in the *Fmo1, 2, 4* (-/-) (-8.5%) mice compared to the WT, but this wasn't statistically significant.

Blood plasma lipids were analysed from the lipoic acid-treated mice (Figure 5.12.1b). The total cholesterol, HDL cholesterol, LDL cholesterol and triglycerides were all higher (15.9%, 15.8%, 10.2% and 18.4% respectively) in the *Fmo1, 2, 4* (-/-) mice than the WT mice, but none of these values are significant. When compared to those values on a normal diet, there is very little change in cholesterol concentration from a normal to a lipoic acid diet in any of the mice.

Plasma solutes were also measured in the lipoic acid-treated mice (Figure 5.12.2). Chloride was lower in *Fmo1, 2, 4* (-/-) mice, -2.1% ($p<0.05$) and potassium was 10.4% higher ($p<0.05$) compared to the WT males. The level of iron in the plasma increased in the KO animals compared to the WT. The *Fmo1, 2, 4* (-/-) males had 42% more iron ($p<0.05$) than the WT mice.

The histology of the male livers is shown in Figure 5.12.4. Both have little or no fat in the liver, i.e. no red dots where Oil Red O has stained. Another example of how the WT and KO response to lipoic acid is very similar.

(a)

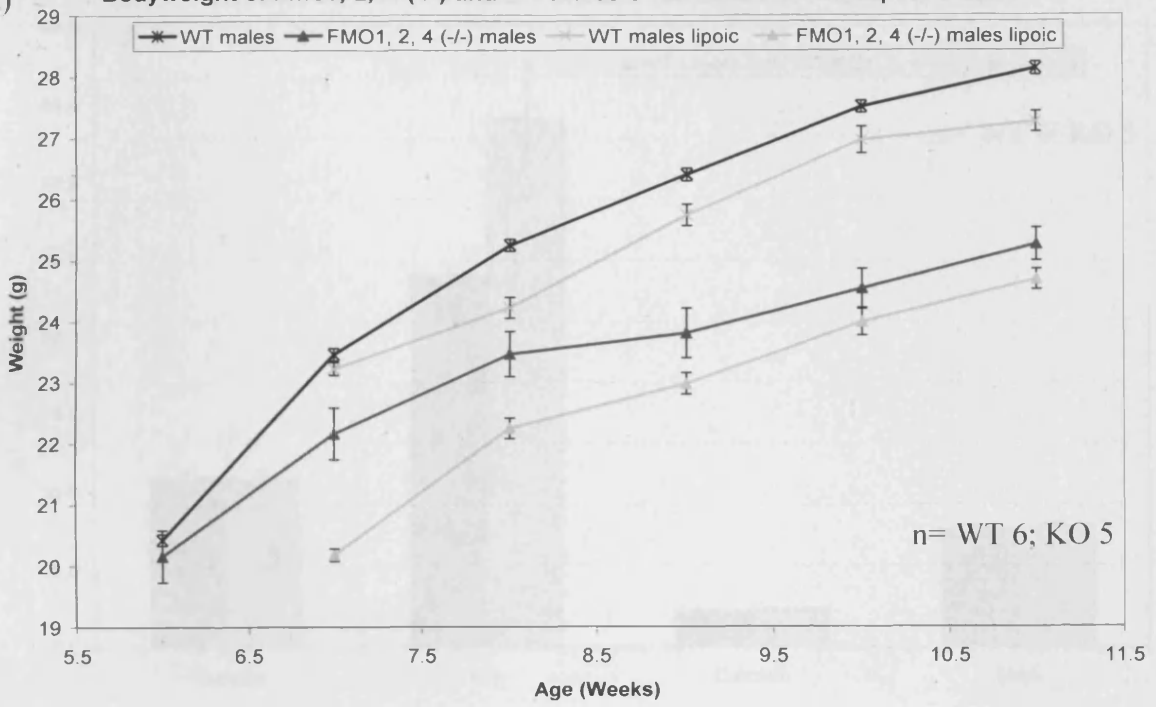

(b)

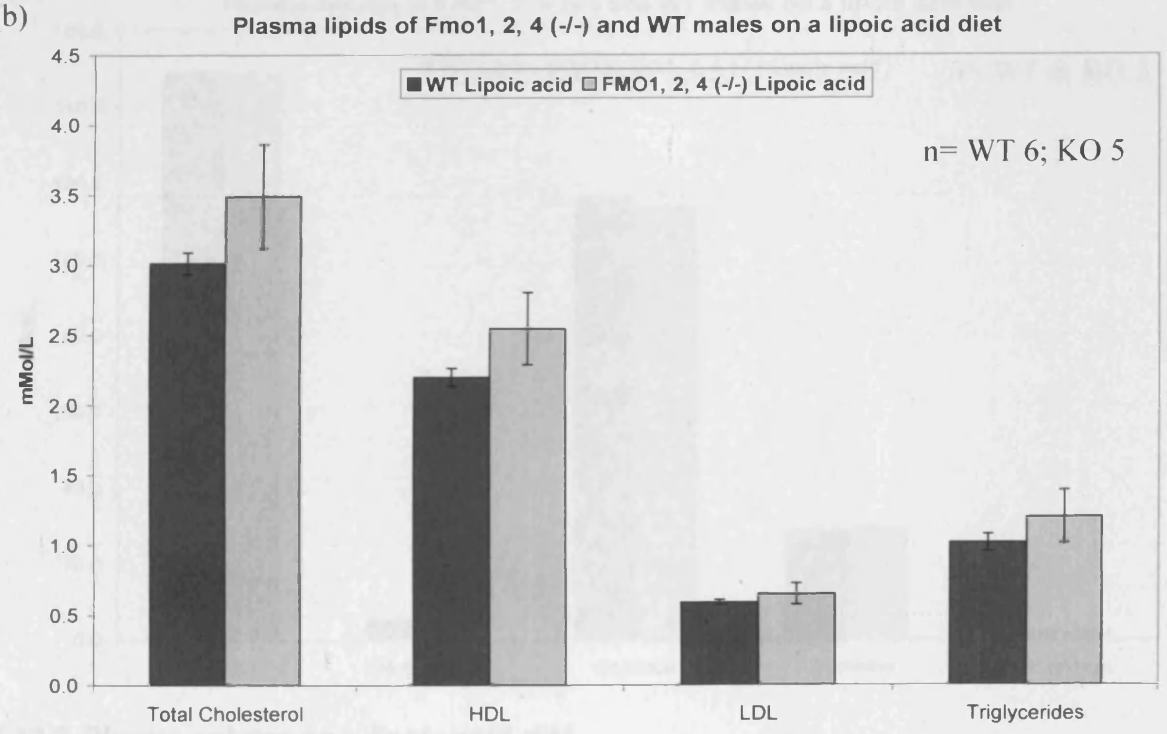

5.12.1 Bodyweight and plasma lipids on a lipoic acid diet

Bodyweights (a) and plasma lipids (b) of *Fmo1, 2, 4* (-/-) and WT males on a 0.1% lipoic acid diet. * is $p<0.05$, ** is $p<0.005$. Error bars are SEM.

(a)

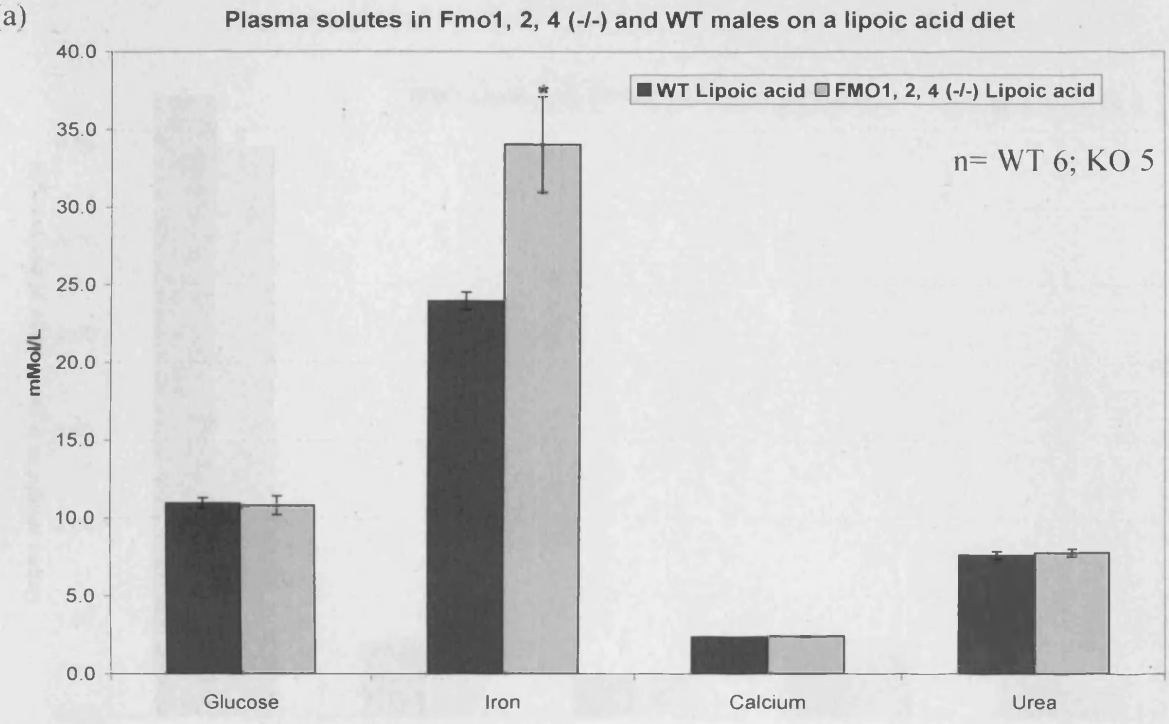

(b)

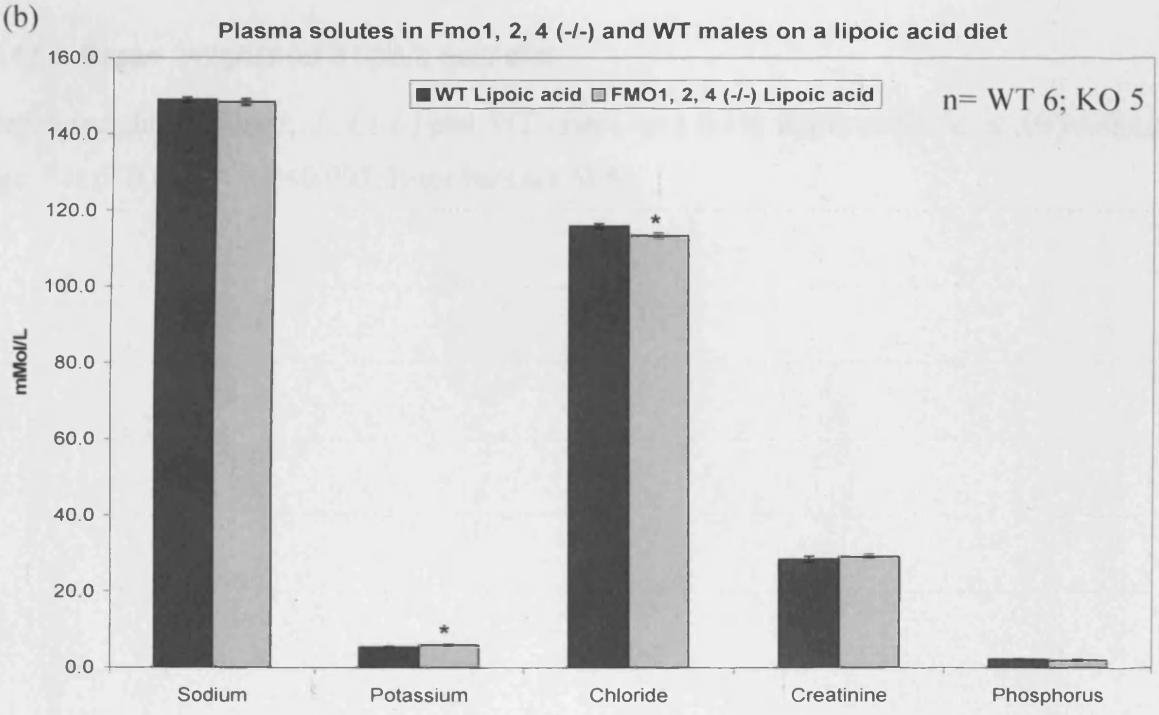

5.12.2 Plasma solutes on a lipoic acid diet

Plasma solutes of *Fmo1, 2, 4* (-/-) and WT males on a 0.1% lipoic acid diet at 10 weeks of age. * is $p<0.05$, ** is $p<0.005$. Error bars are SEM.

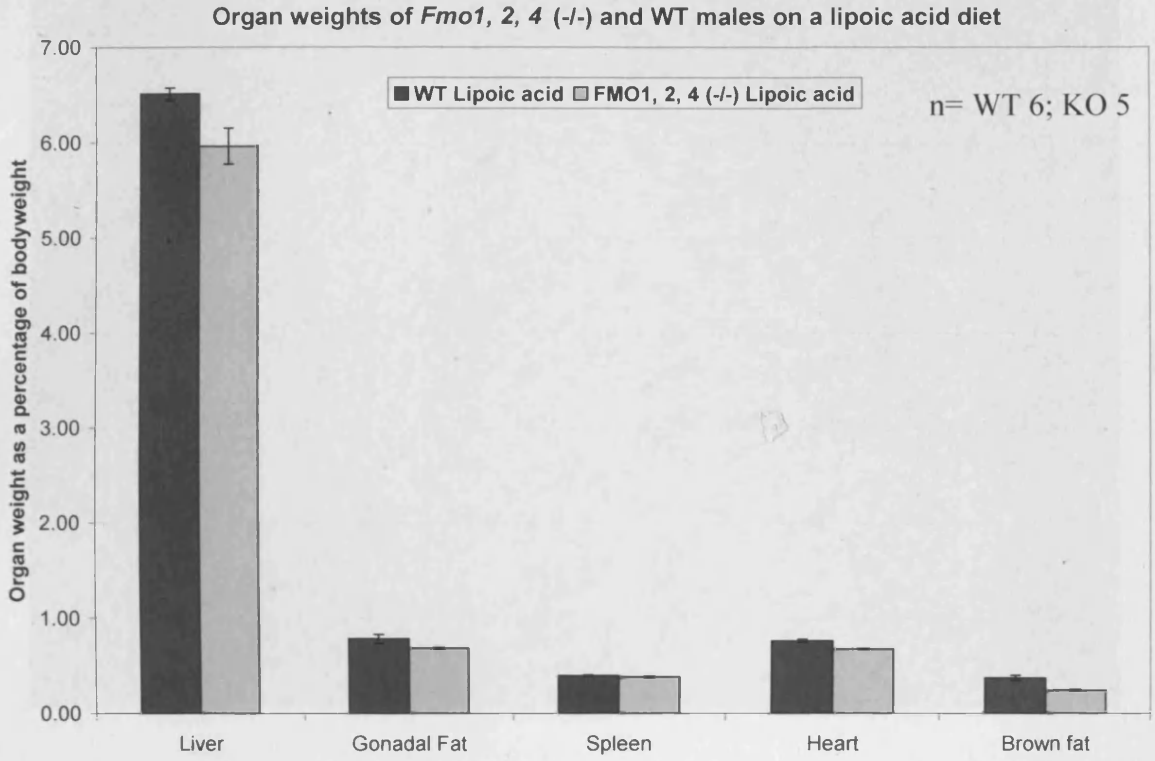

5.12.3 Organ weights on a lipoic acid diet

Organ weights of *Fmo1, 2, 4* (-/-) and WT males on a 0.1% lipoic acid diet at 10 weeks of age. * is $p<0.05$, ** is $p<0.005$. Error bars are SEM.

(a)

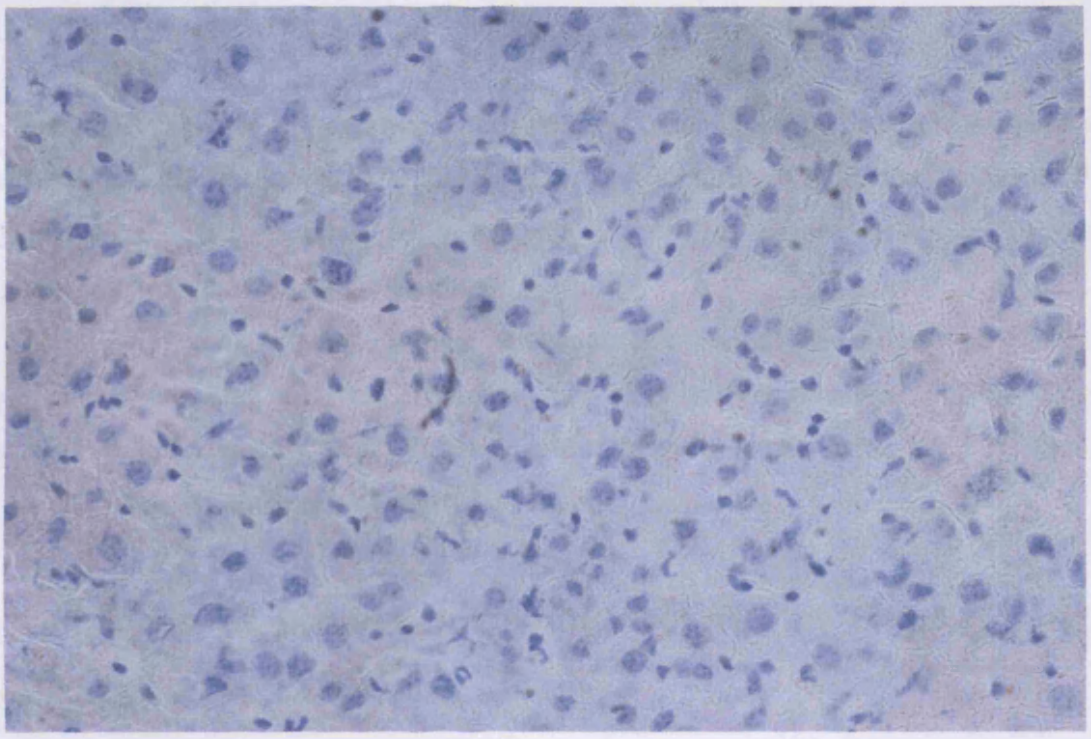

(b)

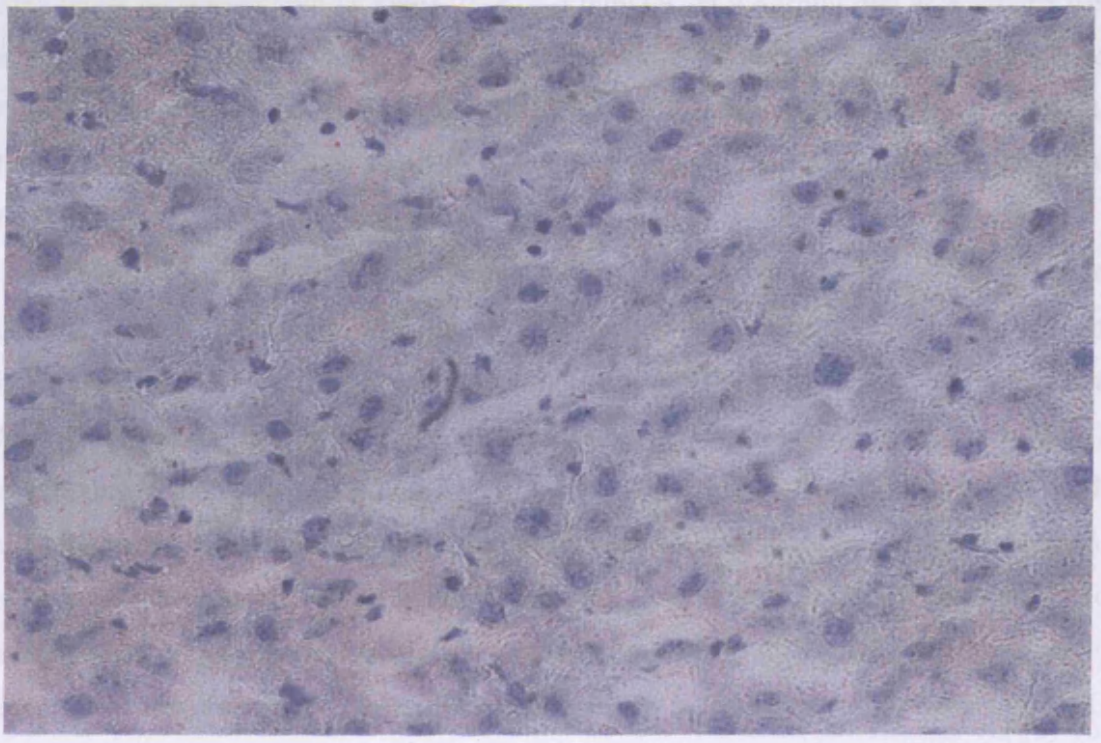

5.12.4 Liver histology in Fmo1, 2, 4 (-/-) and WT males on a lipoic acid diet

A representative photograph of the liver histology in *Fmo1, 2, 4* (-/-) males (a) and WT males (b) at 10 weeks of age on a 0.1% lipoic acid diet. Error bars are SEM.

5.13 Organ weight analysis of *Fmo1, 2, 4* (-/-) females

The liver, spleen, brown fat, heart and front adipose tissue (gonadal fat) were weighed in 4 week old females (Figure 5.14.1). They have a pronounced reduction in gonadal fat compared to the WT females, 61% less fat. This is interesting given the increased bodyweight in the *Fmo1, 2, 4* (-/-) females.

The *Fmo1, 2, 4* (-/-) female mice at 4 weeks are shorter (15%) than that of the WT female mice of the same age. This difference is not seen in the male *Fmo1, 2, 4* (-/-) mice at all at any age. Unfortunately we don't have data for the older female mice, but at 22 weeks of age on a high fat diet, there is no length difference.

5.14 Analysis of plasma lipids and solutes in *Fmo1, 2, 4* (-/-) females

Plasma lipids were measured in *Fmo1, 2, 4* (-/-) females on a normal diet at 8 and 15 weeks of age (Figure 5.14.2). The *Fmo1, 2, 4* (-/-) females had 39% and 42% more total cholesterol at 8 and 15 weeks respectively than the WT females. Similarly HDL cholesterol was 44% and 48% higher than the WT at 8 and 15 weeks respectively; the LDL cholesterol being 33% and 43% higher in the KO females at those same two ages.

Along with the plasma lipids, some plasma solutes were measured, glucose, iron, calcium and urea. There was a significant difference between female *Fmo1, 2, 4* (-/-) mice and WT females at 8 weeks of age in iron concentration (Figure 5.14.4). The female *Fmo1, 2, 4* (-/-) mice had 45 μMol/L of iron compared to the WT females who have 32 μMol/L. The level remains higher than the WT at 15 weeks (not significant). Iron homeostasis is tightly regulated and is mainly controlled by the absorption of iron through the intestine. A high plasma iron level can be due to certain anaemias (e.g. thalassemia), an increase in food intake, haemochromatosis (an uncontrolled absorption of iron through the intestine), or liver disease. The measurement of plasma iron alone is not sufficient to imply iron overload. In view of this plasma ferritin would have to be measured as well to define the total iron binding capacity. What is really interesting is that the female *Fmo1, 2, 4* (-/-) mice also have more calcium (2.43 mMol/L) than the WT females (2.34 nMol/L) at 9 weeks of age. Calcium

has been shown to reduce iron absorption in the intestine (Barton et al., 1983; Hallberg et al., 1992) and this may be a response by the females to get iron levels in check, which could be thought of as successful given that the iron elevation at 15 weeks is not significant, and there is no longer an increased calcium concentration. The *Fmo1, 2, 4* (-/-) females at 15 weeks also show a slightly higher blood glucose concentration (not significant) compared to the WT females.

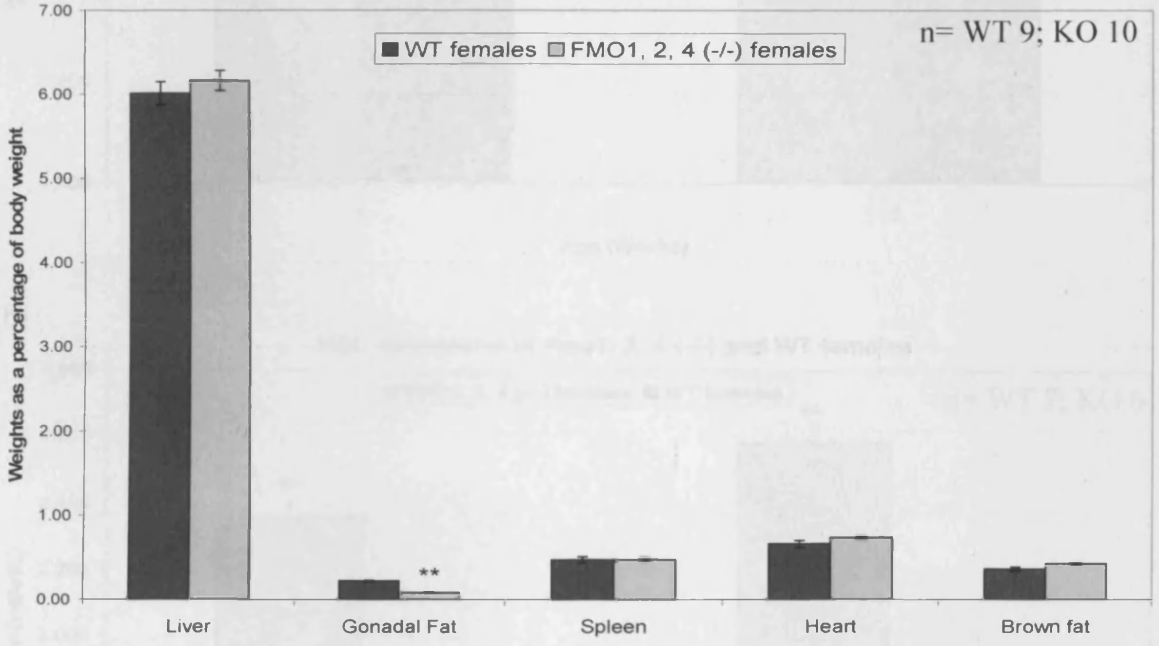

5.14.1 Organ weights of Fmo1, 2, 4 (-/-) females at 4 weeks of age

The organ weights as a percentage of body weight of *Fmo1, 2, 4* (-/-) and WT females at 4 weeks of age. ** is $p<0.005$. Error bars are SEM.

(a)

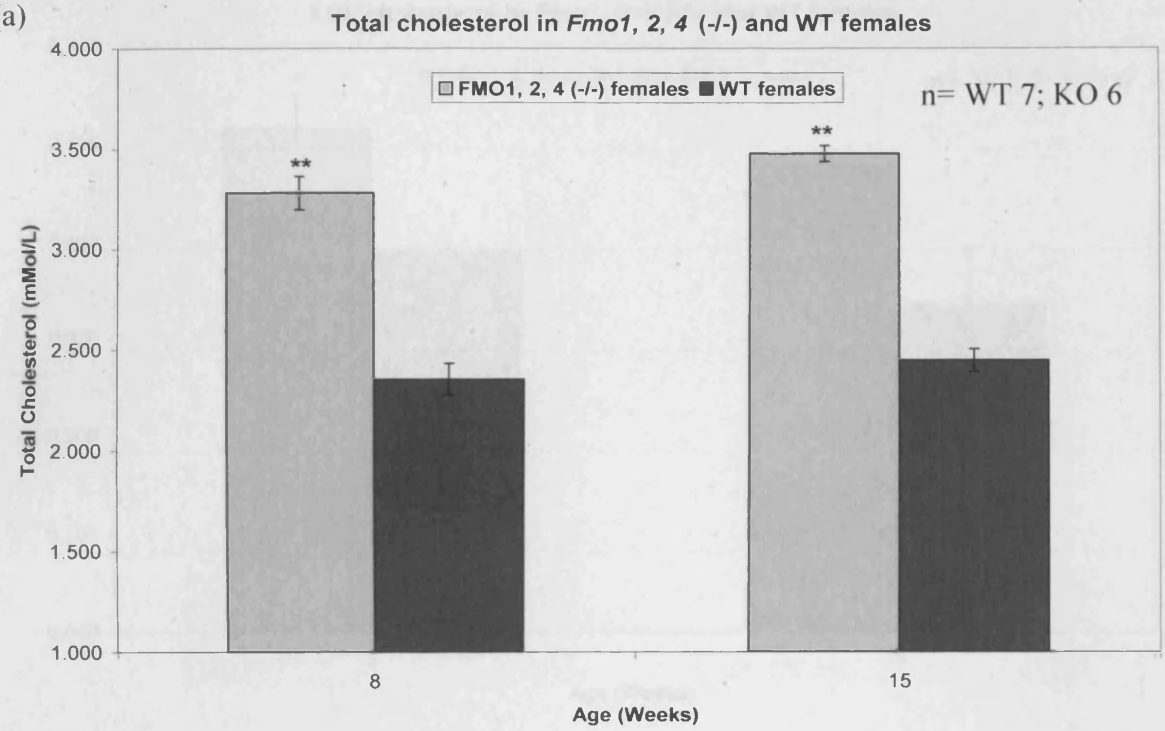

(b)

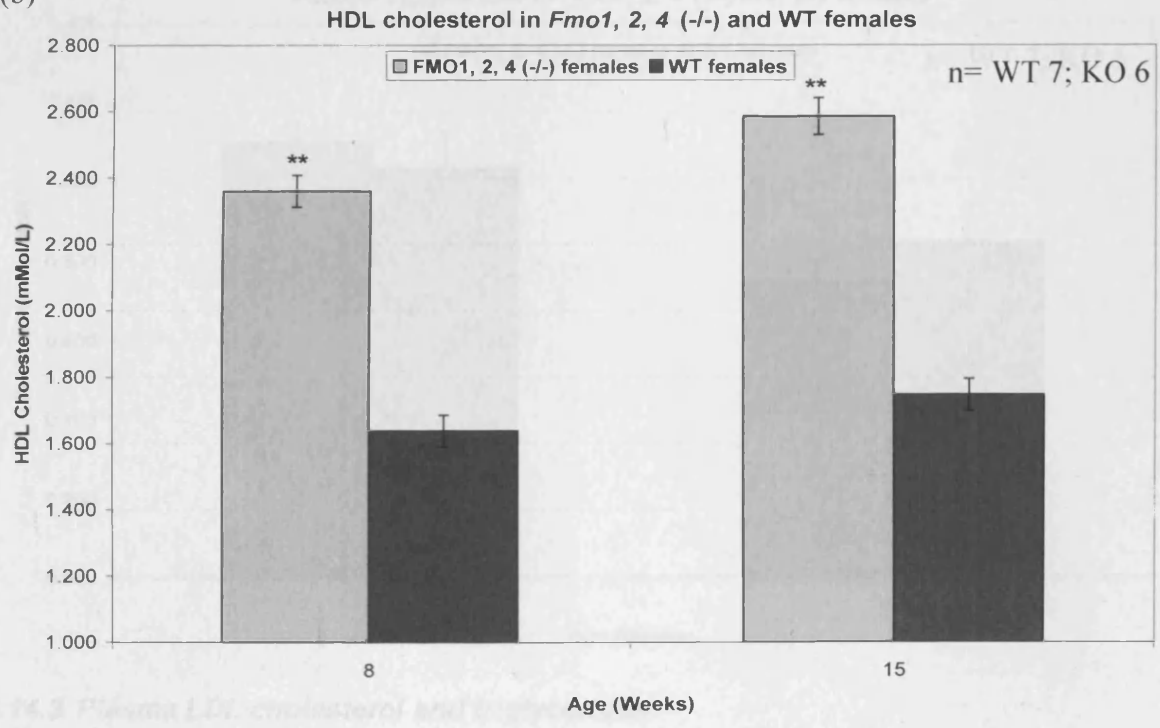

5.14.2 Plasma total and HDL cholesterol

The plasma lipids in *Fmo1, 2, 4* (-/-) and WT females on a normal diet, total cholesterol (a); HDL cholesterol (b) at 8 and 15 weeks of age.*is $p<0.05$,**is $p<0.005$. Error bars are SEM.

(a)

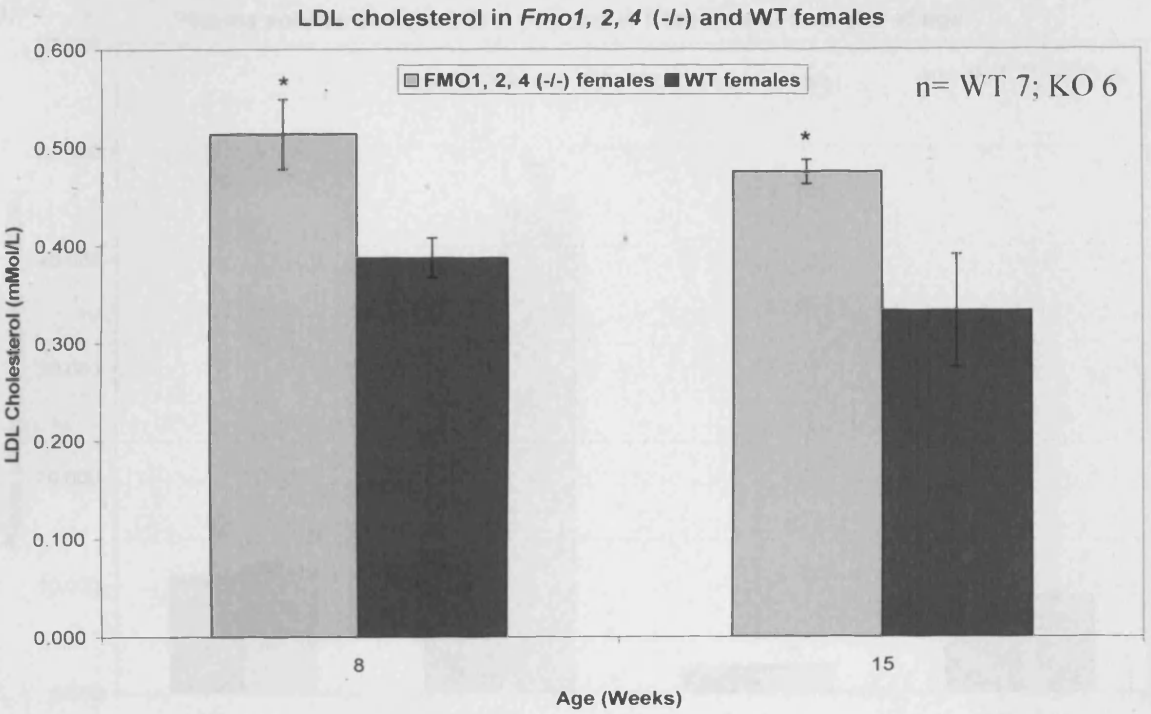

(b)

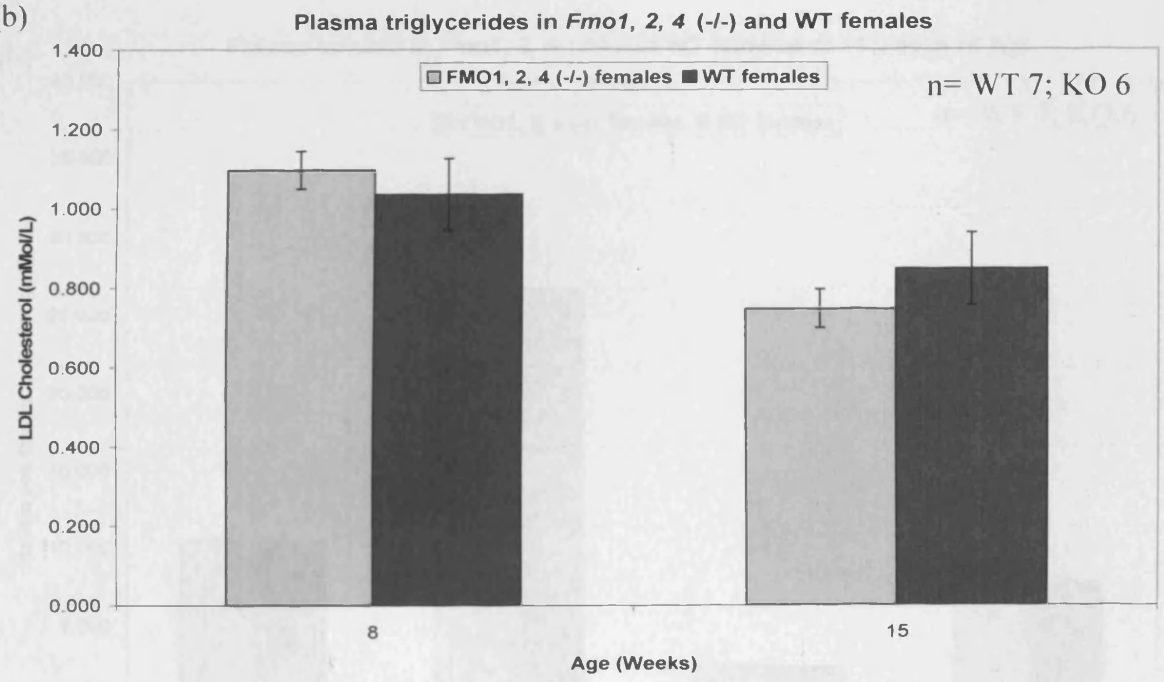

5.14.3 Plasma LDL cholesterol and triglycerides

The plasma lipids in *Fmo1, 2, 4* (-/-) and WT females on a normal diet, LDL cholesterol (a) and triglycerides (b) at 8 and 15 weeks of age. * is $p<0.05$, ** is $p<0.005$. Error bars are SEM.

(a)

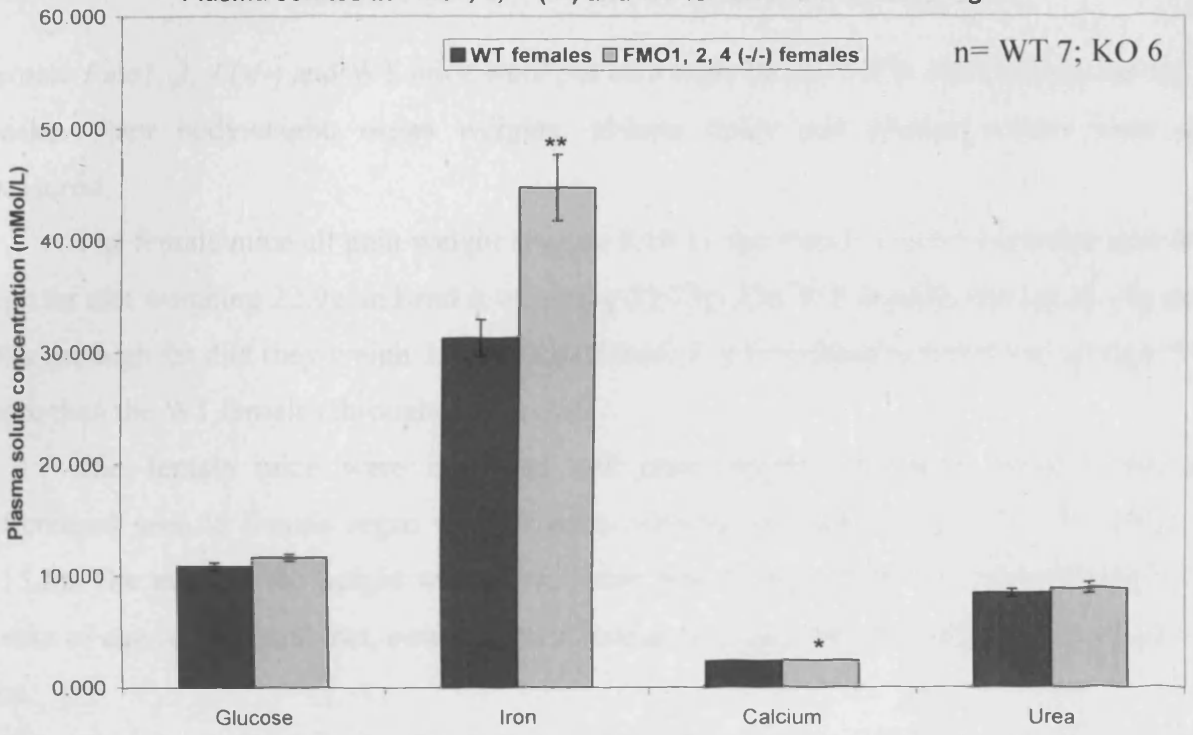

(b)

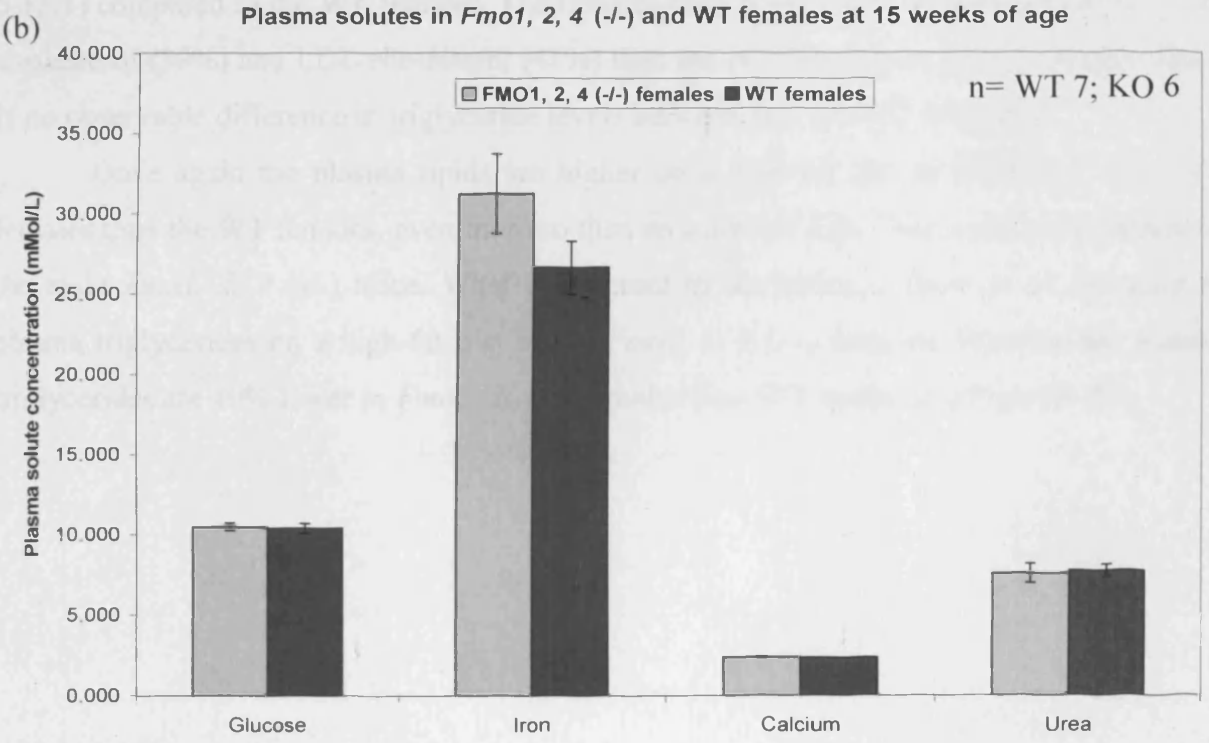

5.14.4 Plasma solutes

The plasma solutes in *Fmo1, 2, 4* (-/-) and WT females on a normal diet at 9 (a) and 15 (b) weeks of age. * is $p<0.05$, ** is $p<0.005$. Error bars are SEM.

5.15 Analysis of *Fmo1, 2, 4* (-/-) females on a high-fat diet

Female *Fmo1, 2, 4* (-/-) and WT mice were put on a high-fat diet (35% cholesterol) diet for 7 weeks. Their bodyweight, organ weights, plasma lipids and plasma solutes were all measured.

The female mice all gain weight (Figure 5.15.1), the *Fmo1, 2, 4* (-/-) females start the high fat diet weighing 22.9g and end it weighing 33.73g. The WT females start at 22.35g and after the high fat diet they weigh 32.94g. The *Fmo1, 2, 4* (-/-) females weigh on average 5% more than the WT females throughout the diet.

The female mice were dissected and their organs measured. There were no differences seen in female organ weights on a high-fat diet between KO and WT (Figure 5.15.2). The gonadal fat weight which was much less in the *Fmo1, 2, 4* (-/-) females at 4 weeks of age on a normal diet, now weighs a similar amount to the WT females on a high-fat diet.

The plasma lipids in the *Fmo1, 2, 4* (-/-) females are higher on a high fat diet (Figure 5.15.1) compared to the WT females. The females have higher total cholesterol (40%), HDL cholesterol (39%) and LDL cholesterol (41%) than the WT females on a high fat diet. There is no observable difference in triglyceride levels between WT and KO females.

Once again the plasma lipids are higher on a high-fat diet in the *Fmo1, 2, 4* (-/-) females than the WT females, even more so than on a normal diet. This is the same pattern as the male *Fmo1, 2, 4* (-/-) mice. What is different to the males is there is no lowering of plasma triglycerides on a high-fat diet in the *Fmo1, 2, 4* (-/-) females. Whereas the plasma triglycerides are 40% lower in *Fmo1, 2, 4* (-/-) males than WT males on a high-fat diet.

(a)

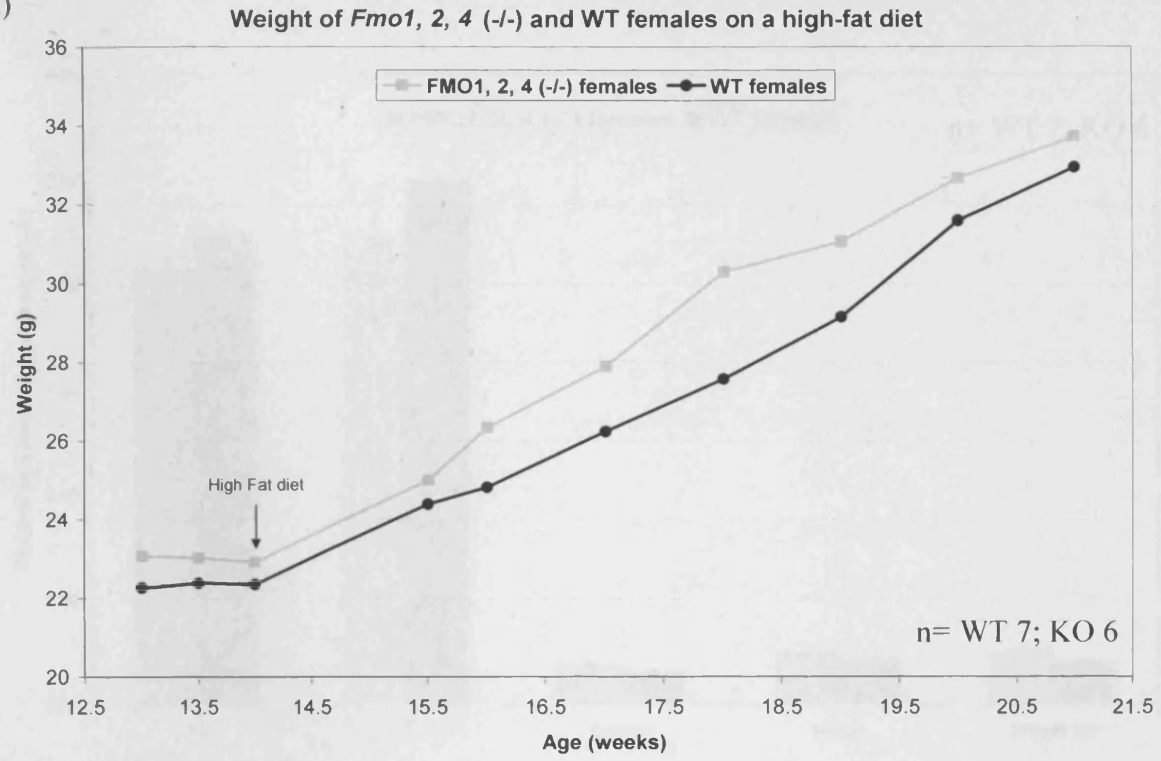

(b)

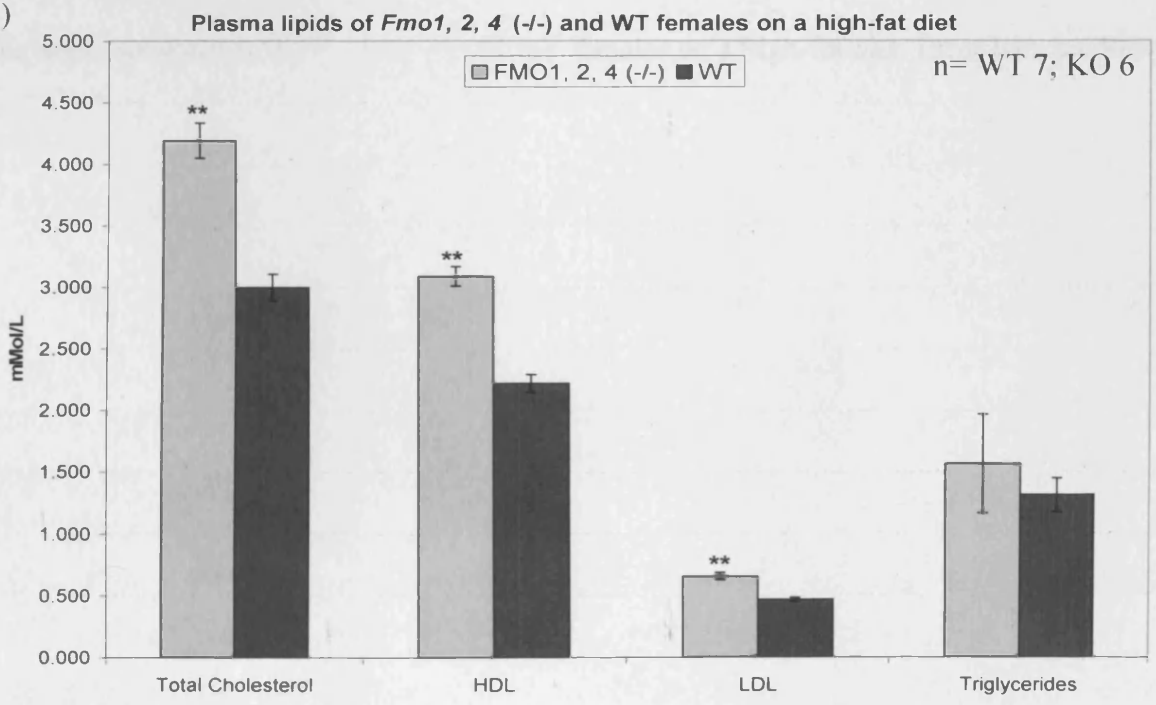

5.15.1 Bodyweight and plasma lipids of females on a high-fat diet

The bodyweight (a) and plasma lipids (b) of *Fmo1, 2, 4* (-/-) and WT females on a high-fat diet. * is $p<0.05$, ** is $p<0.005$. Error bars are SEM.

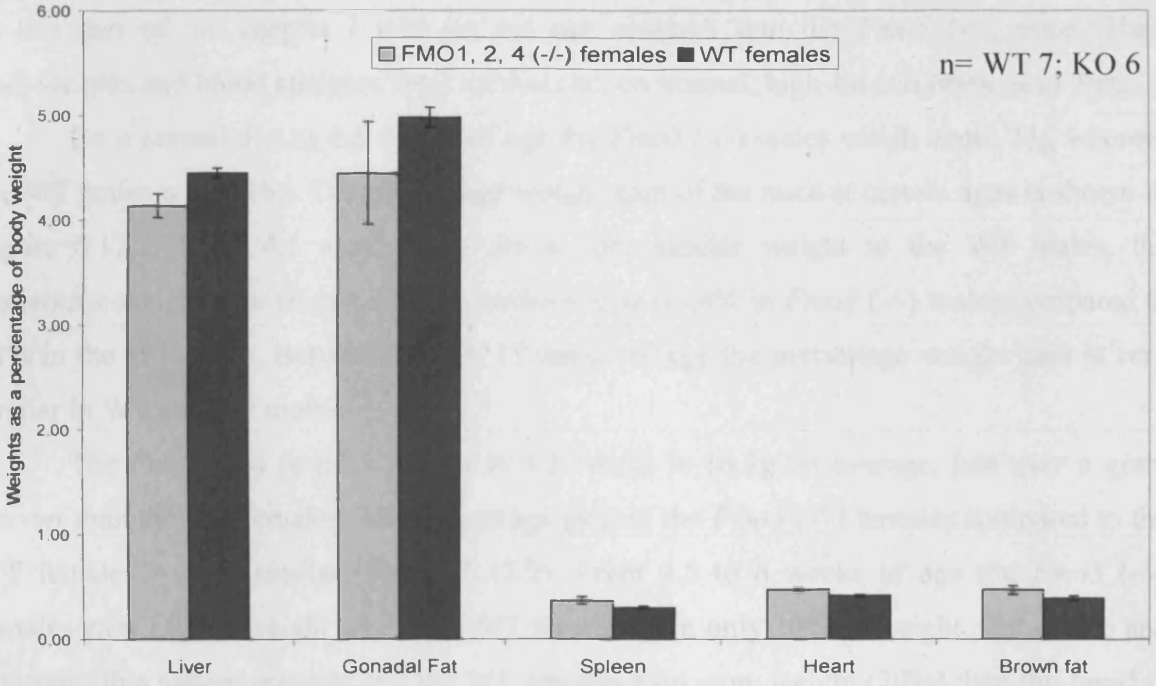

5.15.2 Organ weights of Fmo1, 2, 4 (-/-) females on a high-fat diet

The organ weights of *Fmo1, 2, 4* (-/-) and WT females on a high-fat diet. Error bars are SEM.

5.16 Investigation into *Fmo5* (-/-) mice on a normal diet

In this part of the chapter I will set out our research into the *Fmo5* (-/-) mice. Their bodyweights and blood analyses were carried out, on normal, high-fat and lipoic acid diets.

On a normal diet at 4.5 weeks of age the *Fmo5* (-/-) males weigh about 23g whereas the WT males weigh 16g. The percentage weight gain of the mice at certain ages is shown in Figure 5.17.2. From 4.5 weeks they are a very similar weight to the WT males, the percentage weight gain from 6.5 to 10 weeks of age is 24% in *Fmo5* (-/-) males compared to 31% in the WT males. Between 10 and 17 weeks of age the percentage weight gain is very similar in WT and KO males.

The *Fmo5* (-/-) females weight at 4.5 weeks is 16.3g on average, just over a gram heavier than the WT females. The percentage gain of the *Fmo5* (-/-) females compared to the WT females is very similar (Figure 5.17.2). From 4.5 to 6 weeks of age the *Fmo5* (-/-) females gain 14% in weight whilst the WT females gain only 10% in weight. Between 6 and 10 weeks this pattern reverses and the WT females gain more weight (20%) than the *Fmo5* (-/-) females (12%). This pattern continues but is less pronounced from 10 to 14 weeks where the WT females gain 12% in weight and the *Fmo5* (-/-) females gain 9.5% in weight. Overall the weight of *Fmo5* (-/-) females is very similar to that of WT females.

5.17 Blood plasma lipids in *Fmo5* (-/-) mice

The *Fmo5* (-/-) males have 22% and 16% lower HDL cholesterol at 15 and 22 weeks respectively. Whilst their LDL cholesterol is 16% lower at 15 weeks, but 38 % higher at 22 weeks of age. The *Fmo5* (-/-) females have slightly lower HDL cholesterol at 15 and 22 weeks (9% and 5% respectively) and higher LDL cholesterol at 15 weeks (22%) but slightly lower (2%) at 22 weeks (Figure 5.17.3).

In the *Fmo5* (-/-) females, the same applies; there is no difference in the triglyceride concentrations between them and the WT females at 15 and 22 weeks of age (Figure 5.17.4). There is a difference between *Fmo5* (-/-) males and WT males (Figure 5.17.4). At 15 weeks their triglyceride content is very similar (0.8 and 0.85 mMol/L respectively), but whilst the WT male mice triglyceride concentration increases at 22 weeks of age to 1.8 mMol/L, the

Fmo5 (-/-) male mice concentration stays at a similar level to that of 15 weeks (0.84 mMol/L).

Fmo5 (-/-) males have less iron (22 μMol/L) compared to the WT males (29 μMol/L) at 22 weeks of age (Figure 5.17.7 and 5.17.8). The *Fmo5* (-/-) females also have a reduced iron level (not significant) at the same age.

(a)

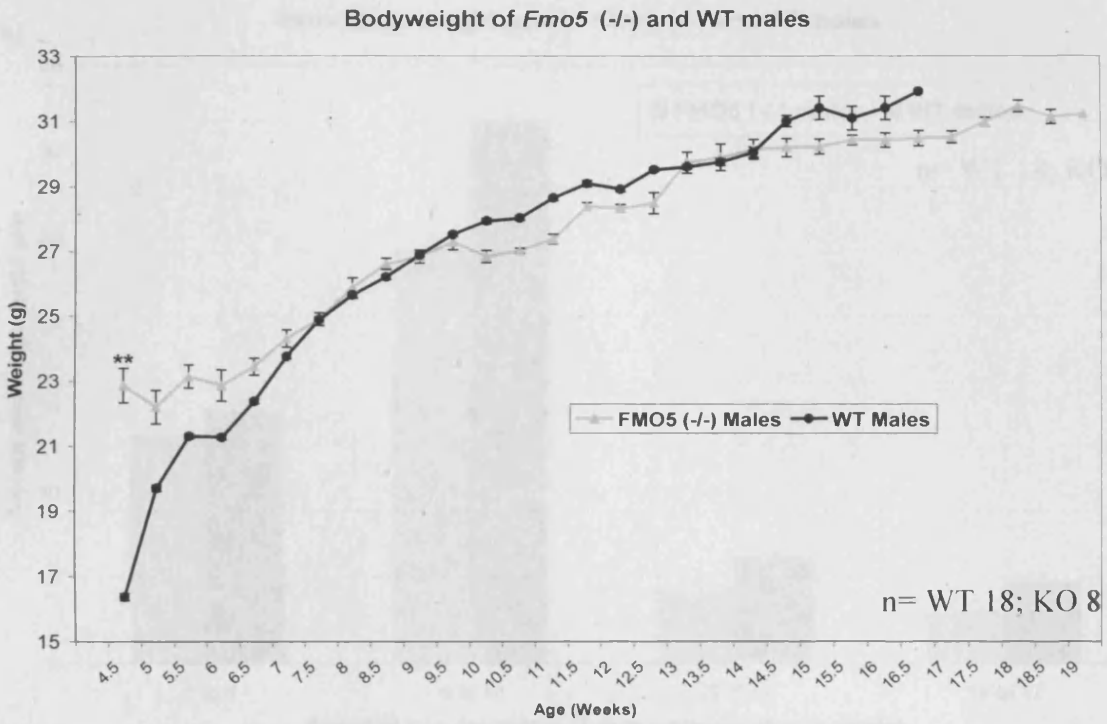

(b)

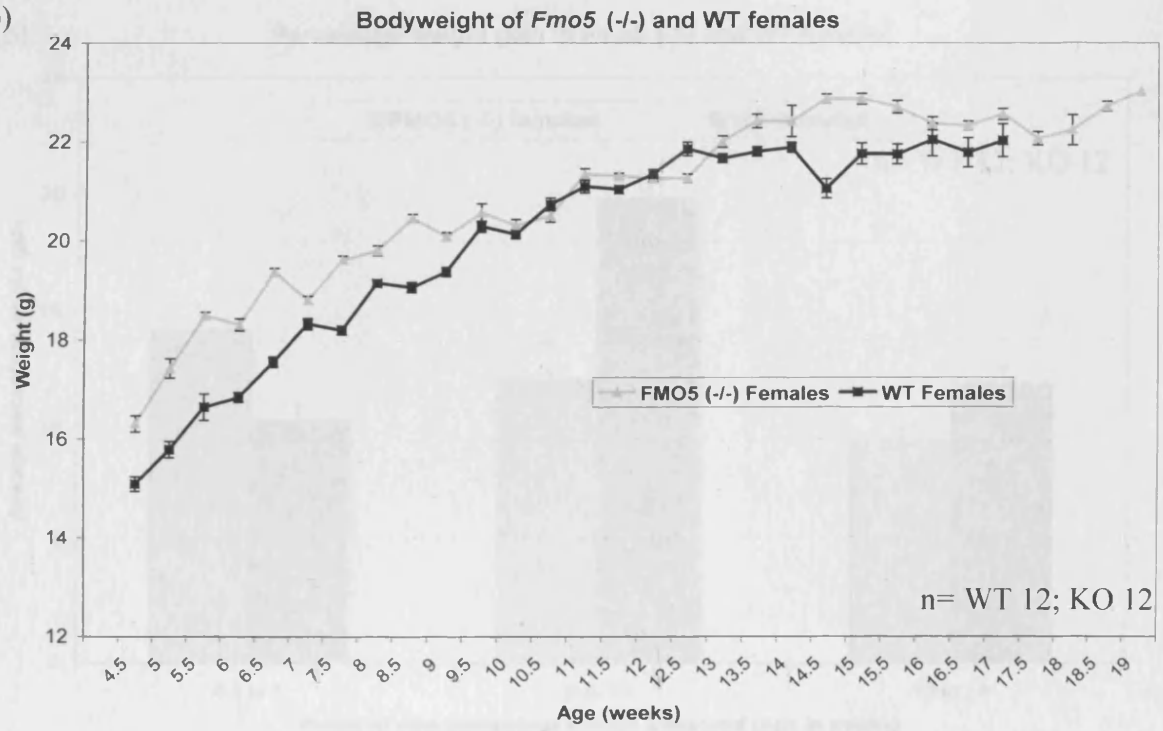

5.17.1 Bodyweights of Fmo5 (-/-) and WT males and females

The bodyweight of *Fmo5* (-/-) and WT males (a) and females (b) on a normal diet. Error bars are SEM.

(a)

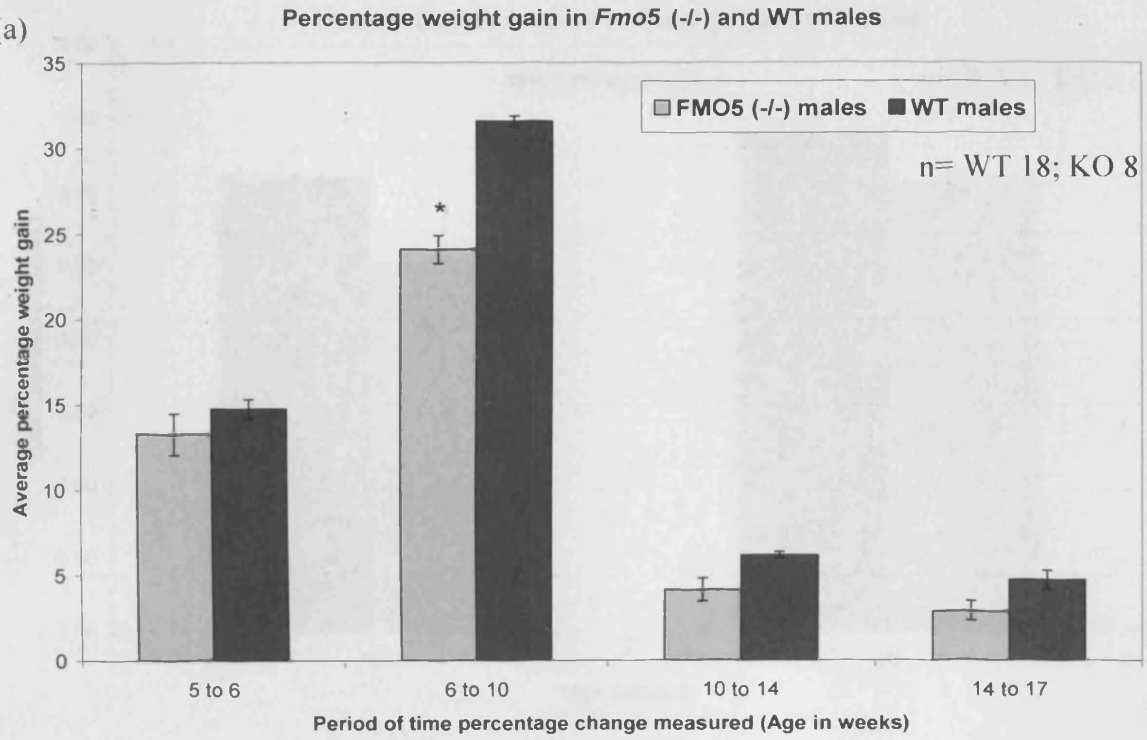

(b)

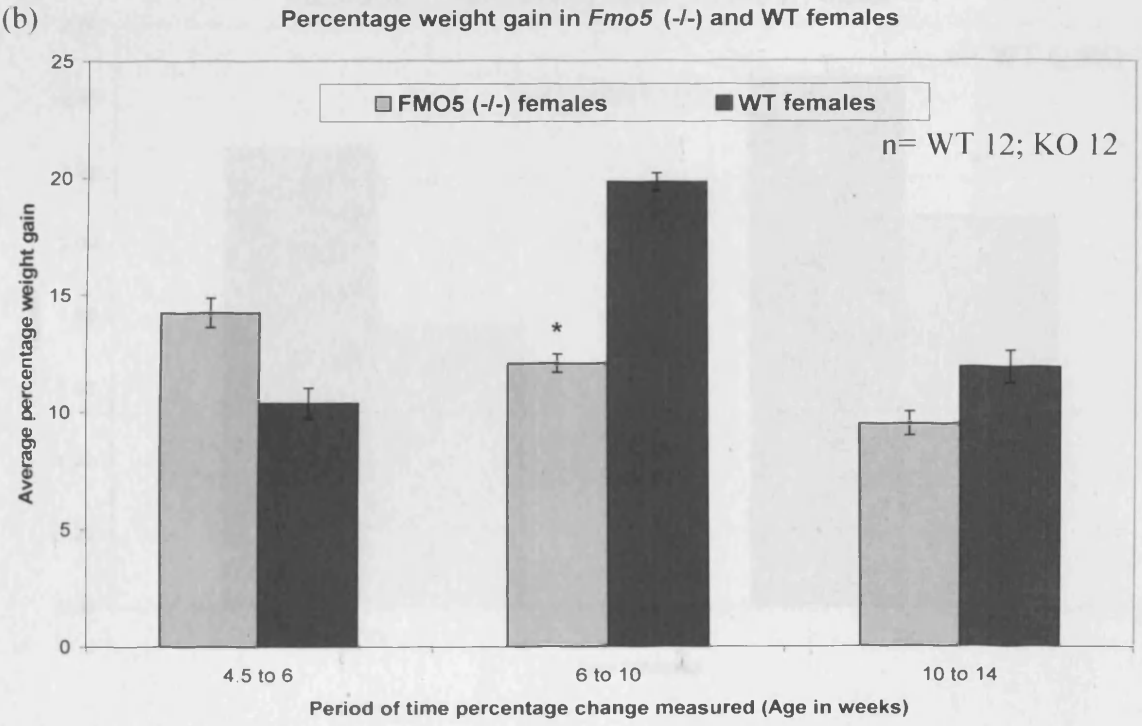

5.17.2 Percentage weight gain of Fmo5 (-/-) mice

The percentage weight gain of *Fmo5* (-/-) and WT males (a) and females (b) on a normal diet. * is $p<0.05$. Error bars are SEM.

(a)

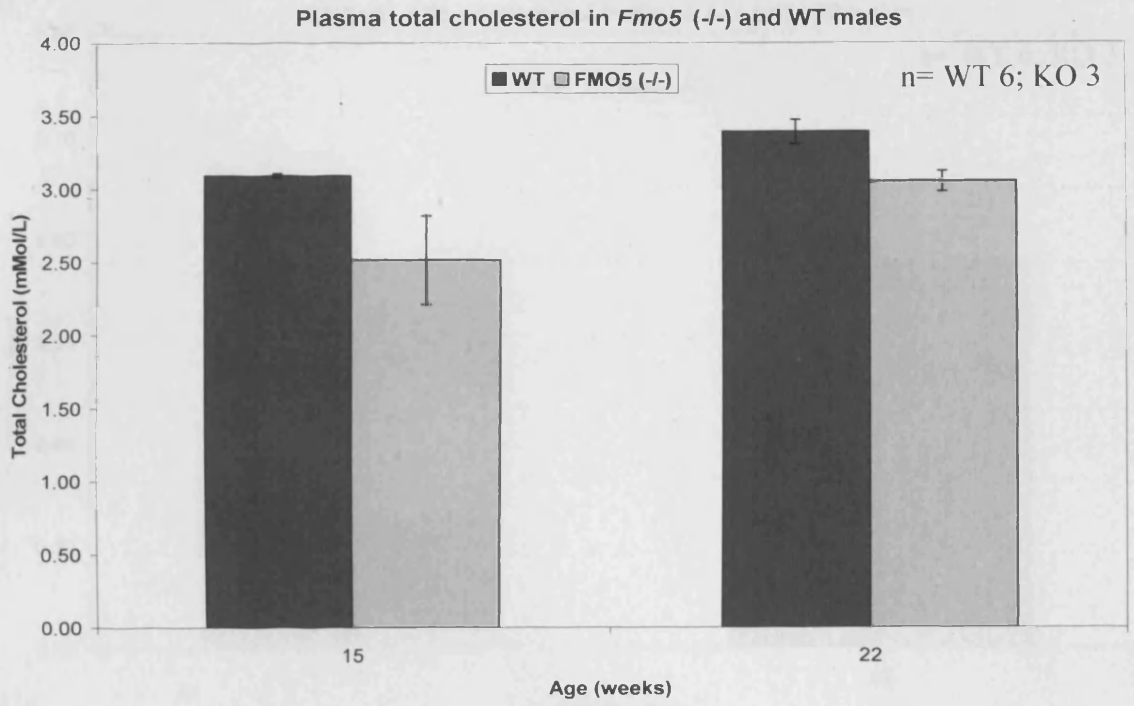

(b)

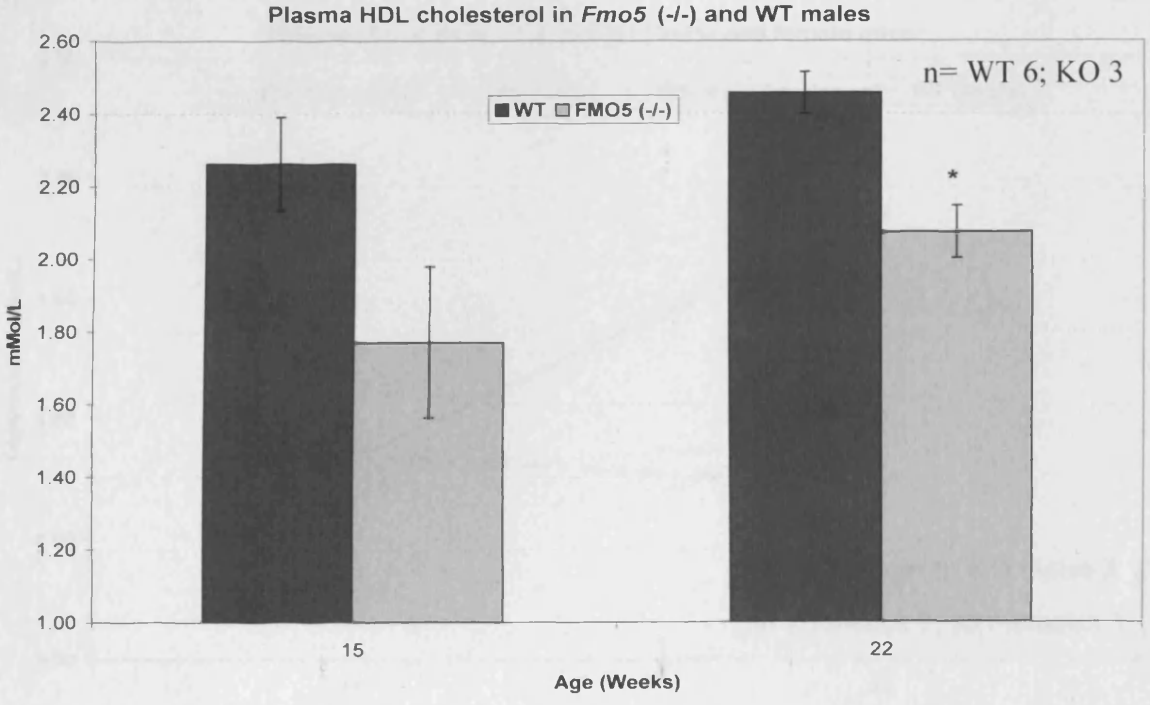

5.17.3 Plasma total and HDL cholesterol in male Fmo5 (-/-) mice

The plasma total cholesterol (a) and HDL cholesterol (b) of *Fmo5* (-/-) and WT males on a normal diet. * is $p<0.05$. Error bars are SEM.

(a)

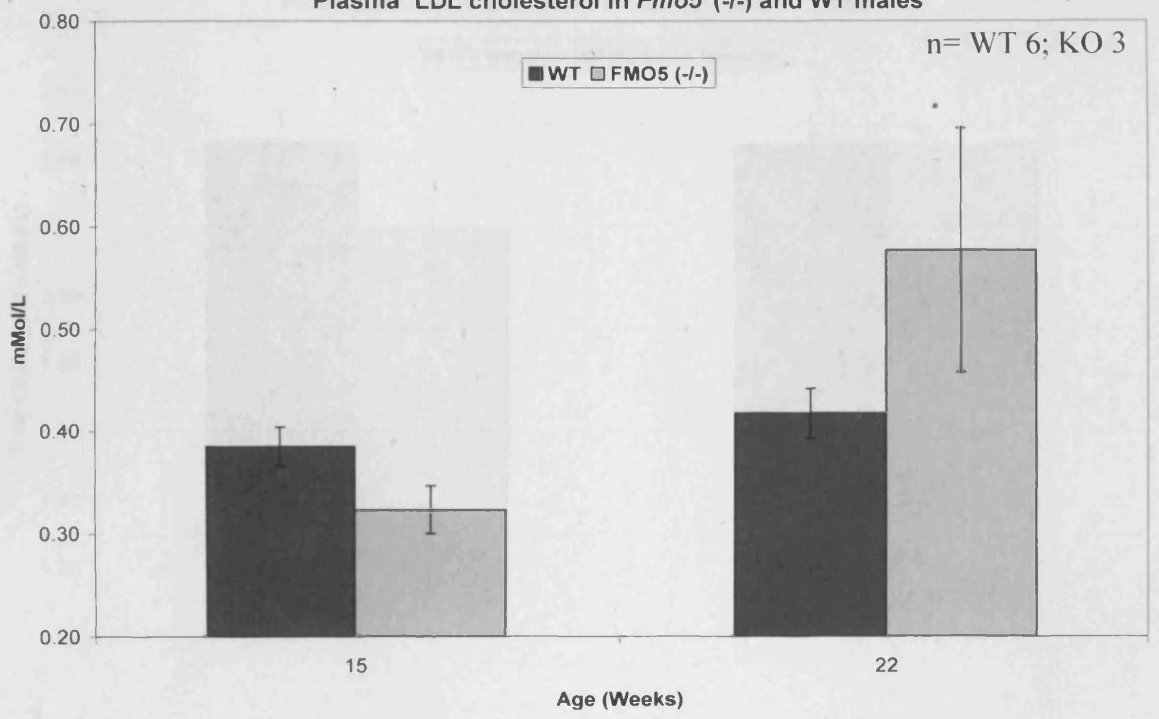

(b)

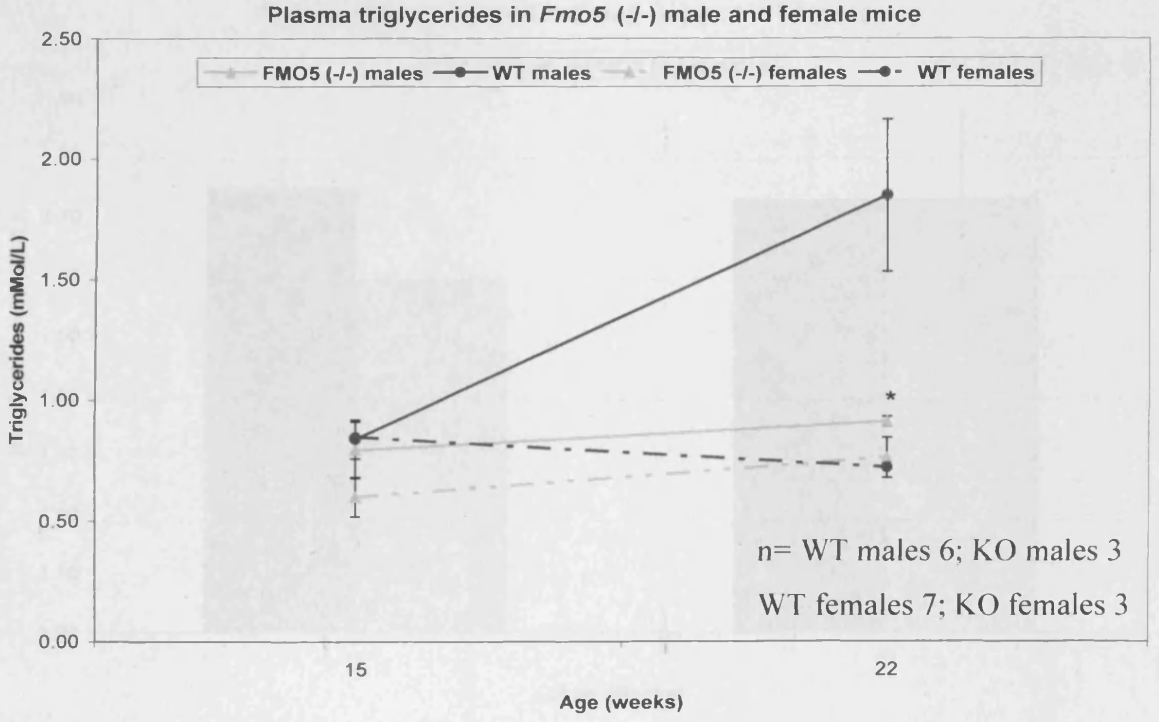

5.17.4 Plasma LDL cholesterol and triglycerides in Fmo5 (-/-) mice

The plasma LDL cholesterol in *Fmo5* (-/-) and WT males (a) and triglycerides (b) in *Fmo5* (-/-) and WT males and females on a normal diet. * is $p<0.05$. Error bars are SEM.

(a)

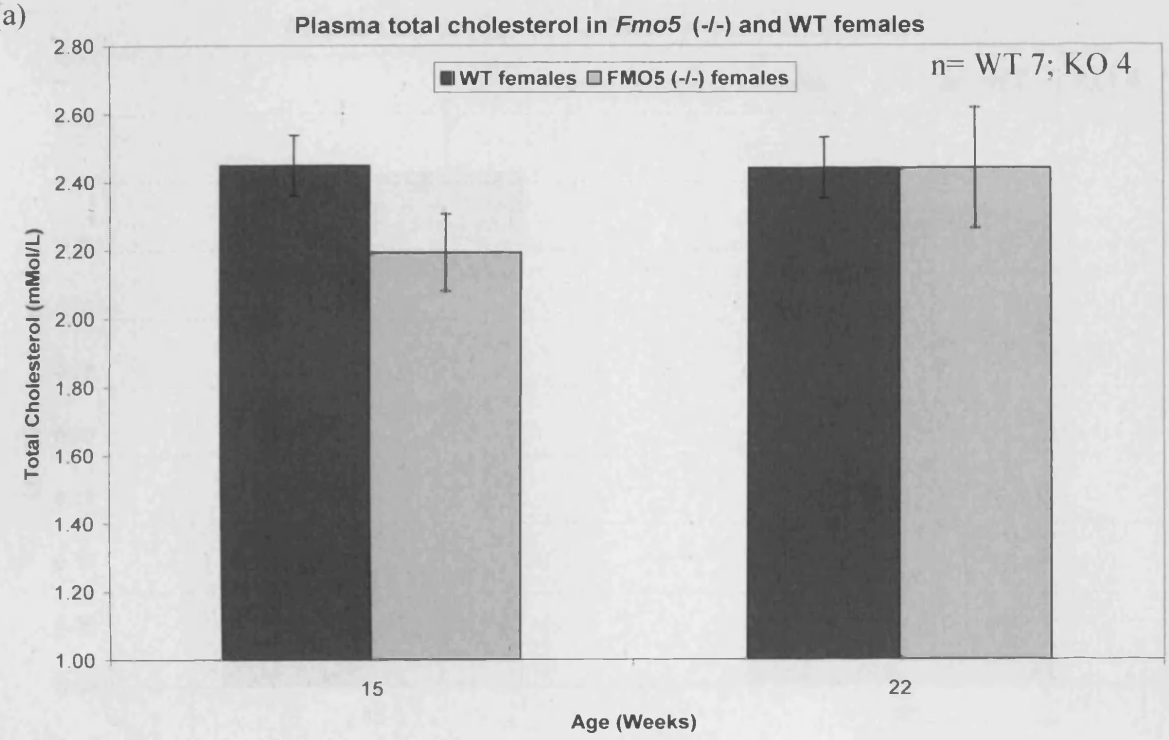

(b)

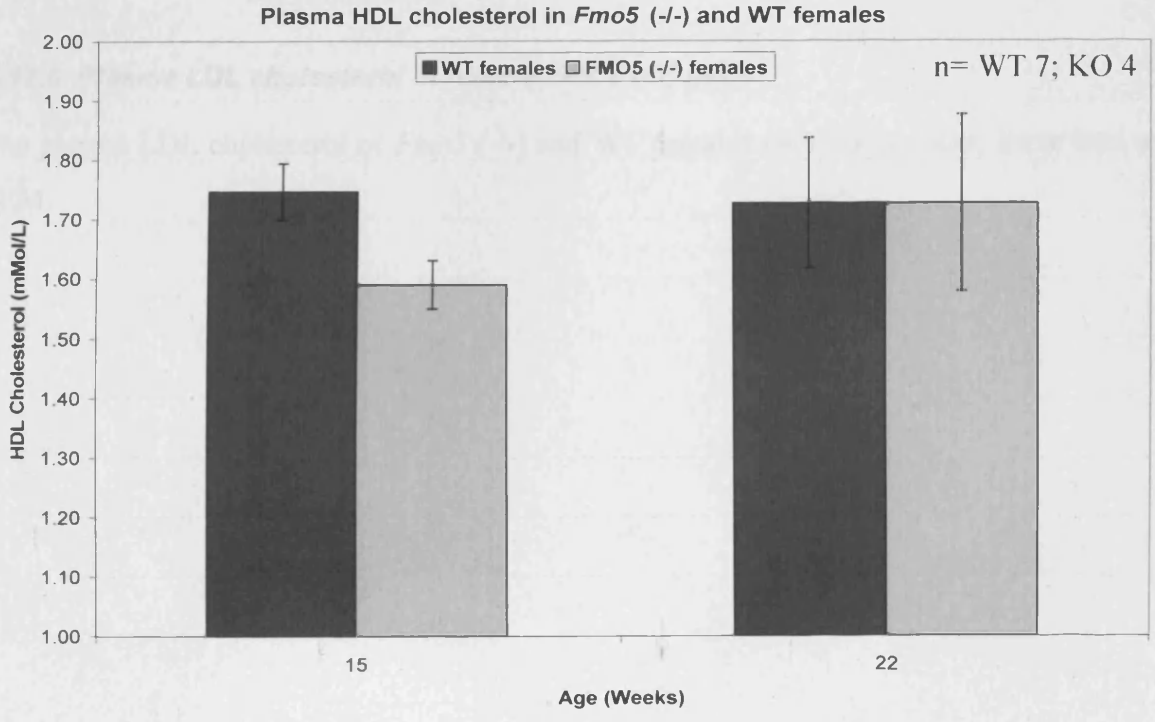

5.17.5 Plasma total and HDL cholesterol in female Fmo5 (-/-) mice

The plasma total cholesterol (a) and HDL cholesterol (b) of *Fmo5* (-/-) and WT females on a normal diet. Error bars are SEM.

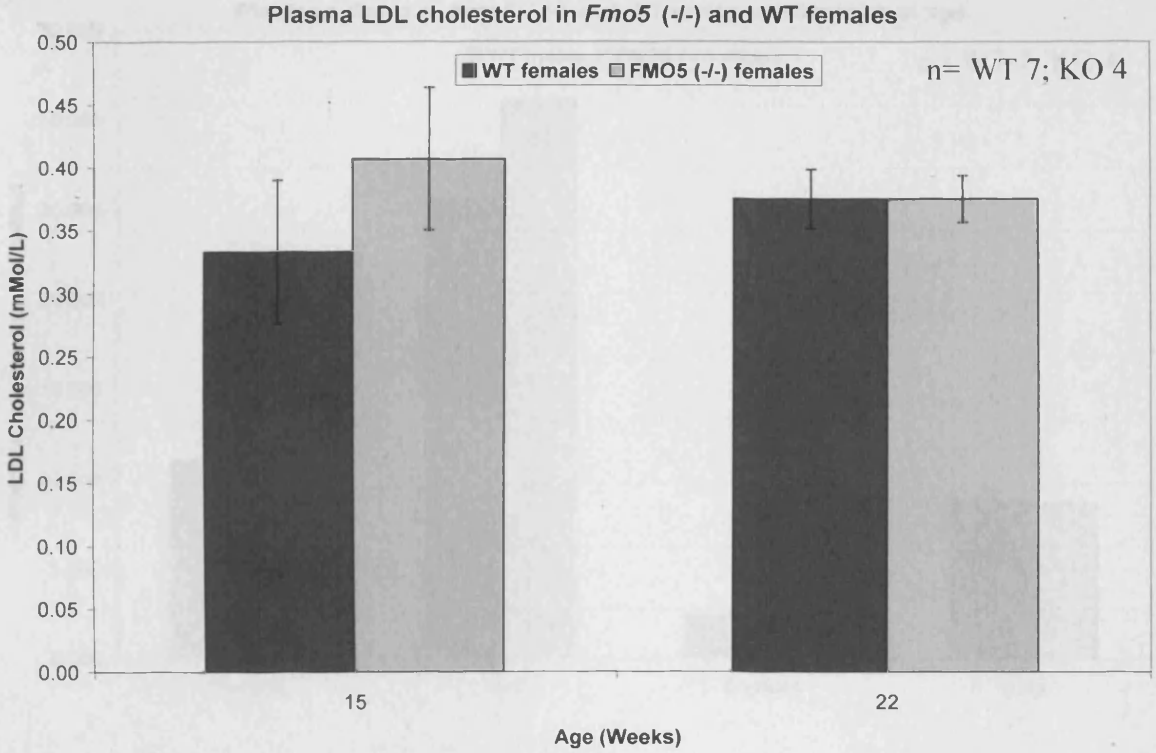

5.17.6 Plasma LDL cholesterol in female Fmo5 (-/-) mice

The plasma LDL cholesterol of *Fmo5* (-/-) and WT females on a normal diet. Error bars are SEM.

(a)

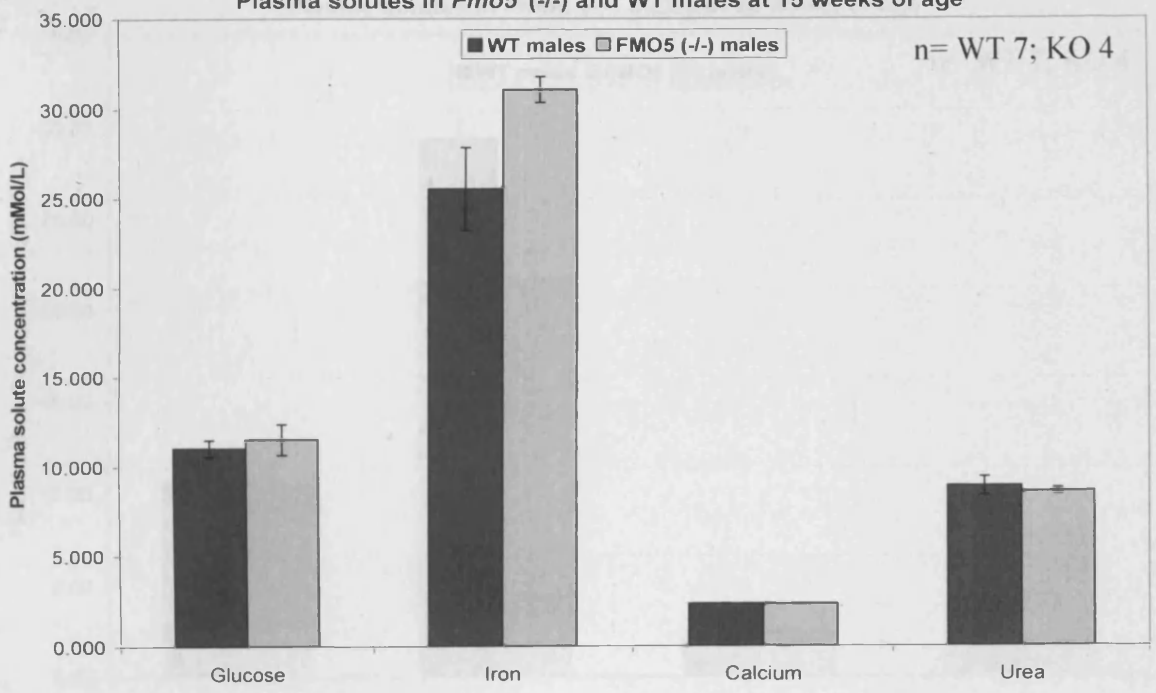

(b)

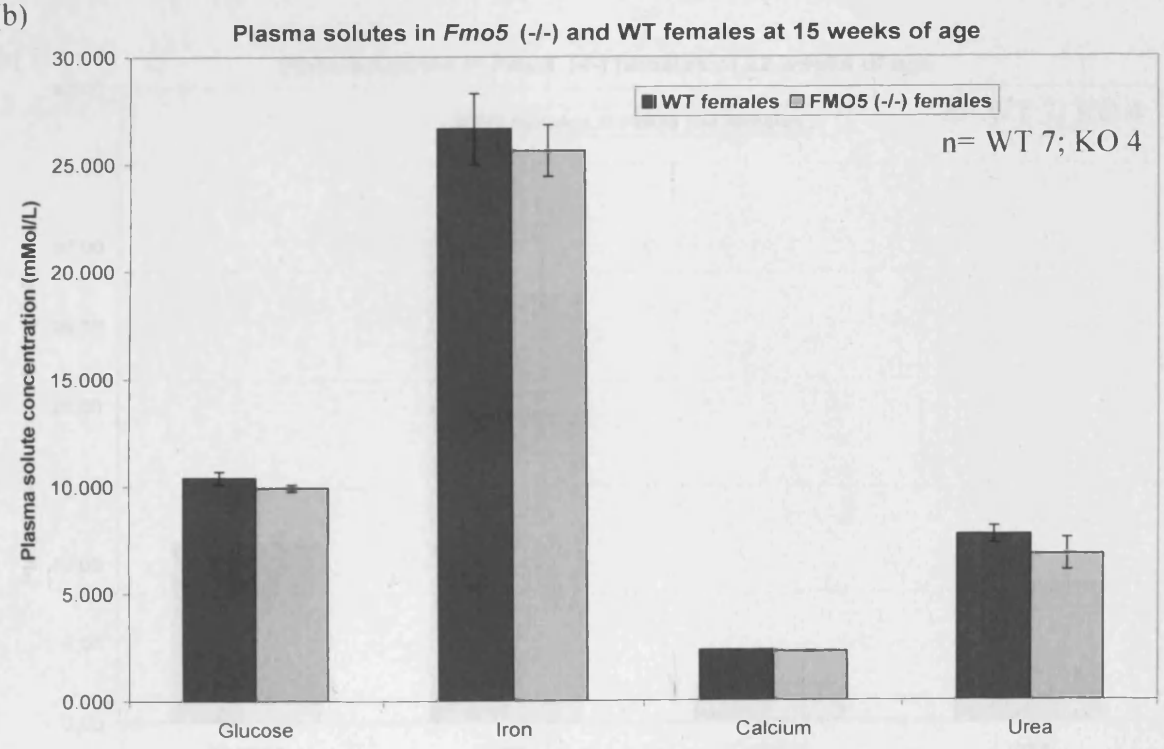

5.17.7 Plasma solutes in Fmo5 (-/-) mice at 15 weeks of age

The plasma solutes of *Fmo5* (-/-) and WT males (a) and females (b) on a normal diet. Error bars are SEM.

(a)

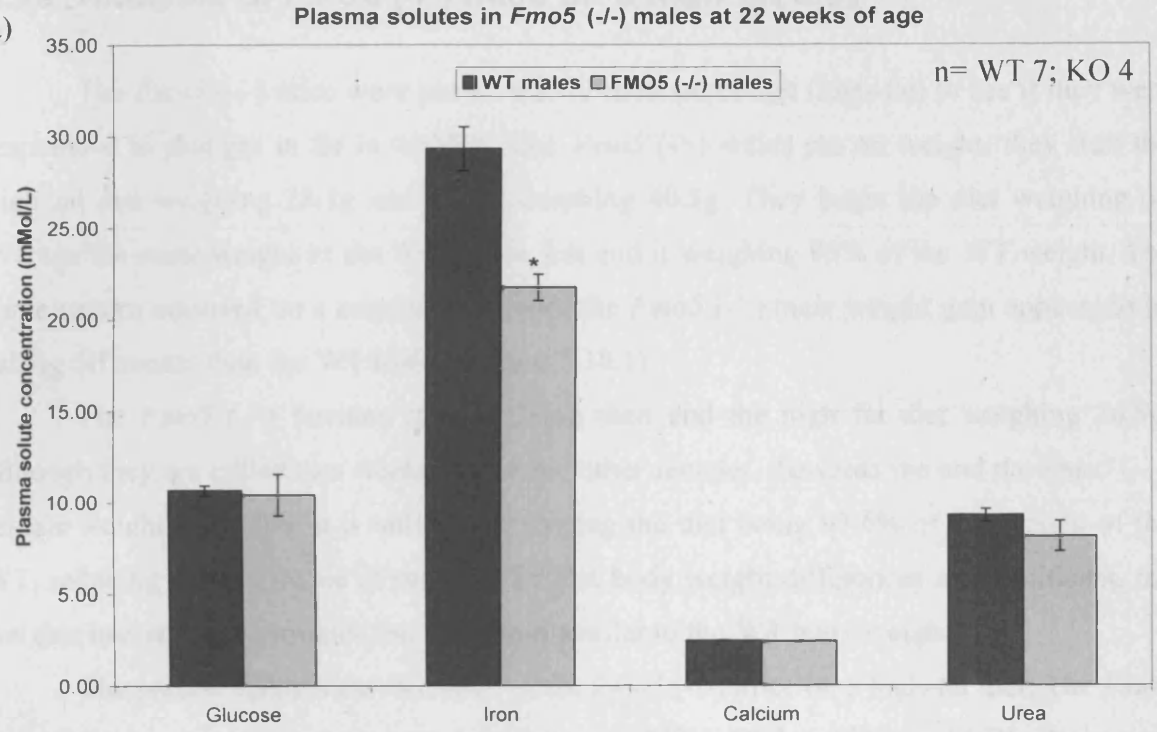

(b)

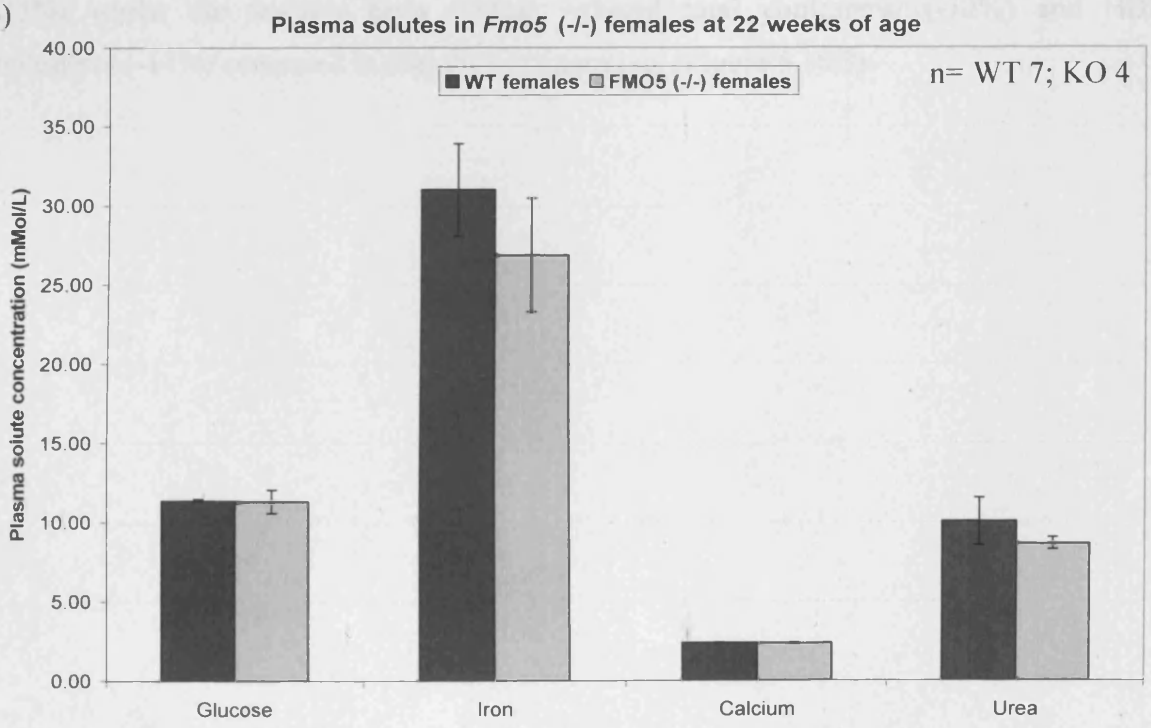

5.17.8 Plasma solutes in Fmo5 (-/-) mice at 22 weeks of age

The plasma solutes of *Fmo5* (-/-) and WT males (a) and females (b) on a normal diet. * is $p<0.05$. Error bars are SEM.

5.18 Analysis of *Fmo5* (-/-) mice on a high-fat diet

The *Fmo5* (-/-) mice were put on a 35% cholesterol diet (high-fat) to see if they were responsive to changes in fat in the diet. The *Fmo5* (-/-) males put on weight, they start the high fat diet weighing 28.1g and end it weighing 40.5g. They begin the diet weighing on average the same weight as the WT males, but end it weighing 95% of the WT weight. The same pattern occurred on a normal diet where the *Fmo5* (-/-) male weight gain appears to be tailing off sooner than the WT males (Figure 5.18.1).

The *Fmo5* (-/-) females start at 21.1g then end the high fat diet weighing 26.9g, although they are culled two weeks before the other females. Towards the end the *Fmo5* (-/-) female weight looks like it is tailing off, starting the diet being 97.6% of the weight of the WT, reducing to 92%. None of the high fat diet body weight differences are significant, the weights become more variable but also more similar to the WT body weight.

The plasma lipids were measured in the *Fmo5* (-/-) mice on a high-fat diet. The *Fmo5* (-/-) males have reduced plasma total cholesterol (-17%), HDL (-15%) and LDL cholesterol (-35%) whilst the females have slightly reduced total cholesterol (-12%) and HDL cholesterol (-14%) compared to their WT counterparts (Figure 5.18.3).

(a)

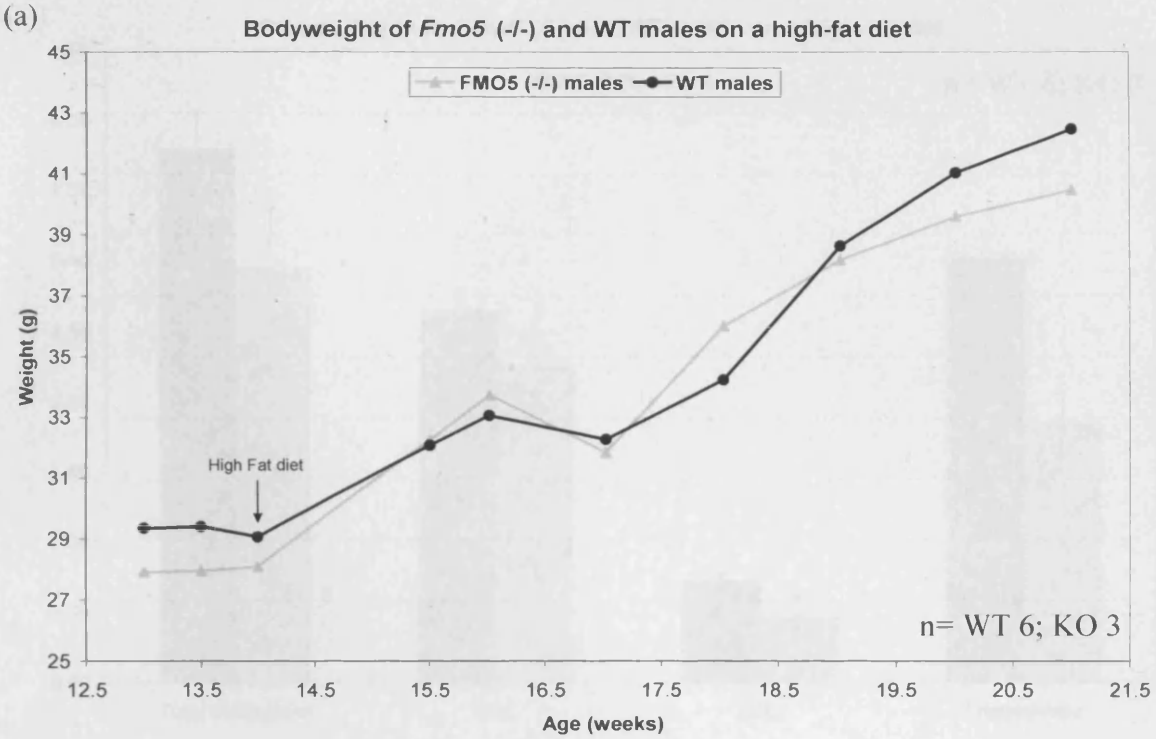

(b)

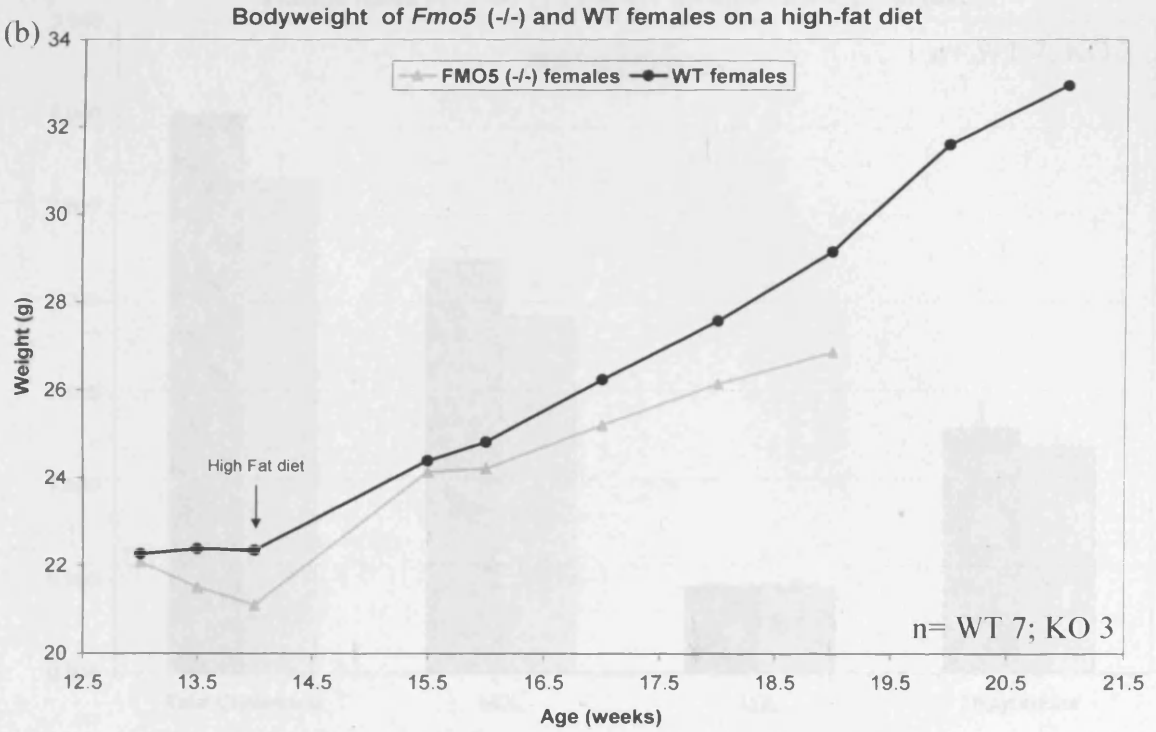

5.18.1 Bodyweight in Fmo5 (-/-) mice on a high-fat diet

The bodyweight of *Fmo5* (-/-) and WT males (a) and females (b) on a high-fat diet.

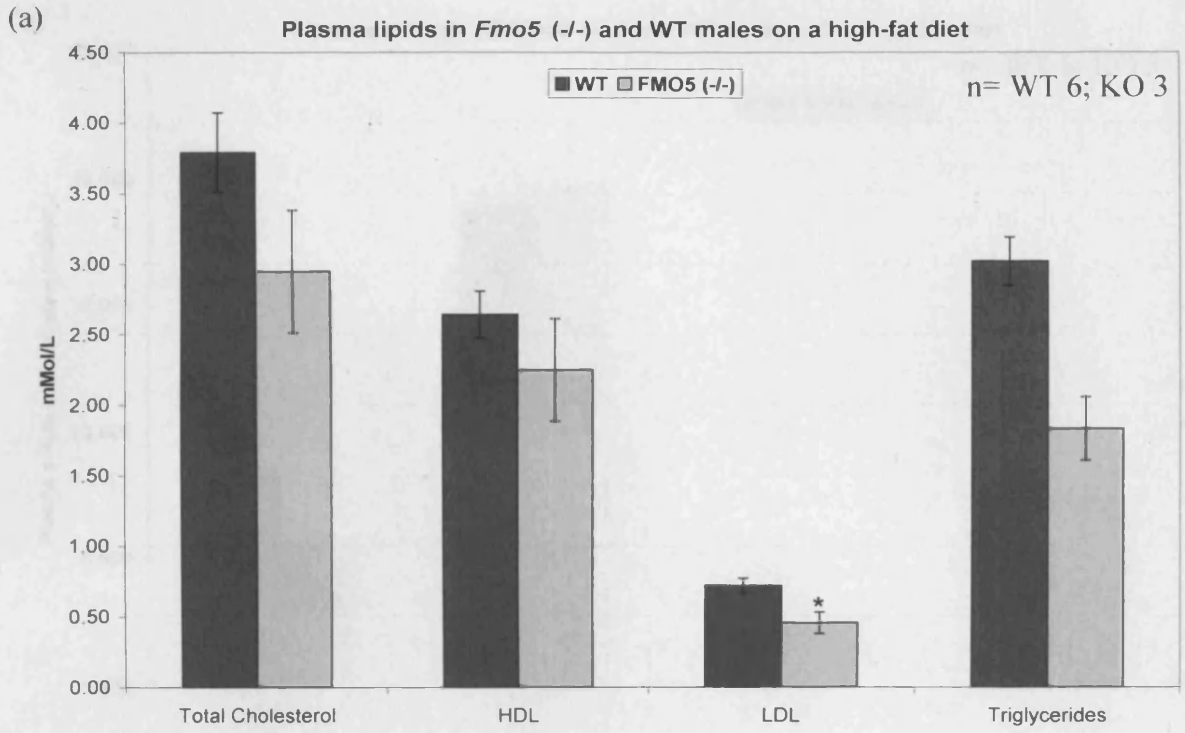

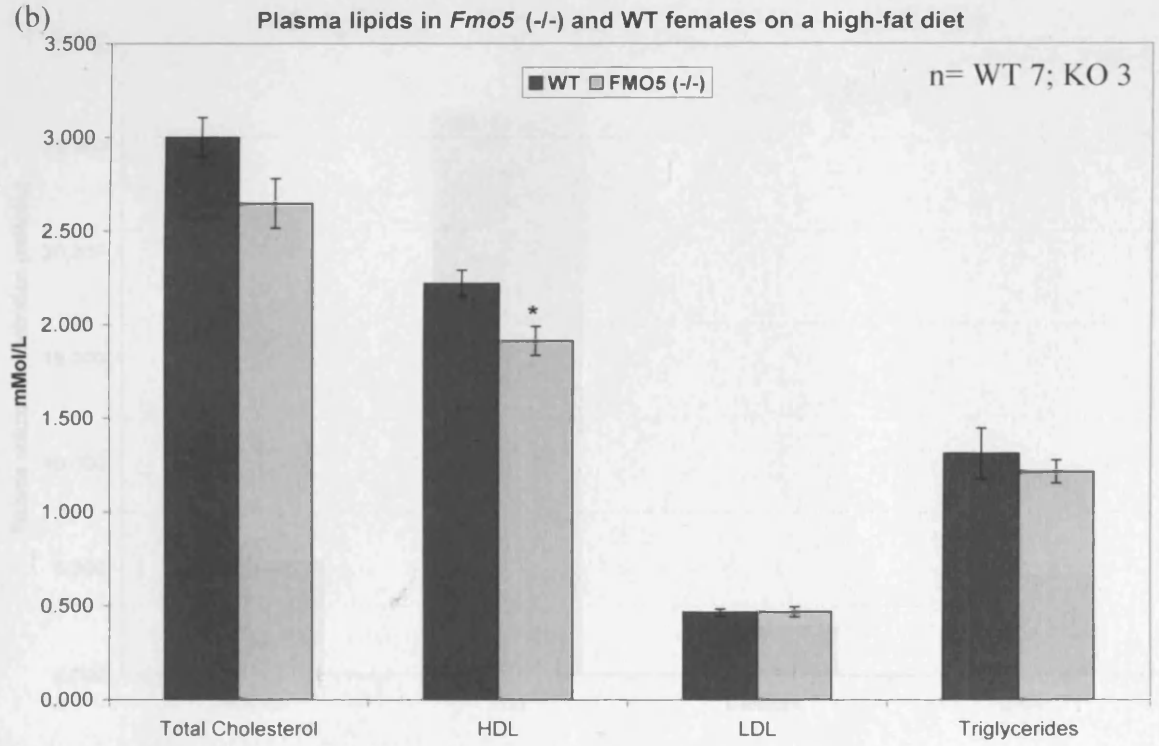

5.18.2 Plasma lipids in Fmo5 (-/-) mice on a high-fat diet

The plasma lipids of *Fmo5* (-/-) and WT males (a) and females (b) on a high-fat diet. * is $p<0.05$. Error bars are SEM.

(a)

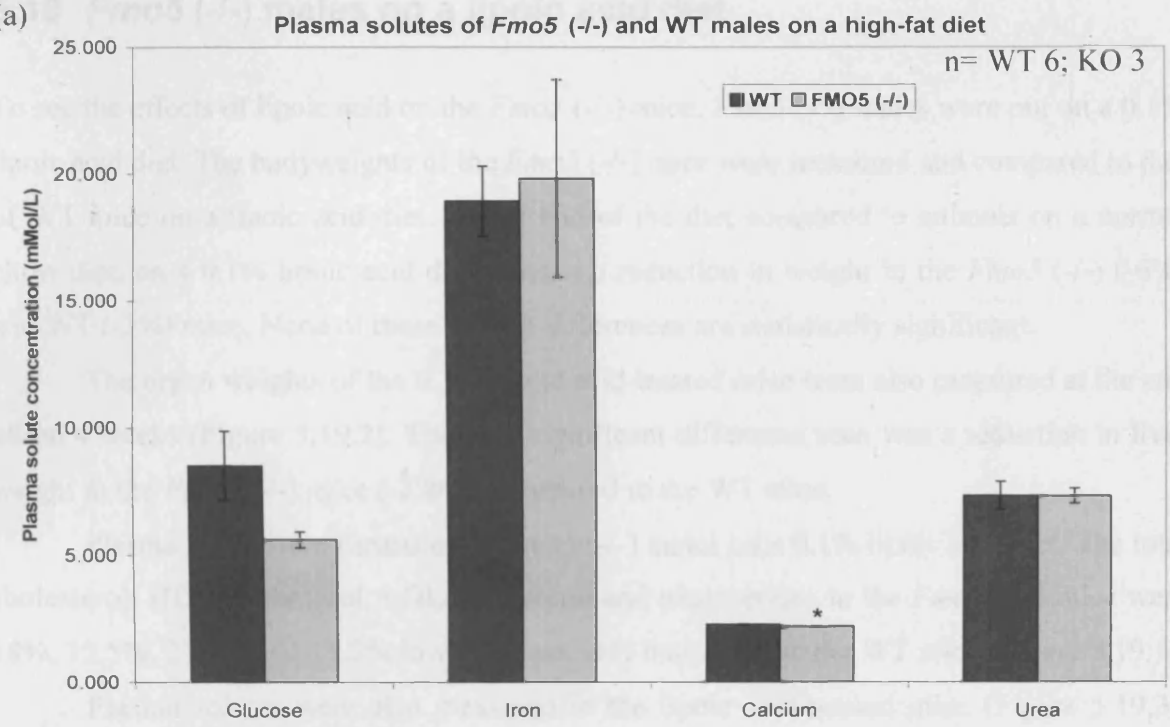

(b)

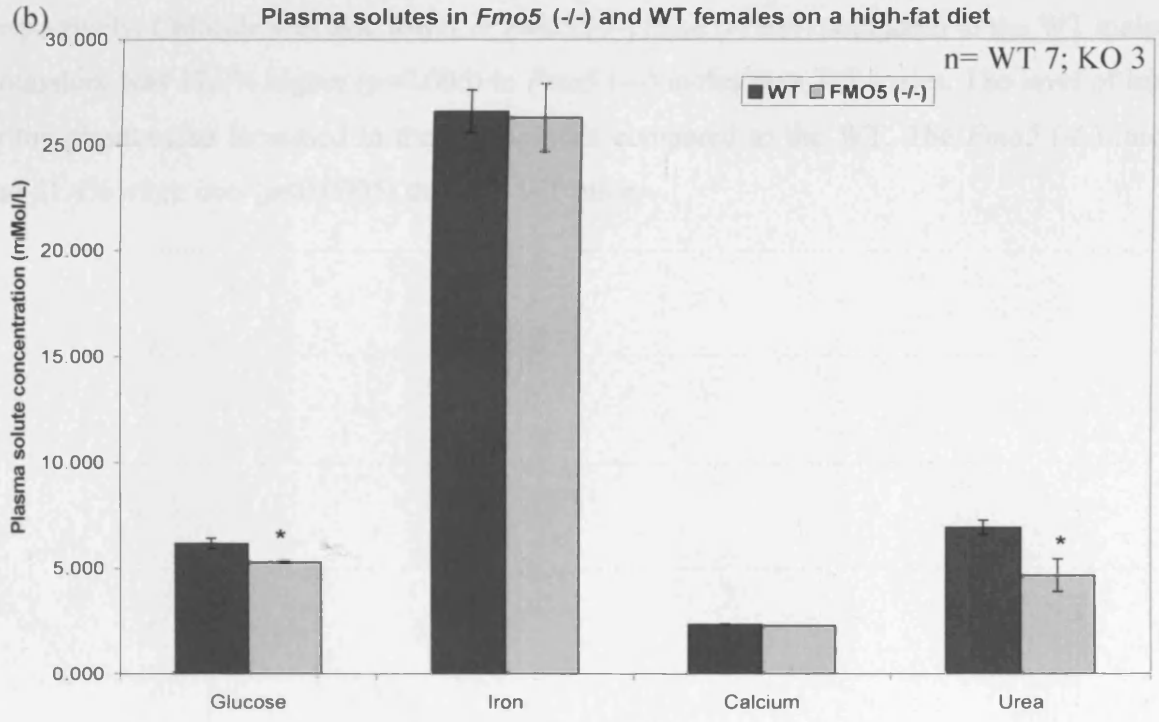

5.18.3 Plasma solutes in Fmo5 (-/-) mice on a high-fat diet

The plasma solutes of *Fmo5* (-/-) and WT males (a) and females (b) on a high-fat diet. * is $p<0.05$. Error bars are SEM.

5.19 *Fmo5* (-/-) males on a lipoic acid diet

To see the effects of lipoic acid on the *Fmo5* (-/-) mice, *Fmo5* (-/-) males were put on a 0.1% lipoic acid diet. The bodyweights of the *Fmo5* (-/-) mice were measured and compared to that of WT mice on a lipoic acid diet. At the end of the diet compared to animals on a normal chow diet, on a 0.1% lipoic acid diet there is a reduction in weight in the *Fmo5* (-/-) (-6%) and WT (-3%) mice. None of these weight differences are statistically significant.

The organ weights of the 0.1% lipoic acid-treated mice were also measured at the end of the 4 weeks (Figure 5.19.2). The only significant difference seen was a reduction in liver weight in the *Fmo5* (-/-) mice (-2.8%), compared to the WT mice.

Plasma lipids were measured in *Fmo5* (-/-) males on a 0.1% lipoic acid diet. The total cholesterol, HDL cholesterol, LDL cholesterol and triglycerides in the *Fmo5* (-/-) mice were 18%, 15.5%, 21.5% and 15.3% lower respectively than those in the WT mice (Figure 5.19.1).

Plasma solutes were also measured in the lipoic acid-treated mice (Figure 5.19.3). Calcium and phosphorous were significantly lower in the *Fmo5* (-/-) mice, -3% and -20.4% respectively. Chloride was also lower in *Fmo5* (-/-) mice (-1.6%) compared to the WT males. Potassium was 17.9% higher ($p<0.005$) in *Fmo5* (-/-) males than WT males. The level of iron in the plasma also increased in the KO animals compared to the WT. The *Fmo5* (-/-) mice had 51.4% more iron ($p<0.0005$) than the WT mice.

(a)

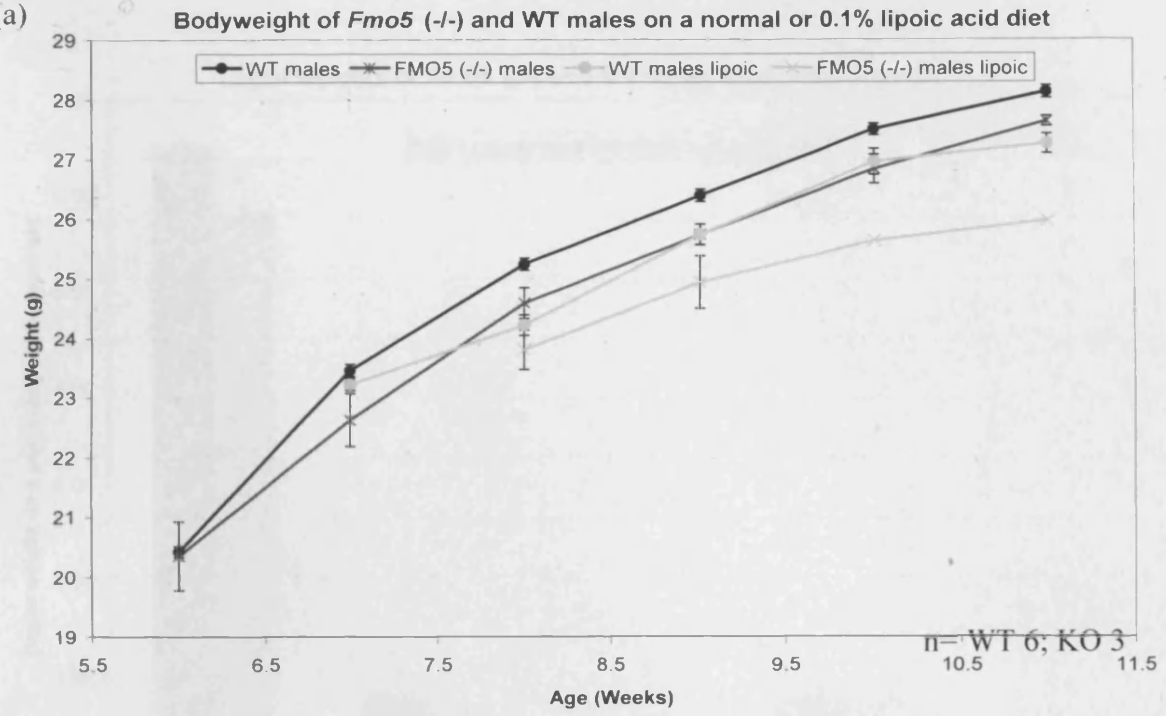

(b)

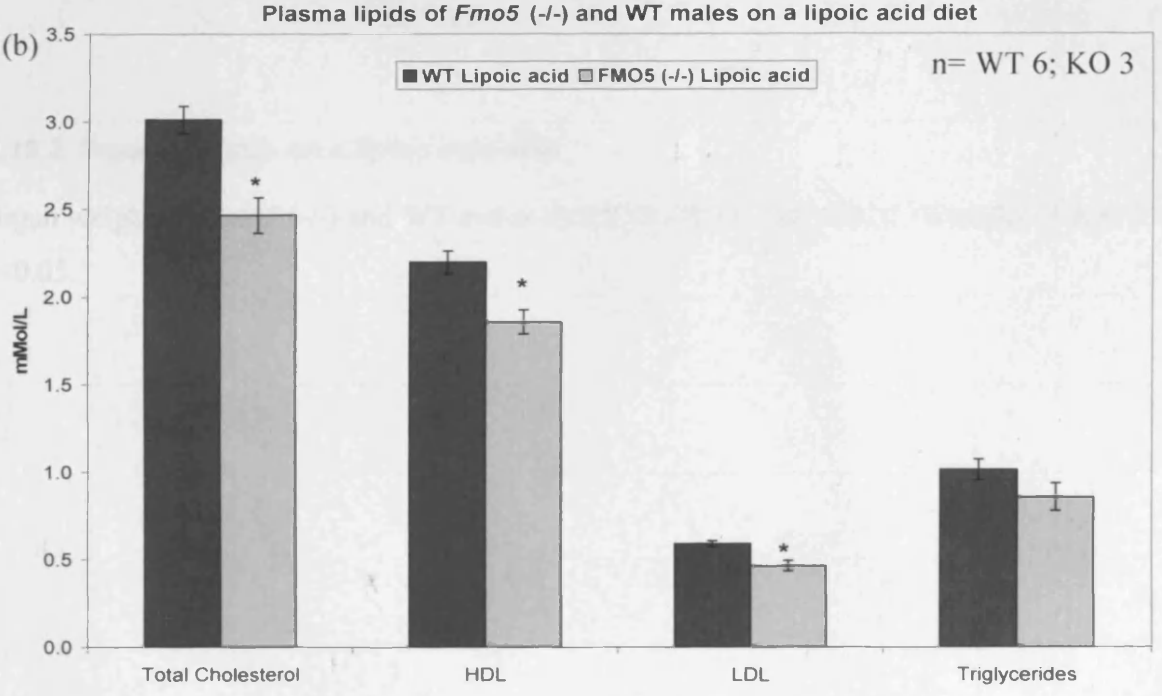

5.19.1 Bodyweight and blood plasma lipids on a lipoic acid diet

Bodyweight (a) and blood plasma lipids (b) in *Fmo5* (-/-) and WT males on a 0.1% lipoic acid diet at 10 weeks of age. The iron concentration is in µMol/L. * is $p<0.05$, ** is $p<0.005$. Error bars are SEM.

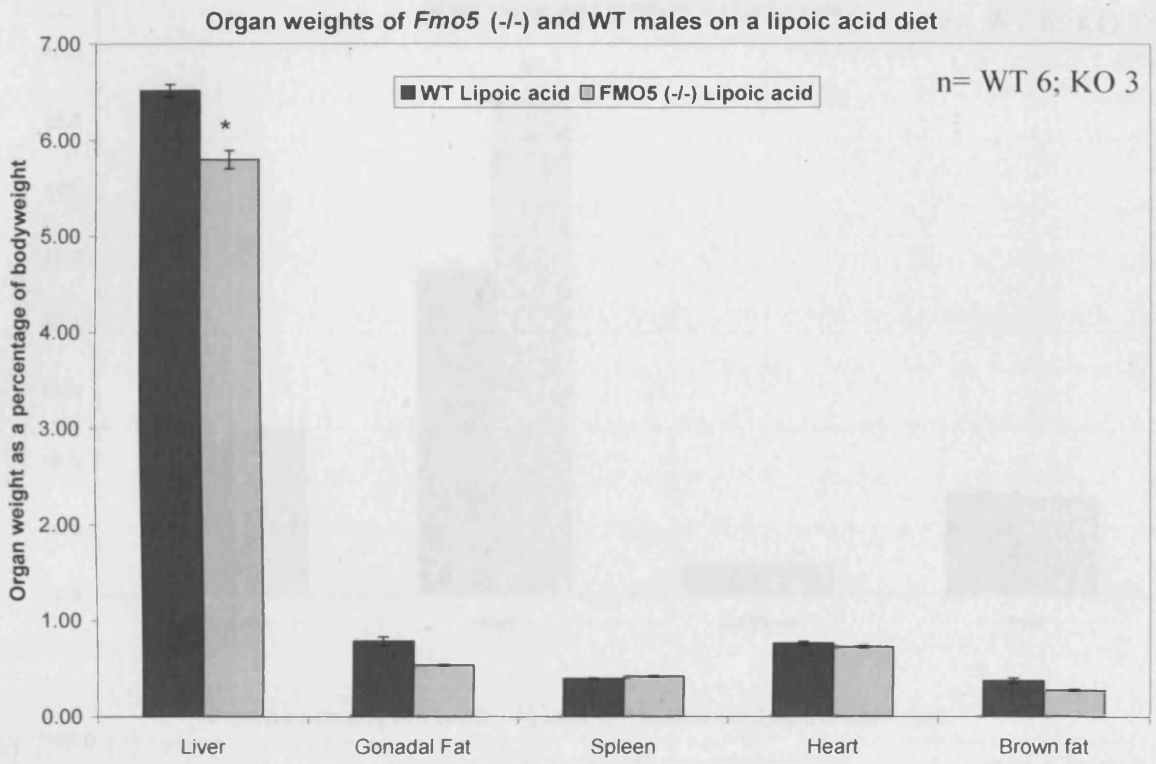

5.19.2 Organ weights on a lipoic acid diet

Organ weights in *Fmo5* (-/-) and WT males on a 0.1% lipoic acid diet at 10 weeks of age. * is $p<0.05$.

(a)

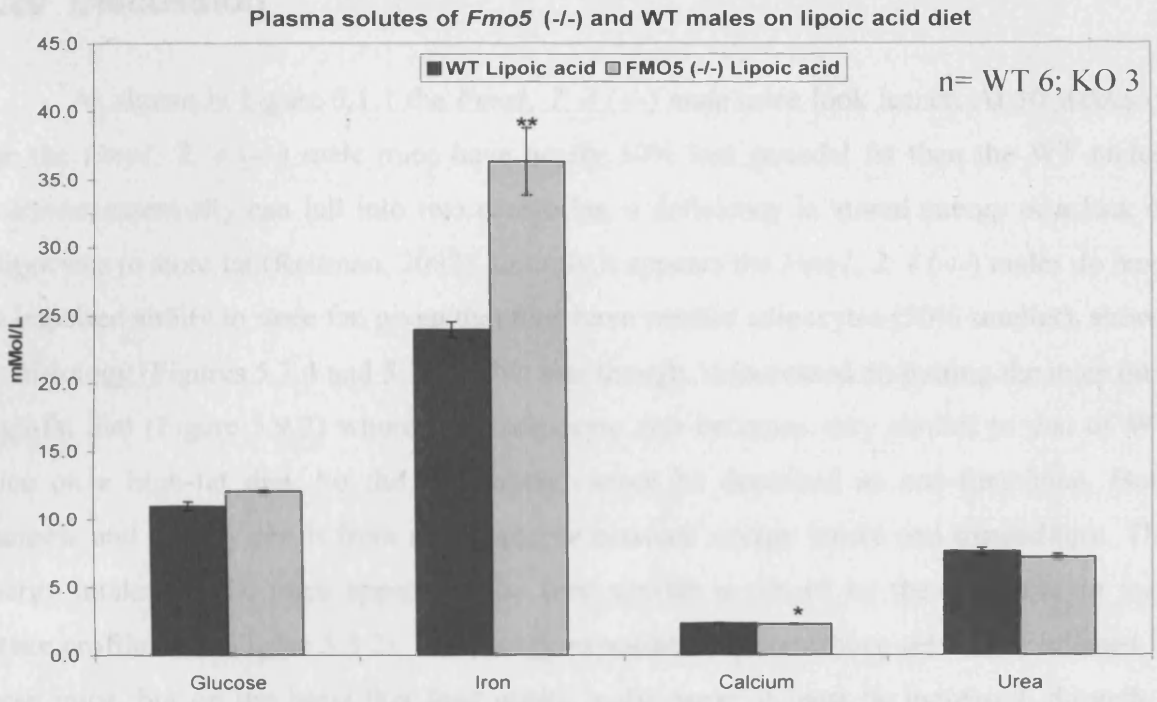

(b)

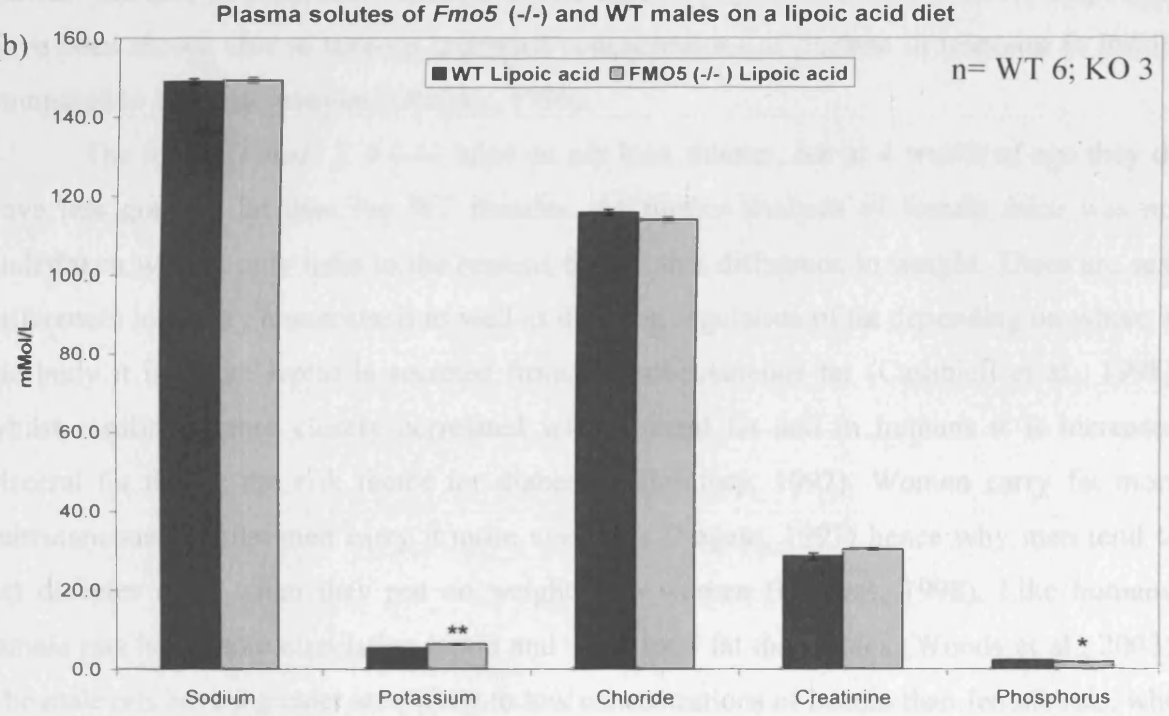

5.19.3 Blood plasma solutes on a lipoic acid diet

Blood plasma solute concentration in *Fmo5* (-/-) and WT males (a) and (b) on a 0.1% lipoic acid diet at 10 weeks of age. The iron concentration is in µMol/L. * is $p<0.05$, ** is $p<0.005$. Error bars are SEM.

5.20 Discussion

As shown in Figure 5.1.1 the *Fmo1, 2, 4* (-/-) male mice look leaner. At 10 weeks of age the *Fmo1, 2, 4* (-/-) male mice have nearly 50% less gonadal fat than the WT males. Leanness essentially can fall into two categories, a deficiency in stored energy or a lack of adipocytes to store fat (Reitman, 2002). Initially it appears the *Fmo1, 2, 4* (-/-) males do have an impaired ability to store fat, given that they have smaller adipocytes (50% smaller), shown by histology (Figures 5.7.4 and 5.7.5). This size though, is increased on putting the mice on a high-fat diet (Figure 5.9.2) where their adipocyte size becomes very similar to that of WT mice on a high-fat diet. So the adipocytes cannot be described as non-functional. Both leanness and obesity result from an imbalance between energy intake and expenditure. The energy intake for the mice appears to be very similar as shown by the similarity in feed intake profiles (see Figure 5.3.2). The energy expenditure is something yet to be evaluated in these mice, but on the basis that feed intake is the same, it must be increased, through a general increase in metabolic turnover or increase in physical activity. Smaller adipocytes have been shown able to take-up increased concentrations of glucose in response to insulin compared to larger adipocytes (Olefsky, 1976).

The female *Fmo1, 2, 4* (-/-) mice do not look thinner, but at 4 weeks of age they do have less gonadal fat than the WT females. As further analysis of female mice was not undertaken we can only infer to the reasons behind this difference in weight. There are sex-differences in energy homeostasis as well as different regulation of fat depending on where in the body it is. More leptin is secreted from the subcutaneous fat (Casabiell et al., 1998), whilst insulin is more closely correlated with visceral fat and in humans it is increased visceral fat that is the risk factor for diabetes (Bjorntorp, 1997). Women carry fat more subcutaneously whilst men carry it more viscerally (Legato, 1997) hence why men tend to get diabetes more when they put on weight than women (Despres, 1998). Like humans, female rats have more circulating leptin and more total fat than males (Woods et al., 2003). The male rats have a greater sensitivity to low concentrations of insulin than female rats, who in turn have a greater sensitivity to low concentrations of leptin than male rats (Clegg et al., 2003). Although we have no fat data on the female mice after 4 weeks of age, we do know that the *Fmo1, 2, 4* (-/-) female mice have a greater body weight than the WT females whereas the *Fmo1, 2, 4* (-/-) males weigh less than WT males. We can therefore propose a

reason for this difference. The possibility is that the effect we are seeing is visceral fat specific, which is why the males have shown a pronounced reduction in weight whereas the females have not. Females carry more fat subcutaneously, which perhaps is unaffected, although their visceral fat is still reduced, certainly at 4 weeks of age. Therefore we could come to the conclusion that the difference in weight and fat we are observing is down to insulin regulation, or lack of it. This does not preclude a role for leptin, given the increased weight in the *Fmo1, 2, 4* (-/-) females.

There were no bodyweight differences between WT and *Fmo5* (-/-) animals on a normal diet, in either sex. This is a stark difference to that seen in the *Fmo1, 2, 4* (-/-) animals, where bodyweight is lower in males and higher in females compared to the WT mice.

The differences between KO mouse models continue regarding the plasma lipids on a normal diet. The *Fmo1, 2, 4* (-/-) males and females had higher total-, HDL- and LDL-cholesterol than the WT males at the same age. Surprisingly the *Fmo5* (-/-) males and females had less total- and HDL-cholesterol than the WT mice. Although it is well publicized that HDL cholesterol is the "good cholesterol" and LDL cholesterol is the "bad cholesterol" as an indicator of coronary artery disease, this view is over-simplistic, since both have vital roles in the body. LDL transports cholesterol from the liver to tissues for use e.g. in membrane synthesis, whilst HDL accompanies old/used cholesterol back to the liver for recycling or excretion. The causes of this dichotomy of lipid homeostasis between the KO mouse models are unknown. But adipocytes are one of the largest pools in the body for cholesterol storage and exchange (Angel and Farkas, 1974). So a reduction in adipocyte size could cause a rise in plasma cholesterol levels in the *Fmo1, 2, 4* (-/-) mice.

Seeing the changes in body fat and lipid levels in the KO mice, they were put on a high-fat diet to investigate further the apparent dysregulation of energy homeostasis. On a normal diet there is no difference in the plasma triglyceride concentration between KO and WT animals. High plasma triglycerides do have an association with incidence of cardiovascular disease (Despres et al., 1996), and also insulin resistance (Reaven et al., 1967). But this is not the case here, there is no change to triglycerides on a chow diet, but interestingly on a high-fat diet the plasma triglyceride level in *Fmo1, 2, 4* (-/-) male mice is much lower than that in WT male mice (Figure 5.11.1). In line with this reduction in plasma triglycerides is an increase in plasma total- and HDL-cholesterol. In the WT males only a

steady increase in total-cholesterol is observed, but a marked increase in triglycerides is seen, the concentration almost doubles. Whereas on a normal or high-fat diet in *Fmo1, 2, 4* (-/-) males, the plasma triglycerides stay remarkably the same. Triglyceride levels in plasma are greatly influenced by the intake of dietary fats (as well as endogenous production by the liver and to a lesser extent liberation from adipose) (Weatherby, 2002). So this large increase of triglycerides in the WT males could be thought of as 'normal' given the mice are eating a high-fat diet; the ability of the WT mice to excrete fat is dwarfed by the fat concentration being taken in. Again this isn't seen in *Fmo1, 2, 4* (-/-) male mice on a high-fat diet. They are either successfully using the extra energy they are taking in, or excreting it.

The *Fmo5* (-/-) mice on a high-fat diet have similar or slightly lower plasma lipids than the WT mice. Again this is counter-intuitive, given the amount of fat being eaten. Whilst there is a steady increase in plasma lipid in the WT mice, the reduction in *Fmo5* (-/-) mice again shows a lack of control in lipid homeostasis.

As shown in the liver histology of mice on a normal chow diet, the *Fmo1, 2, 4* (-/-) male mice have fewer triglycerides, stored fat, in the liver than the WT mice at 4 and 10 weeks of age, and at 22 weeks of a age they have a similar amount of fat. It would then make sense that the *Fmo1, 2, 4* (-/-) mice have higher lipids in the blood plasma. The fat is being circulated, not stored in the liver or adipocytes. In the liver histology from the *Fmo1, 2, 4* (-/-) mice on a high-fat diet, they have much more fat in the liver, a similar amount to the WT mice. A fatty liver is caused by an imbalance in hepatic triglycerides for export and the disposal system of the liver (Malnick et al., 2003). The main sources of hepatic fatty acids to make triglycerides are those made by the liver itself and those found in the plasma, the free fatty acids. In more recent work by the laboratory the free fatty acids appeared unchanged in the mice, this leaves us with the possibility of a problem with hepatic de novo lipogenesis. Hepatic lipogenesis is controlled by two main transcription factors, the sterol regulatory element-binding protein (SREBP)-1c which is controlled by nutritional stimulus and the action of insulin (Yokoyama et al., 1993), and the carbohydrate response element-binding protein (CREBP) which is governed by glucose levels (Dentin et al., 2006). Since the high-fat feed was very crumbly and difficult to weigh accurately once in the cages, we are unable to know if the *Fmo1, 2, 4* (-/-) mice ate more high-fat diet than their WT counterparts. So the nutritional stimulus and subsequent effects of glucose and insulin could be the mechanisms involved to increase the amount of fat in the liver but lower plasma triglycerides in the *Fmo1,*

2, 4 (-/-) male mice on a high-fat diet. However, on a normal diet there is no difference in triglyceride levels in the plasma between *Fmo1, 2, 4* (-/-) and WT mice, so a problem with the synthesis of triglycerides by the liver is probably not the case.

At 8 weeks of age on a normal diet the *Fmo1, 2, 4* (-/-) mice have increased levels of iron in their plasma. The *Fmo1, 2, 4* (-/-) female mice have 30% more iron than the WT females and the *Fmo1, 2, 4* (-/-) male mice have more iron than the WT males (20%, not significant). Van Lenten (Van Lenten et al., 1995) suggests a possible correlation between lipid levels and iron homeostasis. In his study the C57BL/6J strain which is more susceptible to fatty streak formation appeared less able to maintain iron homeostasis when challenged with lipid-induced oxidative stress. Liver apoferritin (sequesters iron) was induced in the fatty-streak resistant mice (C3H/HeJ) to a greater level than that observed in the C57BL/6J mice. The increased amount of LDL cholesterol in the *Fmo1, 2, 4* (-/-) mice could perhaps be the cause of the iron dysregulation. This effect is transient because the older mice do not have this difference in plasma iron concentrations. As explained in the results section, an increased calcium concentration in the *Fmo1, 2, 4* (-/-) females could have combated this increase in plasma iron.

The biggest changes for the *Fmo5* (-/-) mice are seen on a 0.1% lipoic acid diet. All of the mice, both of the KO mouse models and the WT each lose about 5% weight on average on this diet. The liver weights in the *Fmo5* (-/-) mice are lighter (-11%) than that of the WT mice. The *Fmo1, 2, 4* (-/-) mice also have a lighter liver than the WT males (-8%, not significant). There are no other differences with regard to organ weights on the lipoic acid diet.

There is a reduction in total-, HDL- and LDL- cholesterol as well as triglycerides in the *Fmo5* (-/-) mice, which is significant, but doesn't appear to vary much from the concentrations on a normal diet at 15 weeks of age. The most interesting alteration in mice on a lipoic acid diet is the change in some of the plasma solutes. There is a 30% increase in plasma iron in the *Fmo1, 2, 4* (-/-) males and a 35% increase in *Fmo5* (-/-) males compared to the WT mice. As discussed in Chapter 3, the promoter of *FMO5* contains a potential upstream-stimulatory factor (USF) binding site. USF is also known to bind to the promoter of haem-oxygenase (HO). HO breaks down haem and is able to shift the redox state of a cell to a more antioxidant status and increase iron efflux (Ferris et al., 1999). Lipoic acid is known to induce the expression of HO (Cheng et al., 2006; Ogborne et al., 2005). What is interesting

then is the increased plasma iron level in both of the KO mouse models compared to the WT on 0.1% lipoic acid diet.

What we had expected to see was a more pronounced reduction in weight in the *Fmo1, 2, 4* (-/-) mice on a lipoic acid diet, presuming that these mice would be less able to metabolise lipoic acid than the WT mice, thus the effects of lipoic acid would be more manifest. But this is not the case, and so lipoic acid and its lack of metabolism is probably not the cause of the gonadal fat reduction in the *Fmo1, 2, 4* (-/-) mice.

5.21 Current work

Work currently being carried out in the laboratory of Prof Elizabeth Shephard has delved a little deeper into questions thrown up by the *Fmo1, 2, 4* (-/-) and *Fmo5* (-/-) mice.

The expression of several fat storage and fat oxidation genes have been studied in the gonadal fat using real-time RT-PCR by Mr Bilal Omar, and there are several differences between WT and *Fmo1, 2, 4* (-/-) males (Figure 5.21.1). PPARγ is a regulator of genes involved in glucose and lipid metabolism, and is highly expressed in adipose tissue. There were no PPARγ expression changes seen between *Fmo1, 2, 4* (-/-) and WT male adipose. This may not be of importance, since phosphorylation is often used to activate nuclear receptors. Activation of PPARγ enhances the uptake of lipids (Martin et al., 1997; Martin et al., 1998) and up-regulates transcription of genes involved in fatty acid uptake (Motojima et al., 1998). Adipocyte fatty acid binding protein (AP2, or FABP4) expression is 2-fold and 9-fold higher in *Fmo1, 2, 4* (-/-) than WT adipose at 10 and 22 weeks of age respectively. Lipoprotein lipase is two-fold higher in the KO male adipose than the WT but only at 10 weeks of age. Fatty acid transport protein 1 (FATP1) expression was similar in WT and KO adipose. Leptin is expressed at a similar level in WT and KO mice until they are fed a high-fat diet, where leptin is expressed 2-fold higher in WT than *Fmo1, 2, 4* (-/-) adipose.

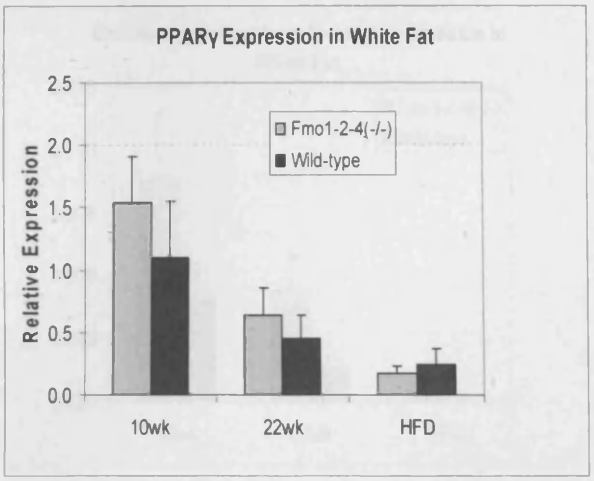

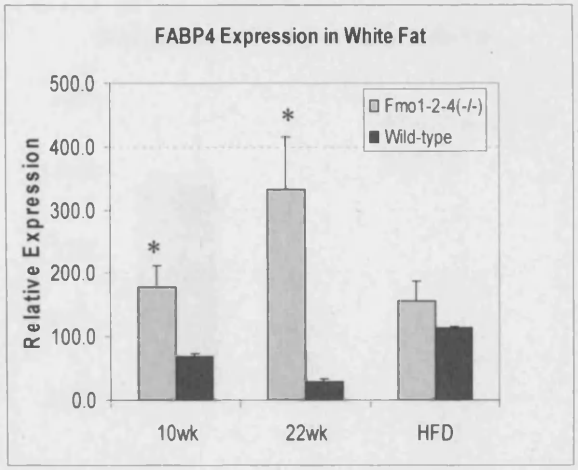

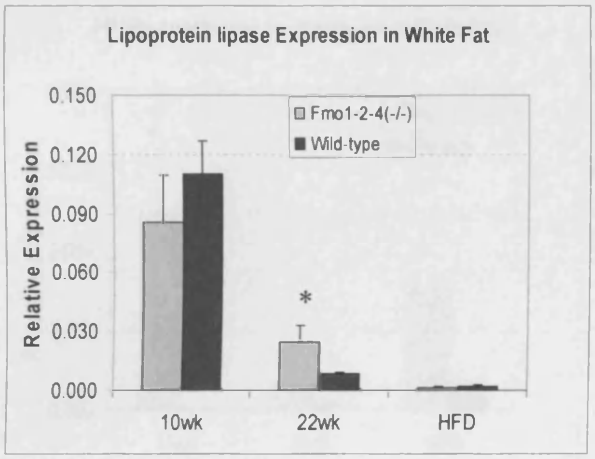

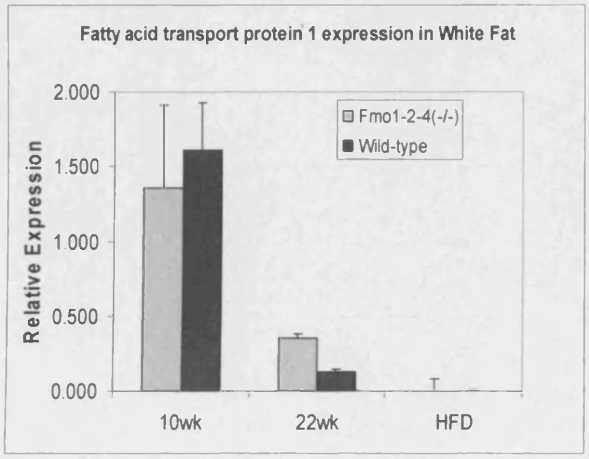

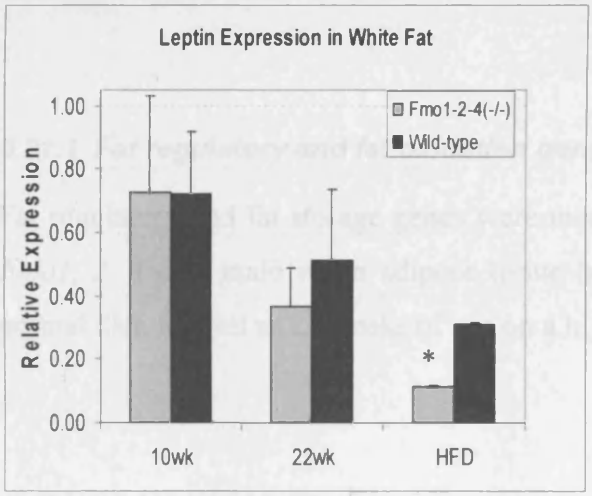

Part 1 of Figure 5.21.1

Lipid regulatory and oxidation genes in Fmo1, 2, 4 (-/-) and WT male adipose.

For full figure legend see next page.

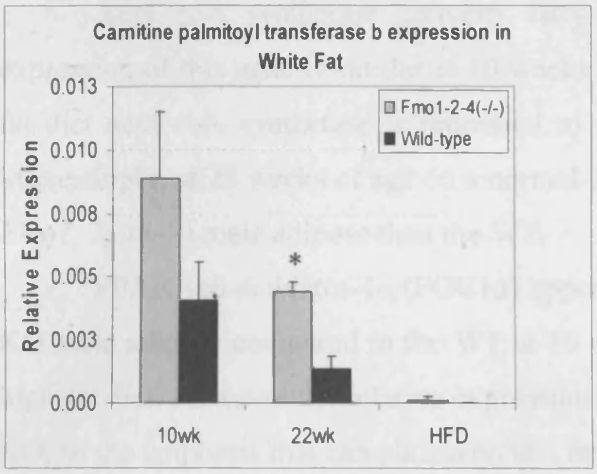

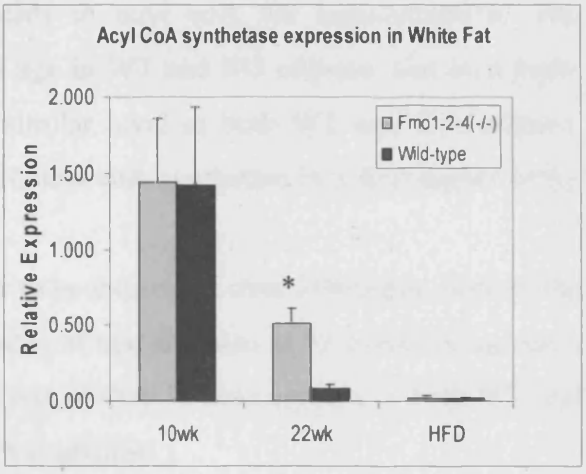

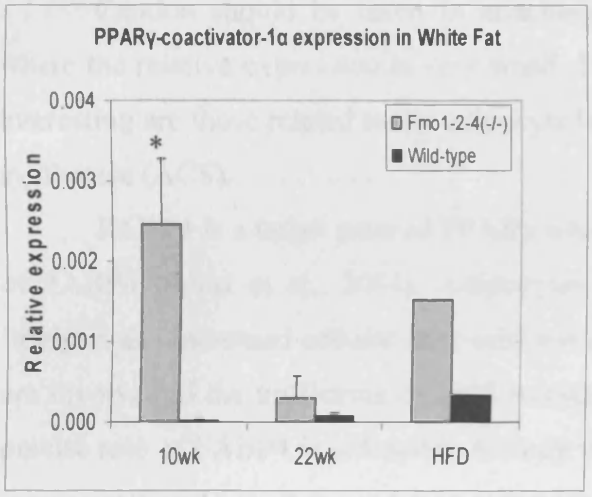

5.21.1 Fat regulatory and fat oxidation genes in WT and KO white adipose

Fat regulatory and fat storage genes were measured using real time RT-PCR from WT and *Fmo1, 2, 4* (-/-) male white adipose tissue (gonadal fat) at 10 and 22 weeks of age on a normal diet, as well as 22 weeks of age on a high-fat diet. n=WT:3, KO:3 for each gene.

Acyl coA synthetase converts fatty acids to acyl coA for beta-oxidation. The expression of this gene is similar at 10 weeks of age in WT and KO adipose, and on a high-fat diet acyl coA synthetase is repressed to a similar level in both WT and KO adipose. Interestingly, at 22 weeks of age on a normal diet, acyl coA synthetase is 5-fold higher in the *Fmo1, 2, 4* (-/-) male adipose than the WT.

PPARγ-co-activator-1α (PGC1α) appears to be expressed over 100 times more in the KO male adipose compared to the WT at 10 weeks of age and also at 22 weeks of age on a high-fat diet. However the relative expression levels of PGC1α are very low in both WT and KO, so the emphasis that can placed on this result is unclear.

Caution should be taken in attaching too much weight to gene expression values where the relative expression is very small. Hence the changes stated above which are most interesting are those related to the adipocyte fatty acid binding protein (FABP4) and acyl coA synthetase (ACS).

FABP4 is a target gene of PPARγ whereby activators of PPARγ lead to up-regulation of FABP4 (Rival et al., 2004). Adipocytes from FABP4 (-/-) mice show a reduction in lipolysis and increased cellular fatty acid levels (Coe et al., 1999). Fatty acid binding proteins are involved in the trafficking of lipid mediators (Hertzel and Bernlohr, 2000), although the precise role of FABP4 is unknown. A study where FABP4 expression levels were measured semi-quantitavely in obese and lean individuals suggested a greater expression of FABP4 in the lean (Fisher et al., 2001). This is interesting when considering the lean *Fmo1, 2, 4* (-/-) male mice. However it has also been up-regulated in patients with 'metabolic syndrome' (a collection of disorders that increase the risk of cardiovascular disease and diabetes) and is secreted during adipogenesis (Cabre et al., 2007).

FABP4 is also known to associate with hormone sensitive lipase (HSL) (Shen et al., 2001; Smith et al., 2004a). HSL hydrolyses triacylglycerol to monoacylglycerol, which eventually becomes glycerol. Glycerol is then exported to the liver and other tissues for the production of glucose. Free fatty acids are esterified using the co-factor acyl CoA to form triacylglycerol. *Acyl CoA synthetase* is up-regulated in the *Fmo1, 2, 4* (-/-) males, clearly the production of triacylglycerol can have two outcomes, storage or mobilisation to form energy via β-oxidation. Since the fat is not being stored in the *Fmo1, 2, 4* (-/-) male adipose, it is probably being used for energy. Whether β-oxidation is up-regulated in *Fmo1, 2, 4* (-/-) male adipose is currently being investigated.

The expression of all five FMOs has been examined in white adipose in WT male mice, something which has not been investigated before. *Fmo1* is highly expressed at 10 weeks of age and is expressed 3-fold lower at 22-weeks of age. It is expressed 3-fold lower at 22 weeks of age on a high-fat diet than at 22 weeks on a normal diet. *Fmo3* shows the same pattern but to a much lower extent, the 10 week expression of *Fmo3* is 7-fold lower than the *Fmo1* expression at the same age. *Fmo5* is not expressed at all at 10 or 22 weeks of age on a normal diet, but interestingly seems to be up-regulated on a high-fat diet. There is no expression of *Fmo2* and *Fmo4* at all in white adipose.

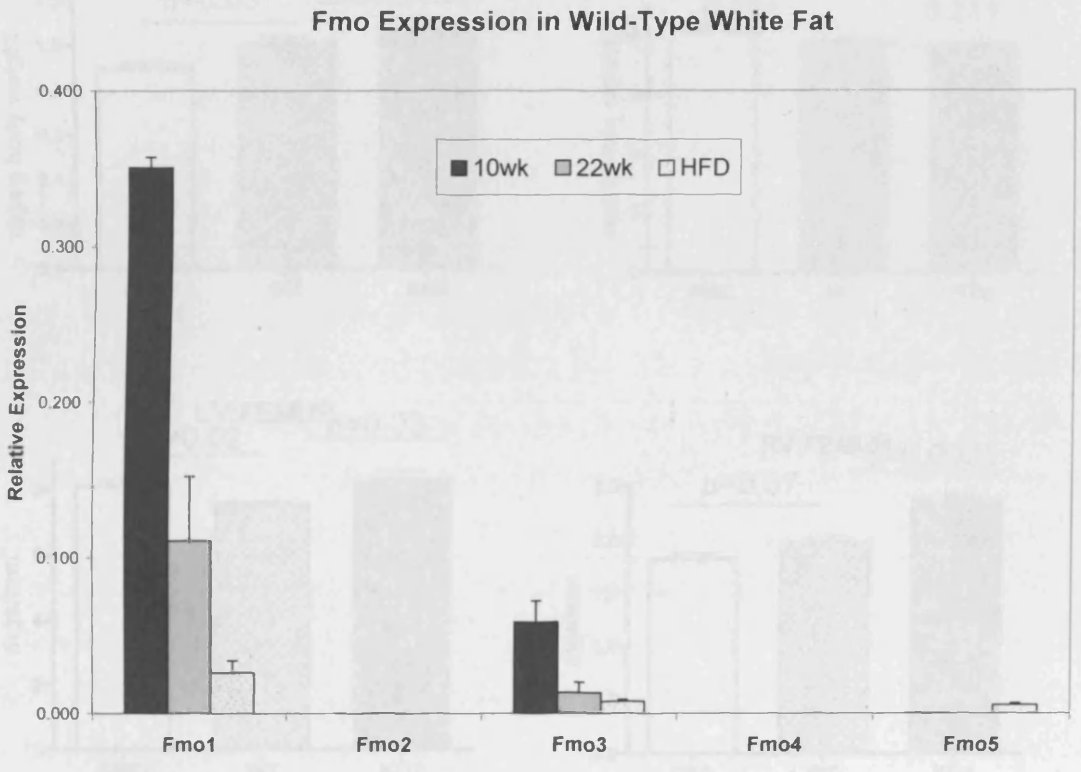

5.21.2 The expression of Fmos in WT male adipose

The expression of *Fmos* was analysed using real-time RT-PCR in WT male adipose at 10 and 22 weeks of age on a normal diet, and at 22 weeks of age on a high-fat diet.

In a series of preliminary experiments the ventricles of the *Fmo1, 2, 4* (-/-) and *Fmo5* (-/-) and WT male hearts have been analysed. When normalised to bodyweight there is a slight reduction in right ventricle weight in the *Fmo1, 2, 4* (-/-) males compared to the WT males. The *Fmo5* (-/-) male right and left ventricles weight is very similar to the WT. When the ventricles are normalised to femur length the left ventricle weights in both *Fmo1, 2, 4* (-/-) and *Fmo5* (-/-) mice are heavier than the WT male ventricles. The right ventricle in the *Fmo5* (-/-) hearts are heavier than the WT, whilst in the *Fmo1, 2, 4* (-/-) males, the right ventricles are a similar weight to the WT. This is an interesting development which requires further study.

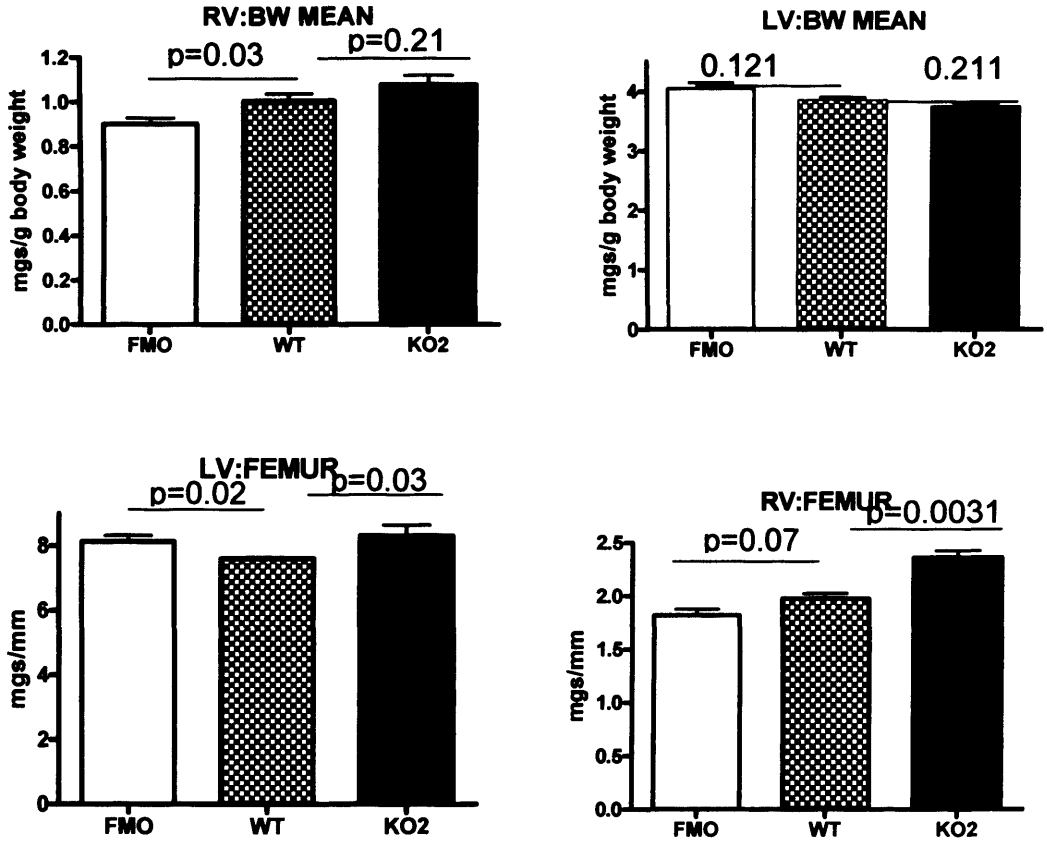

5.21.3 Ventricle weights vs bodyweight or femur length

The ventricles of 10 week old *Fmo1, 2, 4* (-/-), *Fmo5* (-/-) and WT males were measured and normalised to bodyweight or femur length. Where 'FMO' is *Fmo1, 2, 4* (-/-) mice and KO2 is *Fmo5* (-/-) mice.

5.22 Conclusions

Studying the removal of FMOs from mice has thrown up some interesting and unexpected results, made all the more intriguing for the similarities and differences in the response by the separate KO models. What also confuses the issue is the apparent gender-specific effects. Clearly these results could be considered the tip of the iceberg, as a lot more work needs to be undertaken to really understand the, what appears to be, fundamental role in energy homeostasis of FMOs. In the following paragraphs I will set out two possible explanations for these effects in an attempt to clarify our observations.

It has long been speculated that FMOs have a role in the production of reactive oxygen species (ROS). It has been shown that as FAD-OOH in the FMO catalytic cycle breaks down, superoxide anions and hydrogen peroxide are released (Rauckman et al., 1979). Additionally purified porcine liver FMO1 produced superoxide anions at a rate of about 4% of the oxidised NADPH, and FMO2 (purified from rabbit lung) released H_2O_2 from, at most, 40% of the total NADPH oxidised (Tynes et al., 1986). It has thus been surmised that FMOs may have a role in the regulation of redox potential within a cell. This has not been fully investigated so far, but recently the only yeast FMO (yFMO) has been shown to regulate the thiol:disulfide ratio by oxidising glutathione (Suh et al., 1999). The expression levels of yFMO and its activity are modulated by changes in the redox state of the cell (Suh et al., 2000) therefore substantiating a possible role for yFMO in redox regulation and also perhaps other FMOs. We could conclude that the removal of FMO1, 2 and 4 has somehow disrupted the redox status of the cells (hepatocytes and/or adipocytes) causing a disruption in lipid homeostasis. *Fmo1* is up-regulated in the glycerol kinase KO in brown adipose (Rahib et al., 2007). Glycerol kinase catalyses the transfer of phosphate from ATP to glycerol. Adipocytes do not have this enzyme so they cannot metabolise glycerol produced from the breakdown of triacylglycerol. Instead glycerol travels to the liver to be used in glycolysis or gluconeogenesis. The up-regulation of FMO1 in the glycerol kinase KO further points to an association to energy homeostasis.

There are a limited number of known endogenous substrates for FMOs, this is not to say that there are not more. Lipoic acid is one of the known endogenous substrates for porcine FMO1 (Taylor and Ziegler, 1987). It has been shown to reduce weight and increase energy expenditure in rats (Kim et al., 2004). This was the reason for using this substrate as a

basis for part of this research, to see if without certain FMOs, the *Fmo1, 2, 4* (-/-) mice would lose more weight than the WT mice. This was not the case. Although subsequent increases in plasma iron concentrations are intriguing and require further research. It is feasible that there could be another unknown endogenous substrate that goes un-metabolised when FMO1, 2 and 4 are knocked-out. This possibility also has to be further investigated and is no doubt no easy task, as nearly 50 years of research has not thrown up many candidates.

The role for FMO5 remains elusive. FMO5 mRNA levels are similar or higher than FMO3 or FMO1 levels in human and mouse liver respectively. Its degree of expression implies that it has a fundamental role in the liver, if not an endogenous role, than a distinct xenobiotic metabolism role. We need to learn more about the substrate specificity of FMO5 to further our knowledge of its role.

There is a pattern of lower lipid levels in the *Fmo5* (-/-) mice, distinctly lower HDL-cholesterol. Low concentrations of bile salts such as cholate have been shown to induce expression of FMO in mouse and rat liver (Dixit and Roche, 1984; Pettit et al., 1964), but repress it in rabbit (Williams et al., 1985) and pig (Gorrod et al., 1975) liver. Interestingly cholic acid reduces HDL-cholesterol in mice, and this effect is even more pronounced in PXR-null mice (Masson et al., 2005), PXR is known to have a role in bile acid regulation (Handschin and Meyer, 2005). It would be interesting if the reduction of HDL-cholesterol in *Fmo5* (-/-) mice was in any way related to an increased level of cholic acid, perhaps because FMO5 is not there to metabolise it. This would tie in very well with the apparent regulation of FMO5 by PXR and is certainly worth further study.

References

Adesnik M, Bar-Nun S, Maschio F, Zunich M, Lippman A and Bard E (1981) Mechanism of induction of cytochrome P-450 by phenobarbital. *J Biol Chem* 256(20):10340-10345.

Aiken J, Cima L, Schloo B, Mooney D, Johnson L, Langer R and Vacanti JP (1990) Studies in rat liver perfusion for optimal harvest of hepatocytes. *J Pediatr Surg* 25(1):140-144; discussion 144-145.

An J, Ribeiro RC, Webb P, Gustafsson JA, Kushner PJ, Baxter JD and Leitman DC (1999) Estradiol repression of tumor necrosis factor-alpha transcription requires estrogen receptor activation function-2 and is enhanced by coactivators. *Proc Natl Acad Sci U S A* 96(26):15161-15166.

Andersen ML and Tufik S (2006) Does male sexual behavior require progesterone? *Brain Res Rev* 51(1):136-143.

Angel A and Farkas J (1974) Regulation of cholesterol storage in adipose tissue. *J Lipid Res* 15(5):491-499.

Applegate LA, Luscher P and Tyrrell RM (1991) Induction of heme oxygenase: a general response to oxidant stress in cultured mammalian cells. *Cancer Res* 51(3):974-978.

Armanini D, Nacamulli D, Francini-Pesenti F, Battagin G, Ragazzi E and Fiore C (2005) Glycyrrhetinic acid, the active principle of licorice, can reduce the thickness of subcutaneous thigh fat through topical application. *Steroids* 70(8):538-542.

Asai Y, Yamada K, Watanabe T, Keng VW and Noguchi T (2003) Insulin stimulates expression of the pyruvate kinase M gene in 3T3-L1 adipocytes. *Biosci Biotechnol Biochem* 67(6):1272-1277.

Atta-Asafo-Adjei E, Lawton MP and Philpot RM (1993) Cloning, sequencing, distribution, and expression in Escherichia coli of flavin-containing monooxygenase 1C1. Evidence for a third gene subfamily in rabbits. *J Biol Chem* 268(13):9681-9689.

Baes M, Gulick T, Choi HS, Martinoli MG, Simha D and Moore DD (1994) A new orphan member of the nuclear hormone receptor superfamily that interacts with a subset of retinoic acid response elements. *Mol Cell Biol* 14(3):1544-1552.

Bahjat FR, Dharnidharka VR, Fukuzuka K, Morel L, Crawford JM, Clare-Salzler MJ and Moldawer LL (2000) Reduced susceptibility of nonobese diabetic mice to TNF-alpha and D-galactosamine-mediated hepatocellular apoptosis and lethality. *J Immunol* 165(11):6559-6567.

Bajt ML, Knight TR, Lemasters JJ and Jaeschke H (2004) Acetaminophen-induced oxidant stress and cell injury in cultured mouse hepatocytes: protection by N-acetyl cysteine. *Toxicol Sci* 80(2):343-349.

Barber M, Conrad ME, Umbreit JN, Barton JC and Moore EG (2000) Abnormalities of flavin monooxygenase as an etiology for sideroblastic anemia. *Am J Hematol* 65(2):149-153.

Baron J, Redick JA and Guengerich FP (1981) An immunohistochemical study on the localization and distributions of phenobarbital- and 3-methylcholanthrene-inducible cytochromes P-450 within the livers of untreated rats. *J Biol Chem* 256(11):5931-5937.

Bars RG, Bell DR, Elcombe CR, Oinonen T, Jalava T and Lindros KO (1992) Zone-specific inducibility of cytochrome P450 2B1/2 is retained in isolated perivenous hepatocytes. *Biochem J* 282 (Pt 3):635-638.

Barton JC, Conrad ME and Parmley RT (1983) Calcium inhibition of inorganic iron absorption in rats. *Gastroenterology* 84(1):90-101.

Barwick JL, Quattrochi LC, Mills AS, Potenza C, Tukey RH and Guzelian PS (1996) Trans-species gene transfer for analysis of glucocorticoid-inducible transcriptional activation of transiently expressed human CYP3A4 and rabbit CYP3A6 in primary cultures of adult rat and rabbit hepatocytes. *Mol Pharmacol* 50(1):10-16.

Battle MA, Konopka G, Parviz F, Gaggl AL, Yang C, Sladek FM and Duncan SA (2006) Hepatocyte nuclear factor 4alpha orchestrates expression of cell adhesion proteins during the epithelial transformation of the developing liver. *Proc Natl Acad Sci U S A* 103(22):8419-8424.

Bedo G, Vargas M, Ferreiro MJ, Chalar C and Agrati D (2005) Characterization of hypoxia induced gene 1: expression during rat central nervous system maturation and evidence of antisense RNA expression. *Int J Dev Biol* 49(4):431-436.

Benevenga NJ (1974) Toxicities of methionine and other amino acids. *J Agric Food Chem* 22(1):2-9.

Bengtsson G, Julkunen A, Penttila KE and Lindros KO (1987) Effect of phenobarbital on the distribution of drug metabolizing enzymes between periportal and perivenous rat hepatocytes prepared by digitonin-collagenase liver perfusion. *J Pharmacol Exp Ther* 240(2):663-667.

Bieche I, Lerebours F, Tozlu S, Espie M, Marty M and Lidereau R (2004) Molecular profiling of inflammatory breast cancer: identification of a poor-prognosis gene expression signature. *Clin Cancer Res* 10(20):6789-6795.

Bjorntorp P (1997) Body fat distribution, insulin resistance, and metabolic diseases. *Nutrition* 13(9):795-803.

Borbas T, Benko B, Dalmadi B, Szabo I and Tihanyi K (2006) Insulin in flavin-containing monooxygenase regulation. Flavin-containing monooxygenase and cytochrome P450 activities in experimental diabetes. *Eur J Pharm Sci* 28(1-2):51-58.

Bray BJ, Perry NB, Menkes DB and Rosengren RJ (2002) St. John's wort extract induces CYP3A and CYP2E1 in the Swiss Webster mouse. *Toxicol Sci* 66(1):27-33.

Brodfuehrer JI and Zannoni VG (1987) Modulation of the flavin-containing monooxygenase in guinea pigs by ascorbic acid and food restriction. *J Nutr* 117(2):286-290.

Bryzgalova G, Gao H, Ahren B, Zierath JR, Galuska D, Steiler TL, Dahlman-Wright K, Nilsson S, Gustafsson JA, Efendic S and Khan A (2006) Evidence that oestrogen receptor-alpha plays an important role in the regulation of glucose homeostasis in mice: insulin sensitivity in the liver. *Diabetologia* 49(3):588-597.

Buhler R, Lindros KO, Nordling A, Johansson I and Ingelman-Sundberg M (1992) Zonation of cytochrome P450 isozyme expression and induction in rat liver. *Eur J Biochem* 204(1):407-412.

Burgos-Trinidad M, Youngblood GL, Maroto MR, Scheller A, Robins DM and Payne AH (1997) Repression of cAMP-induced expression of the mouse P450 17 alpha-hydroxylase/C17-20 lyase gene (Cyp17) by androgens. *Mol Endocrinol* 11(1):87-96.

Bustamante J, Lodge JK, Marcocci L, Tritschler HJ, Packer L and Rihn BH (1998) Alpha-lipoic acid in liver metabolism and disease. *Free Radic Biol Med* 24(6):1023-1039.

Butler AM and Murray M (1997) Biotransformation of parathion in human liver: participation of CYP3A4 and its inactivation during microsomal parathion oxidation. *J Pharmacol Exp Ther* 280(2):966-973.

Cabre A, Lazaro I, Girona J, Manzanares JM, Marimon F, Plana N, Heras M and Masana L (2007) Fatty acid binding protein 4 is increased in metabolic syndrome and with thiazolidinedione treatment in diabetic patients. *Atherosclerosis* 195(1):e150-158.

Cancado EL, Leitao RM, Carrilho FJ and Laudanna AA (1998) Unexpected clinical remission of cholestasis after rifampicin therapy in patients with normal or slightly increased levels of gamma-glutamyl transpeptidase. *Am J Gastroenterol* 93(9):1510-1517.

Carter ME, Gulick T, Raisher BD, Caira T, Ladias JA, Moore DD and Kelly DP (1993) Hepatocyte nuclear factor-4 activates medium chain acyl-CoA dehydrogenase gene transcription by interacting with a complex regulatory element. *J Biol Chem* 268(19):13805-13810.

Casabiell X, Pineiro V, Peino R, Lage M, Camina J, Gallego R, Vallejo LG, Dieguez C and Casanueva FF (1998) Gender differences in both spontaneous and stimulated leptin secretion by human omental adipose tissue in vitro: dexamethasone and estradiol stimulate leptin release in women, but not in men. *J Clin Endocrinol Metab* 83(6):2149-2155.

Cashman JR (2003) The role of flavin-containing monooxygenases in drug metabolism and development. *Curr Opin Drug Discov Devel* 6(4):486-493.

Cashman JR, Park SB, Berkman CE and Cashman LE (1995) Role of hepatic flavin-containing monooxygenase 3 in drug and chemical metabolism in adult humans. *Chem Biol Interact* 96(1):33-46.

Chanden P (2004).

Chatterjee SS, Bhattacharya SK, Wonnemann M, Singer A and Muller WE (1998) Hyperforin as a possible antidepressant component of hypericum extracts. *Life Sci* 63(6):499-510.

Chen B, Nelson DM and Sadovsky Y (2006) N-myc down-regulated gene 1 modulates the response of term human trophoblasts to hypoxic injury. *J Biol Chem* 281(5):2764-2772.

Chen H, Fantel AG and Juchau MR (2000) Catalysis of the 4-hydroxylation of retinoic acids by cyp3a7 in human fetal hepatic tissues. *Drug Metab Dispos* 28(9):1051-1057.

Chen Y, Kissling G, Negishi M and Goldstein JA (2005) The nuclear receptors constitutive androstane receptor and pregnane X receptor cross-talk with hepatic nuclear factor 4alpha to synergistically activate the human CYP2C9 promoter. *J Pharmacol Exp Ther* 314(3):1125-1133.

Cheng PY, Lee YM, Shih NL, Chen YC and Yen MH (2006) Heme oxygenase-1 contributes to the cytoprotection of alpha-lipoic acid via activation of p44/42 mitogen-activated protein kinase in vascular smooth muscle cells. *Free Radic Biol Med* 40(8):1313-1322.

Cherrington NJ, Cao Y, Cherrington JW, Rose RL and Hodgson E (1998) Physiological factors affecting protein expression of flavin-containing monooxygenases 1, 3 and 5. *Xenobiotica* 28(7):673-682.

Chung WG, Park CS, Roh HK and Cha YN (1997) Induction of flavin-containing monooxygenase (FMO1) by a polycyclic aromatic hydrocarbon, 3-methylcholanthrene, in rat liver. *Mol Cells* 7(6):738-741.

Chung WG, Park CS, Roh HK, Lee WK and Cha YN (2000) Oxidation of ranitidine by isozymes of flavin-containing monooxygenase and cytochrome P450. *Jpn J Pharmacol* 84(2):213-220.

Clegg DJ, Riedy CA, Smith KA, Benoit SC and Woods SC (2003) Differential sensitivity to central leptin and insulin in male and female rats. *Diabetes* 52(3):682-687.

Clement B, Grimaud JA, Campion JP, Deugnier Y and Guillouzo A (1986) Cell types involved in collagen and fibronectin production in normal and fibrotic human liver. *Hepatology* 6(2):225-234.

Coe NR, Simpson MA and Bernlohr DA (1999) Targeted disruption of the adipocyte lipid-binding protein (aP2 protein) gene impairs fat cell lipolysis and increases cellular fatty acid levels. *J Lipid Res* 40(5):967-972.

Coecke S, Debast G, Phillips IR, Vercruysse A, Shephard EA and Rogiers V (1998) Hormonal regulation of microsomal flavin-containing monooxygenase activity by sex steroids and growth hormone in co-cultured adult male rat hepatocytes. *Biochem Pharmacol* 56(8):1047-1051.

Combalbert J, Fabre I, Fabre G, Dalet I, Derancourt J, Cano JP and Maurel P (1989) Metabolism of cyclosporin A. IV. Purification and identification of the rifampicin-inducible human liver cytochrome P-450 (cyclosporin A oxidase) as a product of P450IIIA gene subfamily. *Drug Metab Dispos* 17(2):197-207.

Conney AH, Davison C, Gastel R and Burns JJ (1960) Adaptive increases in drug-metabolizing enzymes induced by phenobarbital and other drugs. *J Pharmacol Exp Ther* 130:1-8.

Conrad ME (1993) Excess iron and catastrophic illness. *Am J Hematol* 43(3):234-236.

Conrad ME and Umbreit JN (1993) A concise review: iron absorption--the mucin-mobilferrin-integrin pathway. A competitive pathway for metal absorption. *Am J Hematol* 42(1):67-73.

Conrad ME, Umbreit JN, Moore EG, Peterson RD and Jones MB (1990) A newly identified iron binding protein in duodenal mucosa of rats. Purification and characterization of mobilferrin. *J Biol Chem* 265(9):5273-5279.

Culling CF, Reid PE, Clay MG and Dunn WL (1974) The histochemical demonstration of O-acylated sialic acid in gastrointestinal mucins. Their association with the potassium hydroxide-periodic acid-schiff effect. *J Histochem Cytochem* 22(8):826-831.

Dabrosin C (2005) Increased extracellular local levels of estradiol in normal breast in vivo during the luteal phase of the menstrual cycle. *J Endocrinol* 187(1):103-108.

Dannan GA, Guengerich FP and Waxman DJ (1986) Hormonal regulation of rat liver microsomal enzymes. Role of gonadal steroids in programming, maintenance, and suppression of delta 4-steroid 5 alpha-reductase, flavin-containing monooxygenase, and sex-specific cytochromes P-450. *J Biol Chem* 261(23):10728-10735.

Das ML and Ziegler DM (1970) Rat liver oxidative N-dealkylase and N-oxidase activities as a function of animal age. *Arch Biochem Biophys* 140(1):300-306.

de Groot G, Koops R, Hogendoorn EA, Goewie CE, Savelkoul TJ and van Vloten P (1988) Improvement of selectivity and sensitivity by column switching in the determination of glycyrrhizin and glycyrrhetic acid in human plasma by high-performance liquid chromatography. *J Chromatogr* 456(1):71-81.

Dentin R, Benhamed F, Hainault I, Fauveau V, Foufelle F, Dyck JR, Girard J and Postic C (2006) Liver-specific inhibition of ChREBP improves hepatic steatosis and insulin resistance in ob/ob mice. *Diabetes* 55(8):2159-2170.

Despres JP (1998) The insulin resistance-dyslipidemic syndrome of visceral obesity: effect on patients' risk. *Obes Res* 6 Suppl 1:8S-17S.

Despres JP, Lamarche B, Mauriege P, Cantin B, Dagenais GR, Moorjani S and Lupien PJ (1996) Hyperinsulinemia as an independent risk factor for ischemic heart disease. *N Engl J Med* 334(15):952-957.

Devereux TR and Fouts JR (1975) Effect of pregnancy or treatment with cetain steroids on N,N-dimethylaniline demethylation and N-oxidation by rabbit liver or lung microsomes. *Drug Metab Dispos* 3(4):254-258.

Diehl AM, Michaelson P and Yang SQ (1994) Selective induction of CCAAT/enhancer binding protein isoforms occurs during rat liver development. *Gastroenterology* 106(6):1625-1637.

Diesel B, Kulhanek-Heinze S, Holtje M, Brandt B, Holtje HD, Vollmar AM and Kiemer AK (2007) Alpha-lipoic acid as a directly binding activator of the insulin receptor: protection from hepatocyte apoptosis. *Biochemistry* 46(8):2146-2155.

Dixit A and Roche TE (1984) Spectrophotometric assay of the flavin-containing monooxygenase and changes in its activity in female mouse liver with nutritional and diurnal conditions. *Arch Biochem Biophys* 233(1):50-63.

Dolphin C, Shephard EA, Povey S, Palmer CN, Ziegler DM, Ayesh R, Smith RL and Phillips IR (1991) Cloning, primary sequence, and chromosomal mapping of a human flavin-containing monooxygenase (FMO1). *J Biol Chem* 266(19):12379-12385.

Dolphin CT, Beckett DJ, Janmohamed A, Cullingford TE, Smith RL, Shephard EA and Phillips IR (1998) The flavin-containing monooxygenase 2 gene (FMO2) of humans, but not of other primates, encodes a truncated, nonfunctional protein. *J Biol Chem* 273(46):30599-30607.

Dolphin CT, Cullingford TE, Shephard EA, Smith RL and Phillips IR (1996) Differential developmental and tissue-specific regulation of expression of the genes encoding three members of the flavin-containing monooxygenase family of man, FMO1, FMO3 and FM04. *Eur J Biochem* 235(3):683-689.

Dolphin CT, Janmohamed A, Smith RL, Shephard EA and Phillips IR (1997) Missense mutation in flavin-containing mono-oxygenase 3 gene, FMO3, underlies fish-odour syndrome. *Nat Genet* 17(4):491-494.

Donaldson RP and Luster DG (1991) Multiple Forms of Plant Cytochromes P-450. *Plant Physiol* 96(3):669-674.

Duescher RJ, Lawton MP, Philpot RM and Elfarra AA (1994) Flavin-containing monooxygenase (FMO)-dependent metabolism of methionine and evidence for FMO3 being the major FMO involved in methionine sulfoxidation in rabbit liver and kidney microsomes. *J Biol Chem* 269(26):17525-17530.

Duffel MW, Graham JM and Ziegler DM (1981) Changes in dimethylaniline N-oxidase activity of mouse liver and kidney induced by steroid sex hormones. *Mol Pharmacol* 19(1):134-139.

Durr D, Stieger B, Kullak-Ublick GA, Rentsch KM, Steinert HC, Meier PJ and Fattinger K (2000) St John's Wort induces intestinal P-glycoprotein/MDR1 and intestinal and hepatic CYP3A4. *Clin Pharmacol Ther* 68(6):598-604.

Dyer KD and Rosenberg HF (2005) The mouse RNase 4 and RNase 5/ang 1 locus utilizes dual promoters for tissue-specific expression. *Nucleic Acids Res* 33(3):1077-1086.

Epstein AC, Gleadle JM, McNeill LA, Hewitson KS, O'Rourke J, Mole DR, Mukherji M, Metzen E, Wilson MI, Dhanda A, Tian YM, Masson N, Hamilton DL, Jaakkola P, Barstead R, Hodgkin J, Maxwell PH, Pugh CW, Schofield CJ and Ratcliffe PJ (2001) C. elegans EGL-9 and mammalian homologs define a family of dioxygenases that regulate HIF by prolyl hydroxylation. *Cell* 107(1):43-54.

Falls JG, Blake BL, Cao Y, Levi PE and Hodgson E (1995) Gender differences in hepatic expression of flavin-containing monooxygenase isoforms (FMO1, FMO3, and FMO5) in mice. *J Biochem Toxicol* 10(3):171-177.

Falls JG, Ryu DY, Cao Y, Levi PE and Hodgson E (1997) Regulation of mouse liver flavin-containing monooxygenases 1 and 3 by sex steroids. *Arch Biochem Biophys* 342(2):212-223.

Ferris CD, Jaffrey SR, Sawa A, Takahashi M, Brady SD, Barrow RK, Tysoe SA, Wolosker H, Baranano DE, Dore S, Poss KD and Snyder SH (1999) Haem oxygenase-1 prevents cell death by regulating cellular iron. *Nat Cell Biol* 1(3):152-157.

Fisher RM, Eriksson P, Hoffstedt J, Hotamisligil GS, Thorne A, Ryden M, Hamsten A and Arner P (2001) Fatty acid binding protein expression in different adipose tissue depots from lean and obese individuals. *Diabetologia* 44(10):1268-1273.

Fleischer A and Rebollo A (2004) Induction of p53-independent apoptosis by the BH3-only protein ITM2Bs. *FEBS Lett* 557(1-3):283-287.

Flodby P, Barlow C, Kylefjord H, Ahrlund-Richter L and Xanthopoulos KG (1996) Increased hepatic cell proliferation and lung abnormalities in mice deficient in CCAAT/enhancer binding protein alpha. *J Biol Chem* 271(40):24753-24760.

Furnes B, Feng J, Sommer SS and Schlenk D (2003) Identification of novel variants of the flavin-containing monooxygenase gene family in African Americans. *Drug Metab Dispos* 31(2):187-193.

Gao H, Bryzgalova G, Hedman E, Khan A, Efendic S, Gustafsson JA and Dahlman-Wright K (2006) Long-term administration of estradiol decreases expression of hepatic lipogenic genes and improves insulin sensitivity in ob/ob mice: a possible mechanism is through direct regulation of signal transducer and activator of transcription 3. *Mol Endocrinol* 20(6):1287-1299.

Gao Y, Jiang HC, Xu J, Pan SH and Li YD (2005) Microencapsulating hepatocytes. *Transplant Proc* 37(10):4589-4593.

Gasser R, Tynes RE, Lawton MP, Korsmeyer KK, Ziegler DM and Philpot RM (1990) The flavin-containing monooxygenase expressed in pig liver: primary sequence, distribution, and evidence for a single gene. *Biochemistry* 29(1):119-124.

Gaullier JM, Halse J, Hoivik HO, Hoye K, Syvertsen C, Nurminiemi M, Hassfeld C, Einerhand A, O'Shea M and Gudmundsen O (2007) Six months supplementation with conjugated linoleic acid induces regional-specific fat mass decreases in overweight and obese. *Br J Nutr* 97(3):550-560.

Gerbal-Chaloin S, Daujat M, Pascussi JM, Pichard-Garcia L, Vilarem MJ and Maurel P (2002) Transcriptional regulation of CYP2C9 gene. Role of glucocorticoid receptor and constitutive androstane receptor. *J Biol Chem* 277(1):209-217.

Ghosh AK, Lacson R, Liu P, Cichy SB, Danilkovich A, Guo S and Unterman TG (2001) A nucleoprotein complex containing CCAAT/enhancer-binding protein beta interacts with an insulin response sequence in the insulin-like growth factor-binding protein-1 gene and contributes to insulin-regulated gene expression. *J Biol Chem* 276(11):8507-8515.

Gong P and Cederbaum AI (2006) Nrf2 is increased by CYP2E1 in rodent liver and HepG2 cells and protects against oxidative stress caused by CYP2E1. *Hepatology* 43(1):144-153.

Gooding PE, Chayen J, Sawyer B and Slater TF (1978) Cytochrome P-450 distribution in rat liver and the effect of sodium phenobarbitone administration. *Chem Biol Interact* 20(3):299-310.

Goodwin B, Gauthier KC, Umetani M, Watson MA, Lochansky MI, Collins JL, Leitersdorf E, Mangelsdorf DJ, Kliewer SA and Repa JJ (2003) Identification of bile acid precursors as endogenous ligands for the nuclear xenobiotic pregnane X receptor. *Proc Natl Acad Sci U S A* 100(1):223-228.

Goodwin B, Hodgson E, D'Costa DJ, Robertson GR and Liddle C (2002) Transcriptional regulation of the human CYP3A4 gene by the constitutive androstane receptor. *Mol Pharmacol* 62(2):359-365.

Goodwin B, Moore LB, Stoltz CM, McKee DD and Kliewer SA (2001) Regulation of the human CYP2B6 gene by the nuclear pregnane X receptor. *Mol Pharmacol* 60(3):427-431.

Gorrod JW, Temple DJ and Beckett AH (1975) The differentiation of N-oxidation and N-dealkylation of N-ethyl-N-methylaniline by rabbit liver microsomes as distinct metabolic routes. *Xenobiotica* 5(8):465-474.

Gorski JC, Vannaprasaht S, Hamman MA, Ambrosius WT, Bruce MA, Haehner-Daniels B and Hall SD (2003) The effect of age, sex, and rifampin administration on intestinal and hepatic cytochrome P450 3A activity. *Clin Pharmacol Ther* 74(3):275-287.

Graham JD, Roman SD, McGowan E, Sutherland RL and Clarke CL (1995) Preferential stimulation of human progesterone receptor B expression by estrogen in T-47D human breast cancer cells. *J Biol Chem* 270(51):30693-30700.

Guan SH, Falick AM, Williams DE and Cashman JR (1991) Evidence for complex formation between rabbit lung flavin-containing monooxygenase and calreticulin. *Biochemistry* 30(41):9892-9900.

Guerra-Araiza C and Camacho-Arroyo I (2000) [Progesterone receptor isoforms: function and regulation]. *Rev Invest Clin* 52(6):686-691.

Guerra-Araiza C, Cerbon MA, Morimoto S and Camacho-Arroyo I (2000) Progesterone receptor isoforms expression pattern in the rat brain during the estrous cycle. *Life Sci* 66(18):1743-1752.

Guerra-Araiza C, Reyna-Neyra A, Salazar AM, Cerbon MA, Morimoto S and Camacho-Arroyo I (2001) Progesterone receptor isoforms expression in the prepuberal and adult male rat brain. *Brain Res Bull* 54(1):13-17.

Guguen-Guillouzo C and Guillouzo A (1983) Modulation of functional activities in cultured rat hepatocytes. *Mol Cell Biochem* 53-54(1-2):35-56.

Halkier BA and Gershenzon J (2006) Biology and biochemistry of glucosinolates. *Annu Rev Plant Biol* 57:303-333.

Hall PM, Stupans I, Burgess W, Birkett DJ and McManus ME (1989) Immunohistochemical localization of NADPH-cytochrome P450 reductase in human tissues. *Carcinogenesis* 10(3):521-530.

Hallberg L, Rossander-Hulten L, Brune M and Gleerup A (1992) Calcium and iron absorption: mechanism of action and nutritional importance. *Eur J Clin Nutr* 46(5):317-327.

Handschin C and Meyer UA (2005) Regulatory network of lipid-sensing nuclear receptors: roles for CAR, PXR, LXR, and FXR. *Arch Biochem Biophys* 433(2):387-396.

Hansen BG, Kliebenstein DJ and Halkier BA (2007) Identification of a flavin-monooxygenase as the S-oxygenating enzyme in aliphatic glucosinolate biosynthesis in Arabidopsis. *Plant J* 50(5):902-910.

Heemers H, Vanderhoydonc F, Roskams T, Shechter I, Heyns W, Verhoeven G and Swinnen JV (2003) Androgens stimulate coordinated lipogenic gene expression in normal target tissues in vivo. *Mol Cell Endocrinol* 205(1-2):21-31.

Heinsbroek RP, van Haaren F, Zantvoord F and van de Poll NE (1987) Effects of pentobarbital and progesterone on random ratio responding in male and female rats. *Psychopharmacology (Berl)* 93(2):178-181.

Hertzel AV and Bernlohr DA (2000) The mammalian fatty acid-binding protein multigene family: molecular and genetic insights into function. *Trends Endocrinol Metab* 11(5):175-180.

Hines RN and McCarver DG (2002) The ontogeny of human drug-metabolizing enzymes: phase I oxidative enzymes. *J Pharmacol Exp Ther* 300(2):355-360.

Hock TD, Nick HS and Agarwal A (2004) Upstream stimulatory factors, USF1 and USF2, bind to the human haem oxygenase-1 proximal promoter in vivo and regulate its transcription. *Biochem J* 383(Pt 2):209-218.

Honkakoski P, Sueyoshi T and Negishi M (2003) Drug-activated nuclear receptors CAR and PXR. *Ann Med* 35(3):172-182.

Honkakoski P, Zelko I, Sueyoshi T and Negishi M (1998) The nuclear orphan receptor CAR-retinoid X receptor heterodimer activates the phenobarbital-responsive enhancer module of the CYP2B gene. *Mol Cell Biol* 18(10):5652-5658.

Horigome H, Homma M, Hirano T and Oka K (2001) Glycyrrhetinic acid induced apoptosis in murine splenocytes. *Biol Pharm Bull* 24(1):54-58.

Hosea NA and Guengerich FP (1998) Oxidation of nonionic detergents by cytochrome P450 enzymes. *Arch Biochem Biophys* 353(2):365-373.

Hough TA, Nolan PM, Tsipouri V, Toye AA, Gray IC, Goldsworthy M, Moir L, Cox RD, Clements S, Glenister PH, Wood J, Selley RL, Strivens MA, Vizor L, McCormack SL, Peters J, Fisher EM, Spurr N, Rastan S, Martin JE, Brown SD and Hunter AJ (2002) Novel phenotypes identified by plasma biochemical screening in the mouse. *Mamm Genome* 13(10):595-602.

Hulst LK, Fleishaker JC, Peters GR, Harry JD, Wright DM and Ward P (1994) Effect of age and gender on tirilazad pharmacokinetics in humans. *Clin Pharmacol Ther* 55(4):378-384.

Inoue H, Ogawa W, Ozaki M, Haga S, Matsumoto M, Furukawa K, Hashimoto N, Kido Y, Mori T, Sakaue H, Teshigawara K, Jin S, Iguchi H, Hiramatsu R, LeRoith D, Takeda K, Akira S and Kasuga M (2004) Role of STAT-3 in regulation of hepatic gluconeogenic genes and carbohydrate metabolism in vivo. *Nat Med* 10(2):168-174.

Ishida M, Ohashi S, Kizaki Y, Naito J, Horiguchi K and Harigaya T (2007) Expression profiling of mouse placental lactogen II and its correlative genes using a cDNA microarray analysis in the developmental mouse placenta. *J Reprod Dev* 53(1):69-76.

Jackson D, Volpert OV, Bouck N and Linzer DI (1994) Stimulation and inhibition of angiogenesis by placental proliferin and proliferin-related protein. *Science* 266(5190):1581-1584.

Janmohamed A, Hernandez D, Phillips IR and Shephard EA (2004) Cell-, tissue-, sex- and developmental stage-specific expression of mouse flavin-containing monooxygenases (Fmos). *Biochem Pharmacol* 68(1):73-83.

Janz KF, Dawson JD and Mahoney LT (2000) Predicting heart growth during puberty: The Muscatine Study. *Pediatrics* 105(5):E63.

Jefferson DM, Clayton DF, Darnell JE, Jr. and Reid LM (1984) Posttranscriptional modulation of gene expression in cultured rat hepatocytes. *Mol Cell Biol* 4(9):1929-1934.

Jeitner TM and Lawrence DA (2001) Mechanisms for the cytotoxicity of cysteamine. *Toxicol Sci* 63(1):57-64.

Jones KC and Ballou DP (1986) Reactions of the 4a-hydroperoxide of liver microsomal flavin-containing monooxygenase with nucleophilic and electrophilic substrates. *J Biol Chem* 261(6):2553-2559.

Jones SA, Moore LB, Shenk JL, Wisely GB, Hamilton GA, McKee DD, Tomkinson NC, LeCluyse EL, Lambert MH, Willson TM, Kliewer SA and Moore JT (2000) The pregnane X receptor: a promiscuous xenobiotic receptor that has diverged during evolution. *Mol Endocrinol* 14(1):27-39.

Jung D, Mangelsdorf DJ and Meyer UA (2006) Pregnane X receptor is a target of farnesoid X receptor. *J Biol Chem* 281(28):19081-19091.

Jungermann K and Katz N (1982) Functional hepatocellular heterogeneity. *Hepatology* 2(3):385-395.

Kaderlik R, Weser, E., and Ziegler DM (1991) Selective loss of flavin-containing monooxygenase in rats on chemically defined diets. *Prog Pharmacol Clin Pharmacol* 8:95-103.

Kahan BD, Kramer WG, Wideman C, Flechner SM, Lorber MI and Van Buren CT (1986) Demographic factors affecting the pharmacokinetics of cyclosporine estimated by radioimmunoassay. *Transplantation* 41(4):459-464.

Kamiya A, Inoue Y and Gonzalez FJ (2003) Role of the hepatocyte nuclear factor 4alpha in control of the pregnane X receptor during fetal liver development. *Hepatology* 37(6):1375-1384.

Kato R, Takahashi A and Omori Y (1971) The mechanism of sex differences in the anesthetic action of progesterone in rats. *Eur J Pharmacol* 13(2):141-149.

Kennedy J (2005) Herb and supplement use in the US adult population. *Clin Ther* 27(11):1847-1858.

Kera Y, Sippel HW, Penttila KE and Lindros KO (1987) Acinar distribution of glutathione-dependent detoxifying enzymes. Low glutathione peroxidase activity in perivenous hepatocytes. *Biochem Pharmacol* 36(12):2003-2006.

Khomenko T, Deng X, Sandor Z, Tarnawski AS and Szabo S (2004) Cysteamine alters redox state, HIF-1alpha transcriptional interactions and reduces duodenal mucosal oxygenation: novel insight into the mechanisms of duodenal ulceration. *Biochem Biophys Res Commun* 317(1):121-127.

Kim MS, Park JY, Namkoong C, Jang PG, Ryu JW, Song HS, Yun JY, Namgoong IS, Ha J, Park IS, Lee IK, Viollet B, Youn JH, Lee HK and Lee KU (2004) Anti-obesity effects of alpha-lipoic acid mediated by suppression of hypothalamic AMP-activated protein kinase. *Nat Med* 10(7):727-733.

Kliewer SA, Moore JT, Wade L, Staudinger JL, Watson MA, Jones SA, McKee DD, Oliver BB, Willson TM, Zetterstrom RH, Perlmann T and Lehmann JM (1998) An orphan nuclear receptor activated by pregnanes defines a novel steroid signaling pathway. *Cell* 92(1):73-82.

Kloss MW, Rosen GM, Rauckman EJ and Padilla GM (1982) Androgenic suppression of mouse hepatic FAD-containing monooxygenase activity. *Life Sci* 31(10):1037-1042.

Kocarek TA, Schuetz EG and Guzelian PS (1990) Differentiated induction of cytochrome P450b/e and P450p mRNAs by dose of phenobarbital in primary cultures of adult rat hepatocytes. *Mol Pharmacol* 38(4):440-444.

Kocarek TA, Schuetz EG, Strom SC, Fisher RA and Guzelian PS (1995) Comparative analysis of cytochrome P4503A induction in primary cultures of rat, rabbit, and human hepatocytes. *Drug Metab Dispos* 23(3):415-421.

Koji T, Nakane PK, Murakoshi M, Watanabe K and Terayama H (1988) Cell density dependent morphological changes in adult rat hepatocytes during primary culture. *Cell Biochem Funct* 6(4):237-243.

Komori M, Nishio K, Kitada M, Shiramatsu K, Muroya K, Soma M, Nagashima K and Kamataki T (1990) Fetus-specific expression of a form of cytochrome P-450 in human livers. *Biochemistry* 29(18):4430-4433.

Koukouritaki SB, Simpson P, Yeung CK, Rettie AE and Hines RN (2002) Human hepatic flavin-containing monooxygenases 1 (FMO1) and 3 (FMO3) developmental expression. *Pediatr Res* 51(2):236-243.

Krause RJ, Lash LH and Elfarra AA (2003) Human kidney flavin-containing monooxygenases and their potential roles in cysteine s-conjugate metabolism and nephrotoxicity. *J Pharmacol Exp Ther* 304(1):185-191.

Krause RJ, Ripp SL, Sausen PJ, Overby LH, Philpot RM and Elfarra AA (1996) Characterization of the methionine S-oxidase activity of rat liver and kidney microsomes: immunochemical and kinetic evidence for FMO3 being the major catalyst. *Arch Biochem Biophys* 333(1):109-116.

Krueger SK, Martin SR, Yueh MF, Pereira CB and Williams DE (2002a) Identification of active flavin-containing monooxygenase isoform 2 in human lung and characterization of expressed protein. *Drug Metab Dispos* 30(1):34-41.

Krueger SK, Williams DE, Yueh MF, Martin SR, Hines RN, Raucy JL, Dolphin CT, Shephard EA and Phillips IR (2002b) Genetic polymorphisms of flavin-containing monooxygenase (FMO). *Drug Metab Rev* 34(3):523-532.

Krusekopf S and Roots I (2005) St. John's wort and its constituent hyperforin concordantly regulate expression of genes encoding enzymes involved in basic cellular pathways. *Pharmacogenet Genomics* 15(11):817-829.

Kusano H, Shimizu S, Koya RC, Fujita H, Kamada S, Kuzumaki N and Tsujimoto Y (2000) Human gelsolin prevents apoptosis by inhibiting apoptotic mitochondrial changes via closing VDAC. *Oncogene* 19(42):4807-4814.

Kyprianou N and Isaacs JT (1989) Expression of transforming growth factor-beta in the rat ventral prostate during castration-induced programmed cell death. *Mol Endocrinol* 3(10):1515-1522.

Lang DH and Rettie AE (2000) In vitro evaluation of potential in vivo probes for human flavin-containing monooxygenase (FMO): metabolism of benzydamine and caffeine by FMO and P450 isoforms. *Br J Clin Pharmacol* 50(4):311-314.

Lang DH, Yeung CK, Peter RM, Ibarra C, Gasser R, Itagaki K, Philpot RM and Rettie AE (1998) Isoform specificity of trimethylamine N-oxygenation by human flavin-containing monooxygenase (FMO) and P450 enzymes: selective catalysis by FMO3. *Biochem Pharmacol* 56(8):1005-1012.

Larsen-Su S and Williams DE (1996) Dietary indole-3-carbinol inhibits FMO activity and the expression of flavin-containing monooxygenase form 1 in rat liver and intestine. *Drug Metab Dispos* 24(9):927-931.

Larsen-Su SA, Krueger SK, Yueh MF, Pereira CB and Williams DE (2002) Developmental regulation of flavin-containing monooxygenase form 1 in the liver and kidney of fetal and neonatal rabbits. *Biochem Pharmacol* 63(7):1353-1359.

Lattard V, Lachuer J, Buronfosse T, Garnier F and Benoit E (2002) Physiological factors affecting the expression of FMO1 and FMO3 in the rat liver and kidney. *Biochem Pharmacol* 63(8):1453-1464.

Lawton MP, Gasser R, Tynes RE, Hodgson E and Philpot RM (1990) The flavin-containing monooxygenase enzymes expressed in rabbit liver and lung are products of related but distinctly different genes. *J Biol Chem* 265(10):5855-5861.

Leape LL (1995) Preventing adverse drug events. *Am J Health Syst Pharm* 52(4):379-382.

Lee H and Paik SG (2006) Regulation of BNIP3 in normal and cancer cells. *Mol Cells* 21(1):1-6.

Lee MY, Clark JE and Williams DE (1993) Induction of flavin-containing monooxygenase (FMO B) in rabbit lung and kidney by sex steroids and glucocorticoids. *Arch Biochem Biophys* 302(2):332-336.

Lee MY, Smiley S, Kadkhodayan S, Hines RN and Williams DE (1995) Developmental regulation of flavin-containing monooxygenase (FMO) isoforms 1 and 2 in pregnant rabbit. *Chem Biol Interact* 96(1):75-85.

Lee YH, Sauer B, Johnson PF and Gonzalez FJ (1997) Disruption of the c/ebp alpha gene in adult mouse liver. *Mol Cell Biol* 17(10):6014-6022.

Legato MJ (1997) Gender-specific aspects of obesity. *Int J Fertil Womens Med* 42(3):184-197.

Leger JG, Montpetit ML and Tenniswood MP (1987) Characterization and cloning of androgen-repressed mRNAs from rat ventral prostate. *Biochem Biophys Res Commun* 147(1):196-203.

Lehmann JM, McKee DD, Watson MA, Willson TM, Moore JT and Kliewer SA (1998) The human orphan nuclear receptor PXR is activated by compounds that regulate CYP3A4 gene expression and cause drug interactions. *J Clin Invest* 102(5):1016-1023.

Lemaigre FP, Courtois SJ, Lafontaine DA and Rousseau GG (1989) Evidence that the upstream stimulatory factor and the Sp1 transcription factor bind in vitro to the promoter of the human-growth-hormone gene. *Eur J Biochem* 181(3):555-561.

Li T and Chiang JY (2006) Rifampicin induction of CYP3A4 requires pregnane X receptor cross talk with hepatocyte nuclear factor 4alpha and coactivators, and suppression of small heterodimer partner gene expression. *Drug Metab Dispos* 34(5):756-764.

Liang CP and Tall AR (2001) Transcriptional profiling reveals global defects in energy metabolism, lipoprotein, and bile acid synthesis and transport with reversal by leptin treatment in ob/ob mouse liver. *J Biol Chem* 276(52):49066-49076.

Lin FT and Lane MD (1994) CCAAT/enhancer binding protein alpha is sufficient to initiate the 3T3-L1 adipocyte differentiation program. *Proc Natl Acad Sci U S A* 91(19):8757-8761.

Lin L, Qian Y, Shi X and Chen Y (2005) Induction of a cell stress response gene RTP801 by DNA damaging agent methyl methanesulfonate through CCAAT/enhancer binding protein. *Biochemistry* 44(10):3909-3914.

Liu W and Saint DA (2002) A new quantitative method of real time reverse transcription polymerase chain reaction assay based on simulation of polymerase chain reaction kinetics. *Anal Biochem* 302(1):52-59.

Lowis S, Eastwood MA and Brydon WG (1985) The influence of creatinine, lecithin and choline feeding on aliphatic amine production and excretion in the rat. *Br J Nutr* 54(1):43-51.

Luo Z and Hines RN (2001) Regulation of flavin-containing monooxygenase 1 expression by ying yang 1 and hepatic nuclear factors 1 and 4. *Mol Pharmacol* 60(6):1421-1430.

Malnick SD, Beergabel M and Knobler H (2003) Non-alcoholic fatty liver: a common manifestation of a metabolic disorder. *Qjm* 96(10):699-709.

Martin G, Schoonjans K, Lefebvre AM, Staels B and Auwerx J (1997) Coordinate regulation of the expression of the fatty acid transport protein and acyl-CoA synthetase genes by PPARalpha and PPARgamma activators. *J Biol Chem* 272(45):28210-28217.

Martin G, Schoonjans K, Staels B and Auwerx J (1998) PPARgamma activators improve glucose homeostasis by stimulating fatty acid uptake in the adipocytes. *Atherosclerosis* 137 Suppl:S75-80.

Massey V (1994) Activation of molecular oxygen by flavins and flavoproteins. *J Biol Chem* 269(36):22459-22462.

Masson D, Lagrost L, Athias A, Gambert P, Brimer-Cline C, Lan L, Schuetz JD, Schuetz EG and Assem M (2005) Expression of the pregnane X receptor in mice antagonizes the cholic acid-mediated changes in plasma lipoprotein profile. *Arterioscler Thromb Vasc Biol* 25(10):2164-2169.

Masuyama H, Hiramatsu Y, Mizutani Y, Inoshita H and Kudo T (2001) The expression of pregnane X receptor and its target gene, cytochrome P450 3A1, in perinatal mouse. *Mol Cell Endocrinol* 172(1-2):47-56.

Matys V, Fricke E, Geffers R, Gossling E, Haubrock M, Hehl R, Hornischer K, Karas D, Kel AE, Kel-Margoulis OV, Kloos DU, Land S, Lewicki-Potapov B, Michael H, Munch R, Reuter I, Rotert S, Saxel H, Scheer M, Thiele S and Wingender E (2003) TRANSFAC: transcriptional regulation, from patterns to profiles. *Nucleic Acids Res* 31(1):374-378.

Miller MM, James RA, Richer JK, Gordon DF, Wood WM and Horwitz KB (1997) Progesterone regulated expression of flavin-containing monooxygenase 5 by the B-isoform of progesterone receptors: implications for tamoxifen carcinogenicity. *J Clin Endocrinol Metab* 82(9):2956-2961.

Milligan SR and Finn CA (1997) Minimal progesterone support required for the maintenance of pregnancy in mice. *Hum Reprod* 12(3):602-607.

Moore LB, Goodwin B, Jones SA, Wisely.GB, Serabjit-Singh CJ, Willson TM, Collins JL and Kliewer SA (2000) St. John's wort induces hepatic drug metabolism through activation of the pregnane X receptor. *Proc Natl Acad Sci U S A* 97(13):7500-7502.

Motojima K, Passilly P, Peters JM, Gonzalez FJ and Latruffe N (1998) Expression of putative fatty acid transporter genes are regulated by peroxisome proliferator-activated receptor alpha and gamma activators in a tissue- and inducer-specific manner. *J Biol Chem* 273(27):16710-16714.

Muckenthaler M, Roy CN, Custodio AO, Minana B, deGraaf J, Montross LK, Andrews NC and Hentze MW (2003) Regulatory defects in liver and intestine implicate abnormal hepcidin and Cybrd1 expression in mouse hemochromatosis. *Nat Genet* 34(1):102-107.

Muller WE, Singer A, Wonnemann M, Hafner U, Rolli M and Schafer C (1998) Hyperforin represents the neurotransmitter reuptake inhibiting constituent of hypericum extract. *Pharmacopsychiatry* 31 Suppl 1:16-21.

Murphy BC, Chiu T, Harrison M, Uddin RK and Singh SM (2002) Examination of ethanol responsive liver and brain specific gene expression, in the mouse strains with variable ethanol preferences, using cDNA expression arrays. *Biochem Genet* 40(11-12):395-410.

Murray GI, Barnes TS, Sewell HF, Ewen SW, Melvin WT and Burke MD (1988) The immunocytochemical localisation and distribution of cytochrome P-450 in normal human hepatic and extrahepatic tissues with a monoclonal antibody to human cytochrome P-450. *Br J Clin Pharmacol* 25(4):465-475.

Nelson DR (1999) Cytochrome P450 and the individuality of species. *Arch Biochem Biophys* 369(1):1-10.

Nelson DR, Koymans L, Kamataki T, Stegeman JJ, Feyereisen R, Waxman DJ, Waterman MR, Gotoh O, Coon MJ, Estabrook RW, Gunsalus IC and Nebert DW (1996) P450 superfamily: update on new sequences, gene mapping, accession numbers and nomenclature. *Pharmacogenetics* 6(1):1-42.

Nolten LA, van Schaik FM, Steenbergh PH and Sussenbach JS (1994) Expression of the insulin-like growth factor I gene is stimulated by the liver-enriched transcription factors C/EBP alpha and LAP. *Mol Endocrinol* 8(12):1636-1645.

Nyberg SL, Remmel RP, Mann HJ, Peshwa MV, Hu WS and Cerra FB (1994) Primary hepatocytes outperform Hep G2 cells as the source of biotransformation functions in a bioartificial liver. *Ann Surg* 220(1):59-67.

Ogborne RM, Rushworth SA and O'Connell MA (2005) Alpha-lipoic acid-induced heme oxygenase-1 expression is mediated by nuclear factor erythroid 2-related factor 2 and p38 mitogen-activated protein kinase in human monocytic cells. *Arterioscler Thromb Vasc Biol* 25(10):2100-2105.

Ohmi N, Yoshida H, Endo H, Hasegawa M, Akimoto M and Higuchi S (2003) S-oxidation of S-methyl-esonarimod by flavin-containing monooxygenases in human liver microsomes. *Xenobiotica* 33(12):1221-1231.

Okey AB (1990) Enzyme induction in the cytochrome P-450 system. *Pharmacol Ther* 45(2):241-298.

Olefsky JM (1976) The effects of spontaneous obesity on insulin binding, glucose transport, and glucose oxidation of isolated rat adipocytes. *J Clin Invest* 57(4):842-851.

Olsavsky KM, Page JL, Johnson MC, Zarbl H, Strom SC and Omiecinski CJ (2007) Gene expression profiling and differentiation assessment in primary human hepatocyte cultures, established hepatoma cell lines, and human liver tissues. *Toxicol Appl Pharmacol* 222(1):42-56.

Osada S, Yamamoto H, Nishihara T and Imagawa M (1996) DNA binding specificity of the CCAAT/enhancer-binding protein transcription factor family. *J Biol Chem* 271(7):3891-3896.

Overby LH, Buckpitt AR, Lawton MP, Atta-Asafo-Adjei E, Schulze J and Philpot RM (1995) Characterization of flavin-containing monooxygenase 5 (FMO5) cloned from human and guinea pig: evidence that the unique catalytic properties of FMO5 are not confined to the rabbit ortholog. *Arch Biochem Biophys* 317(1):275-284.

Parsons B, MacLusky NJ, Krey L, Pfaff DW and McEwen BS (1980) The temporal relationship between estrogen-inducible progestin receptors in the female rat brain and the time course of estrogen activation of mating behavior. *Endocrinology* 107(3):774-779.

Pascussi JM, Busson-Le Coniat M, Maurel P and Vilarem MJ (2003) Transcriptional analysis of the orphan nuclear receptor constitutive androstane receptor (NR1I3) gene promoter: identification of a distal glucocorticoid response element. *Mol Endocrinol* 17(1):42-55.

Pascussi JM, Drocourt L, Fabre JM, Maurel P and Vilarem MJ (2000) Dexamethasone induces pregnane X receptor and retinoid X receptor-alpha expression in human hepatocytes: synergistic increase of CYP3A4 induction by pregnane X receptor activators. *Mol Pharmacol* 58(2):361-372.

Perrot-Applanat M, Logeat F, Groyer-Picard MT and Milgrom E (1985) Immunocytochemical study of mammalian progesterone receptor using monoclonal antibodies. *Endocrinology* 116(4):1473-1484.

Pettit FH, Orme-Johnson W and Ziegler DM (1964) The requirement for flavin adenine dinucleotide by a liver microsmal oxygenase catalyzing the oxidation of alkylaryl amines. *Biochem Biophys Res Commun* 16(5):444-448.

Physicians-Desk-Reference (1992) Physicians Desk Reference, Medical Economics Data, Montvale, NJ.

Pivato LS, Constantin RP, Ishii-Iwamoto EL, Kelmer-Bracht AM, Yamamoto NS, Constantin J and Bracht A (2006) Metabolic effects of carbenoxolone in rat liver. *J Biochem Mol Toxicol* 20(5):230-240.

Potgieter HC, Ubbink JB, Bissbort S, Bester MJ, Spies JH and Vermaak WJ (1997) Spontaneous oxidation of methionine: effect on the quantification of plasma methionine levels. *Anal Biochem* 248(1):86-93.

Poulsen LL and Ziegler DM (1979) The liver microsomal FAD-containing monooxygenase. Spectral characterization and kinetic studies. *J Biol Chem* 254(14):6449-6455.

Prince MI, Burt AD and Jones DE (2002) Hepatitis and liver dysfunction with rifampicin therapy for pruritus in primary biliary cirrhosis. *Gut* 50(3):436-439.

Rae JM, Johnson MD, Lippman ME and Flockhart DA (2001) Rifampin is a selective, pleiotropic inducer of drug metabolism genes in human hepatocytes: studies with cDNA and oligonucleotide expression arrays. *J Pharmacol Exp Ther* 299(3):849-857.

Rahib L, MacLennan NK, Horvath S, Liao JC and Dipple KM (2007) Glycerol kinase deficiency alters expression of genes involved in lipid metabolism, carbohydrate metabolism, and insulin signaling. *Eur J Hum Genet* 15(6):646-657.

Rahimian R, Van Breemen C, Karkan D, Dube G and Laher I (1997) Estrogen augments cyclopiazonic acid-mediated, endothelium-dependent vasodilation. *Eur J Pharmacol* 327(2-3):143-149.

Ramos RA, Nishio Y, Maiyar AC, Simon KE, Ridder CC, Ge Y and Firestone GL (1996) Glucocorticoid-stimulated CCAAT/enhancer-binding protein alpha expression is required for steroid-induced G1 cell cycle arrest of minimal-deviation rat hepatoma cells. *Mol Cell Biol* 16(10):5288-5301.

Rasooly R, Kelley DS, Greg J and Mackey BE (2007) Dietary trans 10, cis 12-conjugated linoleic acid reduces the expression of fatty acid oxidation and drug detoxification enzymes in mouse liver. *Br J Nutr* 97(1):58-66.

Rastegar M, Rousseau GG and Lemaigre FP (2000) CCAAT/enhancer-binding protein-alpha is a component of the growth hormone-regulated network of liver transcription factors. *Endocrinology* 141(5):1686-1692.

Rauckman EJ, Rosen GM and Kitchell BB (1979) Superoxide radical as an intermediate in the oxidation of hydroxylamines by mixed function amine oxidase. *Mol Pharmacol* 15(1):131-137.

Reaven GM, Lerner RL, Stern MP and Farquhar JW (1967) Role of insulin in endogenous hypertriglyceridemia. *J Clin Invest* 46(11):1756-1767.

Reitman ML (2002) Metabolic lessons from genetically lean mice. *Annu Rev Nutr* 22:459-482.

Rhoades RA, Tanner, George A. (2003) Medical Physiology. Second Edition:781.

Rich KJ, Sesardic D, Foster JR, Davies DS and Boobis AR (1989) Immunohistochemical localization of cytochrome P450b/e in hepatic and extrahepatic tissues of the rat. *Biochem Pharmacol* 38(19):3305-3322.

Ripp SL, Itagaki K, Philpot RM and Elfarra AA (1999) Species and sex differences in expression of flavin-containing monooxygenase form 3 in liver and kidney microsomes. *Drug Metab Dispos* 27(1):46-52.

Rival Y, Stennevin A, Puech L, Rouquette A, Cathala C, Lestienne F, Dupont-Passelaigue E, Patoiseau JF, Wurch T and Junquero D (2004) Human adipocyte fatty acid-binding protein (aP2) gene promoter-driven reporter assay discriminates nonlipogenic peroxisome proliferator-activated receptor gamma ligands. *J Pharmacol Exp Ther* 311(2):467-475.

Rojiani MV, Finlay BB, Gray V and Dedhar S (1991) In vitro interaction of a polypeptide homologous to human Ro/SS-A antigen (calreticulin) with a highly conserved amino acid sequence in the cytoplasmic domain of integrin alpha subunits. *Biochemistry* 30(41):9859-9866.

Rouer E, Rouet P, Delpech M and Leroux JP (1988) Purification and comparison of liver microsomal flavin-containing monooxygenase from normal and streptozotocin-diabetic rats. *Biochem Pharmacol* 37(18):3455-3459.

Salvi M, Fiore C, Armanini D and Toninello A (2003) Glycyrrhetinic acid-induced permeability transition in rat liver mitochondria. *Biochem Pharmacol* 66(12):2375-2379.

Salvi M, Fiore C, Battaglia V, Palermo M, Armanini D and Toninello A (2005) Carbenoxolone induces oxidative stress in liver mitochondria, which is responsible for transition pore opening. *Endocrinology* 146(5):2306-2312.

Salway J (1999) Metabolism at a Glance (2nd Edition).

Samadani U, Porcella A, Pani L, Johnson PF, Burch JB, Pine R and Costa RH (1995) Cytokine regulation of the liver transcription factor hepatocyte nuclear factor-3 beta is mediated by the C/EBP family and interferon regulatory factor 1. *Cell Growth Differ* 6(7):879-890.

Saville B, Wormke M, Wang F, Nguyen T, Enmark E, Kuiper G, Gustafsson JA and Safe S (2000) Ligand-, cell-, and estrogen receptor subtype (alpha/beta)-dependent activation at GC-rich (Sp1) promoter elements. *J Biol Chem* 275(8):5379-5387.

Schenkman JB and Jansson I (2003) The many roles of cytochrome b5. *Pharmacol Ther* 97(2):139-152.

Schlaich NL (2007) Flavin-containing monooxygenases in plants: looking beyond detox. *Trends Plant Sci* 12(9):412-418.

Schuetz EG, Schinkel AH, Relling MV and Schuetz JD (1996) P-glycoprotein: a major determinant of rifampicin-inducible expression of cytochrome P4503A in mice and humans. *Proc Natl Acad Sci U S A* 93(9):4001-4005.

Scott RE, Wu-Peng XS and Pfaff DW (2002) Regulation and expression of progesterone receptor mRNA isoforms A and B in the male and female rat hypothalamus and pituitary following oestrogen treatment. *J Neuroendocrinol* 14(3):175-183.

Seglen PO (1976) Preparation of isolated rat liver cells. *Methods Cell Biol* 13:29-83.

Shah YM, Ma X, Morimura K, Kim I and Gonzalez FJ (2007) Pregnane X receptor activation ameliorates DSS-induced inflammatory bowel disease via inhibition of NF-kappaB target gene expression. *Am J Physiol Gastrointest Liver Physiol* 292(4):G1114-1122.

Shen WJ, Liang Y, Hong R, Patel S, Natu V, Sridhar K, Jenkins A, Bernlohr DA and Kraemer FB (2001) Characterization of the functional interaction of adipocyte lipid-binding protein with hormone-sensitive lipase. *J Biol Chem* 276(52):49443-49448.

Sirica AE, Richards W, Tsukada Y, Sattler CA and Pitot HC (1979) Fetal phenotypic expression by adult rat hepatocytes on collagen gel/nylon meshes. *Proc Natl Acad Sci U S A* 76(1):283-287.

Smirlis D, Muangmoonchai R, Edwards M, Phillips IR and Shephard EA (2001) Orphan receptor promiscuity in the induction of cytochromes p450 by xenobiotics. *J Biol Chem* 276(16):12822-12826.

Smith AJ, Sanders MA, Thompson BR, Londos C, Kraemer FB and Bernlohr DA (2004a) Physical association between the adipocyte fatty acid-binding protein and hormone-sensitive lipase: a fluorescence resonance energy transfer analysis. *J Biol Chem* 279(50):52399-52405.

Smith AR, Shenvi SV, Widlansky M, Suh JH and Hagen TM (2004b) Lipoic acid as a potential therapy for chronic diseases associated with oxidative stress. *Curr Med Chem* 11(9):1135-1146.

Steward AR, Dannan GA, Guzelian PS and Guengerich FP (1985) Changes in the concentration of seven forms of cytochrome P-450 in primary cultures of adult rat hepatocytes. *Mol Pharmacol* 27(1):125-132.

Suh JK, Poulsen LL, Ziegler DM and Robertus JD (1999) Yeast flavin-containing monooxygenase generates oxidizing equivalents that control protein folding in the endoplasmic reticulum. *Proc Natl Acad Sci U S A* 96(6):2687-2691.

Suh JK, Poulsen LL, Ziegler DM and Robertus JD (2000) Redox regulation of yeast flavin-containing monooxygenase. *Arch Biochem Biophys* 381(2):317-322.

Suolinna EM, Penttila KE, Winell BM, Sjoholm AC and Lindros KO (1989) Drug metabolism by periportal and perivenous rat hepatocytes. Comparison of phase I and

phase II reactions and their inducibility during culture. *Biochem Pharmacol* 38(8):1329-1334.

Swales K, Plant N, Ayrton A, Hood S and Gibson G (2003) Relative receptor expression is a determinant in xenobiotic-mediated CYP3A induction in rat and human cells. *Xenobiotica* 33(7):703-716.

Syvertsen C, Halse J, Hoivik HO, Gaullier JM, Nurminiemi M, Kristiansen K, Einerhand A, O'Shea M and Gudmundsen O (2007) The effect of 6 months supplementation with conjugated linoleic acid on insulin resistance in overweight and obese. *Int J Obes (Lond)* 31(7):1148-1154.

Takamura T, Sakurai M, Ota T, Ando H, Honda M and Kaneko S (2004) Genes for systemic vascular complications are differentially expressed in the livers of type 2 diabetic patients. *Diabetologia* 47(4):638-647.

Tani Y, Yamamoto H, Kawaji A, Mizuno H, Fukushige J, Hosokawa T and Doi K (1999) Hepatic cytochrome P450 and flavin-containing monooxygenase in male Nts:Mini rat, a transgenic rat carrying antisense RNA transgene for rat growth hormone. *Toxicol Lett* 106(2-3):159-169.

Taylor KL and Ziegler DM (1987) Studies on substrate specificity of the hog liver flavin-containing monooxygenase. Anionic organic sulfur compounds. *Biochem Pharmacol* 36(1):141-146.

Tijet N, Boutros PC, Moffat ID, Okey AB, Tuomisto J and Pohjanvirta R (2006) Aryl hydrocarbon receptor regulates distinct dioxin-dependent and dioxin-independent gene batteries. *Mol Pharmacol* 69(1):140-153.

Tirona RG, Lee W, Leake BF, Lan LB, Cline CB, Lamba V, Parviz F, Duncan SA, Inoue Y, Gonzalez FJ, Schuetz EG and Kim RB (2003) The orphan nuclear receptor HNF4alpha determines PXR- and CAR-mediated xenobiotic induction of CYP3A4. *Nat Med* 9(2):220-224.

Tokyol C, Karaorman G and Bastug M (2005) Effects of acute and adaptive hypoxia on heat shock protein expression in hepatic tissue. *High Alt Med Biol* 6(3):247-255.

Tynes RE, Sabourin PJ, Hodgson E and Philpot RM (1986) Formation of hydrogen peroxide and N-hydroxylated amines catalyzed by pulmonary flavin-containing monooxygenases in the presence of primary alkylamines. *Arch Biochem Biophys* 251(2):654-664.

Umbreit JN, Conrad ME, Moore EG, Desai MP and Turrens J (1996) Paraferritin: a protein complex with ferrireductase activity is associated with iron absorption in rats. *Biochemistry* 35(20):6460-6469.

Vaananen H (1986) The distribution of cytochrome P-450-mediated drug oxidation and glutathione in periportal and perivenous rat hepatocytes after phenobarbital treatment. *J Hepatol* 2(2):174-181.

Van Lenten BJ, Prieve J, Navab M, Hama S, Lusis AJ and Fogelman AM (1995) Lipid-induced changes in intracellular iron homeostasis in vitro and in vivo. *J Clin Invest* 95(5):2104-2110.

Vegeto E, Shahbaz MM, Wen DX, Goldman ME, O'Malley BW and McDonnell DP (1993) Human progesterone receptor A form is a cell- and promoter-specific repressor of human progesterone receptor B function. *Mol Endocrinol* 7(10):1244-1255.

Venkatraman MS, Chittiboyina A, Meingassner J, Ho CI, Varani J, Ellis CN, Avery MA, Pershadsingh HA, Kurtz TW and Benson SC (2004) Alpha-Lipoic acid-based PPARgamma agonists for treating inflammatory skin diseases. *Arch Dermatol Res* 296(3):97-104.

Vignati LA, Bogni A, Grossi P and Monshouwer M (2004) A human and mouse pregnane X receptor reporter gene assay in combination with cytotoxicity measurements as a tool to evaluate species-specific CYP3A induction. *Toxicology* 199(1):23-33.

Villar D, Vara-Vega A, Landazuri MO and.Del Peso L (2007) Identification of a region on HIF prolyl 4-hydroxylases that determines their specificity for the oxygen degradation domains. *Biochem J.*

Vlasov IA and Volkov AM (2004) [Dependence of heart weight on body weight in patients with cardiovascular diseases]. *Fiziol Cheloveka* 30(4):62-68.

Vostrov AA, Quitschke WW, Vidal F, Schwarzman AL and Goldgaber D (1995) USF binds to the APB alpha sequence in the promoter of the amyloid beta-protein precursor gene. *Nucleic Acids Res* 23(14):2734-2741.

Wang D and Sul HS (1997) Upstream stimulatory factor binding to the E-box at -65 is required for insulin regulation of the fatty acid synthase promoter. *J Biol Chem* 272(42):26367-26374.

Wang H, Hagenfeldt-Johansson K, Otten LA, Gauthier BR, Herrera PL and Wollheim CB (2002) Experimental models of transcription factor-associated maturity-onset diabetes of the young. *Diabetes* 51 Suppl 3:S333-342.

Wang ND, Finegold MJ, Bradley A, Ou CN, Abdelsayed SV, Wilde MD, Taylor LR, Wilson DR and Darlington GJ (1995) Impaired energy homeostasis in C/EBP alpha knockout mice. *Science* 269(5227):1108-1112.

Wang T, Shankar K, Ronis MJ and Mehendale HM (2000) Potentiation of thioacetamide liver injury in diabetic rats is due to induced CYP2E1. *J Pharmacol Exp Ther* 294(2):473-479.

Wang YR, Xiao XZ, Huang SN, Luo FJ, You JL, Luo H and Luo ZY (1996) Heat shock pretreatment prevents hydrogen peroxide injury of pulmonary endothelial cells and macrophages in culture. *Shock* 6(2):134-141.

Waxman DJ (1999) P450 gene induction by structurally diverse xenochemicals: central role of nuclear receptors CAR, PXR, and PPAR. *Arch Biochem Biophys* 369(1):11-23.

Waxman DJ and Azaroff L (1992) Phenobarbital induction of cytochrome P-450 gene expression. *Biochem J* 281 (Pt 3):577-592.

Waxman DJ and O'Connor C (2006) Growth hormone regulation of sex-dependent liver gene expression. *Mol Endocrinol* 20(11):2613-2629.

Weatherby D, Ferguson, S. (2002) Blood Chemistry and CBC Analysis.

Wentworth JM, Agostini M, Love J, Schwabe JW and Chatterjee VK (2000) St John's wort, a herbal antidepressant, activates the steroid X receptor. *J Endocrinol* 166(3):R11-16.

Wilkening S, Stahl F and Bader A (2003) Comparison of primary human hepatocytes and hepatoma cell line Hepg2 with regard to their biotransformation properties. *Drug Metab Dispos* 31(8):1035-1042.

Williams DE, Hale SE, Muerhoff AS and Masters BS (1985) Rabbit lung flavin-containing monooxygenase. Purification, characterization, and induction during pregnancy. *Mol Pharmacol* 28(4):381-390.

Williams DE, Ziegler DM, Nordin DJ, Hale SE and Masters BS (1984) Rabbit lung flavin-containing monooxygenase is immunochemically and catalytically distinct from the liver enzyme. *Biochem Biophys Res Commun* 125(1):116-122.

Wong HR, Mannix RJ, Rusnak JM, Boota A, Zar H, Watkins SC, Lazo JS and Pitt BR (1996) The heat-shock response attenuates lipopolysaccharide-mediated apoptosis in cultured sheep pulmonary artery endothelial cells. *Am J Respir Cell Mol Biol* 15(6):745-751.

Woods SC, Gotoh K and Clegg DJ (2003) Gender differences in the control of energy homeostasis. *Exp Biol Med (Maywood)* 228(10):1175-1180.

Wrighton SA, Maurel P, Schuetz EG, Watkins PB, Young B and Guzelian PS (1985) Identification of the cytochrome P-450 induced by macrolide antibiotics in rat liver as the glucocorticoid responsive cytochrome P-450p. *Biochemistry* 24(9):2171-2178.

Yanagimoto T, Itoh S, Sawada M and Kamataki T (1997) Mouse cytochrome P450 (Cyp3a11): predominant expression in liver and capacity to activate aflatoxin B1. *Arch Biochem Biophys* 340(2):215-218.

Yeung CK, Lang DH, Thummel KE and Rettie AE (2000) Immunoquantitation of FMO1 in human liver, kidney, and intestine. *Drug Metab Dispos* 28(9):1107-1111.

Yokoyama C, Wang X, Briggs MR, Admon A, Wu J, Hua X, Goldstein JL and Brown MS (1993) SREBP-1, a basic-helix-loop-helix-leucine zipper protein that controls transcription of the low density lipoprotein receptor gene. *Cell* 75(1):187-197.

Yueh MF, Krueger SK and Williams DE (1997) Pulmonary flavin-containing monooxygenase (FMO) in rhesus macaque: expression of FMO2 protein, mRNA and analysis of the cDNA. *Biochim Biophys Acta* 1350(3):267-271.

Zhang J and Cashman JR (2006) Quantitative analysis of FMO gene mRNA levels in human tissues. *Drug Metab Dispos* 34(1):19-26.

Zhang J, Cerny MA, Lawson M, Mosadeghi R and Cashman JR (2007) Functional activity of the mouse flavin-containing monooxygenase forms 1, 3, and 5. *J Biochem Mol Toxicol* 21(4):206-215.

Zhao GQ, Liaw L and Hogan BL (1998) Bone morphogenetic protein 8A plays a role in the maintenance of spermatogenesis and the integrity of the epididymis. *Development* 125(6):1103-1112.

Ziegler DM and Pettit FH (1966) Microsomal oxidases. I. The isolation and dialkylarylamine oxygenase activity of pork liver microsomes. *Biochemistry* 5(9):2932-2938.

Appendix

Primers

hFMO5 -2443 F ggggtacCAGTTCCACATGCATGTGCATC (11/22)

hFMO5 -1723 F ggggtaccGACCAGCTTGAGCAACATAGTG (11/22)

hFMO5 -1031 F ggggtaCCTCACTATACTCCAGCACTCAG (12/23)

hFMO5 -531 F ggggtaccGCTCGGCTCTTAAGACGCGAGTC (12/23)

hFMO5 +9 R ggagatctGCGCTCAACAGATCCTTCAGCTG (12/23)